EABR
Experimental and Applied Biomedical Research
ISSN 2956-0454
eISSN 2956-2090
VOL 25 No 2
June, 2024.



sciendo

**ISSN 2956-0454**



**Print**

Faculty of Medical Sciences, University of Kragujevac

**Indexed in**

EMBASE/Excerpta Medica, Index Copernicus, BioMedWorld, KoBSON, SCIndeks, Chemical Abstracts Service, Cabell's Directory, Celdes, CNKI Scholar (China National Knowledge Infrastructure), CNPIEC, EBSCO Discovery Service, Elsevier - SCOPUS, Google Scholar, J-Gate, Naviga (Softweco), Primo Central (ExLibris), ReadCube, SCImago (SJR), Summon (Serials Solutions/ProQuest), TDOne (TDNet), WorldCat (OCLC)

**Address:**

Experimental and Applied Biomedical Research, Faculty of Medical Sciences,
University of Kragujevac 69 Svetozara Markovica Street, 34000 Kragujevac, PO Box 124, Serbia

https:/medf.kg.ac.rs/eabr
https://sciendo.com/journal/SJECR

EABR is published four times annually

Experimental and Applied Biomedical Research is categorized as a scientific journal of M51 category by the Ministry of Education, Science and Technological Development of the Republic of Serbia

CIP - Каталогизација у публикацији
Народна библиотека Србије, Београд

61

**EABR** : Experimental and Applied Biomedical Research / editor in chief Vladimir Zivkovic. - Vol. 25, no. 2 (jun. 2024)- . - Kragujevac : Faculty of Medical Sciences, University of Kragujevac, 2024- (Kragujevac : Faculty of Medical Sciences, University of Kragujevac). - 30 cm

Tromesečno. - Je nastavak: Serbian Journal of Experimental and Clinical Research = ISSN 1820-8665
ISSN 2956-0454 = EABR. Experimental and Applied Biomedical Research
COBISS.SR-ID 81208329

**TABLE OF CONTENTS**

# BASIC PRINCIPLES OF ANTIBIOTICS DOSING IN PATIENTS WITH SEPSIS AND ACUTE KIDNEY DAMAGE TREATED WITH CONTINUOUS VENOVENOUS HEMODIAFILTRATION

Aleksandra Nikolić[1], Sasa Jaćović[2], Željko Mijailović[3,5], Dejan Petrović[4,5]

[1]*Apoteka Kragujevac, Kragujevac, Serbia*
[2]*Medicines and Medical Devices Agency of Serbia, Belgrade, Serbia*
[3]*Clinic for Infectious Disease, Clinical Center Kragujevac, Kragujevac, Serbia*
[4]*Clinic for Urology, Nephrology and Dialysis, Clinical Center Kragujevac, Kragujevac, Serbia*
[5]*Faculty of Medical Sciences, University of Kragujevac, Kragujevac, Serbia*

Received: 16.12.2018.
Accepted: 25.12.2018.

**Corresponding author:**

**Prof. dr Dejan Petrovic**

Faculty of Medical Sciences, University of Kragujevac, Clinic of Urology, Nephrology and Dialysis, University Clinical Center Kragujevac, Kragujevac, Serbia

E-mail: dejan.petrovic@fmn.kg.ac.rs

## ABSTRACT

*Sepsis is the leading cause of acute kidney damage in patients in intensive care units. Pathophysiological mechanisms of the development of acute kidney damage in patients with sepsis may be hemodynamic and non-hemodynamic. Patients with severe sepsis, septic shock and acute kidney damage are treated with continuous venovenous hemodiafiltration. Sepsis, acute kidney damage, and continuous venovenous hemodiafiltration have a significant effect on the pharmacokinetics and pharmacodynamics of antibiotics. The impact dose of antibiotics is increased due to the increased volume of distribution (increased administration of crystalloids, hypoalbuminemia, increased capillary permeability syndrome toproteins). The dose of antibiotic maintenance depends on renal, non-renal and extracorporeal clearance. In the early stage of sepsis, there is an increased renal clearance of antibiotics, caused by glomerular hyperfiltration, while in the late stage of sepsis, as the consequence of the development of acute renal damage, renal clearance of antibiotics is reduced. The extracorporeal clearance of antibiotics depends on the hydrosolubility and pharmacokinetic characteristics of the antibiotic, but also on the type of continuous dialysis modality, dialysis dose, membrane type, blood flow rate, dialysis flow rate, net filtration rate, and effluent flow rate. Early detection of sepsis and acute kidney damage, early target therapy, early administration of antibiotics at an appropriate dose, and early extracorporeal therapy for kidney replacement and removal of the inflammatory mediators can improve the outcome of patients with sepsis in intensive care units.*

***Keywords***: *Sepsis, acute kidney damage, antibiotics, continuous venovenous hemodiafiltration (CVVHDF).*

sciendo

UDK: 616.94-085
616.61-008.64
615.33.015.4
Eabr 2024; 25(2):93-102
DOI: 10.2478/sjecr-2018-0071

## INTRODUCTION

Sepsis is the leading cause of acute kidney damage in patients in intensive care units (1, 2). It is defined as the systemic inflammatory response syndrome to the proven bacterial-induced infection, and a severe sepsis as the sepsis associated with Sequential Organ Failure Assessment - SOFA score ≥ 2.0. Severe sepsis progresses to a septic shock, which is defined as a persistent hypotension that does not repair after resuscitation with 0.9% NaCl solution of crystalloid at a dose of 40-60 mL/kg in the first hour, requiring the use of the vasopressor norepinephrine in a dose > 5 μg/kg/min for maintenance of mean arterial blood pressure at values ≥ 65 mmHg, associated with clinical data for hypoperfusion (serum lactate concentration greater than 2.0 mmol/L) and organ dysfunction (SOFA score ≥ 2.0) (3, 4). The mortality rate of patients with severe sepsis, septic shock and acute kidney damage is 50-80% (5-9). Patients in intensive care units with severe sepsis, septic shock and acute kidney damage require extended hospitalization, kidney replacement therapy, have high cost of treatment and an increased risk of developing insufficiency of multiple organ systems and unwanted outcomes (5-9). Early detection of sepsis and acute kidney damage, early target therapy, early administration of antibiotics at an appropriate dose, and early extracorporeal therapy to replace the kidney function and removing the inflammatory mediators can correct the outcome in patients with sepsis in intensive care units (5-9). Sepsis, acute kidney damage, and CVVHDF significantly influence the pharmacokinetics and pharmacodynamics of antibiotics (10, 11). The results of the study show that 25-60% of these patients have a substitute therapy concentration of antibiotics in blood (10, 11).

### Acute damage and kidney function disorder in sepsis

Based on the Kidney Disease: Improving Global Outcomes classification, acute kidney injury (AKI) is defined as a serum creatinine concentration increase of ≥ 0.3 mg/dL (≥ 26.5 μmol/L) during the course of 48h or as an increase serum creatinine concentrations for ≥ 1.5 times compared to basal serum creatinine concentration over the past seven days and/or as a diuresis of less than 0.5 mL/kg/h for at least 6h (12).

Pathophysiological mechanisms of AKI development in patients with sepsis can be hemodynamic and non-hemodynamic (13-15). Hemodynamic pathophysiological mechanisms include: hypoperfusion of kidneys, increased intra-abdominal pressure, increased central venous pressure and stoppage of blood flow in the venous kidney system (13-15). The non-hemodynamic pathophysiological mechanisms include: enhanced systemic and local response of the host immune system to infection, increased formation and secretion of proinflammatory mediators ("cytokine storm"), dysfunction of the kidney small blood vessels endothelium, kidney parenchyma infiltration by immune system cells (monocytes, neutrophils) activation of epithelial cells of proximal tubules through activation of Toll-like receptors - TLRs and oxidative stress (13-17).

### Treatment of acute damage and disorders of kidney function caused by sepsis

In patients with sepsis and AKI, the severity of renal impairment and the presence of absolute criteria for the treatment of acute dialysis should be assessed: resistant hyperkalemia ($K^+$ > 6.5 mmol/L with or without electrocardiographic changes), resistant hypervolemia (furosemide resistant edema), severe metabolic acidosis (pH arterial blood ≤ 7.15), complications of high azotemia (uremic encephalopathy, uremic pericarditis) (18, 19). In the absence of absolute criteria, treatment with dialysis should be initiated if the severe form of AKI (KDIGO3 stage) is diagnosed, and in patients with severe sepsis and rapid deterioration of AKI, treatment with dialysis should be initiated at stage 2 (KDIGO2) (modulation of response of systemic and local immune system to infection) (20-22). Before making a decision to initiate treatment with dialysis in patients with sepsis and mild to moderate AKI (KDIGO 1/2), there should be assessment of the severity of the clinical condition of the patient including the renal function reserve, potency for complications, and the presence of clinical conditions that adversely affect the kidney function (intraabdominal hypertension, mechanical ventilation with positive ventilation pressure, nephrotoxic antibiotics, radiocontrast agents) (20-22). Patients with severe sepsis/septic shock who are hemodynamically unstable, with AKI and multiple organ systems failure, increased serum inflammation mediator concentrations (IL-6 ≥ 1000 pg/mL), increased catabolism and hypervolemia, require treatment with CVVHDFwith PMMA (Polymethylmethacrylate), standard and modified AN69ST membrane (Acrylonitrile 69 Surface-Treated) (20-26). CVVHDF with PMMA membrane, which has the ability to adsorb the inflammatory mediators, is administered at a dose of 35 ml/kg/h, during 24-72 hours, and substantially ensures hemodynamic stability and homeostasis of the systemic and local immune system response of the host to infection (preventing the development of “cytokine storms”). When the concentration of IL-6 (Interleukin-6) is reduced below 1000 pg/mL, the treatment is continued with standard CVVHDF, with an ultrafiltration of 35 mL/kg/h (dose of CVVHDF = 35 mL/kg/h) (20-29). For evaluation of the efficiency of the filter (AN69ST), serial measurement of effluent and blood concentrations of urea in patients - FUN/BUN (measurement at every 12h) is used. The filter is effective if the ratio FUN/BUN is ≥ 0.80, and values less than 0.80 indicate the risk of thrombosis of the filter (30, 31). CVVHDF-AN69ST is effective if the ratio of delivered and prescribed dialysis is ≥ 80% (the effective treatment time should be ≥ 20h) (30, 31).

### The effect of sepsis, acute kidney damage, and CVVHDFon the pharmacokinetics of antibiotics

In patients with AKI, the absorption of antibiotics from the gastrointestinal tract is reduced due to: the use of a proton pump blocker, mucous membrane edema due to hypervolemia, disorders of structure and function of the bowels, altered gastrointestinal motility, cholestasis in sepsis and shock

conditions (antibiotics are administered in the form of i.v. bolus or i.v. infusion) (10, 11). The volume of antibiotic distribution in these patients has been increased due to: increased administration of crystalloid solutions (early target therapy), reduced serum albumin concentrations (increased fraction of free antibiotic concentration in blood), decreased antibody affinity for binding to plasma proteins and increased capillary permeability syndrome to proteins (10, 11). Hypoalbuminemia is present in 40-50% of patients with sepsis and acute kidney damage. There is a particularly high increase of volume of distribution of hydrosoluble antibiotics, such as aminoglycosides, ß-lactam antibiotics and glycopeptide antibiotics: vancomycin and daptomycin (10, 11). Increased antibiotic distribution volume requires a higher loading dose compared to the standard impact dose (maintenance of antibiotic therapeutic concentration) (10, 11). The maintenance dose depends on the metabolism of the antibiotic in the liver and the degree of renal function (antibiotic excretion). It is calculated from the following equation: MD = standard dose x (CLCr of the patient/normal CLCr), where CLCr is the clearance of endogenous creatinine (10, 11).

In the early stage of sepsis, glomerular hyperfiltration is developed. Glomerular hyperfiltration - Augmented Renal Clearance - ARC is defined as CLCr> 130 mL/min/1.73m$^2$ (32-35). The prevalence of ARC in patients in intensive care units with sepsis and brain injury (subarachnoid bleeding) is 50-85% (32-35). Inflammation mediators released during the Systemic Inflammatory Response Syndrome - SIRS increase the minute heart volume, reduce vascular resistance, and increase kidney perfusion (↑GFR) (32-35). Glomerular hyperfiltration affects the pharmacokinetics of hydrophilic "time-dependent" antibiotics. Increased clearance of antibiotics shortens its half-life (t1/2) and reduces the area under the concentration-time curve ($AUC_{0-24}$), which directly affects the achievement of the target therapeutic values of pharmacodynamic parameters (inadequate therapy) (32-35). In the presence of ARC, the standard dose of beta lactam antibiotics is not sufficient to maintain the free antibiotic concentration above the minimum inhibitory concentration (fT > MIC ≥ 100%) over the dosage interval (32-35). The optimal dose of meropenem in patients with ARC is 2.0 g/8h, in the form of i.v. infusion for 3.0h, and the dose of cefepime is 2.0 g/6-8h, in the form of i.v. infusion over 3.0h. The standard dose of vancomycin is not sufficient to provide AUC/MIC > 400. In patients with ARC, impact i.v. dose of vancomycin should be 25-30 mg/kg and then continued with a maintenance dose of 45 mg/kg/24h (administered every8 hours or as a continuous IV infusion), with appropriate monitoring of the therapeutic levels of vancomycin in plasma (target therapeutic concentration: 15-20 mg/L) (31-34). In the late stage of sepsis, due to the development of acute kidney damage, renal clearance of antibiotics is reduced (32-35).

The extracorporeal antibiotic clearance ($CL_{EC}$) depends on the following: molecular weight, plasma protein binding degree, and the volume of antibiotic distribution. Hydrosoluble antibiotics with low molecular weight (MW < 500 Da), low volume of distribution (Vd < 1.0 L/kg) and low plasma protein binding (PB < 80%, fu > 0.20) have large extracorporeal clearance (36-39). The group of antibiotics with low molecular weight, low volume of distribution, low plasma protein binding rates and small non-renal clearance, which are being removed in significant amounts during the CVVHDF session, include: aminoglycoside antibiotics, vancomycin, phosphomycin, and flucytosine (36-39). High-volume antibiotics (Vd > 1.0 L/kg) and/or high plasma protein binding rates (PB > 80%, fu < 0.20) have small extracorporeal clearance since a significant antibiotic fraction is found in the extravascular section (36-39). Flucloxacillin binds to plasma proteins in high percentage (PB ≥ 94%, fu < 0.06) and therefore it is not removed in significant amounts during the CVVHDF session (36-39). The two most important parameters for antibiotic dosing in patients treated with CVVHDF are pharmacokinetic properties of antibiotics and CVVHDF doses, expressed as the total effluent flow rate (Qef) (36-39). With CVVHDF, Qef represents the sum of the dialysis flow rate (Qd), the rate of the solution for substitution flow rate (Qs), and the rate of net ultrafiltration (Qnuf): Qef = Qd + Qs + Qnuf. Qef significantly influences the pharmacokinetics of antibiotics, the prediction of extracorporeal antibody clearance, and the achievement of the target therapeutic concentration of antibiotics in plasma of the patients (36-39). According to the KDIGO recommendations, Qef in patients with AKI should be 20-25 mL/kg/h, and in patients with sepsis and AKI 35 mL/kg/h (36-39). The total clearance of antibiotics in patients with AKI and CVVHDF is calculated from the formula: CLtot = $CL_{EC}$ + $CL_R$ + $CL_{NR}$, where: $CL_{EC}$ is extracorporal clearance, $CL_R$is renal clearance and $CL_{NR}$ non-renal clearance. The diffusion clearance (Qd x Sd) of the antibiotic in CVVHDF depends on the molecular weight of the antibiotic, the blood flow (Qb), and the dialysate flow (Qd), while convective clearance (Qef x Sc) depends on the total effluent flow rate (Qef) and the coefficient of scaling (36-39). The saturation coefficient (Sd) is calculated from the formula: Sd = Cd/Cp, where: Cd is the antibiotic concentration in the dialysate, and Cp is the plasma antibiotic concentration. The coefficient of scaling - Sc is calculated from the equation: Sc = Cef/Cp, where: Cef is the concentration of antibiotics in the effluent, and Cp is the plasma antibiotic concentration (36-39). In CVVHDF, extracorporal clearance is calculated from the formula: $CL_{CCVHDF}$ = Qef x Sd, where: Qef is the total effluent flow rate and Sd is the saturation coefficient (35-38). Extracorporeal clearance significantly contributes to the overall antibiotic clearance if it is greater than 25% ($Fr_{EC}$ > 25%). Contribution of the extracorporeal clearance to the total antibiotic clearance is calculated from the equation: $Fr_{EC} = CL_{EC}/(CL_{EC} + CL_R + C_{NR})$, where: $CL_{EC}$ is extracorporeal clearance, $CL_R$ is renal clearance, and $C_{NR}$ is non-renal clearance (36-39).

Factors that affect antibiotic clearance during the CVVHDF session include factors specific to: patients, antibiotics (pharmacokinetics, pharmacodynamics), and CVVHDF modality of dialysis. Factors specific to the CVVHDF modality of the dialysis include: dialysate flow rate (Qd), replacement rate of the substitution solution (Qs), net ultrafiltration rate (Qnuf), total ultrafiltration rate (Quf =

Qs + Qnuf), total effluent flow rate (Qef = Qd + Qs + Qnuf), dialysis membrane type (high-velocity membranes), and the dilution method (pre-conditioning, post-dilution). Pre-dialysis (substitution solution used before the filter) reduces antibiotic clearance. Vancomycin clearance is 25% higher if the solution for substitution is applied after the filter (post-dilution) (36-39). Another factor affecting the antibiotic clearance during the CVVHDF modality of the dialysis is the age of the filter (duration of treatment). The Sieving coefficient of scaling of the antibiotic decreases during the CVVHDF session (it is highest in the first dialysis hours) due to the precipitation of proteins along the membrane surface and the reduction in the number of non-trombosed filter capillaries (36-39). Larger Qef and Sc provide higher clearance of antibiotics, and this may result in subdosing, the absence of target antibiotic therapeutic concentration, and a lower survival rate of these patients (36-39).

The antibiotic dose adjustment factor in the CVVHDF patients is calculated from the equation: Q = 1 - (fe x (1 - KF)), where: fe is the fraction of the medicine excreted in urine in an unchanged form, KF - the ratio of the current clearance of endogenous creatinine and normal endogenous creatinine clearance (normal clearance of endogenous creatinine = 120 mL/min). The new adjusted dose - $D_R$ is calculated from the formula: $D_R$ = Dnorm x Q, where: Dnorm is the dose predicted for normal kidney function and Q is the dose adjustment factor (40, 41).

**Pharmacokinetic and pharmacodynamic properties of antibiotics**

Based on the pharmacokinetic and pharmacodynamic characteristics, antibiotics can be divided into three groups. The first group consists of antibiotics whose antibacterial effect depends on the concentration of medicine in plasma ("concentration dependent" antibiotics), the second group consists of antibiotics whose antibacterial effect depends on the length of exposure to the antibiotic ("time-dependent" antibiotics), and the third group consists of antibiotics whose antibacterial effect depends on the plasma drug concentration, but also on the duration of exposure to the antibiotic ("concentration-dependent" and "time-dependent" antibiotics) (40-43).

The first group of antibiotics include: aminoglycosides, daptomycin, and fluoroquinolones. The antibacterial effect of these antibiotics is achieved only when the maximum plasma antibiotic concentration is reached. The main pharmacodynamic parameter for assessing the efficacy of these antibiotics is to measure the maximum plasma antibiotic concentration (Cmax) and the ratio of the maximum plasma antibiotic concentration to the minimum inhibitory antibiotic concentrations (Cmax/MIC). The main parameter for evaluating the efficacy of antibiotics from the second group is the determination of the percentage of T > MIC (Minimal Inhibitory Concentration) (the estimated time during 24 hours when the plasma antibiotic concentration is greater than its minimum inhibitory concentration (%T > MIC)) (39-42). This antibiotic group includes beta-lactam antibiotics (40-43). The third group consists of antibiotics whose antibacterial effect depends on the concentration, but also on the time of exposure to the antibiotic (40-43). The antibacterial effect is assessed by measuring the ratio of the area under the concentration-time curve for 24 hours and the minimum inhibitory antibiotic concentration ($AUC_{0-24}$/MIC) (40-43). This group of antibiotics includes: fluoroquinolones, tigecycline, linezolid, and glycopeptide antibiotics (vancomycin) (40-43).

Gentamicin (Gentamicin) is a hydrosoluble antibiotic, with molecular weight - MW = 477 Da, a small volume of distribution - Vd = 0.25 L/kg, and a low plasma proteins binding level - PB = 10-20% (fu = 0.80-0.90). It belongs to the group of antibiotics whose antibacterial effect depends on its plasma concentration ("concentration-dependent" antibiotic group) (40-43). The therapeutic concentration of gentamicin in plasma is 1.0-2.0 μg/L. Its maximum blood concentration is 6-8 mg/L, and it is achieved 30 minutes after the application of the impact dose of 2-2.5 mg/kg (IV infusion) (40-43). After the applied impact dose, it is continued with 1.0-1.5 mg/kg/24h (40-42). The target value of the Cmax/MIC ratio should be at least 8-10 (Cmax/MIC = 8-10) (40-43).

Amikacin is a hydrosoluble antibiotic, with molecular weight - MW = 585.6 Da, a small volume of distribution - Vd = 0.22-0.29 L/kg and a low plasma protein binding level - PB < 20% (40-44). It is used to treat serious infections caused by Gram negative microorganisms in patients in intensive care units. It belongs to a group of antibiotics whose antibacterial effect depends on the concentration of the medicine in the plasma ("concentration-dependent" antibiotic). It is administered at a dose of 7.5 mg/kg/12h, in the form of an IV infusion, for 30 minutes and requires dose adjustment depending on the degree of renal function (40-44). Amikacin is removed in significant amounts during the CVVHDF session. $CL_{CVVHDF}$ of amikacin is calculated from the formula: $CL_{CVVHDF}$ = Qef x fu, where: Qef is the total effluent flow rate, and the fu - fraction of amikacin not bound to plasma proteins (fu = 0.80). Qef represents a dose of CVVHDF modality of dialysis. It is calculated from the equation: Qef = Qd + Qs + Qnuf. In patients with AKI in the absence of sepsis, the dose of dialysis is Qef = 20-25 mL/kg/h, and in patients with severe sepsis, septic shock and AKI, the dose of dialysis is - Qef = 35 mL/kg/h (43). The average $CL_{CVVHDF}$of amikacin is 2.86 ± 0.41 L/h, and the coefficient of scaling for amikacin is - Sc = 0.83 ± 0.05 (44). Amikacin is a small hydrophilic antibiotic, which is significantly removed during the CVVHDF session. The recommended dose of amikacin being 10 mg/kg does not provide optimal therapeutic concentration in patients treated with CVVHDF. The results of the study show that in these patients, amikacin should be administered at an impact dose of 15-30 mg/kg, in the form of an IV infusion for 30 minutes and then continue with the appropriate dose every 24h or 36h (7.5 mg/kg/24-48h) (44, 45). The target pharmacodynamic parameters for assessing the efficacy of amikacin are: AUC/MIC ≥ 70, Cmax/MIC = 8-10 (≥ 8) and MIC ≤ 2.5 mg/L (45, 46).

Daptomycin has a molecular weight - MW = 1650 Da and volume of distribution - Vd = 0.1 L/kg. It is associated with a high percentage of plasma protein binding (PB = 90-92%, fe = 0.08-0.10) (47, 48). It is used to treat infections caused by Methicillin (MRSA) resistant Staphylococcus aureus, Vancomycin Resistant Enterococcus (VRE) and other Gram-positive microorganisms. It belongs to the group of "concentration-dependent" antibiotics, and the most important pharmacodynamic parameter for assessing the effectiveness of antibacterial action is the ratio of the area under the concentration-time curve (AUC) and the minimum inhibitory concentration (MIC) - $AUC_{0-24}$/MIC (MIC = 3-4 μg/mL) (47, 48). The efficacious antibacterial effect of daptomycin exists if $AUC_{0-24}$/MIC is ≥ 666 (47, 48). In patients with endogenous creatinine clearance greater than 30 ml/min it is administered at a dose of 6 mg/kg every 24 hours (IV infusion over 30 minutes), and when the endogenous creatinine clearance drops below 30 mL/min, it is administered in the same dose, but every 48h (47, 48). The recommended dose of daptomycin in patients treated with CVVHDF is the same as in patients with clearance greater than 30 mL/min (6 mg/kg/24h) (46, 47). One group of authors recommends that the dose of daptomycin in patients with severe sepsis, septic shock and AKI treated with CVVHDF should be 8 mg/kg/48h (47, 48). Daptomycin acts toxically to skeletal musculature: it causes weakness and pain of transverse-striated musculature, and creatinine kinase concentration is ten times higher than the upper normal limit (47, 48). Serum creatinine phosphokinase (CPK) monitoring is required in patients using daptomycin (47, 48).

Linezolid (Linezolid) has a molecular weight - MW = 337 Da, a small volume of distribution - Vd = 0.6-0.8 L/kg and low percentage of plasma protein binding - PB = 30% (fu = 0.70) (49, 50). It is a moderately lipophilic antibiotic that belongs to the group of "time-dependent" antibiotics. The linezolid dosing regimen may be intermittent or continuous. Intermittently, linezolid is applied IV at a dose of 600 mg/12h, and continuously, as an impact dose of 300 mg, and then continued at a dose of 900 mg/24h, in the form of a continuous IV infusion. In patients with severe sepsis treated with CVVHDF, high-dose linezolid can be administered intermittently or continuously. Intermittently, intravenously at a dose of 600 mg/8h or continuously, as a high dose of 600 mg, and then continued at a dose of 1200 mg/24h, in the form of a continuous IV infusion (49, 50). The best parameter for assessing the antibacterial effect of linezolid is the $AUC_{24}$/MIC ratio, which should be 50 for Staphylococcus pneumoniae ($AUC_{24}$/MIC = 50), and 85 for Staphylococcus aureus ($AUC_{24}$/MIC = 85). The maximum antibacterial effect of linezolid is achieved when T > MIC is ≥ 85% and $AUC_{0-24}$/MIC ratio is > 100 (49, 50).

Vancomycin has a molecular weight - MW = 1450 Da, volume of distribution - Vd = 0.47 -1.1 L/kg and plasma protein binding percentage - PB = 10-50% (51-53). Depending on the antibacterial effect, it belongs to the third group of "concentration-dependent" and "time-dependent" antibiotics. The best parameter for the evaluation of the efficacy of vancomycin is $AUC_{0-24}$/MIC ratio, which should be greater than 400 mg/hxL (provides eradication of Methicillin-resistant Staphylococcus aureus) (51-53). Vancomycin is applied IV at an impact dose of 15-20 mg/kg, and then continued at 10-40 mg/kg/day, depending on the degree of renal function. The therapeutic concentration of vancomycin in plasma is 15-20 mg/L (51-53). In patients treated with standard intermittent hemodialysis, the dose of vancomycin depends on the diabetic membrane flow rate: "low-flux" versus "high-flux" (54). The results of clinical trials show that vancomycin is removed in significant amounts during the CVVHDF session (> 50% of the total amount of vancomycin is eliminated via kidneys). The dose of CVVHDF significantly affects the clearance of vancomycin. With the increase in the CVVHDF dose, vancomycin clearance is increased by at least 30%. CVVHDF clearance of vancomycin corresponds to the clearance of endogenous creatinine of 25-50 mL/min. Bearing this in mind, some authors consider that the vancomycin impact dose should be 35 mg/kg (IV infusion for 4h), and further treatment should be continued continuously i.v. through the infusion of vancomycin at a dose of 14 mg/kg/24h (51-54).

Beta-lactam antibiotics are widely used as the first-line antibiotics for the treatment of infections in patients in intensive care units. The use of standard doses in patients treated with continuous dialysis modalities may result in an inadequate therapeutic concentration of these antibiotics in the serum (subdosage, increased risk of development of resistance). The group of beta-lactam antibiotics include: ceftazidime (CEF), cefepime (CEF) and piperacillin/tazobactam (TZP) (55-57). They belong to the group of "time-dependent" antibiotics. The best pharmacodynamic parameter for the evaluation of the antibacterial effect is %T > MIC (T > MIC ≥ 40% for CEF, T > MIC > 75% for TZP) (55-57). The results of the tests carried out so far indicate that the standard intermittent dose of ceftazidime does not provide the target values of the pharmacodynamic parameters in all patients with severe infection treated with CVVHDF (56, 57). CVVHDF removes a significant amount of ceftazidime. The maximum effective serum ceftazidic concentration is 4-5 times higher than the MIC (> 4-5 x MIC) (MIC for ceftazidime is ≤ 4 mg/L) (56, 57). Ceftazidime is the third generation of cephalosporins, with molecular weight of 636.6 Da. It binds with plasma proteins in low percentage (fu = 0.90), and about 90% of ceftazidime is excreted in the urine in an unchanged form (fe = 0.90), and the coefficient of scaling of ceftazidime in the CVVHDF session is Sc = 0.81 ± 0.11. The $CL_{CVVHDF}$ of ceftazidime is calculated from the equation: $CL_{CVVHDF}$ = Sc x Qef = fu x Qef, where: Sc is the coefficient of scaling, fu is the fraction of ceftazides not bound to plasma proteins, and Qef - the total effluent flow rate (dose of CVVHDF modality of dialysis). The average $CL_{CVVHDF}$ of ceftazidime is 33.6 ppm 4.0 mL/min (56, 57). $CL_{CVVHDF}$ in total clearance of ceftazides participates with 55%. One of the dosing regimens recommended in patients with severe infection treated with CVVHDF is ceftazidime administration in the form of an impact dose of 2.0 g IV

infusion, and then continued treatment with a continuous 3.0 g/24h IV infusion over 72h (during CVVHDF) (56, 57).

Cefepime is a fourth-generation cephalosporin, which has a wide range of effects on Gram-positive and Gram-negative bacteria. It has a small volume of distribution - Vd = 0.3 L/kg and binds in low percentage to plasma proteins (fu = 0.97). The Sieving coefficient (the coefficient of cefepime scaling is - Sc = 0.93, and the saturation coefficient - Sd = 1.03. $CL_{CVVHDF}$ of cefepime is significant and is calculated from the equation: $CL_{CVVHDF}$ = fu x Qef, where: fu is fraction of cefepime not bound to plasma proteins (fu = 0.97) and Qef - the total effluent flow rate (dialysis dose). Qef is calculated from the equation: Qef = Qd + Qs + Qnuf. In patients with AKI, in the absence of sepsis, Qef = 20-25 mL/kg, and in patients with severe sepsis, septic shock and AKI, Qef = 35 mL/kg/h (56, 57). The dose of cefepime in patients treated with CVVHDF should be IV 1.0 g/12h or IV 2.0 g/24h (56, 57) Cefepime belongs to the "time-dependent" group and the antibacterial effect is effective if T > MIC ≥ 40-50% and $AUC_{0-24}$/MIC ratio ≥ 100 (57, 58).

Piperacillin/tazobactam, Tazocin® is one of the most frequently used combinations of antibiotics for the treatment of serious infections in patients in intensive care units. They have a wide range of antibacterial effects involving Gram-positive and Gram-negative bacteria (Pseudomonas aeruginosa) (59, 60). They are applied in a standard dose of 4.5g (Piperacillin 4.0 g + Tazobactam 0.5g), in the form of an IV infusion for 20 minutes, at different dosing intervals: 4h, 6h and 8h (59, 60). It belongs to the group of "time-dependent" antibiotics, and the antibacterial effect is effective if T > MIC ≥ 100% (59, 60). Both piperacillin and tazobactam have a low molecular weight, low plasma protein binding rates and are removed during the CVVHDF session in high percentage. The extracorporeal cleansing of piperacillin/tazobactam is calculated from the equation: CLCVVHDF = Sc x Qef, where: Sc is Sieving coefficient/coefficient of scaling (Sc = fu), fu - fraction of piperacillin/tazobactam not bound to plasma proteins and Qef - flow rate of total effluent (dose of CVVHDF modality of dialysis) (59, 60). Extracorporeal clearance has a significant role in the total clearance of piperacillin/tazobactam (≥ 25% of total clearance) (59, 60).

Colistin is used to treat Gram-negative bacteria that are resistant to a large number of antibiotics - MDR (Multi Drug-Resistant): Acinetobacter baumannii and Pseudomonas aeruginosa (61-63). Colistin has a small volume of distribution - Vd = 0.3-0.4 L/kg and in high percentage is excreted in an unchanged form via kidneys (fe = 80%) (59-61). Antibacterial effect depends on the concentration of colistin in plasma (belonging to the group of "concentration-dependent" antibiotics) (61-63). It is administered intravenously in the form of an inactive colistin methanesufonate (CMS), which is designated as CBA (Colistin Base Activity) in most countries (80 mg CMS = 30 mg CBA, conversion factor is 2.7). In some countries, colistin is expressed in international units (1.000.000 IU = 30 mg CBA). These diverse descriptions have led to confusion in daily clinical work. Impact dose in the IV bolus is 10,000,000 IU (300 mg CBA); it is applied for 30 minutes, and then continues with IVapplication at a dose of 3,000,000 IU/8h (12h after the impact dose) for two weeks (conventional dosing regimen). The dosage should be adjusted to the degree of renal function (61-63). According to the EMA and FDA recommendations, dosing of colistin should provide a target mean concentration of colystin balance of 2.0 mg/L (Css = 2.0 mg/L). The AUC/MIC ratio is used to assess the antibacterial effect (61-63). In patients treated with CVVHDF, the extracorporeal clearance of colistin can be calculated from the following formula: $CL_{CRRT}$ = Qef x ER, where: Qef is the total effluent flow rate, and the ER is the extraction index. The extract index of colistin is calculated from the formula: ER = 2 x Ceff/(Cin + Cout), where: Ceff is the concentration of colistin in the effluent, Cin is the concentration of colistin before the filter, and Cout is the concentration of colistin after the filter. The coefficient of scaling for colistin is - Sc = 0.35. Extracorporeal clearance of colistin is significant and accounts for 43-59% of total colistin clearance. The concentration of colistin after the filter ≥ 70% of the colistin concentration before the filter may indicate a reduced elimination of colistin during a dialysis session (61-63). An increased risk of nephrotoxicity occurs if the concentration of colistin is in balance (after seven days of administration) > 3.0 mg/L. The nephrotoxic effect occurs as a result of the accumulation of colistin in the epithelial cells of the proximal tubule (tubulointerstition damage), within 72h after the administration of colistin (63, 64). As the consequence of the increased accumulation of colistin in the epithelial cells of the proximal tubule, the development of acute kidney damage occurs. The most common are AKI Stages 1 and 2, and less than 3% of patients require dialysis treatment (64). The main risk factors for the development of the nephrotoxic effect induced by the use of colistin are the following: age, liver disease, basal intensity of glomerular filtration, and hemoglobin concentration in blood. The blood hemoglobin concentration changes the oxygenation of the kidney tissue and increases the risk of AKI (64).

Meropenem is a carbapenem hydrophilic antibiotic used to treat severe infections caused by Gram-positive and Gram-negative bacteria, including Pseudomonas aeruginosa and Acinetobacter species (65). Meropenem has a low molecular weight, a small volume of distribution (Vd = 0.30-0.35 L/kg), low percentage of binding to plasma proteins (fu = 0.98) and is significantly removed during the course of the CVVHDF (65). It belongs to the group of "time-dependent" antibiotics, and the antibacterial effect is effective if T > MIC ≥ 40% (65). The minimum inhibitory concentration of meropenem is ≤ 2.0 mg/L (MIC ≤ 2.0 mg/L) (65). It is applied at a dose of 500-1000 mg/8-12h. When determining the dosing regimen, conditions that affect the pharmacokinetics of meropenem should be considered: hypoproteinemia, different residual diuresis, different continuous dialysis modalities, and different doses of the same CRRT modality of the dialysis. For sensitive microorganisms, in which the minimum inhibitory concentration of meropenem is MIC ≤ 2.0 mg/L, the target pharmacodynamic parameter that assesses the effectiveness of the antibacterial effect of meropenem should be T

> MIC ≥ 40%. In these patients, meropenem is administered at a dose of 500 mg/8h in the IV infusion for 30 min. However, in the case of severe infections of microorganisms that require minimal inhibitor meropenem concentration of MIC = 2.0-4.0 mg/L, T > MIC should be ≥ 100% (65). In these patients, meropenem is administered at a dose of 500 mg/8h, in the form of an extended intravenous infusion over 3h (65). Resistance to meropenem is defined as the minimum inhibitory concentration of meropenem - MIC > 4.0 mg/L (65).

Ertapenem is a carbapenem antibiotic used to treat severe infections caused by Gram-negative bacteria (65). It is associated with a high percentage of plasma proteins (85-95% in healthy volunteers, fu = 0.05-0.15), and in patients with AKI, the free medicine fraction increases to 20-40% (fu = 0.20-0.40) (66). It belongs to the group of "time-dependent" antibiotics, and the main pharmacodynamic parameter for assessing the efficacy of ertapenem is $AUC_{0-24}$/MIC ratio ($AUC_{0-24}$/MIC ≥ 40%) (66). In patients with endogenous creatinine clearance less than 30 ml/min, IV dose of ertapenem is 500 mg/24h, in patients with standard hemodialysis is also 500 mg/24h, and it is applied after a hemodialysis session, whereas in patients treated with continuous dialysis modalities (CVVHDF), ertapenem is administered at a dose of 1.0 g/24h (66).

Doripenem is a new carbapenem antibiotic with little available data for optimal dosing in patients with sepsis and AKI treated with continuous dialysis modalities (67). It belongs to the group of "time-dependent" antibiotics, and the main pharmacodynamic parameter for assessing the effectiveness of its antibacterial effect is T > MIC ≥ 40% (67). It is low in molecular weight (MW = 438.5 Da), low in percentage of plasma protein binding (PB = 10%, fu = 0.90), has an unchanged form of excretion in urine (fe = 0.70), and is significantly removed in the course of CVVHDF. The extrapolation index of doripenem is calculated from the equation: % ER = ((Ca - Cv) x 100)/Ca, where: Ca is the concentration of doripenem in the patient's blood before the filter and Cv is the concentration of doripenem in blood after the filter. $CL_{CVVHDF}$ of doripenem moderately contributes to its overall clearance (30%) (67). In patients with normal kidney function, it is administered at a dose of 500-100 mg/8h, in the form of an IV infusion over 60 minutes, and in patients treated with CVVHDF for sensitive microorganisms (MIC ≤ 4.0 mg/L), a dose of 500 mg/12h is administered (67).

Fluoroquinolones (Levofloxacin, Ciprofloxacin) are lipophilic antimicrobials, which fall into the group of "concentrations-dependent" antibiotics (target Cmax = 4-5 μg/mL) (68-70). The main pharmacodynamic parameters for assessing the effectiveness of the antibacterial effect of fluoroquinolones are Cmax/MIC ratio ≥ 10 and $AUC_{0-24}$/MIC ratio ≥ 100-125 (good ciprofloxycin dosing indicator) (68-70). Levofloxacin is applied IV at a dose of 250 mg/24h or 500 mg/48h, while ciprofloxacin is administered IV. at a dose of 400 mg/12h (i.e. infusion over 60 min) (per os 500 mg/12h). In patients with endogenous creatinine clearance less than 30 mL/min is administered IV. The dose of ciprofloxacin is 400 mg/24h (per os 500 mg/24h). If the patient is treated with intermittent standard hemodialysis, ciprofloxacin is administered at a dose of 400 mg/24h (per os 500 mg/24h), the medicine is applied after HD, and in patients treated with CVVHDF, IV infusion of administered ciprofloxacin is 400 mg/12-24h (68-70). The CVVHDF fluoroquinolone clearance is calculated from the equation: $CL_{CVVHF}$ = Sc x Quf, where: Sc is the coefficient of scaling (sieving coefficient), and Quf - the rate of the total ultrafiltrate flow. The coefficient of scaling is calculated from the equation: Sc = 2 x Cuf/(Ca + Cv), where: Cuf is the concentration of the medicine in the ultrafiltrate or effluent (Cuf = Cef), Ca is the concentration of the medicine before the filter and Cv is the concentration of the medicine after the filter. The total flow rate of the total ultrafilter is calculated from the equation Quf = Qs + Qnuf, where: Qs is the rate of flow of the solution for substitution and Qnuf is the rate of net ultrafiltration. The coefficient of scaling for levofloxacin is 0.67, and for ciprofloxacin 0.63 (0.70 ± 0.06) (68, 69). The contribution of $CL_{CVVHF}$ to total system clearance is calculated from the equation ($CL_{CVVHF}$/CLs) x 100, where CLs is the total system clearance (68, 69). With CVVHDF, fluoroquinolone clearance is calculated from the equation: $CL_{CVVHDF}$ = Sd x Qef, where: Sd is the saturation coefficient, and Qef is the flow rate of the total effluent. The coefficient of saturation is calculated from the equation: Sd = Cef/(Ca + Cv), where: Cef is the concentration of the medicine in the effluent, Ca is the concentration of the medicine before the filter and Cv is the concentration of the medicine after the filter. The flow rate of the total effluent - Qef = Qd + Qs + Qnuf, where: Qd is the dialysis flow rate, Qs is the rate of flow of the solution for substitution and Qnuf is the net ultrafiltration rate. The coefficient of saturation for levofloxacin is 0.56, and for ciprofloxacin 0.63. $CL_{CVVHDF}$ of ciprofloxacin can be calculated from the equation: $CL_{CVVHDF}$ = fu x Qef, where: fu is the fraction of ciprofloxacin not bound to the plasma protein (fu = 0.60-0.78), and Qef - flow rate of the total effluent (Qef = 35 mL/kg/h). An increase in the dose of CVVHDF (↑Qef) increases the clearance of ciprofloxacin. $CL_{CVVHDF}$ of creatinine is equivalent to the clearance of $CL_{CVVHDF}$ of ciprofloxacin. In the situations of inability to measure ciprofloxacin plasma concentrations, $CL_{CVVHDF}$ creatinine should be determined. The contribution of $CL_{CVVHDF}$ to the total system clearance is calculated from the equation ($CL_{CVVHDF}$/CLs) x 100, where CLs is the total system clearance. $CL_{CVVHDF}$ of fluoroquinolones contributes to 40% of the total system clearance. The results of the studies showed that the optimal IV dose of levofloxacin in patients treated with CRRT/CVVHDF is 250mg/24h, and for ciprofloxacin 400 mg/24h (68, 69). In patients with severe sepsis, septic shock and AKI treated with CVVHDF, with a filter containing AN69 membrane and a dialysis dose of Qef = 35 mL/kg/h, to achieve pharmacokinetic and pharmacodynamic goals (Cmax/MIC ≥ 10, $AUC_{0-24}$/MIC ≥ 100 for MIC ≤0.50 mg/L) a dose of 400 mg/12h of ciprofloxacin is required, and in patients with concomitant liver insufficiency it is 400 mg/24h (in order to optimize and individualize ciprofloxacin, the function of the liver should also be evaluated) (69, 70).

## ACKNOWLEDGMENTS

The authors would like to thank the Ministry of Education, Science and Technological Development of the Republic of Serbia for the project N$^0$175014, whose funds were used as one of the sources for the financial support of this scientific paper.

## CONFLICT OF INTEREST

The authors declare no financial or commercial conflict of interest.

## REFERENCES

1. Singbartl K, Kellum JA. AKI in the ICU: definition, epidemiology, risk stratification, and outcomes. Kidney Int 2012; 81(9): 819-25.
2. Ostermann M, Joannidis M. Acute Kidney Injury 2016: diagnosis and diagnostics workup. Crit Care 2016; 20(1): 299-312.
3. Singer M, Deutschman CS, Seymour CW, Shankar-Hari M, Annane D, Bauer M, et al. The Third International Consensus Definitions for Sepsis and Septic Shock (Sepsis-3). JAMA 2016; 315(8): 801-10.
4. Angus DC, Van der Pol T. Severe Sepsis and Septic Shock. N Engl J Med 2013; 369(9): 840-51.
5. Martensson J, Bellomo R. Sepsis-Induced Acute Kidney Injury. Crit Care Clin 2015; 31(4): 649-660.
6. Swaminathan S, Rosner MH, Okusa MD. Emerging Therapeutic Targets of Sepsis-Associated Acute Kidney Injury. Semin Nephrol 2015; 35(1): 38-54.
7. Rizo-Topete L, Ronco C. Critical Care Nephrology: A Multidisciplinary Approach. Blood Purif 2017; 43: 53-6.
8. Petrović D, Mijailović Ž, Popovska B, Miloradović V, Đurđević P. Sepsis and cardiorenal syndrome: etiopathogenesis, diagnosis and treatment. Ser J Exp Clin Res 2013; 14(4): 181-7.
9. Hamzagić N, Nikolić T, Popovska Jovičić B, Čanović P, Jaćović S, Petrović D. Acute kidney damage: definition, classification and optimal time of hemodialysis. Ser J Exp Clin Res 2017; DOI: 10.1515/sjecr-2017-0050.
10. Fissell WH. Antimicrobial Dosing in Acute Renal Replacement Therapy. Adv Chronic Kidney Dis 2013; 20(1): 85-93.
11. Shaw AR, Mueller BA. Antibiotic Dosing in Continuous Renal Replacement Therapy. Adv Chronic Kidney Dis 2017; 24(4): 219-27.
12. Udy AA, Roberts JA, Boots RJ, Paterson DL, Lipman J. Augmented Renal Clearance: Implications for Antibacterial Dosing in the Critically ill. Clin Pharmacokinet 2010; 49(1): 1-16.
13. Udy AA, Roberts JA, Shorr AF, Boots RJ, Lipman J. Augmented renal clearance in septic and traumatized patients with normal plasma creatinine concentrations: identifying at-risk patients. Crit Care 2013; 17: R35.
14. Hobbs AL, Shea KM, Roberts KM, Daley MJ. Implications of Augmented Renal Clearance on Drug Dosing Critically Ill Patients: A Focus on Antibiotics. Pharmacotherapy 2015; 35(11): 1063-75.
15. Mahmoud SH, Shen C. Augmented Renal Clearance in Critical Illness: An Important Consideration in Drug Dosing. Pharmaceutics 2017; 9(3): 36-63.
16. KDIGO Clinical Practice Guideline for Acute Kidney Injury. AKI Dewfinition. Kidney Int Suppl 2012; 2(1): 19-36.
17. Zarbock A, Gomez H, Kellum JA. Sepsis-induced AKI revisited: pathophysiology, prevention and future therapies. Curr Opin Crit Care 2014; 20(6): 588-95.
18. Gomez H, Ince C, Backer DD, Pickkers P, Payen D, Hotchkiss J, Kellum JA. A Unified Theory of Sepsis-Induced Acute Kidney Injury: Inflammation, microcirculation dysfunction, bioenergetics and the tubular cell adaptation to injury. Shock 2014; 41(1): 3-11.
19. Doi K. Role of kidney injury in sepsis. J Intensive Care 2016; 4: 17. DOI: 10.1186/s40560-016-0146-3.
20. Kellum JA, Chawla LS. Cell-cycle arrest and acute kideny injury: the light and the dark side. Nephrol Dial Transplant 2016; 31(1): 16-22.
21. Lameire N, Vanmassenhove, Van Biesen W, Vanholder R. The cell cycle biomarkers: promising research, but do not oversell them. Clin Kidney J 2016; 9(3): 353-8.
22. Palevsky PM. Renal Replacement Therapy in Acute Kidney Injury. Adv Chronic Kidney Dis 2013; 20(1): 76-84.
23. Heung M, Yessayan L. Renal Replacement Therapy in Acute Kidney Injury: Controversies and Consensus. Crit Care Clin 2017; 33(2): 365-78.
24. Bagshaw SM, Cruz DN, Gibney RTN, Ronco C. A proposed algorithm for initiation of renal replacement therapy in adult critically ill patients. Crit Care 2009; 13(6): 317-25
25. Wald R, Bagshaw SM. The Timing of Renal Replacement Therapy Initiation in Acute Kidney Injury. Semin Nephrol 2016; 36(1): 78-84.
26. Shiao CC, Huang TM, Spapen HD, Honore PM, Wu VC. Optimal timing of renal replacement therapy initiation in acute kidney injury: the elephant felt by the blidmen? Crit Care 2017; 21: 146. DOI: 10.1186/s13054-017-1713-2.
27. Bagshaw SM, Wald R. Strategies for the optimal timing to start renal replacement therapy in critically ill patients with acute kidney injury. Kidney Int 2017; 91(2): 1022-32.
28. Murugan R, Hoste E, Mehta RL, Samoni S, Ding X, Rosner MH, Kellum JA, Ronco C on behalf of the Acute Disease Quality Initiative (ADOQI) Consensus Group. Precision Fluid Management in Continuous Renal Replacement Therapy. Blod Purif 2016; 42(3): 266-78.
29. Macedo E, Mehta RL. Continous Dialysis Therapies: Cor Curriculum 2016. Am J Kidney Dis 2016; 68(4): 645-57.
30. Rimmele T, Kellum JA. Clinical review: Blood purification for sepsis. Crit Care 2011; 15(1): 205. DOI: 10.1186/cc9411.
31. Oda S, Aibiki M, Ikeda T, Imaizumi H, Endo S, Ochai R, Kotani J, Shime N, Nishida O, Noguchi T, Matsuda N,

Hirasawa H and Sepsis Registry Committee of The Japanese Society of Intensive Care Medicine. The Japanese guidelines for the management of sepsis. J Intesive Care 2014; 2: 55. DOI: 10.1186/s40560-014-0055-2.
32. Hattori N, Oda S. Cytokine-adsorbing hemofilter: old but new modality for septic acute kidney injury. Renal Replacement Therapy 2016; 2: 41. (DOI: 10.1186/s41100-016-0051-1.
33. Tanaka A, Inaguma D, Nakamura T, Watanabe T, Ito E, Kamegai N, et al. Effect of continuous hemodiafiltration using an AN69ST membrane in patients with sepsis. Renal Replacement Therapy 2017; 3: 12. (DOI: 10.1186/s41100-017-0093z).
34. Baldwin I, Fealy N. Clinical Nursing for the Application of Continuous Renal Replacement Therapy in the Intensive Care Unit. Semin Dial 2009; 22(2): 189-93.
35. Bagshaw SM, Chakravarthi MR, Ricci Z, Tolwani A, Neri M, De Rosa S, Kellum JA, Ronco C, on behalf of the ADQI Consensus Group. Precision Continuous Renal Replacement Therapy and Solute Control. Blood Purif 2016; 42(3): 238-47.
36. Nolin TD, Aronoff GR, Fissel WH, Jain L, Madabushi R, Reynolds K, et al. Pharmacokinetic Assessment in Patients Receiving Continuous RRT: Perspectives from the Kidney Health Initiative. Clin J Am Soc Nephrol 2015; 10(1): 159-64.
37. Böhler J, Donauer J, Keller F. Pharmacokinetic principles during continuous renal replacement therapy: Drugs and dosage. Kidne Int 1999; 56(Suppl 72): 24-8.
38. Churchwell MD, Mueller BA. Drug Dosing During Continuous Renal Replacement Therapy. Semin Dial 2009; 22(2): 185-8.
39. Lewis SJ, Mueller BA. Antibiotics Dosing in Patients With Acute Kidney Injury: "Enough But Not Too Much". J Intensive Care Med 2016; 31(3): 164-76.
40. Choi G, Gomersall CD, Tian Q, Joynt GM, Li AMMY, Lipman J. Principles of Antibacterial Dosing in Continuous Renal Replacement Therapy. Blood Purif 2010; 30(3): 195-212.
41. Bugge JF. Pharmacokinetics and drug dosing adjustment during continuous venovenous hemofiltration or hemodiafiltration in critically patients. Acta Anaesthesiol Scand 2001; 45(8): 929-34.
42. Blot SI, Pea F, Lipman J. The effect of pathophysiology on pharmacokinetics in the critically ill patient-Concepts appraised by the example of antimicrobial agents. Adv Drug Del Rev 2014; 77(1): 3-11.
43. Honore PM, Jacobs R, De Waele E, Spapen HD. Applyng pharmacokinetic /pharmacodynamic principles for optimizing antimicrobial therapy during continuous renal replacement therapy. Anaestesiol Intensive Therapy 2017; 49(5): 412-8.
44. Taccone FS, De Backer D, Laterre PF, Spapen H, Dugernier T, Delattre I, et al. Pharmacokinetics of loading dose of amikacin in septic patients undergoing continuous renal replacement therapy. Int J Antimicrob Agents 2011; 37(6): 531-5.
45. Roger C, Wallis SC, Muller L, Saissi G, Lipman J, Lefrant JY, Roberts JA. Influence of Renal Replacement Modalities on Amikacin Population Pharmacokinetics in Critically Ill Patients on Continuous Renal Replacement Therapy. Antimicrob Agents Chemother 2016; 60(8): 4901-9.
46. De Winter S, Wauters J, Meersseman W, Verhaegen J, Wijngaerden EV, Peetermans W, et al. Higher versus standard amikacin single dose in emergency departemnt patients with severe sepsis and septic shock: a randomised controlled trial. Int J Antimicrob Agents 2018; 51(4): 562-70.
47. D'Avolio A, Pensi D, Baietto L, Pacini G, Di Perri G, De Rosa FG. Daptomycin Pharmacokinetics and Pharmacodynamics in Septic and Critically Ill Patients. Drugs 2016; 76(12): 1161-74.
48. Soraluce A, Asin-Prieto E, Rodriquet-Gascon A, Barrasa H, Mayner J, Carcelero E, et al. Population pharmacokinetics of daptomycin in critically ill patients. Int J Antimicrob Agents 2018; 52(2): 158-65.
49. Villa G, Di Maggio P, De Gaudio AR, Novelli A, Antoniotti R, Ficcadori E, Adembri C. Effects of continuous renal replacement therapy on linezolid pharmacokinetic /phamacodynamics: a systematic review. Crit Care 2016; 20(1): 374.
50. Taubert M, Zander J, Frechen S, Scharf C, Frey L, Vogeser M, Fuhr U, Zoller M. Optimization of linezolid therapy in the critically ill: the effect of adjusted infusion regimens. J Antimicrob Chemother 2017; 72(8): 2304-10.
51. Beumier M, Roberts JA, Kabtouri H, Hites M, Cotton F, Wolf F, et al. A new regimen for continuous infusion of vancomycin during continuous renal replacement therapy. J Antimicrob Chemother 2013; 68(12): 2859-65.
52. Roberts JA, Taccone FS, Udy AA, Vincent JL, Jacobs F, Lipman J. Vancomycin Dosing in Critically Ill Patients: Robust Methods for Improved Continuous-Infusion Regimens. Antimicrob Agents Chemother 2011; 55(6): 2704-9.
53. Vandecasteele SJ, Vriese ASD, Tacconelli E. The pharmacokinetics and pharmacodynamics of vancomycin in clinical practice: evidence and uncerainies. J Antimicrob Chemother 2013; 68(4): 743-48.
54. Filippone EJ, Kraft WK, Farber JL. The Nephrotoxicity of Vancomycin. Clin Pharm Ther 2017; 102(3): 459-469.
55. Beumier M, Casu GS, Hites M, Seyler L, Cotton F, Vincent JL, et al. β-lactam antibiotic concentrations during continuous rena replacement therapy. Crit Care 2014; 18: R105.
56. Mariat C, Venet C, Jehl F, Mwewa S, Lazarevic V, Diconne E, et al. Continuous infusion of ceftazidime in critically ill patients undergoing continuous venovenous haemodiafiltration: pharmacokinetic evaluation and dose recommendation. Crit Care 2016; 10(1): R26.
57. Isla A, Gascon AR, Maynar J, Pedraz JL. Cefepime and continuous renal replacement therapy (CRRT): In vitro pemeability of two CRRT membranes and pharmacokinetics in four critically patients. Clin Ther 2005; 27(5): 599-608.
58. Malone RS, Fish DN, Abraham E, Teitelbaum I. Pharmacokinetics of Cefepime during Continuous Renal

Replacement Therapy in Critically Ill Patients. Antimicrob Agents Chemotherapy 2001; 45(11): 3148-55.
59. Roger C, Cotta MO, Muller L, Wallis SC, Lipman J, Lefrant JY, Roberts JA. Impact of renal replacement modalities on the clearance of pipracillin-tazobactam administered via continuous infusion in critically ill patients. Int J Antimicrob Agents 2017; 50(2): 227-31.
60. Asin-Prieto E, Rodriguez-Gascon A, Troconiz I, Soraluce A, Maynar J, Sanchez-Izquierdo JA, et al.Population pharmacokinetics of piperacillin and tazobactam in critically ill patients undergoing continuous renal replacement therapy: application to pharmacokinetic/pharmacodynamic analysis. J Antimicrob Chemother 2014; 69(1): 180-9.
61. Menna P, Salvatorelli E, Mattei A, Cappiello D, Minotti G, Carassiti M. Modified Colistin Regimen for Critically ill Patients with Acute Renal Impairment and Continuous Renal Replacement Therapy. Chemotherapy 2018; 63(1): 35-8.
62. Markou N, Fousteri M, Markantonis SL, Zidianakis B, Hroni D, Boutzouka E, Baltopoulos G. Colistin pharmacokinetics in intensive care units patients on continuous venovenous haemodiafiltration: an observational study. J Antimicrob Chemother 2012; 67(10): 2459-62.
63. Fiaccadori E, Antonucci E, Morabito S, dAvolio A, Maggiore U, Regolisti G. Colistin Use in Patients With Reduced Kidney Function. Am J Kidney Dis 2016; 68(2): 196-306.
64. Miano TA, Lautenbach E, Wilson FP, Guo W, Borovskiy Y, Hennessy. Attributable Risk and Time Course of Colistin-Associated Acute Kidney Injury. Clin J Am Soc Nephrol 2018; 13(4): 542-50.
65. Ulldemolnis M, Soy D, Liaurado-Serra M, Vaquer S, Castro P, Rodriquez AH, et al. Meropenem Population Pharmacokinetics in Critically Ill Patients with Septic Shock and Continuous Renal Replacement Therapy: Influence of Residual Diuresis on Dose Requirements. Antimicrobial Agenst Chemother 2015; 59(9): 5520-8.
66. Eyler RF, Vilay AM, Nader AM, Heung M, Pleva M, Sowinski KM, et al. Pharmacokinetics of Ertapenem in Critically Ill Patients Receiving Continuous Venovenous Hemodialysis or Hemodiafiltration. Antimicrob Agents Chemother 2014; 58(3): 1320-6.
67. Roberts JA, Udy AA, Bulitta JB, Stuart J, Jarrett P, Starr T, et al. Doripenem population pharmacokinetics and dosing requirements for critically ill patients receiving continuous venovenous haemodiafiltration. J Antimicrob Chemother 2014; 69(9): 2508-16.
68. Malone RS, Fish DN, Abraham E, Teitelbaum I. Pharmacokinetics of Levofloxacin and Ciprofloxacin during Continuous Renal Replacement Therapy in Critically Ill Patients. Antimicrob Agents Chemother 2001; 45(10): 2949-54.
69. Wallis S, Mullany D, Lipman J, Rickard C. Pharmacokinetics of ciprofloxacin in ICU patients on continuous veno-venous haemodiafiltration. Int Care Med 2001; 27(4): 665-72.
70. Spooner AM, Deegan C, Darcy DM, Gowing CM, Donnelly MB, Corrigan OI. An evaluation of ciprofloxacin pharmacokinetics in critically ill patients undergoing continuous veno-venous haemodiafiltration. BMC Clinical Pharmacol 2011; 11(1): 11-20.

# THE ACUTE EFFECTS OF DIFFERENT SPIRONOLACTONE DOSES ON OXIDATIVE STRESS IN STREPTOZOTOCIN-INDUCED DIABETIC RATS

Stefan Simovic[1,2], Aleksandra Vranic[3], Petar Ristic[4], Jovana Jeremic[3], Ivan Srejovic[5], Jasna Petrovic[6], Vladimir Jakovljevic[5,7], Stefani Bolevich[8], Sergey Bolevich[7] and Vladimir Zivkovic[5]

[1]*University of Kragujevac, Faculty of Medical Sciences, Department of Internal Medicine, Serbia*
[2]*Clinic for Cardiology, Clinical Center Kragujevac, Serbia*
[3]*University of Kragujevac, Faculty of Medical Sciences, Department of Pharmacy, Serbia*
[4]*Clinic of Endocrinology, Military Medical Academy, Belgrade, Serbia*
[5]*University of Kragujevac, Faculty of Medical Sciences, Department of Physiology, Serbia*
[6] *General Hospital "Valjevo", Valjevo, Serbia*
[6]*Department of Human Pathology, 1st Moscow State Medical University IM Sechenov, Moscow, Russia*
[7]*Department of Pathophysiology, 1st Moscow State Medical University IM Sechenov, Moscow, Russia*

Received: 16.03.2021.
Accepted: 22.03.2021.

**Corresponding author:**

**Stefan Simovic, MD**

University of Kragujevac, Faculty of Medical Sciences, Department of Internal Medicine, Serbia

E-mail: dejan.petrovic@fmn.kg.ac.rs

## ABSTRACT

*Cardiovascular diseases are the leading cause of morbidity and mortality in patients with diabetes mellitus. Increased bioavailability of reactive oxygen species is defined as oxidative stress and is noticed in type 2 DM and reduced antioxidant enzymes expression/activity. Aldosterone, an adrenal hormone, is secreted due to renin-angiotensin-aldosterone system activation, representing one of the fundamental physiological reactions in CVD. Spironolactone, a mineralocorticoid receptor antagonist, uses enhanced coronary microvascular function, suggesting a beneficial role of aldosterone in preventing diabetic cardiovascular complications in patients with type 2 DM. In this study, we evaluated the influence of spironolactone's acute administration on oxidative stress in rats with diabetes mellitus induced by streptozotocin. The present study was carried out on 40 adult male Wistar albino rats (8 weeks old). Rats were randomly divided into 4 groups (10 animals per group): healthy rats treated with 0.1 μM of spironolactone, diabetic rats treated with 0.1 μM of spironolactone, healthy rats treated with 3 μM of spironolactone, and diabetic rats treated with 3 μM of spironolactone. Spironolactone achieved different effects on oxidative stress parameters when given acutely in different doses in diabetic and healthy rats. In lower doses, spironolactone's acute administration reached lowered parameters of oxidative stress in healthy rats better than higher doses of spironolactone. In contrast, in the diabetic group, acute effects of higher doses of spironolactone lowered oxidative stress parameters better than lower spironolactone doses.*

***Keywords***: *Spironolactone, diabetes mellitus, oxidative stress, rats.*

sciendo

UDK: 616.127-008:616.379-008.64-056.24
Ser J Exp Clin Res 2024; 25(2):103-111
DOI: 10.2478/sjecr-2021-0025

## INTRODUCTION

Cardiovascular diseases (CVD) are the leading cause of morbidity and mortality in patients with diabetes mellitus (DM). Currently, DM type 2 affects 347 million worldwide (1), while the risk of mortality is 1.7 times higher in patients with diabetes mellitus than in the non-diabetic population (2). Inflammation, neurohumoral activation and structural remodelling are multiple mechanisms that contribute to cardiovascular disease, whereby one of the primary means contributing to CVD development is oxidative stress (3).

Increased bioavailability of reactive oxygen species (ROS) is defined as oxidative stress and is noticed in type 2 DM and reduced antioxidant enzymes expression/activity (3). One of the many mechanisms correlated with vascular damage induced by oxidative stress is decreased nitric oxide (NO) bioavailability. NO effects are impaired by increased ROS production whereby increased generation of superoxide anion (O2-), a ROS that readily reacts with vascular NO to form peroxynitrite (ONOO−), has been reported in DM2 experimental models (4).

Aldosterone, an adrenal hormone, is secreted due to renin-angiotensin-aldosterone system (RAAS) activation, representing one of the fundamental physiological reactions in CVD (5). The discovery that the concentrations of myocardial aldosterone in typical rodents are multiple times higher than plasma prompted an extraordinary comprehension of the role of mineralocorticoid receptor activation in the CVD (6).

Spironolactone, a mineralocorticoid receptor antagonist, produces positive ionotropic actions in rat heart by increasing diastolic concentration of calcium and myosin ATPase calcium sensitivity (7). This medication utilizes coronary microvascular function, proposing a beneficial role of aldosterone in preventing diabetic cardiovascular complications in patients with type 2 DM (8). Our previous finding suggests that acute application of different spironolactone doses has other effects on healthy and diabetic hearts; In contrast, the dose-dependent effect is observed in diabetic hearts. That effect is absent in healthy ones (9). Based on the above data, aldosterone affects redox status in multiple ways, whereby cardiac-specific overexpression of human MR leads to increased ROS production and expression of NADPH oxidase (10). MR blockade with spironolactone treatment in rat led to decreased ROS formation and NADPH oxidase subunit expression (10).

Regarding pro-oxidative and pro-inflammatory effects of aldosterone in the cardiovascular system (11), and considering that aldosterone concentration increases in DM (12), our study aimed to evaluate the impact of different spironolactone dosages on oxidative stress in streptozotocin-induced DM diabetic rats.

## MATERIALS AND METHODS

### Animals and experimental design

The present investigation was done on 40 grown-up male Wistar albino rats (8 weeks old and boy weight of 200 ± 30g). They were housed under controlled natural conditions: temperature 25°C with a built-up photo time of 12 h light/day. The rats had free access to food and water - ad libitum. Rats were randomly randomized into 4 groups (10 animals for each group): (1) healthy rats treated with 0.1 μM of spironolactone (n=10); (2) diabetic rats treated with 0.1 μM of spironolactone (n=10); (3) healthy rats treated with 3 μM of spironolactone (n=10); (4) diabetic rats treated with 3 μM of spironolactone (n=10). Acute administration of spironolactone was achieved through the Langedorff apparatus directly in the isolated heart.

### Ethical approval

All experimental procedures were done per current legislation (EU Directive for the Protection of Vertebrate Animals used for Experimental and other Scientific Purposes 86/609/EES) and ethics standards. Animals were cared as per the Guide for the Care and Use of Laboratory Animals (National Research Council 1996). The study was conducted under the Basic & Clinical Pharmacology & Toxicology policy for experimental and clinical studies (13). The investigation protocol was approved by the Ethics committee for experimental animal well being of the Faculty of Medical Sciences of the University of Kragujevac.

### Diabetic rat model

Before DM induction, 2 weeks of adjustment was given. To build up a rat model of experimentally induced type 1 DM, which imitates similar pathophysiology in the human population, over-night fasting rats were infused with a single intraperitoneal portion of streptozocin (STZ) (60 mg/kg) (Sigma-Aldrich, St. Louis, Missouri, USA) dissolved down in cold, fresh 0.01 mol/L citrate buffer of fresh or solidified 1mL aliquots at 20 °C (0.1 mol/L citric acid, 0.1 mol/L sodium citrate), pH 4.5. DM was confirmed 72h later when blood glucose levels were above 11.1 mmol/L. Animals that developed DM were held in similar conditions and followed for the next 4 weeks.

### Isolated rat heart preparation

On the 29th day after inducement of type 1 DM, rats were anaesthetized with ketamine (10 mg/kg) and xylazine (5 mg/kg) and afterwards euthanized by cervical disengagement (Schedule 1 of the Animals/Scientific Procedures, Act 1986, UK). Following a fast thoracotomy and quick cardiac arrest by superfusion with super cold isotonic saline, the hearts were speedily extracted and attached to the Langendorff apparatus (Langendorff apparatus, Experimentia LTD, 1062 Budapest, Hungary) through aortic cannulation and afterwards were perfused with Krebs-Henseleit solution for retrograde perfusion under continuously expanding coronary

perfusion pressure (CPP) (CPP from 40 $cmH_2O$ to 120 $cmH_2O$). Krebs-Henseleit solution was utilized for retrograde perfusion (in mmol/L: NaCl 118, KCl 4.7, $CaCl_2$, x 2 $H_2O$ 2.5, $MgSO_4$ x 7 $H_2O$ 1.7, $NaHCO_3$ 25, $KH_2PO_4$ 1.2, glucose 11 and pyruvate 2). The buffer was balanced with 95% $O_2$ and 5% $CO_2$, with a pH estimation of 7.4 and a temperature of 37 °C.

After the heart perfusion foundation, the arrangements were balanced within 30 min with a basal CPP of 70 $cmH_2O$. Following the adjustment period, the perfusion pressure was diminished to 50 and 40 $cmH_2O$, and afterwards, step by step expanded to 60, 80, 100, and 120 $cmH_2O$ to set up coronary autoregulation. Testing began following the control test to keep away from undesirable time-dependent consequences. The spironolactone application (0.1 and 3 _mol/L) went on until accomplishing a steady stream, yet not under 5 min for each estimation of perfusion pressure. After the sensor (transducer BS4 73-0184, Experimetria Ltd., Budapest, Hungary) placing into the left ventricle, the accompanying cardiodynamic parameters were ceaselessly enlisted: the maximum and minimum rate of pressure development in the left ventricle (dp/dtmax, dp/dtmin), systolic and diastolic left ventricle pressure (SLVP, DLVP), pulse (HR), and coronary flow (CF) on every one of foreordained estimations of perfusion pressure (40, 60, 80, 100, and 120 $cmH_2O$). CF was estimated by flowmetry. Every heart was its control.

**Biochemical analysis**

Markers of oxidative stress were estimated spectrophotometrically in the gathered examples of coronary venous effluent. Samples were collected after adjustment of the coronary flow and after medication administration for every perfusion pressure. We performed quantification of nitrites (the measure of NO discharged), superoxide anion radical ($O_2^-$), and hydrogen peroxide ($H_2O_2$) and indirect quantification of the index of lipid peroxidation using receptive thiobarbituric substances (TBARS), for all examples.

**Determination of hydrogen peroxide ($H_2O_2$)**

Estimation of hydrogen peroxide depended on the oxidation of phenol red by hydrogen peroxide in a response catalyzed by horseradish peroxidase (HRPO) (14). A sum of 200 µl of perfusate was accelerated with 800 ml of freshly arranged phenol red solution, followed by the addition of 10 µl of (1:20) HRPO (made ex-tempore). A sufficient volume of distilled water was utilized as a blank test (rather than coronary venous gushing). The level of $H_2O_2$ was measured at 610 nm.

**Determination of nitrites ($NO_2^-$)**

Nitric oxide decays quickly to frame stable metabolite nitrite/nitrate products. Nitrites can, in this manner, be utilized as an index of NO generation using a spectrophotometric strategy utilizing the Griess reagent. Nitrites ($NO_2^-$) were determined as an index of NO creation with Griess reagent (forms purple diazocomplex) (15). Briefly, 0.5 ml of the perfusate was accelerated with 200 µl of 30% sulfosalicylic acid, vortexed for 30 min and centrifuged at 3000 x g. Equal volumes of the supernatant and Griess reagent containing 1 % sulphanilamide in 5 % phosphoric acid/0.1 % naphthalene ethylenediamine-dihydrochloride was added and balanced out for 10 min in the dark and estimated spectrophotometrically at 550 nm. Distilled water was utilized as a clear test.

**Determination of superoxide anion radicals ($O_2^-$)**

Superoxide anion radical concentrations were estimated utilizing the NTB (Nitro Blue Tetrazolium) reagent in TRIS buffer (assay mixture) with coronary venous effluent. The estimation was performed at a wavelength of 550 nm. Distilled water was utilized as a blank test (16).

**Determination of the index of lipid peroxidation measured as TBARS**

The lipid peroxidation list was determined indirectly by estimating the results of the response with thiobarbituric acid (TBARS or Thiobarbituric Acid Reactive Substances). Briefly, 1% thiobarbituric acid (TBA) in 0.05 M NaOH was incubated with coronary venous effluent at 100˚C for 15 min and afterwards, spectrophotometrically estimated at a wavelength of 530 nm. Distilled water was utilized as a blank test (17).

**Drugs**

STZ and spironolactone were purchased from Sigma-Aldrich Chemie GmbH Eschenstr. 5, 82024 Taufkirchen, Germany.

**Statistics**

Statistical investigation of experimental information incorporated the following essential descriptive statistics: the mean value (X) ± standard deviation (SD). Results and variables from healthy and diabetic rat hearts perfused with various spironolactone dosages (0.1 or 3 µM/L) were compared with every parameter at each CPP. The following factual tests were utilized to test the measurable statistical significance of the outcomes and to affirm the speculation: Independent T-test. A database analysis of the results was performed using programming software SPSS 18th (SPSS Inc., Chicago, IL, USA). P values lower than 0.05 ($p<0.05$) were considered to be significant, while p values lower than 0.01 ($p<0.01$) were viewed as highly significant.

## RESULTS

### Hydrogen peroxide ($H_2O_2$)

After spironolactone application in the dose of 0.1μM, the hydrogen peroxide levels did not significantly differ in healthy and diabetic rats (Fig 1a). However, after perfusion with 3μM of spironolactone, levels of hydrogen peroxide significantly decreased in diabetic rats when compared to healthy rats at all CPPs, with higher significance at 80 - 120 cm$H_2O$ ($p<0.01$) (Fig 2a). When we compared levels of $H_2O_2$ between healthy rats treated with 0.1μM and 3μM of spironolactone, no significant differences were noted at any CPP (Fig 3a). Significantly lower levels of $H_2O_2$ were noticed in diabetic rats treated with 3μM at 80, 100 and 120 cm $H_2O$ compared to diabetic rats treated with 0.1μM of spironolactone (Fig 4a). The most significant increase in the level of $H_2O_2$ was achieved with 0.1μM of spironolactone at CPP of 40 cm $H_2O$ compared to control, while 3μM lowered the level of $H_2O_2$ the most in diabetic rats at CPP of 120 cm $H_2O$ (Table 1.)

### Nitrites ($NO_2^-$)

NO activity was measured as nitrite. Its level was significantly higher in diabetic rats perfused with 0.1 μM of spironolactone than healthy rats perfused with the same dose of spironolactone at CPPs at 100 and 120 cm $H_2O$ ($p<0.05$). Simultaneously, the level of nitrites did not significantly differ at lower CPPs (Fig 1b). When diabetic and healthy hearts were perfused with 3μM of spironolactone, levels of nitrites were markedly higher in healthy hearts only at CPP at 120 cm $H_2O$ ($p<0.05$), while at lower CPPs, no significant differences were observed, but there is a noticeable trend in the rise of the level of nitrites in healthy hearts (Fig 2b). The same evident trend was also observed when we compared levels of nitrites between healthy rats treated with 0.1μM and 3μM of spironolactone, with significantly higher levels of nitrites in healthy rats treated with 3μM of spironolactone when compared to healthy rats treated with 0.1μM of spironolactone (Fig 3b). In contrast, when we compared the level of nitrites in diabetic rats treated with 0.1μM and 3μM of spironolactone, there were no significant differences in nitrites' levels (Fig 4b). The dose of 0.1μM of spironolactone increased the level of $NO_2^-$ the most in healthy rats compared to healthy control at CPP 40 cm $H_2O$, while the most significant decrease in the level of $NO_2^-$ was observed between the same rats at CPP 120 cm $H_2O$ (Table 1.).

### Superoxide anion radical ($O_2^-$)

In diabetic rats perfused with 0.1 μM of spironolactone compared with healthy rats perfused with the same dose of spironolactone level of $O_2^-$ was significantly increased at 80 - 120 cm $H_2O$ ($p<0.01$) (Fig 1c), but when both groups were perfused with 3μM of spironolactone, levels of $O_2^-$ were significantly higher in healthy rats at 40, 60 and 120 cm $H_2O$ ($p<0.05$) (Fig 2c). Level of $O_2^-$ did not significantly differ between healthy rats treated with 0.1μM and 3μM of spironolactone (Fig 3c). However, a significantly higher level of $O_2^-$ was observed in diabetic rats treated with 0.1μM of spironolactone compared to diabetic rats treated with 3μM od spironolactone at 60, 80, 100 and 120 cm $H_2O$ (Fig 4c). Spironolactone in the dose of 0.1μM increased the level of $O_2^-$ for 67.14% in diabetic rats when compared with diabetic control at CPP 120 cm $H_2O$, while the same quantity of spironolactone decreased the level of $O_2^-$ for 53.58% in healthy rats when compared to healthy control at CPP 60 cm $H_2O$ (Table 1.).

### Index of lipid peroxidation (measured as TBARS)

After spironolactone application in the dose of 0.1μM, the levels of TBARS did not significantly differ in healthy and diabetic rats (Fig 1d). After perfusion with 3μM of spironolactone in diabetic rats, significantly lower levels of TBARS was observed at 80 - 120 cm $H_2O$ (Fig 2d). When we compared the level of TBARS between healthy rats treated with 0.1μM and 3μM of spironolactone, in the group treated with 3μM of spironolactone, we noticed significant higher values compared to the group treated with 0.1μM of spironolactone at 80 - 120 cm $H_2O$ (Fig 3d). Significantly lower levels of TBARS were observed in diabetic rats treated with 3μM of spironolactone when we compared them to diabetic rats treated with 0.1μM of spironolactone (Fig 4d). Levels of TBARS increased the most when 3μM of spironolactone was applied to healthy rats at CPP of 120 cm $H_2O$ compared to healthy control. In contrast, spironolactone in the same dose lowered TBARS the most in diabetic rats at CPP 80 cm $H_2O$ (Table 1.).

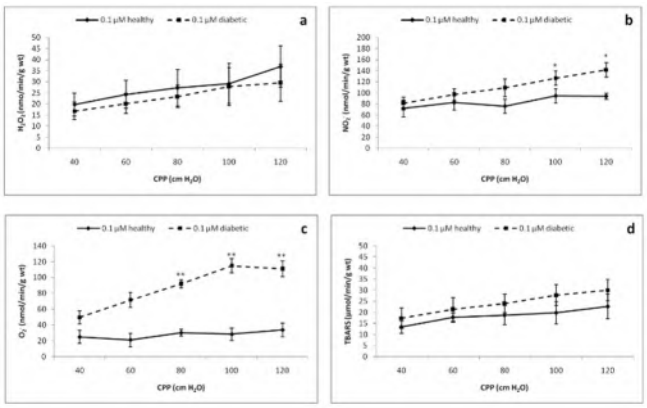


**Figure 1.** Parameters of oxidative stress in healthy rats perfused with 0.1 μM of spironolactone compared with diabetic rats perfused with 0.1 μM of spironolactone.
(a) Hydrogen peroxide (H2O2) (b) Nitrites (NO2-)
(c) Superoxide anion radical (O2-) (d) Index of lipid peroxidation (measured as TBARS). Data is presented as mean ± SD. CPP, coronary perfusion pressure.

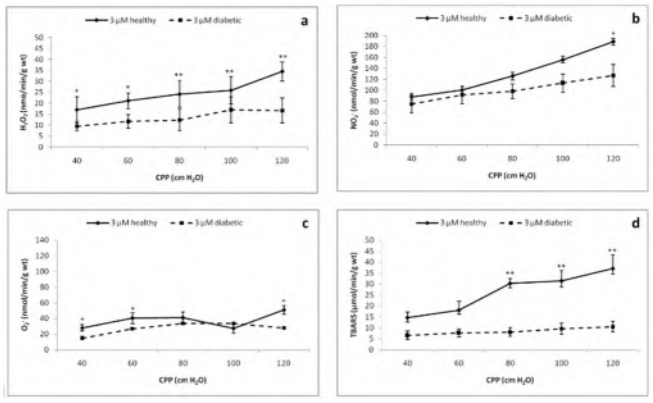

**Figure 2.** Parameters of oxidative stress in healthy rats perfused with 3 µM of spironolactone compared with diabetic rats perfused with 3 µM of spironolactone. (a) Hydrogen peroxide (H2O2) (b) Nitrites (NO2-) (c) Superoxide anion radical (O2-) (d) Index of lipid peroxidation (measured as TBARS). Data is presented as mean ± SD. CPP, coronary perfusion pressure.

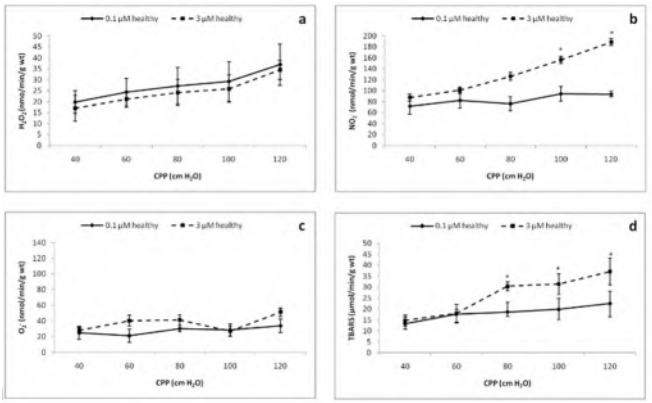

**Figure 3.** Parameters of oxidative stress in healthy rats perfused with 0.1 µM of spironolactone compared with healthy rats perfused with 3 µM of spironolactone. (a) Hydrogen peroxide ($H_2O_2$) (b) Nitrites ($NO_2^-$) (c) Superoxide anion radical ($O_2^-$) (d) Index of lipid peroxidation (measured as TBARS). Data is presented as mean ± SD. CPP, coronary perfusion pressure.

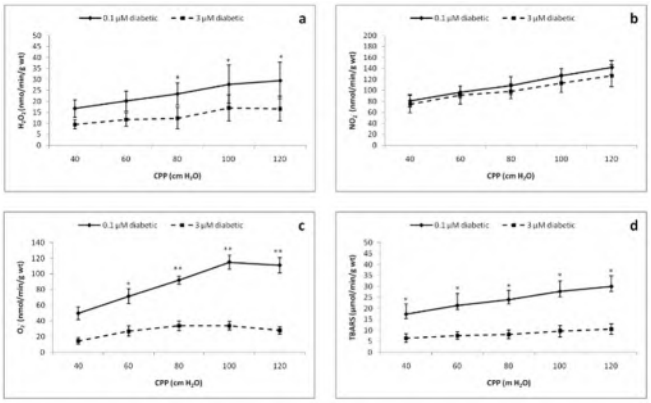

**Figure 4.** Parameters of oxidative stress in diabetic rats perfused with 0.1 µM of spironolactone compared with diabetic rats perfused with 3 µM of spironolactone. (a) Hydrogen peroxide ($H_2O_2$) (b) Nitrites ($NO_2^-$) (c) Superoxide anion radical ($O_2^-$) (d) Index of lipid peroxidation (measured as TBARS). Data is presented as mean ± SD. CPP, coronary perfusion pressure.

**Table 1.** Percentage of reduction or increase in the each of the parameters of oxidative stress in healthy and diabetic rats treated with different spironolactone doses.

| | | **40 cm$H_2O$** | **60 cm$H_2O$** | **80 cm$H_2O$** | **100 cm$H_2O$** | **120 cm$H_2O$** |
|---|---|---|---|---|---|---|
| **$H_2O_2$** | 0.1 µM spironolactone healthy vs. control | +20.49 | +1.34 | +1.30 | -7.57 | 0.00 |
| | 3 µM spironolactone healthy vs. control | +11.12 | -3.88 | +0.79 | -12.62 | +9.40 |
| | 0.1 µM spironolactone diabetic vs. diabetic | -0.12 | -11.62 | -0.28 | +8.73 | -8.08 |
| | 3 µM spironolactone diabetic vs. diabetic | -12.22 | -33.73 | -37.84 | -20.12 | -43.83 |

| | | 40 $cmH_2O$ | 60 $cmH_2O$ | 80 $cmH_2O$ | 100 $cmH_2O$ | 120 $cmH_2O$ |
|---|---|---|---|---|---|---|
| $NO_2^-$ | 0.1 μM spironolactone healthy vs. control | +13.69 | -10.83 | -20.12 | -19.92 | -31.26 |
| | 3 μM spironolactone healthy vs. control | -2.03 | -13.64 | -0.36 | -4.74 | +0.90 |
| | 0.1 μM spironolactone diabetic vs. diabetic | +4.12 | -6.74 | -4.91 | +1.26 | -0.98 |
| | 3 μM spironolactone diabetic vs. diabetic | -3.46 | -11.98 | -14.09 | -9.54 | -11.25 |
| $O_2^-$ | 0.1 μM spironolactone healthy vs. control | +5.55 | -53.58 | -14.75 | +41.34 | -16.96 |
| | 3 μM spironolactone healthy vs. control | +16.83 | -6.04 | -16.97 | -20.30 | -11.92 |
| | 0.1 μM spironolactone diabetic vs. diabetic | -21.85 | -3.80 | +32.66 | +19.34 | +67.14 |
| | 3 μM spironolactone diabetic vs. diabetic | +6.31 | -32.84 | -25.24 | -15.17 | -46.94 |
| TBARS | 0.1 μM spironolactone healthy vs. control | +7.85 | +1.32 | -6.91 | -10.89 | -9.93 |
| | 3 μM spironolactone healthy vs. control | +7.64 | +5.60 | +27.74 | +28.50 | +31.63 |
| | 0.1 μM spironolactone diabetic vs. diabetic | +5.25 | -6.02 | -7.06 | +0.60 | -3.87 |
| | 3 μM spironolactone diabetic vs. diabetic | -13.61 | -48.17 | -49.53 | -46.99 | -47.15 |

Percentage of reduction or increase in the each of the parameters of oxidative stress in healthy rats, healthy rats treated with 0.1 μM and 3 μM of spironolactone and diabetic rats treated with 0.1 μM and 3 μM of spironolactone. Sign (-) stands for reduction and sign (+) stands for increase in the level of the parameters of oxidative stress. Data is presented as percentage.

## DISCUSSION

The present study aimed to assess the acute effect of spironolactone administration on oxidative stress parameters in STZ-induced DM isolated heart rats. Besides, we have also examined the acute effect of different spironolactone doses on oxidative stress parameters in the above mentioned isolated heart rats.

Besides hypertension, DM is one of the most common factors contributing to CVD, putting CVD at the top of the scale of mortality worldwide. Acceleration of atherosclerosis increases the arteries' stiffness; thus, earlier onset of CVD, such as coronary artery disease, heart failure, arrhythmias, is one of the primary mechanisms by which DM contributes to the development of CVD.

Development of diabetic cardiomyopathy, characterized by interstitial and perivascular fibrosis, thickening of basal membranes of capillaries and hypertrophy of cardiomyocytes are one of the most critical consequences of DM (18-21). State of hyperglycemia through activation of different signal pathways leads to inflammation, increased ROS synthesis, and remodelling of the extracellular matrix of heart muscle (22). Those mechanisms lead to myocardial fibrosis, respectively increased rigidity, reduced ability for myocardial relaxation and increased stiffness of the endocardium. Abnormalities in calcium homeostasis, increased synthesis of ROS, and mitochondrial dysfunction are also some of the mechanisms involved in the development of diabetic cardiomyopathy. Simultaneously, activation of RAAS, one of the main ones, plays a crucial role in manifesting the consequences of chronic hyperglycemia (23, 24). One of RAAS activation effects is increased ROS synthesis and thus changes in activation genes leading to increased fibrosis of the heart, apoptosis, and necrosis (25). Beside increased ROS synthesis, consequential activation of angiotensin II receptors type 1 and MR can also lead to myocardial fibrosis (26). When activation of angiotensin II receptors type 1 and MR are compared, AT1 receptor blockade protects the heart from diabetic complications short-termly, while MR blockade provides long-term protection (27).

For chronic administration of spironolactone, MR's non-selective antagonist has been previously reported to lower the myocardial fibrosis, however, without effect on

cardiodynamic parameters (28). Our previous research has documented a different impact of acute spironolactone administration on healthy and diabetic rats with better effects of higher spironolactone doses in diabetic rats, while in a healthy one, the same effect was observed with lower spironolactone doses (9). And our current findings are consistent with the previous one, showing the same effect of spironolactone on oxidative stress parameters as on parameters of cardiac dynamics in healthy and diabetic hearts. Levels of $H_2O_2$ were significantly lower in the group of diabetic rats treated with 3μM then in the healthy rats treated with the same dose of spironolactone. Simultaneously, no significant differences were noted when diabetic and healthy rats treated with 0.1μM of spironolactone were compared and when healthy rats treated with 0.1μM were compared with healthy rats treated with 3μM of spironolactone. Previous research has concluded that chronic administration of spironolactone lowers levels of $H_2O_2$, while it has also been proved that spironolactone enhances the activity of catalase, an antioxidant enzyme with effects on $H_2O_2$ (29, 30). Levels of $NO_2^-$ did not significantly differ between our groups, except when we compared healthy and diabetic rats treated with 0.1μM of spironolactone at higher values of CPP where better effect were observed in healthy rats; and when we compared healthy rats treated with 0.1μM of spironolactone and healthy rats treated with 3μM of spironolactone again at higher values of CPP (100 and 120 cm $H_2O$), confirming our earlier conclusion that spironolactone has better effects in heathy rats when given in lower doses. Similar results were observed when we looked at $O_2^-$ levels, as well as TBARS levels.

Some of the findings we observed in our previously published research regarding different effects of different spironolactone doses on parameters of cardiodynamics could be explained by these findings of oxidative stress. In the literature, spironolactone improved eNOS, endothelial nitric oxide synthase improving coronary flow (3). It has also been reported that spironolactone improves NO/soluble guanylyl cyclase mediated response inducing vasodilatation (30). Beside improved function of eNOS, it has been shown that vitamin E levels were significantly higher in STZ-induced DM rat hearts that were treated with spironolactone, either by its enhanced production or suppressed consumption (3). It has also been shown that MR antagonists have only partial protection in diabetic eNOS knock-out mice in comparison to fully protected diabetic wild-type mice (31). Spironolactone also leads to lower levels of TBARS, which can point protective effects of spironolactone towards biomembranes, which contain numerous polyunsaturated free fatty acids.

In summary, different spironolactone doses achieved different effects on parameters of oxidative stress. While better effects in healthy rats were achieved with lower amounts of spironolactone, in diabetic rats, better outcomes were achieved with higher doses of spironolactone. These results coincide with our previous results regarding cardiodynamic parameters. Therefore, one explanation for the same effect of different spironolactone doses on cardiodynamic parameters in diabetic and healthy rats could be that the higher the dose of spironolactone, the better its impact on oxidative stress and, therefore, cardiac function. It has been shown that the state of hyperglycemia enhances MR transcriptional activity, and the reason for better spironolactone effect on diabetic hearts in higher dose could be explained by overexpression of MR in diabetic hearts, thus blocking it with higher spironolactone concentrations better result is achieved (32). In healthy hearts, the same effect is observed with lower spironolactone concentrations because there is no MR overexpression. These discoveries likewise concur with the recently revealed level after which perfusion with higher spironolactone groupings does not have any extra impact on myocardial contractility (33). Besides the reported plateau for spironolactone, it has also been shown that different spironolactone doses did not change the concentrations of pro-inflammatory cytokines (IL-1β, IL-6 and IL-8) in human coronary artery endothelial cells treated with 5.5mM dextrose (34).

Our study's main limitations are the lack of a causal relationship between the spironolactone effect on cardiodynamics and on parameters of oxidative stress. While oxidative stress induces MR activation, oxidative stress is subsequently increased by MR activation in a feedback loop, we could not determine whether the spironolactone effect is achieved directly by influencing cardiodynamic parameters and consequently changing the levels of parameters of oxidative stress or primarily by modification of parameters of oxidative stress and after that cardiodynamic parameters, however, the causal link exists (35, 36). Therefore, further research is needed to investigate the spironolactone effect on the relationship between cardiodynamic and parameters of oxidative stress and determine the definitive mechanism of action of different spironolactone dosage on diabetic hearts.

## CONCLUSION

Spironolactone, a non-selective MR antagonist, achieved different effects on oxidative stress parameters when given acutely in different doses in diabetic and healthy rats. In lower doses, spironolactone's acute administration lowered the parameters of oxidative stress in healthy rats better than higher doses of spironolactone. In contrast, in the diabetic group, acute effects of higher doses of spironolactone lowered oxidative stress parameters better than lower doses of spironolactone.

## ACKNOWLEDGEMENTS

The work has been done at the Department of Physiology, Faculty of Medical Sciences, University of Kragujevac, Kragujevac, Serbia.

## CONFLICT OF INTEREST

The authors report no conflicts of interest.

## REFERENCES


1. Zimmet P, Alberti KG, Shaw J. Global and societal implications of the diabetes epidemic. Nature 2001;414:782-787.
2. Leon BM, Maddox TM. Diabetes and cardiovascular disease: Epidemiology, biological mechanisms, treatment recommendations and future research. World J Diabetes 2015;6(13):1246-1258.
3. Mayyas F, Alzoubi KH, Bonyan R. The role of spironolactone on myocardial oxidative stress in rat model of streptozotocin-induced diabetes. Cardiovasc Ther 2017;35(2): e12242.
4. Silva MAB, Bruder-Nascimento T, Cau SBA, Lopes RAM, Mestriner FLAC, Fais RS, et al. Spironolcatone treatment attenuates vascular dysfunction in type 2 diabetic mice by decreasing oxidative stress and restoring NO/GC signaling. Front Physiol 2015;6:269.
5. Silva MA, Cau SB, Lopes RA, Manzato CP, Neves KB, Bruder-Nascimento T, et al. Mineralocorticoid receptor blockade prevents vascular remodeling in a rodent model of type 2 diabetes mellitus. Clin Sci (Lond.) 2015;129(7):533-545.
6. Delcayre C. and Silvestre JS. Aldosterone and the heart: towards a physiological function? Cardiovasc Res 1999;43(1):7-12.
7. Patel BM, Kakadiya J, Goyal RK, Mehta AA. Effect of Spironolactone on Cardiovascular Complications Associated with Type-2 Diabetes in Rats. Exp Clin Endocrinol Diabetes 2013;121:441-447.
8. Garg R, Rao AD, Baimas-George M, Hurwitz S, Foster C, Shah RV, et al. Mineralocorticoid receptor blockade improves coronary microvascular function in individuals with type 2 diabetes. Diabetes 2015;64(1):236-42.
9. Vranic A, Simovic S, Ristic P, Nikolic T, Stojic I, Srejovic I, et al.. The acute effects of different spironolactone doses on cardiac function in streptozotocin-induced diabetic rats. Can J Physiol Pharmacol 2017;95(11):1343-1350.
10. Stas S, Whaley-Connell A, Habibi J, Appesh L, Hayden MR, Karuparthi PR, et al. Mineralocorticoid receptor blockade attenuates chronic overexpression of the renin-angiotensin-aldosterone system stimulation of reduced nicotinamide adenine dinucleotide phosphate oxidase and cardiac remodeling. Endocrinology 2007;148:3773 -3780.
11. Toda N, Nakanishi S, Tanabe S. Aldosterone affects blood flow and vascular tone regulated by endothelium-derived NO: therapeutic implications. Br J Pharmacol 2013;168:519-533.
12. Hollenberg NK, Stevanovic R, Agarwal A, Lansang MC, Price DA, Laffel LM, et al. Plasma aldosterone concentration in the patient with diabetes mellitus. Kidney Int 2004;65:1435-1439.
13. 13.Tveden-Nyborg P, Bergmann TK, Lykkesfeldt J. Basic & Clinical Pharmacology & Toxicology Policy for Experimental and Clinical studies. Basic Clin Pharmacol Toxicol 2018;123(3):233-235.
14. Pick E, Keisari Y. A simple colometric method for the measurement of hydrogen peroxide by cells in culture. J Immunol Methods 1980;38:161-170.
15. Green LC, Wagner DA, Glogowski J, Skipper PI, Wishnok JS, Tannenbaum SR Analysis of nitrate, nitrite and (15N) nitrate in biological fluids. Anal Biochem 1982;126:131-138.
16. Auclair C, Voisin E. Nitroblue Tetrazolium reduction. In: Greenwald RA (ed) Handbook of methods for oxygen radical research. CRP Press, Boca Raton, 1985. pp 123-132.
17. Ohkawa H, Ohishi N, Yagi K. Assay for lipid peroxides in animal tissues by thiobarbituric acid reaction. Anal Biochem 1979;95:351-358.
18. Hayat SA, Patel B, Khattar RS, Malik RA. Diabetic cardiomyopathy: mechanisms, diagnosis and treatment Clinical Science 2004;107:539-557.
19. Li YW, Aeno WS. Diabetes Mellitus and Cardiovascular Disease. J Clinic Experiment Cardiol 2011;2:114.
20. Rubler S, Dlugash J, Yuceoglu YZ, Kumral T, Branwood AW, Grishman A. New type of cardiomyopathy associated with diabetic glomerulosclerosis. Am J Cardiol 1972;30:595-602.
21. Van Hoeven KH, Factor SM. A comparison of the pathological spectrum of hypertensive, diabetic, and hypertensive - diabetic heart disease. Circulation 1990;82:848-85.
22. Poornima IG, Parkih P, Shanon RP. Diabetic Cardiomyopathy: search for unifying hypoyhesis Circ Res 2006;98:596-605.
23. Watanabe K, Thandavarayan RA, Harima M, Sari FR, Gurusamy N, Veeraveedu PT, et al. Role of Differential Signaling Pathways and Oxidative Stress in Diabetic Cardiomyopathy. Curr Cardiol Rev 2010;6:280-290.
24. Hunyady L, Catt KJ. Pleiotropic AT1 receptor signaling pathways mediating physiological and pathogenic actions of angiotensin II. Molecular Endocrinol 2006;20:953-970.
25. Frustaci A, Kajstura J, Chimenti C, Jakoniuk I, Leri A, Maseri A. et al. Myocardial cell death in human diabetes. Circ Res 2000;87:1123-1132.
26. Robert V, Heymes C, Silvestre JS. Angiotensin AT1receptor subtype as a cardiac target of aldosterone: role in aldosterone salt induced fibrosis. Hypertension 1999;33:981-986.
27. Nagatomo Y, Meguro T, Ito H, Koide K, Anzai T, Fukuda K. et al. Significance of AT1 receptor independent activation of mineralocorticoid receptor in murine diabetic cardiomyopathy. PLoS One 2014;9(3):e93145.
28. Verma S, Violet GY, Badiwala M, Anderson JT, Mc Niel LH. Working heart function in diabetes is not improved by spironolactone treatment Can J Physiol Pharmacol 2003;81:493-496.
29. Ojeda-Cervantes M, Barrera-Chimal J, Alberú J, Pérez-Villalva R, Morales-Buenrostro LE, Bobadilla NA. Mineralocorticoid receptor blockade reduced oxidative

stress in renal transplant recipients: a double-blind, randomized pilot study. Am J Nephrol 2013;37(5):481-90.
30. Silva MA, Bruder-Nascimento T, Cau SB, Lopes RA, Mestriner FL, Fais RS, Touyz, RM, Tostes RC. Spironolactone treatment attenuates vascular dysfunction in type 2 diabetic mice by decreasing oxidative stress and restoring NO/GC signaling. Front Physiol 2015;6:269.
31. Kosugi T, Heining M, Nakayama T, Matsuo S, Nakagawa T. eNOS Knockout Mice with Advanced Diabetic Nephropathy Have Less Benefit from Renin-Angiotensin Blockade than from Aldosterone Receptor Antagonists. Am J Path 2010;176(2):619-629.
32. Hayashi T, Shibata H, Kurihara I, Yokota K, Mitsuishi Y, Ohashi, K, et al. High Glucose Stimulates Mineralocorticoid Receptor Transcriptional Activity Through the Protein Kinase C β Signaling. Int Heart J 2017;58:794-802.
33. Barbato JC, Mulrow PJ, Shapiro JI and Franco-Saenz R. Rapid effects of aldosterone and spironolactone in the isolated working rat heart. Hypertension 2002;40(2):130-135.
34. Haas MJ, Jurado-Flores M, Hammoud R, Feng V, Gonzales K, Onstead-Haas L, Mooradian AD. The Effects of Known Cardioprotective Drugs on Proinflammatory Cytokine Secretion from Human Coronary Artery Endothelial Cells. Am J Therapeut 2019;26(3):e321-e332.
35. Shibata S, Nagase M, Yoshida S, Kawarazaki W, Kurihara H, Tanaka H, Miyoshi J. Modification of mineralocorticoid receptor function by Rac1 GTPase: implication in proteinuric kidney disease. Nat Med 2008;14:1370-1376.
36. Kawakami-Moori F and Shimosawa T. Oxidative Stress and Mineralocorticoid Receptor Signaling in the Brain: Possible Therapeutic Targets for Dementia. Ann Clin Exp Hypertesion 2012;2(2):1015-1020.

# DNA AND BSA-BINDING STUDIES OF DINUCLEAR PALLADIUM(II) COMPLEXES WITH 1,5-NAPHTIRIDINE BRIDGING LIGANDS

Snezana Rajkovic[1], Andjela A. Franich[1], Vojislav Cupurdija[2,3] and Marija D. Zivkovic[4]

[1] *University of Kragujevac, Faculty of Science, Department of Chemistry, Kragujevac, Serbia*
[2] *University of Kragujevac, Faculty of Medical Sciences, Department of Internal Medicine, Kragujevac, Serbia*
[3] *University Clinical Center, Clinic for Pulmonology, Kragujevac, Serbia*
[4] *University of Kragujevac, Faculty of Medical Sciences, Department of Pharmacy, Kragujevac, Serbia*

Received: 22.01.2021.
Accepted: 24.02.2021.

**Corresponding author:**

**Marija D. Zivkovic**

University of Kragujevac, Faculty of Medical Sciences, Department of Pharmacy, Serbia

E-mail: mzivkovic@kg.ac.rs

## ABSTRACT

*The interactions of metal complexes with important biomolecules such as deoxyribonucleic acid (DNA) or bovine serum albumin (BSA) are responsible for their antitumor activity due to different modes of interaction with DNA and their transport through the blood system to cells and tissues via serum albumin. Therefore, the dinuclear palladium(II) complexes, [{Pd(en)Cl}$_2$(μ-1,5-nphe)](NO$_3$)$_2$ (Pd1) and [{Pd(1,3-pd)Cl}$_2$(μ-1,5-nphe)](NO$_3$)$_2$ (Pd2) (en is ethylenediamine, 1,3-pd is 1,3-propylenediamine and 1,5-nphe is the bridging 1,5-naphthyridine ligand) were synthesized and characterized by different spectroscopic methods. The UV-Vis and fluorescence emission spectroscopy were applied for evaluation of binding modes of Pd1 and Pd2 complexes to DNA as well as their interaction with BSA. The emission spectra indicate that the investigated Pd1 and Pd2 complexes can displace the ethidium bromide intercalator from DNA/EtBr molecules and act as intercalators showing strong interactions with DNA. The fluorescence intensity showes that Pd1 and Pd2 complexes can bind to BSA and then be transported to the cell.*

***Keywords***: *Dinuclear palladium(II) complexes; 1,5-naphthyridine; DNA; bovine serum albumin (BSA).*

sciendo

UDK: 575.113
546.562-386
Eabr 2024; 25(2):113-125
DOI: 10.2478/sjecr-2021-0030

## INTRODUCTION

Palladium(II) complexes are interesting due to their similarity with the corresponding platinum(II) complexes, so they can be used as model molecules for investigation of the antitumor action mechanism of cisplatin and other platinum chemotherapeutics. Reactivity of palladium(II) complexes is $10^4$-$10^5$ times higher in relation to analogous with platinum(II) (1-4).

Although the first results did not show significant antitumor activity of the palladium(II) complexes, they were nevertheless studied more widely. It is considered that the lower activity of these complexes is a consequence of very fast ligands exchange and the inability of the complex to reach the biological target without changes in structure, which increases the risk of adverse effects on biochemical processes in the cell. Since the main reason for the poor biological activity of these palladium complexes lies in its thermodynamic and kinetic lability, it was necessary to make a good selection of ligands, and thus the leaving groups, in the synthesis. In order to overcome such problems, a large number of palladium(II) complexes containing chelating ligands, have been synthesized in order to reduce the reactivity of palladium(II) ion, and increase the stability of the obtained compounds (5). The reactivity and lipophilicity, as well as the antitumor activity of the complex itself, depend on the choice of appropriate ligands. With increasing of compound lipophilicity, its cytotoxicity also increases (6,7). The leaving group must not be extremely labile because it is necessary for the complex to sustain its structural integrity *in vivo* long enough. For example, 1,10-phenanthroline mononuclear and dinuclear palladium(II) complexes show very good antitumor activity (8). It is assumed that one of the main reasons for good cytotoxicity, in addition to lipophilicity, is the presence of the N-H group, more precisely the hydrogen atom that is suitable for the formation of the hydrogen bonds. This allows more efficient coordination of nucleic acids, containing the electron donor nitrogen atoms, for the palladium(II) ion. So far, only in medicine, the radioactive isotope $^{103}$Pd has been used for treatment of fast-growing prostate cancer (9,10).

Numerous palladium complexes with ligands such as putrescine, spermine, edta-type ligands and coumarin derivatives have been synthesized and showed cytotoxic activity approximately equal or even better than cisplatin (11,12). Studies based on the biological activity of mononuclear palladium(II) complexes with ethylenediamine ligand have shown enhanced cytotoxic activity against human leukemia cell lines, relative to cisplatin and other platinum(II) complexes (13). Ethylenediamine dinuclear palladium(II) complexes with pyridine derivatives and phenanthroline as ligands have also shown cytotoxic activity, as well as the ability to reduce the viability of cervical tumor cells (14). The synthesis of palladium(II) complexes with voluminous *N*-donor ligands leads to the formation of *trans*-complexes, due to the steric effect. *Trans*-isomers of palladium(II) complexes have shown better cytotoxicity compared to corresponding *cis*-isomers (15).

Deoxyribonucleic acid (DNA), important biopolymer in the human body, forms different conformations under physiological conditions, because of interactions that occur within the molecule itself (16-18). DNA has a role to store and transmit encoded genetic data, which includes transcription, replication, and translation into proteins. Investigating the mechanism of action of cisplatin as a highly represented cytostatic in the treatment of different cancers, it was found that reversible and irreversible binding to the DNA molecule occur. Reversible bonding refers to the formation of covalent bonds between platinum(II) ions and nitrogen atoms from purine and pyrimidine bases, namely N7-nitrogen atoms from guanine, N7 and N1-atoms from adenine and N3-atom from cytosine and thymine (19, 20). NMR spectroscopy and X-ray analysis have shown that interlinked bonds between DNA molecules and metal ions can be formed in different ways. Analogous to platinum(II), studies of palladium(II) complexes interactions with DNA have been performed (21,22).

Serum albumins are a class of blood proteins whose primary function is the transport of molecules and regulation of osmotic pressure in the blood plasma. They play an important role in the transport of metal ions and their complexes to cells and tissues. The concentration of serum albumin in the blood is about $7.0 \cdot 10^{-4}$ M (23,24). Human serum albumin (HSA) and bovine serum albumin (BSA) belong to the group of the most studied proteins (23,25). Bovine serum albumin possesses amino acid sequence that has 76% similarity to the human serum albumin (23,26). Investigations of the interactions of serum albumin proteins and transition metal ion complexes used as drugs, is of great importance, because it can lead to a decrease or increase in the biological activity of the drug, as well as to the occurrence of new modes of complex transport. Rapid degradation of many drugs in the body, reduces their therapeutic power. HSA and BSA, as drug transporters, can be used to increase the half-lives of peptides and small molecules that are rapidly subject to degradation. In this way, serum albumins regulate the bioavailability of drugs and bioactive molecules. Due to the extraordinary binding capacity of different ligands, they are also used as model systems for studying interactions with bioactive molecules (27,28).

In this paper, we report synthesis and spectroscopic characterization of two dinuclear palladium(II) complexes with 1,5-naphthyridine bridging ligand, [{Pd(en)Cl}2(μ-1,5-nphe)](NO3)2 (**Pd1**) and [{Pd(1,3-pd)Cl}2(μ-1,5-nphe)](NO3)2 (**Pd2**). UV-Vis spectrometry and fluorescent measurements are applied for investigation of the reactions of palladium(II) complexes (**Pd1** and **Pd2**) with DNA and bovine serum albumin (BSA), which results can provide mechanism of their antitumor activity and their possibility to interact with important biomolecules as well as mode of these interactions.

## EXPERIMENTAL

### Materials

Chemicals and reagents ethylenediamine (en), 1,3-propylenediamine (1,3-pd), 1,5-naphthyridine (1,5-nphe), deoxyribonucleic acid isolated from calf thymus (CT-DNA), bovine serum albumin (BSA), ethidium bromide (EtBr), 0.01 M phosphate buffer and $K_2[PdCl_4]$ were purchased from Sigma-Aldrich Chemical Co. Bidistilled water was used to prepare a solution of these reagents. Other chemicals used in this work were commercial products of analytical purity and were purchased from a domestic manufacturer.

### Instrumental methodes

All pH measurements were performed at 25 °C. For this purpose, a pH meter Mettler Toledo Seven Copmact S220-U was used, which was calibrated in relation to Mettler Toledo buffer solutions for pH = 4.0 and pH = 7.0. The measured pH values were not corrected for the deuterium effect.

Elemental microanalysis for C, H, and N parameters were performed in the Microanalytical Department of the Institute of Chemistry, Faculty of Chemistry, University of Belgrade.

$D_2O$ as the solvent and TSP (trimethyl-silylpropane-3-sulfonate) as the reference standard were used to record the $^1H$ and $^{13}C$ NMR spectrum. The spectra were recorded on a Varian Gemini 200 MHz spectrometer. All reactions were performed in 5 mm diameter NMR cuvettes.

Electronic absorption spectra were recorded on a Shimadzu UV-Vis spectrophotometer. Concentrations of dinuclear palladium(II) complexes were $5 \cdot 10^{-5}$ mol/dm$^3$. The electron absorption spectra were recorded in the wavelength range 200–500 nm at 25 °C and the experimental results were processed using the computer program Microsoft Office Excel 2003.

Infra-red (IR) spectra were recorded on a Perkin-Elmer Spectrum One FT-IR spectrometer using the KBr technique, in the wavelength range of 450 - 4000 cm$^{-1}$.

Fluorescence measurements were performed on an RF-1501 PC spectrophotometer (Shimadzu, Japan).

### Synthesis of $[Pd(en)Cl_2]$ and $[Pd(1,3\text{-}pd)Cl_2]$ complexes

Mononuclear palladium(II) complexes $[Pd(en)Cl_2]$ and $[Pd(1,3\text{-}pd)Cl_2]$ (en and 1,3-pd, are bidentate coordinated diamine ligands ethylenediamine and 1,3-propylenediamine, respectively) were synthesized according to a modified procedure previously described in the literature (29-31).

0.1632 g ($5.00 \cdot 10^{-4}$ mol) of $K_2[PdCl_4]$ was dissolved in 25 cm$^3$ of water and the resulting brown solution was transferred to a 100 cm$^3$ double-necked flask supplied with reflux condenser and dropper. The pH value of the solution was adjusted to about 2-3 by adding a solution of HCl with a concentration of 0.1 M. Obtained solution was heated on a water bath, with slow instilment of an equimolar amount ($5.00 \cdot 10^{-4}$ mol) of ethylenediamine or 1,3-propylenediamine. Instilment is performed slowly for one hour with constant heating, stirring and occasional control of pH values (pH 2-3). During the reaction, the color of the solution changes from brown to light yellow. After refluxing for 5 h, the reaction mixture was left at room temperature overnight. The complexes crystallized from aqueous solution at room temperature. The obtained crystals were filtered off, washed with ethanol and air dried. The yield was about 90%.

### Synthesis of dinuclear $[\{Pd(en)Cl\}_2(\mu\text{-}1,5\text{-}nphe)](NO_3)_2$ and $[\{Pd(1,3\text{-}pd)Cl\}_2(\mu\text{-}1,5\text{-}nphe)](NO_3)_2$ complexes

Dinuclear palladium(II) complexes, $[\{Pd(en)Cl\}_2(\mu\text{-}1,5\text{-}nphe)](NO_3)_2$ (**Pd1**) and $[\{Pd(1,3\text{-}pd)Cl\}_2(\mu\text{-}1,5\text{-}nphe)](NO_3)_2$ (**Pd2**), were obtained from the corresponding mononuclear complexes according to a modified procedure previously described in the literature (32-34).

In 5 cm$^3$ of dimethylformamide 0.0572 g ($3.37 \cdot 10^{-4}$ mol) of $AgNO_3$ was dissolved and a suspension of the mononuclear $[Pd(en)Cl_2]$ or $[Pd(1,3\text{-}pd)Cl_2]$ complex ($3.43 \cdot 10^{-4}$ mol) in 10 cm$^3$ of dimethylformamide was added. The reaction mixture was leaved overnight with stirring at room temperature and in the dark. Precipitated AgCl was removed by filtration and in the pale yellow solution of palladium(II) complex, $[Pd(en)(dmf)Cl]^+$ or $[Pd(1,3\text{-}pd)(dmf)Cl]^+$, solution of 1,5-naphthyridine (1,5-nphe) in dimethylformamide (molar ratio 2 : 1) was edded dropwise. The reaction mixture was stirred at room temperature for about 4 h in the dark. The volume of the solution was reduced by evaporation of dimethylformamide on a rotary vacuum evaporator.

After the addition of about 20 cm$^3$ of dichloromethane, a light yellow precipitate of the complex $[\{Pd(en)Cl\}_2(\mu\text{-}1,5\text{-}nphe)](NO_3)_2$ and $[\{Pd(1,3\text{-}pd)Cl\}_2(\mu\text{-}1,5\text{-}nphe)](NO_3)_2$ was obtained. The resulting precipitate of dinuclear palladium(II) complexes was separated by filtration, washed with methanol, then ether and air dried. The yield of dinuclear palladium(II) complexes was 65% for **Pd1** and 50% for **Pd2**.

Anal. Calcd. for **Pd1** ($C_{12}H_{22}N_8Cl_2O_6Pd_2$: FW = 658,11): C, 21.90%; H, 3.37%; N, 17.03%. Found: C, 22.11%; H, 3.26%; N, 17.29%. $^1H$ NMR (200 MHz, $D_2O$, δ, ppm): 8.14 (m, 2H, H3, H7), 9.58 (m, 2H, H4, H8), 10.21 (d, 2H, H2, H6). $^{13}C$ NMR (50 MHz, $D_2O$, δ, ppm): 130 (C3, C7), 143 (C4a, C8a), 147 (C4, C8), 160 (C2, C6). IR (KBr, ν, cm$^{-1}$): ~3226, 3100 (N-H stretch); 1582, 1509 (C=C/C=N 1,5-naphthyridine group stretch); 1373, 1356, 1336 ($\nu_{as}(NO_3)$). UV-vis ($H_2O$, $\lambda_{max}$, nm): 303 ($\varepsilon = 7.8 \cdot 10^3$ M$^{-1}$cm$^{-1}$), 314 ($\varepsilon = 8.0 \cdot 10^3$ M$^{-1}$cm$^{-1}$).

Anal. Calcd. for **Pd2** ($C_{14}H_{26}N_8Cl_2O_6Pd_2$: FW = 686,15): C, 24.51%; H, 3.82%; N, 16.33%. Found: C, 24.28%; H, 3.55%; N, 16.53%. $^1H$ NMR (200 MHz, $D_2O$, δ, ppm): 8.23 (m, 2H, H3, H7), 9.55 (d, 2H, H4, H8), 10.17 (d, 2H, H2,

H6). $^{13}C$ NMR (50 MHz, $D_2O$, δ, ppm): 131 (C3, C7), 143 (C4a, C8a), 146 (C4, C8), 160 (C2, C6). IR (KBr, ν, $cm^{-1}$): ~3241, 3135 (N-H stretch); 1659, 1600, 1589, 1510 (C=C/C=N 1,5-naphthyridine group stretch); 1367, 1295 ($\nu_{as}(NO_3)$). UV-vis ($H_2O$, $\lambda_{max}$, nm): 303 ($\varepsilon = 7.5 \cdot 10^3$ $M^{-1}cm^{-1}$), 313 ($\varepsilon = 7.2 \cdot 10^3$ $M^{-1}cm^{-1}$).

**Interactions of complexes with CT-DNA**

**UV-Vis spectrophotometric measurements**

Interactions of [{Pd(en)Cl}$_2$($\mu$-1,5-nphe)]$(NO_3)_2$ and [{Pd(1,3-pd)Cl}$_2$($\mu$-1,5-nphe)]$(NO_3)_2$ complexes with deoxyribonucleic acid isolated from calf thymus (CT-DNA) were investigated using UV-Vis spectrophotometry. Based on these measurements, the internal binding constant ($K_b$) of CT-DNA molecules for dinuclear palladium(II) complexes was determined. A 0.01 M phosphate buffer solution (pH = 7.4) was used to prepare the solutions for UV-Vis measurements. All reactions were performed at 37 ºC. The concentration of CT-DNA was determined from the ratio of UV absorbance at 260 and 280 nm ($A_{260}/A_{280}$). An absorption ratio of 1.8 to 1.9 indicates that CT-DNA has been released from the protein portion, and such a solution was stored at 4 °C for no longer than 7 days. The concentration of CT-DNA was determined based on UV absorption at 260 nm and extinction coefficient $\varepsilon = 6600$ $M^{-1}cm^{-1}$ (35,36).

To determine the internal binding constant ($K_b$) of CT-DNA molecules and dinuclear palladium(II) complexes, UV-Vis spectra of the solution obtained by mixing dinuclear palladium(II) complexes with CT-DNA were recorded. In all solutions, the concentration of palladium(II) complex was constant ($4.51 \cdot 10^{-5}$ M), while the concentration of CT-DNA was in the interval (0 - 9.02) $\cdot$ $10^{-5}$ M ([complex] / [ CT-DNA] = 0.0 - 2.0). The internal binding constants ($K_b$) were determined according to the equation: $[DNK]/(\varepsilon_a-\varepsilon_f) = [DNK]/(\varepsilon_b-\varepsilon_f) + 1/K_b \cdot (\varepsilon_b-\varepsilon_f)$ (37), where [DNA] is the concentration of CT-DNA, $\varepsilon_a$ and $\varepsilon_b$ are the extinction coefficients of the free complex and the complex when the CT-DNA molecule is bound to it, respectively. The extinction coefficient $\varepsilon_f$ was defined from the calibration curve obtained by determining the absorption of the free complex at different concentrations. The extinction coefficient $\varepsilon_a$ was calculated based on Lambert-Beer's law, as the ratio of the absorption of the tested solution ($A_{obs}$) and the concentration of the complex in that solution ($A_{obs}$-DNA)/[complex]. The obtained results are presented graphically as the dependence of $[DNK]/(\varepsilon_a-\varepsilon_f)$ *versus* [DNK]. The slope of the obtained line has the value $1/(\varepsilon_b-\varepsilon_f)$, while the segment on the *y* axis is $1/K_b \cdot (\varepsilon_b-\varepsilon_f)$. The internal binding constant ($K_b$) was determined from the ratio of the slope of the line and the segment on the *y* axis.

**Fluorescent measurements**

Interactions of dinuclear palladium(II) complexes, [{Pd(en)Cl}$_2$($\mu$-1,5-nphe)]$(NO_3)_2$ and [{Pd(1,3-pd)Cl}$_2$($\mu$-1,5-nphe)]$(NO_3)_2$, with CT-DNA in the presence of ethidium bromide (3,8-diamino-5-ethyl-6-phenylphenanthridium bromide, EtBr) were examined using emission fluorescence spectroscopy. A solution of palladium(II) complex was added in to the mixture of EtBr and CT-DNA ($1.28 \cdot 10^{-5}$ M) in a 1: 1 molar ratio, so that obtained solution have concentration ratio of Pd(II) complex and CT-DNA in range from 0.0 to 0.9. All reactions were carried out in 0.01 M phosphate buffer (pH = 7.4). In order to examine the competitive reactions of the interaction of dinuclear palladium(II) complexes and EtBr with CT-DNA, fluorescent spectra of EtBr/CT-DNA were recorded in the absence and presence of dinuclear Pd(II) complexes. The emission spectra were recorded in the wavelength range 550 - 750 nm, with extinction at 527 nm and fluorescent emission at 612 nm. The Stern-Volmer constant ($K_{sv}$) was determined based on the equation: $I_0/I = 1 + K_{sv}[Q]$ (38), where $I_0$ and I are the fluorescence intensities before and after the addition of the palladium(II) complex to the EtBr/CT-DNA solution, while [Q] is the concentration of the Pd(II) complex. The obtained results are presented graphically as the dependence of $I_0/I$ from [Q]. The Stern-Volmer constant ($K_{sv}$) was obtained from the slope of the acquired line. The stability constant ($K_a$) as well as the number of binding sites (n) was obtained based on the equation: $\log (I_0–I)/I = \log K_a + n \cdot \log[Q]$ (39-41). The obtained results are presented graphically as the dependence of $\log (I_0–I)/I$ from the log[Q]. The value of $K_a$ was obtained from the intersection of the line with the *y* axis, and the number of connecting points (n) from the slope of the line.

**Interactions of Pd(II) complexes with albumin**

Emission fluorescence spectroscopy were used to examine interactions of dinuclear palladium(II) complexes [{Pd(en)Cl}$_2$($\mu$-1,5-nphe)]$(NO_3)_2$ and [{Pd(1,3-pd)Cl}$_2$($\mu$-1,5-nphe)]$(NO_3)_2$ with bovine serum albumin (BSA). Emission spectra were recorded in the wavelength range 300–500 nm, with extinction at 295 nm (32). The binding effect of the tested albumin complexes was observed based on the reduction of the albumin emission intensity ($1.6 \cdot 10^{-6}$ M in 0.01 M PBS) to 352 nm after the addition of palladium(II) complexes $(0\text{-}4.0) \cdot 10^{-5}$ M. All emission spectra were recorded under the same experimental conditions.

The Stern-Volmer constant ($K_{sv}$) was determined based on the equation: $I_0/I = 1 + K_{sv}[Q] = 1 + k_q\tau_0[Q]$, where $I_0$ is the initial fluorescence intensity of tryptophan in BSA, and I is the fluorescence intensity of tryptophan in BSA after addition of palladium(II) complex in protein solution, $k_q$ is the fluorescence quenching constant, $\tau_0$ is the average time for fluorescence of albumin in the absence of the complex and [Q] is the concentration of the complex. The binding constant ($K_a$) as well as the number of binding sites (n) were obtained on the basis of Scatchard's equation: $\log(I_0–I)/I = \log K_a + n \cdot \log[Q]$. The results are presented graphically as the

dependence of log($I_0$–I)/I from log [Q], the value of $K_a$ is aquired from the intersection of the obtained line with the *y* axis, and the number of connecting points (n) from the slope of the line.

## RESULTS AND DISCUSSION

In this work, two dinuclear palladium(II) complexes, [{Pd(en)Cl}$_2$($\mu$-1,5-nphe)](NO$_3$)$_2$ (**Pd1**) and [{Pd(1,3-pd)Cl}$_2$($\mu$-1,5-nphe)](NO$_3$)$_2$ (**Pd2**), containing 1,5-naphthyridine (1,5-nphe) as bridging ligand, while ethylenediamine (en) and 1,3-propylenediamine (1,3-pd) are bidentate coordinated diamine ligands, were synthesized and characterized by elemental microanalysis, NMR ($^1$H and $^{13}$C), IR spectroscopy and UV-Vis spectrophotometry. **Figure 1** shows the structural formulas of ligands, and the synthesized dinuclear palladium(II) complexes. Interactions of dinuclear palladium(II) complexes with calf thymus deoxyribonucleic acid (CT-DNA) were investigated using UV-Vis spectrophotometry and fluorescence spectroscopy. In addition, fluorescence spectroscopy was used to study the interaction of **Pd1** and **Pd2** complexes with bovine serum albumin (BSA).

**Figure 1.** Structural formulas of 1,5-naphthyridine (1,5-nphe), ethylenediamine (en) and 1,3-propylenediamine (1,3-pd), and dinuclear palladium(II) complexes **Pd1** and **Pd2**.

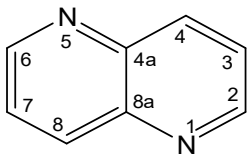


1,5-naphthyridine (1,5-nphe)

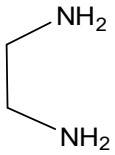


ethylenediamine (en)

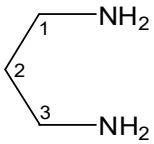


1,3-propylenediamine (1,3-pd)

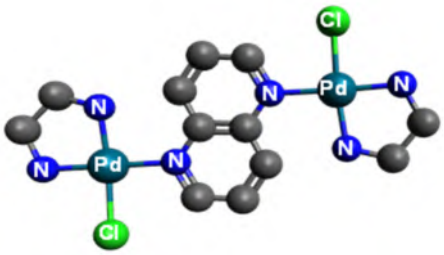


[{Pd(en)Cl}$_2$($\mu$-1,5-nphe)](NO$_3$)$_2$ (**Pd1**)

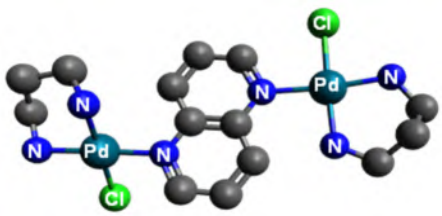


[{Pd(1,3-pd)Cl}$_2$($\mu$-1,5-nphe)](NO$_3$)$_2$ (**Pd2**) (**Pd2**),

### Synthesis and characterization of dinuclear palladium(II) complexes

Dinuclear palladium(II) complexes, [{Pd(en)Cl}$_2$($\mu$-1,5-nphe)](NO$_3$)$_2$ (**Pd1**) and [{Pd(1,3-pd)Cl}$_2$($\mu$-1,5-nphe)](NO$_3$)$_2$ (**Pd2**), were obtained from the corresponding mononuclear complexes according to a modified procedure previously described in the literature (32-34).

As shown in **Figure 1**, the synthesized dinuclear palladium(II) complexes have the same bridging 1,5-naphthyridine ligand and different bidentate coordinated diamine ligands. $^1$H and $^{13}$C NMR spectra of 1,5-naphthyridine, ethylediamine, 1,3-propylenediamine as well as **Pd1** and **Pd2** complexes were recorded in $D_2O$ as solvent. NMR data for ligands and dinuclear palladium(II) complexes is given in Table 1, while $^1$H and $^{13}$C NMR spectra of **Pd1** and **Pd2** complexes in **Figure 2**.

**Table 1.** $^{1}H$ and $^{13}C$ NMR chemical shifts (δ, ppm) for 1,5-naphthyridine (1,5-nphe), ethylenediamine (en), 1,3-propylenediamine (1,3-pd) and the corresponding dinuclear palladium(II) complexes

| ligand/ complex | NMR shifts | | | | | | | | |
|---|---|---|---|---|---|---|---|---|---|
| | $^{1}H$ | | | | $^{13}C$ | | | | |
| | H2, H6 | H4, H8 | H3, H7 | alifatic protons | C2, C6 | C4, C8 | C3, C7 | C4a, C8a | L |
| **1,5-nphe** | 8.57 *dd* | 7.89 *d* | 7.48 *dd* | | 154 | 139 | 128 | 144 | |
| **en** | | | | 2.64 *s* ($CH_2$) | | | | | 45 ($CH_2$) |
| **Pd1** | 10.21 *d* | 9.58 *d* | 8.14 *m* | 2.76 *m* ($CH_2$) | 160 | 147 | 130 | 143 | 50 ($CH_2$) |
| **1,3-pd** | | | | 1.60 *m* (H2, $CH_2$) 2.47 *m* (H1,H3,$CH_2$) | | | | | 29 (C2, $CH_2$) 39 (C1,C3, $H_2$) |
| **Pd2** | 10.17 *d* | 9.55 *d* | 8.23 *m* | 1.85 *m* (H2,$CH_2$) 2.76 *m* (H1,H3,$CH_2$) | 160 | 146 | 131 | 143 | 30 (C2, $CH_2$) 43,44 (C1,C3, $CH_2$) |

In the $^{1}H$ NMR spectrum of free 1,5-naphthyridine, two multiplets (doublet-doublets, *dd*) occur at 7.48 (H3, H7) and 8.57 (H2, H6) ppm, derive from the equivalent protons of the two condensed pyridine rings. The doublet at 7.89 ppm originates from the H4 and H8 protons of 1,5-nphe.

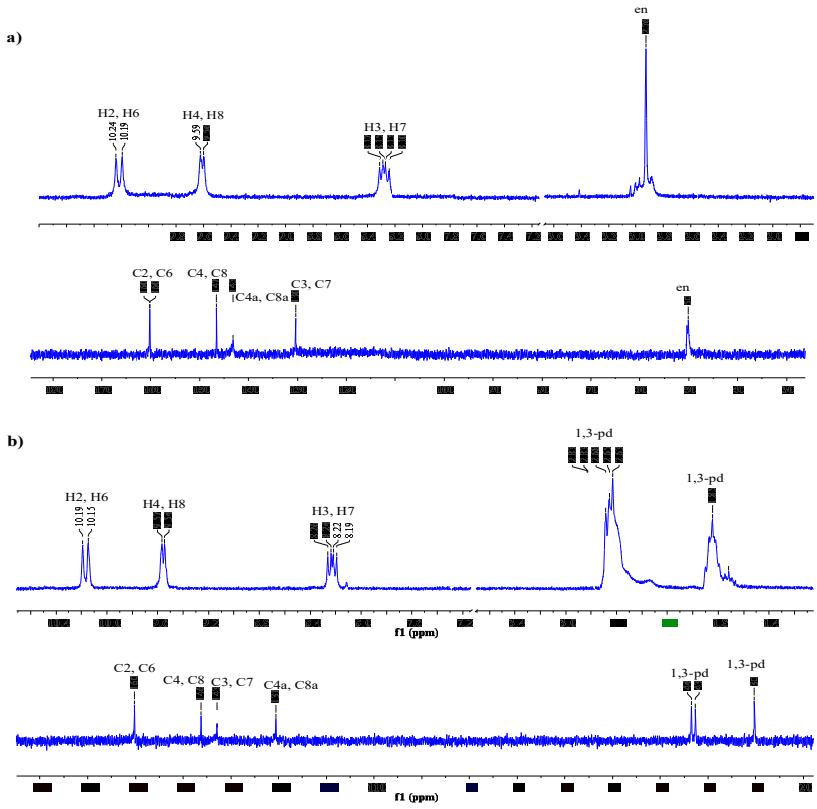


**Figure 2.** $^{1}H$ and $^{13}C$ NMR spectra of [{Pd(en)Cl}$_2$(μ-1,5-nphe)](NO$_3$)$_2$ **(Pd1)** and [{Pd(1,3-pd)Cl}$_2$(μ-1,5-nphe)](NO$_3$)$_2$ **(Pd2)** complexes.

After coordination of diamine ligand to the palladium(II) ion, the signal shifts downfield (**Fig. 2** and Table 1). The shifts of the signals, which correspond to the 1,5-nphe protons after coordination for the palladium(II) ion, are a consequence of the delocalization of the charge transmitted through the pyridine rings (20,32,42). The multiplet at 2.76 ppm in the $^{1}$H NMR spectrum of the **Pd1** complex, correspond to methylene protons of bidentate coordinated ethylenediamine. This signal was shifted by $\Delta\delta = 0.12$ ppm downfield in regard to free ethylenediamine. In the aliphatic part of the $^{1}$H NMR spectrum of the **Pd2** complex, two multiplets appear at 1.85 and 2.60 ppm due to the $CH_2$ protons at position 2 and the $CH_2$ protons at position 1 and 3 (**Fig. 1**, Table 1). Signals derived from these protons after coordination were shifted downfield ($\Delta\delta = 0.25$ ppm for methylene protons at position 2 and $\Delta\delta = 0.19$ ppm for same protons at positions 1 and 3) in regards to the uncoordinated 1,3-pd.

In the $^{13}$C NMR spectra of the **Pd1** and **Pd2** complexes, in the aromatic region, four signals from the carbon atoms of the 1,5-naphthyridine ligand (C2 and C6, C4 and C8, C4a and C8a, C3 and C7) appears. The position of these signals differs significantly from those of the uncoordinated 1,5-nphe (Table 1). After coordination of 1,5-nphe for Pd(II) the signals for the carbon atoms in the heterocyclic aromatic ring move downfield. The signal at 50 ppm originating from from the carbon atoms of bidentate-coordinated ethylediamine in **Pd1**, are shifted by $\Delta\delta = 5$ ppm in regarde to the uncoordinated en ligand. Also, in the spectrum of the **Pd2** complex, the signals corresponding to the C atoms of the coordinated 1,3-pd ligand are shifted by $\Delta\delta = 1$-5 ppm downfield relative to the signals of the uncoordinated ligand.

### UV-Vis spectrophotometry

The UV-Vis spectra of the Pd1, Pd2 complexes and free 1,5-nphe ligand are given in Figure 3. The first absorption maximum is located in the wavelength range of 296 to 310 nm, while the second maximum is in the range of 310 to 320 nm. All absorption maxima of the synthesized complexes have a batochromic shift after the coordination of 1,5-naphthyridine, due to π….π electron transitions in the heterocyclic 1,5-nphe ligand.

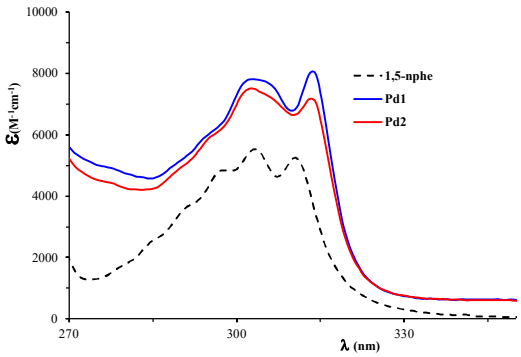


**Figure 3.** UV-Vis spectra of dinuclear $[\{Pd(en)Cl\}_2(\mu\text{-}1,5\text{-nphe})]^{2+}$ and $[\{Pd(1,3\text{-pd})Cl\}_2(\mu\text{-}1,5\text{-nphe})]^{2+}$ complexes and free 1,5-nphe ligand.

### IR spectroscopy

IR spectra of Pd1 and Pd2 complexes, recorded in the wavelength range 4000 - 450 cm-1, show bands corresponding to coordinated 1,5-nphe ligand, as well as bands of bidentate coordinated ethylenediamine (en) and 1,3-propylenediamine (1,3-pd) (Fig. 4).

In the IR spectra of dinuclear palladium(II) complexes, two very strong bands in the range of 3280 - 3098 $cm^{-1}$ were observed, which correspond to asymmetric and symmetric vibrations of the coordinated amino group of ethylenediamine and 1,3-propylenediamine. The medium-strength band in the region of 1500–1650 $cm^{-1}$ correspond to the C = C and C = N vibrations of the aromatic 1,5-naphthyridine ring. A strong and wide band at ~1364 - 1384 $cm^{-1}$ indicates the existence of $NO_3^-$ ions in the outer coordination sphere of dinuclear palladium(II) complexes.

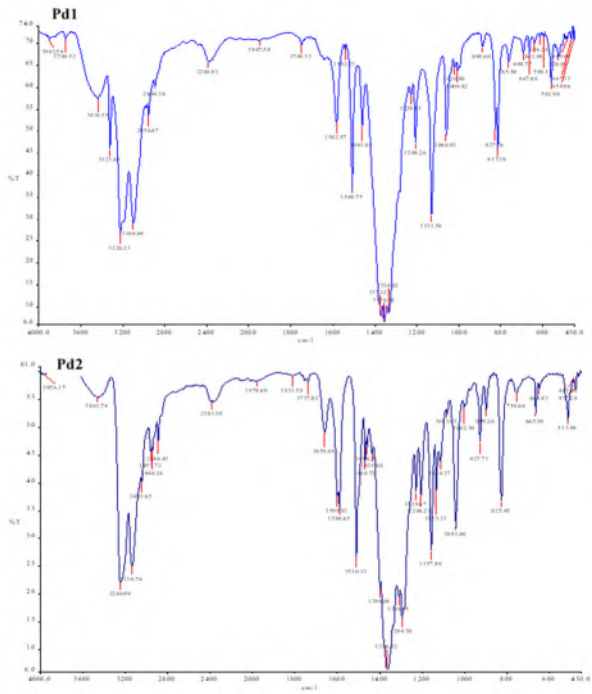


**Figure 4.** IR spectra of **Pd1** and **Pd2** complexes, KBr, 4000-450 $cm^{-1}$.

### Interactions of dinuclear palladium(II) complexes with DNA

#### UV-Vis spectrophotometric measurements

UV-Vis spectrophotometry is a simple and efficient method, which is used to determine the mode of coordination or interaction of metal complexes with deoxyribonucleic acid (DNA). Transition metal complexes can interact with DNA covalently or noncovalently (43). Coordination of DNA molecules, most commonly via N7 atoms from guanine to a metal ion, creates a covalent bond, while noncovalent interactions include intercalation, hydrogen bond formation, and electrostatic interactions. After the interaction of the metal complex

with the DNA, the intensity of the absorbance may decrease (hypochromic effect) or increase (hyperchromic effect). Also, the absorption maximum may have a batochromic or hypsochromic shift. Based on the obtained results of UV-Vis spectrophotometry, the internal binding constants (stability constants) of DNA to the metal ion, can be calculated. The UV-Vis spectra of $[\{Pd(en)Cl\}_2(\mu\text{-}1,5\text{-nphe})]^{2+}$ and $[\{Pd(1,3\text{-pd})Cl\}_2(\mu\text{-}1,5\text{-nphe})]^{2+}$ complexes in the absence and presence of different concentrations of CT-DNA, ([complex] / [CT-DNA] = (0.0 - 2.00)·$10^{-4}$ M) are shown in Figure 5.

After the addition of CT-DNA to the solution of dinuclear palladium(II) complexes, a hyperchromic effect (increase of the absorption maximum) in UV-Vis spectra can be observed, based on which it can be concluded that the complex interacts with CT-DNA. The hyperchromic effect indicates that our complexes with CT-DNA achieve interactions of electrostatic nature or π→π* interactions which occurs as a consequence of the interactions of aromatic rings in complexes with bases in CT-DNA (44).

The internal binding constants ($K_b$) were calculated from the change in absorption at the appropriate wavelength after the addition of CT-DNA according to the equation given in the Experimental part (2.5.1). The obtained results are presented graphically as the dependence of [DNK]/($\varepsilon_a$-$\varepsilon_f$) from DNA concentration. The slope of the obtained line has the value 1/($\varepsilon_b$-$\varepsilon_f$), while the segment on the *y* axis is 1/$K_b$·($\varepsilon_b$-$\varepsilon_f$). The internal binding constant ($K_b$) is determined from the ratio of the slope of the line and the segment on the *y* axis (Fig. 5). The obtained values for the internal binding constants ($K_b$) are shown in Table 2. Based on $K_b$, we can conclude that strong interactions occur between investigated Pd(II) complexes and CT-DNA, which are characteristic for intercalators.

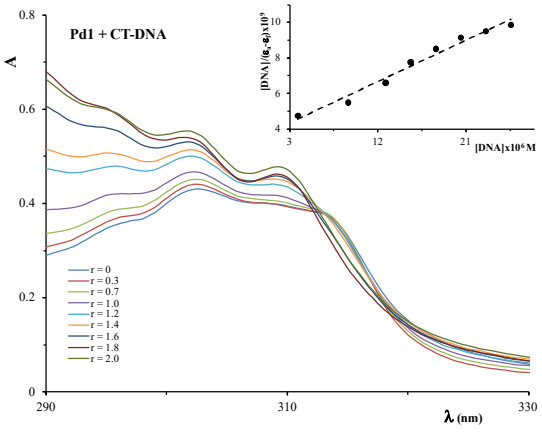


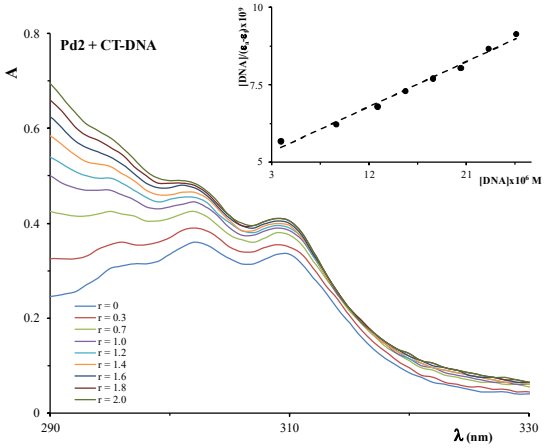


**Figure 5.** Absorption spectra of $[\{Pd(en)Cl\}_2(\mu\text{-}1,5\text{-nphe})]^{2+}$ and $[\{Pd(1,3\text{-pd})Cl\}_2(\mu\text{-}1,5\text{-nphe})]^{2+}$ complexes in 0.01 M phosphate buffer before and after addition of CT-DNA. [Pd(II) complex] = 4.51·$10^{-5}$ M, [DNA] = (0 - 2.00)·$10^{-4}$ M.

$K_b$ values of the tested complexes are about 10 times lower then the same for the typical intercalator ethidium bromide (EtBr) to DNA, ($K_b = 1.23 \cdot 10^5$ $M^{-1}$) (45), indicating that the interactions of the Pd(II) complexes are weaker compared to EtBr. The higher value of $K_b$ for the **Pd1** complex compared to the **Pd2**, indicates that the **Pd1** complex has a higher affinity of interaction with CT-DNA, which can be attributed to the smaller steric effect of the bidentate coordinated five-membered ethylenediamine ring compared to the six-membered 1,3-propylenediamine ring in **Pd2**. The change in Gibbs energy (ΔG, Table 2) of the Pd(II)/CT-DNA adduct was calculated using the following equation: $\Delta G = -RT\ln K_b$. Negative values of Gibbs energy indicate spontaneous interaction of dinuclear palladium(II) complexes, **Pd1** and **Pd2**, with CT-DNA.

| complex | $K_b \cdot 10^4$ ($M^{-1}$) | ΔG (kJ/mol) | H |
|---|---|---|---|
| $[\{Pd(en)Cl\}_2(\mu\text{-}1,5\text{-nphe})]^{2+}$ | (7.50 ± 0.05) | -28.93 | 22.42 |
| $[\{Pd(1,3\text{-pd})Cl\}_2(\mu\text{-}1,5\text{-nphe})]^{2+}$ | (4.00 ± 0.03) | -27.31 | 25.77 |

**Table 2.** Internal binding constants ($K_b$), changes in Gibbs energy (ΔG) and hypochromism (H) of the investigated dinuclear palladium(II) complexes, **Pd1** and **Pd2**, with CT-DNA

**Fluorescent measurements**

Fluorescence emission spectroscopy was used for studying the interactions of dinuclear Pd1 and Pd2 complexes with the CT-DNA molecule and ethidium bromide (EtBr) as a typical intercalator. Changes in EtBr/CT-DNA emission spectra

after addition of the complex solution, decrease or increase in fluorescent emission, indicates that the complex replaces EtBr, and a new adduct of CT-DNA/Pd(II) complex is formed (46).

The emission spectra of EtBr/CT-DNA in the presence of Pd1 and Pd2 complexes are shown in Figure 6. Addition of palladium(II) complex (with increasement of complex concentration) leads to a decreasement of the emission intensity at 612 nm, indicating competition reaction between EtBr and the tested Pd(II) complexes in relation to CT-DNA. Extrusion of EtBr from the EtBr/CT-DNA with Pd(II) complex proves that intercalation the Pd(II) complex occured.

The intensity of the interaction of **Pd1** and **Pd2** complexes with CT-DNA was determined based on the Stern-Volmer constant ($K_{sv}$) using the Sten-Volmer equation: $I_0/I = 1 + K_{sv}[Q]$, where $I_0$ and I are the fluorescence intensities before and after the addition of palladium(II) complex in EtBr/CT-DNA solution, while [Q] is the concentration of Pd(II) complex. The obtained results are graphically presented as the dependence of $I_0/I$ from [Q]. The Stern-Volmer constant ($K_{sv}$) was determined from the slope of the obtained line.

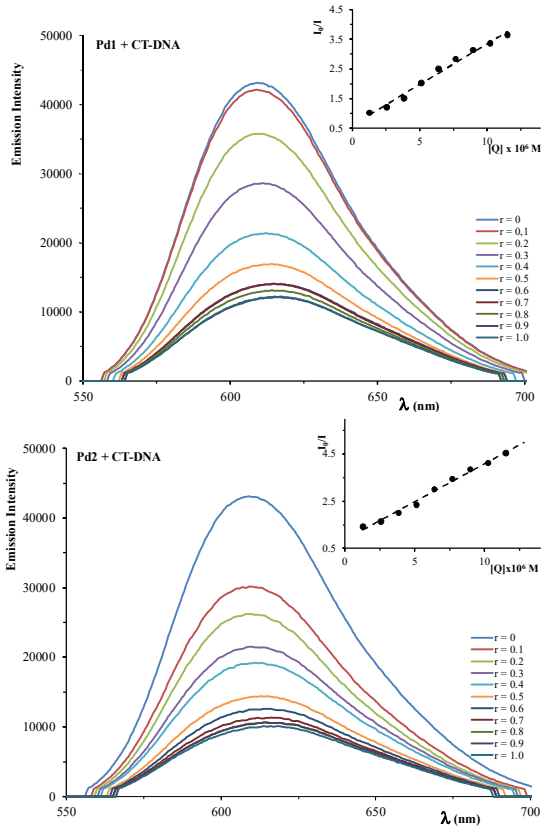


**Figure 6.** EtBr/CT-DNA emission spectra in the presence of $[\{Pd(en)Cl\}_2(\mu\text{-}1,5\text{-nphe})]^{2+}$ and $[\{Pd(1,3\text{-pd})Cl\}_2(\mu\text{-}1,5\text{-nphe})]^{2+}$ complex. [EtBr] = $1.28 \cdot 10^{-5}$ M, [DNA] = $1.28 \cdot 10^{-5}$ M, [Pd(II) complex] = $(0 - 1.28) \cdot 10^{-5}$ M. Inserted graph: Dependence of $I_0/I$ from concentration [Q].

From $K_{sv}$ values (Table 3), it can be concluded that the investigated dinuclear palladium(II) complexes show high affinity for CT-DNA and can displace EtBr from the EtBr/CT-DNA adduct. The stability constant ($K_a$) was determined from the experimental results, as well as the number of binding sites (Table 3), showing that the $K_a$ follows the $K_{sv}$ values. The obtained values for the Stern-Volmer constant ($K_{sv}$), the stability constant ($K_a$) and the number of binding sites (n) confirm that the dinuclear Pd(II) complexes, **Pd1** and **Pd2**, reacts with CT-DNA by intercalating between two nucleotide strands of DNA and displacing EtBr. These results are in agreement with the $K_b$ values obtained by UV-Vis spectrophotometry. The higher number of binding sites for the **Pd1** complex, once again indicates the stronger interaction of this complex with CT-DNA compared to the **Pd2** complex.

**Table 3.** Stern-Volmer constant ($K_{sv}$), stability constant ($K_a$) and number of binding sites (n) of the investigated dinuclear palladium(II) complexes with CT-DNA.

| complex | $K_{sv} \cdot 10^5$ ($M^{-1}$) | $K_a \cdot 10^5$ ($M^{-1}$) | n |
|---|---|---|---|
| $[\{Pd(en)Cl\}_2(\mu\text{-}1,5\text{-nphe})]^{2+}$ | (4.50 ± 0.04) | (8.80 ± 0.02) | 1.7 |
| $[\{Pd(1,3\text{-pd})Cl\}_2(\mu\text{-}1,5\text{-nphe})]^{2+}$ | (2.80 ± 0.06) | (2.50 ± 0.05) | 1.1 |

**Interactions of dinuclear Pd(II) complexes, Pd1 and Pd2, with BSA**

Serum albumin, as the most common blood plasma protein, is one of the most studied proteins (23,25). It plays an important role in the transport of metal ions and their complexes through the blood system to cells and tissues. Bovine serum albumin (BSA) is the most studied serum albumin due to its structural similarity to human serum albumin (HSA). Namely, human serum albumin contains one tryptophan at the Trp-214 position, while BSA contains two tryptophan residues, Trp-134 and Trp-214. The bovine serum albumin (BSA) solution shows intense fluorescent emission at $\lambda_{em,\,max}$ = 352 nm, and after excitation at 295 nm (47). After the addition of the **Pd1** or **Pd2** complex to the BSA solution, the fluorescence intensity at λ = 352 nm decrease (**Fig. 7**) based on it can be concluded that the tested complexes interact with this biomolecule. The decrease in fluorescence intensity can be attributed to changes in protein structure, which occur due to changes in the tryptophan environment in BSA, because of protein binding to complexes (48).

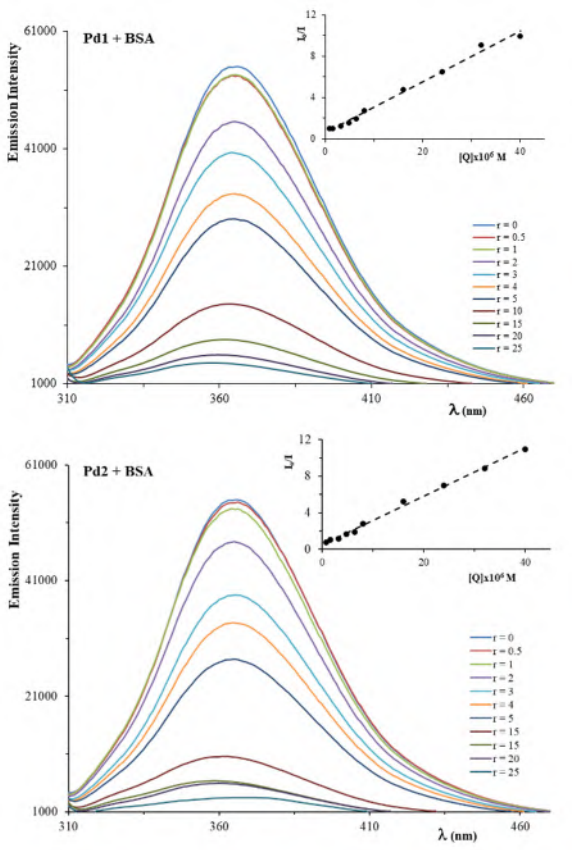


**Figure 7.** BSA emission spectra in the presence of $[\{Pd(en)Cl\}_2(\mu\text{-}1,5\text{-nphe})]^{2+}$ and $[\{Pd(1,3\text{-pd})Cl\}_2(\mu\text{-}1,5\text{-nphe})]^{2+}$ complexes. [BSA] = $1.60\cdot10^{-6}$ M, [Pd(II) complex] = $(0 - 4.00)\cdot10^{-5}$ M; $\lambda_{ex}$ = 295 nm. Inserted graph: Dependence of Io/I from concentration [Q].

The values of the dynamic Stern-Volmer constant ($K_{sv}$) and the fluorescence quenching constant ($k_q$) for complex interactions with BSA were determined using the Stern-Volmer equation. The values of the constants $K_{sv}$ and $k_q$ for the interaction of the studied **Pd1** and **Pd2** complexes with BSA are given in Table 4. In addition, Table 4 shows the values of binding constants ($K_a$) as well as the number of albumin binding sites (n) for Pd(II) complexes, which were obtained on the basis of Scatchard's equation (Experimental part 2.6). The obtained results are graphically presented as the dependence of $\log(I_0–I)/I$ from $\log[Q]$, the value of $K_a$ is obtained from the intersection of the line with the *y* axis, and the number of connecting points (n) from the slope of the line.

Based on the linearity in Stern-Volmer graphs, it can be concluded that both complexes lead to the quenching of tryptophan emission in the BSA molecule. $K_{sv}$ values for **Pd1** and **Pd2** complex (Table 4) indicate a very similar binding affinity of BSA for the tested complexes. The values of n for both complexes are 1.8, which indicates that there are approximately two possible sites in the protein suitable for complex binding. The quenching constants ($k_q$) are greater than $10^{10}$ and indicate a static emission quenching mechanism (49). $K_a$ value leads to conclusion that the **Pd1** and **Pd2** complexes can bind to BSA and thus be transported to the cell and hydrolyze the bond with BSA at the appropriate site in the cell.

**Table 4.** Stern-Volmer constant ($K_{sv}$), quenching constant ($k_q$), binding constant ($K_a$) and number of binding sites (n) for interactions between BSA and dinuclear **Pd1** and **Pd2** complexes.

| complex | $K_{sv}\cdot10^5$ ($M^{-1}$) | $k_q\cdot10^{12}$ ($M^{-1}s^{-1}$) | $K_a\cdot10^9$ ($M^{-1}$) | n |
|---|---|---|---|---|
| $[\{Pd(en)Cl\}_2(\mu\text{-}1,5\text{-nphe})]^{2+}$ | (2.80 ± 0.03) | (28 ± 2) | (1.20 ± 0.05) | 1.8 |
| $[\{Pd(1,3\text{-pd})Cl\}_2(\mu\text{-}1,5\text{-nphe})]^{2+}$ | (3.90 ± 0.04) | (39 ± 1) | (1.20 ± 0.02) | 1.8 |

## CONCLUSION

In this paper, two dinuclear complexes, $[\{Pd(en)Cl\}_2(\mu\text{-}1,5\text{-nphe})](NO_3)_2$ (**Pd1**) and $[\{Pd(1,3\text{-pd})Cl\}_2(\mu\text{-}1,5\text{-nphe})](NO_3)_2$ (**Pd2**), (ethylenediamine (en) and 1,3-propylenediamine (1,3-pd) are bidentate coordinated diamine ligands and 1,5-naphthyridine (5-nphe) bridging ligand) were synthesized. The structure of these complexes was confirmed based on the results of elemental microanalysis, UV-Vis, IR, NMR ($^1H$ and $^{13}C$) spectroscopy.

Interactions of synthesized dinuclear palladium(II) complexes with deoxyribonucleic acid were investigated using UV-Vis spectrophotometry and fluorescence spectroscopy. UV-Vis spectrophotometric data showed that after the addition of CT-DNA to the solution of dinuclear palladium(II) complexes, a hyperchromic effect occurs, based on which we can conclude that the complex interacts with CT-DNA without changing its structure. Higher value of $K_b$ for complex **Pd1** indicates that this complex has greater binding affinity in comparison to **Pd2**. The emission spectra demonstrate that the investigated **Pd1** and **Pd2** complexes can displace the ethidium bromide intercalator from the CT-DNA/EtBr adduct. From the high Stern-Volmer constants ($K_{sv}$) values it can be concluded that these Pd(II) complexes act as intercalators showing strong interactions with DNA, and higher value of the stability constant ($K_a$) for **Pd1** confirms results from UV-Vis spectrophotometry. Stronger binding of **Pd1** complex to the DNA helix can be attributed to the smaller steric effect of the five-membered ethylenediamine ligand in relation to the six-membered 1,3-propylenediamine ring.

Fluorescence spectroscopy were used for investigation of interactions of **Pd1** and **Pd2** complexes with bovine serum albumin (BSA). The fluorescence intensity of tryptophan decreases proportionally to the increasement in the total concentration of the added complex. From calculated values of the constants ($K_{sv}$ and $K_a$) it can be concluded that **Pd1** and **Pd2** complexes can bind to BSA and then be transported to the cell. Also, the number of binding sites (n) show that two binding sites of BSA are accessible for interaction with these metal complexes.

The results obtained in this paper contribute to a better understanding of the interactions of dinuclear palladium(II) complexes containing 1,5-naphthyridine as a bridging ligand, with biologically important molecules, such as DNA and BSA.

## ACKNOWLEDGMENT

This work was financially supported by the Ministry of Education, Science and Technological Development of the Republic of Serbia (Agreement No. 451-03-68/2020-14/200122) and the Faculty of Medical Sciences, University of Kragujevac (JP02/20, JP11/16, JP10/16).

## CONFLICT OF INTEREST

Authors declare no conflict of interest.

## REFERENCES

1. Cotton FA, Wilkinson G. *Advanced inorganic chemistry*, John Wiley & Sons Inc., New York, (1972).
2. Janković V. *Hemijski elementi, Zavod za udžbenike i nastavna sredstva, Beograd*, 2002.
3. Matwiyoff A, Asprey LB, Wageman WE, Reisfeld MJ, Fukushima E. Fluorine-19 nuclear magnetic resonance studies of diamagnetic fluoride complexes of nickel(IV), palladium(IV), and platinum(IV) in anhydrous hydrogen fluoride solutions. Inorg. Chem., 1969;8(4):750-753.
4. Butour JL, Wimmer S, Wimmer F, Castan P. Palladium(II) compounds with potential antitumour properties and their platinum analogues: a comparative study of the reaction of some orotic acid derivatives with DNA *in vitro*. Chem. Biol. Inter., 1997;104:165-178.
5. Navarro-Ranninger C, Pérez JM, Zamora F, González VM, Masaguer JR, Alonso C. Palladium(II) compounds of putrescine and spermine. Synthesis, characterization, and DNA-binding and antitumor properties. J. Inorg. Biochem. 1993;52:37-49.
6. Ray S, Mohan R, Singh JK, Samantaray MK, Shaikh MM, Panda D, Ghosh P. Anticancer and Antimicrobial Metallopharmaceutical Agents Based on Palladium, Gold, and Silver N-Heterocyclic Carbene Complexes. J.Am. Chem. Soc. 2007;129:15042-15053.
7. Storr T, Thompson KH, Orvig C. Design of targeting ligands in medicinal inorganic chemistry. Chem. Soc. Rev. 2006;35:534-544.
8. Zhao G, Sun H, Lin H, Zhu S, Su X, Chen Y. Palladium(II) complexes with N,N'-dialkyl-1,10-phenanthroline-2,9-dimathanamine: synthesis, characterization and cytotoxic activity. J. Inorg. Biochem. 1998;72:173-177.
9. Potters L, Cao Y, Calugaru E, Torre T, Fearn P, Wang XH. A comprehensive review of CT-based dosimetry parameters and biochemical control in patients treated with permanent prostate brachytherapy. Int. J. Radiat. Oncol.Biol.Phys. 2001;50:605-614.
10. Stone NN, Stock PG. Complications following permanent prostate brachytherapy. Eur. Urol. 2002;41:427-433.
11. Vujić JM, Cvijović M, Kaluderović GN, Milovanović M, Zmejkovski BB, Volarević V, Arsenijević N, Sabo TJ, Trifunović SR. Palladium(II) complexes with R2edda derived ligands. Part IV. O,O′-dialkyl esters of (S,S)-ethylenediamine-N,N′-di-2-(4-methyl)-pentanoic acid dihydrochloride and their palladium(II) complexes: Synthesis, characterization and in vitro antitumoral activity against chronic lymphocytic leukemia (CLL) cells. Eur. J. Med. Chem. 2010;45:3601-3606.
12. Ilić DR, Jevtić VV, Radić GP, Arsikin K, Ristić B, Harhaji-Trajković L, Vuković N, Sukdolak S, Klisurić O, Trajković V, Trifunović SR. Synthesis, characterization and cytotoxicity of a new palladium(II) complex with a coumarine-derived ligand. Eur. J. Med. Chem. 2014;74:502-508.
13. Zhao G, Lin H, Yu P, Sun H, Zhu S, Su X, Chen Y. Ethylenediamine-palladium(II) complexes with pyridine and its derivatives: synthesis, molecular structure and initial antitumor studies. J. Inorg. Biochem. 1999;73:145-149.
14. Gao E, Lin L, Liu L, Zhu M, Wang B, Gao X. Two new palladium(II) complexes: Synthesis, characterization and their interaction with HeLa cells. Dalton Trans. 2012;41:11187-11194.
15. Kapdi AR, Fairlamb IJS. Anti-cancer palladium complexes: a focus on $PdX_2L_2$, palladacycles and related complexes. Chem. Soc. Rev. 2014;43:4751-4777.
16. Cohen GL, Ledner JA, Bauer WR, Ushay HM, Caravana C, Lippard SJ. Sequence dependent binding of cis-dichlorodiammineplatinum(II) to DNA. J. Am. Chem. Soc. 1980;102:2487-2488.
17. Takahara PM, Frederick CA, Lippard SJ. Crystal Structure of the Anticancer Drug Cisplatin Bound to Duplex DNA. J. Am. Chem. Soc. 1996;118:12309-12321.
18. Gately DP, Howell SB. Cellular accumulation of the anticancer agent cisplatin: a review. Br. J. Cancer 1993;67:1171-1176.
19. Komeda S, Kalayada GV, Lutz M, Spek AL, Yamanaka Y, Sato T, Chikuma M, Reedijk J. New Isomeric Azine-Bridged Dinuclear Platinum(II) Complexes Circumvent Cross-Resistance to Cisplatin. J. Med. Chem. 2003;46:1210-1219.
20. Ašanin DP, Živković MD, Rajković S, Warżajtis B, Rychlewska U, Djuran MI. Crystallographic evidence of anion···π interactions in the pyrazine bridged {[Pt(en)Cl]2(μ-pz)}Cl2 complex and a comparative study of the catalytic ability of mononuclear and binuclear platinum(II) complexes in the hydrolysis of N-acetylated l-methionylglycine. Polyhedron 2013;51: 255-262.
21. Chen H, Parkinson JA, Parsons S, Coxall RA, Gould RO, Sadler PJ. Organometallic Ruthenium(II) Diamine Anticancer Complexes: Arene-Nucleobase Stacking and Stereospecific Hydrogen-Bonding in Guanine Adducts. J. Am. Chem. Soc. 2002;124:3064-3082.

22. Chen H, Parkinson JA, Nováková O, Bella J, Wang F, Dawson A, Gould R, Parsons S, Brabec V, Sadler PJ. Induced-fit recognition of DNA by organometallic complexes with dynamic stereogenic centers. Proc. Natl. Acad. Sci. U. S. A. 2003;100:14623-1428.
23. Carter D, Ho JX. Structure of Serum Albumin. Advances in Protein Chemistry 1994;45:153-203.
24. Curry S, Mandelkow H, Brick P, Franks N. Crystal structure of human serum albumin complexed with fatty acid reveals an asymmetric distribution of binding sites. Nat. Struct. Biol. 1998;5:827-835.
25. Brown JR, Shockley P. Lipid and Protein Interactions, Wiley, New York, **1** (1982).
26. Peters T. Serum albumin. Advances in Protein Chemistry 1985;37:161-245.
27. Reynolds JA, Herbert S, Polet H, Steinhardt J. The binding of divers detergent anions to bovine serum albumin. Biochemistry 1967;6:937-947.
28. Sklar LA, Hudson BS, Simoni RD. Conjugated polyene fatty acids as fluorescent probes: binding to bovine serum albumin. Biochemistry 1977;16:5100-5108.
29. Milinković SU, Parac TN, Djuran MI, Kostić NM. Dependence of hydrolytic cleavage of histidine-containing peptides by palladium(II) aqua complexes on the co-ordination modes of the peptides. J. Chem. Soc., Dalton Trans. (1997) 2771-2776.
30. Hohmann H, Eldik R. van. Rate and equilibrium data for substitution reactions of diaqua(ethylenediamine)palladium(II) with chloride in aqueous solution. Inorg. Chim.Acta 1990;174:87-92.
31. Živković MD, Ašanin DP, Rajković S, Djuran MI. Hydrolysis of the amide bond in N-acetylated l-methionylglycine catalyzed by various platinum(II) complexes under physiologically relevant conditions. Polyhedron 2011;30:947-952.
32. Franich AA, Živković MD, Ćoćić D, Petrović B, Milovanović M, Arsenijević A, Milovanović J, Arsenijević D, Stojanović B, Djuran MI, Rajković S. New dinuclear palladium(II) complexes with benzodiazines as bridging ligands: interactions with CT-DNA and BSA, and cytotoxic activity. J. Biol. Inorg. Chem. 2019;24:1009-1022.
33. Zhao G, Lin H, Zhu S, Sun H, Chen Y. Dinuclear palladium(II) complexes containing two monofunctional [Pd(en)(pyridine)Cl]+ units bridged by Se or S. Synthesis, characterization, cytotoxicity and kinetic studies of DNA-binding. J. Inorg. Biochem. 1998;70:219-226.
34. Komeda S, Kalayda GV, Lutz M, Spek AL, Yamanaka Y, Sato T, Chikuma M. J. Reedijk, New Isomeric Azine-Bridged Dinuclear Platinum(II) Complexes Circumvent Cross-Resistance to Cisplatin. J. Med. Chem. 2003;46:1210-1219.
35. Dimiza F, Fountoulaki S, Papadopoulos AN, Kontogiorgis CA, Tangoulis V, Raptopoulou CP, Psycharis V, Terzis A, Kessissoglou DP, Psomas G. Non-steroidal antiinflammatory drug–copper(ii) complexes: Structure and biological perspectives. Dalton Trans. 2011;40:8555-8568.
36. Dimiza F, Perdih F, Tangoulis V, Turel I, Kessissoglou DP, Psomas G. Interaction of copper(II) with the non-steroidal anti-inflammatory drugs naproxen and diclofenac: Synthesis, structure, DNA- and albumin-binding. J. Inorg. Biochem. 2011;105:476-489.
37. Wolf A, Shimer GH, Meehan T. Polycyclic aromatic hydrocarbons physically intercalate into duplex regions of denatured DNA. Biochemistry 1987;26:6392-6396.
38. Liu M. Yuan W, Zhang Q, Yan L, Yang R. Synthesis, characterization and DNA interaction studies of complexes of lanthanide nitrates with tris{2-[(3,4-dihydroxybenzylidene)imino]ethyl}amine. Spectrochim.Acta Part A Mol. Biomol. Spectrosc. 2008;70:1114-1119.
39. Shahabadi N, Maghsudi MM, Ahmadipour Z. Study on the interaction of silver(I) complex with bovine serum albumin by spectroscopic techniques. Spectrochim. Acta, Part A 2012;92:184-188.
40. Li L, Qiong GQ, Dong J, Xu T, Li J. DNA binding, DNA cleavage and BSA interaction of a mixed-ligand copper(II) complex with taurine Schiff base and 1,10-phenanthroline. Photochem.Photobiol. B 2013;125:56-62.
41. Bi S, Pang B, Zhao T, Wang T, Wang Y, Yan L. Binding characteristics of salbutamol with DNA by spectral methods. Spectrochim. Acta, Part A 2013;111:182-187.
42. Ćoćić D, Jovanović S, Nišavić M, Baskić D, Todorović D, Popović S, Bugarčić ŽD, Petrović B. New dinuclear palladium(II) complexes: Studies of the nucleophilic substitution reactions, DNA/BSA interactions and cytotoxic activity. J. Inorg. Biochem. 2017;175:67-79.
43. Novakova O, Chen H, Vrana O, Rodger A, Sadler PJ, Brabec V. DNA Interactions of Monofunctional Organometallic Ruthenium(II) Antitumor Complexes in Cell-free Media. Biochemistry 2003;42:11544-11554.
44. Rizvi MA, Zaki M, Afzal M, Mane M, Kumar M, Shah BA, Srivastav S, Srikrishna S, Peerzada GM, Tabassum S. Nuclear blebbing of biologically active organoselenium compound towards human cervical cancer cell (HeLa): In vitro DNA/HSA binding, cleavage and cell imaging studies. Eur. J. Med. Chem. 2015;90:876-888.
45. Recio Despaigne AA, Da Silva JG, da Costa PR, dos Santos RG, Beraldo H. ROS-Mediated Cytotoxic Effect of Copper(II) Hydrazone Complexes against Human Glioma Cells. Molecules 2014;19:17202-17220.
46. Dhar S, Nethaji M, Chakravarty AR. Effect of charge transfer bands on the photo-induced DNA cleavage activity of [1-(2-thiazolylazo)-2-naphtholato]copper(II) complexes. J. Inorg. Biochem. 2005;99:805-812.
47. Wang Y, Zhang H, Zhang G, Tao W, Tang S. Interaction of the flavonoid hesperidin with bovine serum albumin: A fluorescence quenching study. J. Lumin. 2007;126:211-218.

48. Johansson JS. Binding of the volatile anesthetic chloroform to albumin demonstrated using tryptophan fluorescence quenching. J. Biol. Chem. 1997;272:17961-17965.
49. Psomas G, Kessissoglou DP. Quinolones and non-steroidal anti-inflammatory drugs interacting with copper(II), nickel(II), cobalt(II) and zinc(II): structural features, biological evaluation and perspectives. Dalton Trans. 2013;42:6252-6276.

# CORRELATION OF DIFFERENT ANTHROPOMETRIC METHODS AND BIOELECTRIC IMPEDANCE IN ASSESSING BODY FAT PERCENTAGE OF PROFESSIONAL MALE ATHLETES

Marko Dimitrijevic[1], Dijana Lalovic[2] and Djordje Milovanov[3]

[1]*University of Kragujevac, Faculty of Medical Sciences, Department of Physiology, Kragujevac, Serbia*
[2]*Medical High School "Nadezda Perovic", Zemun, Belgrade, Serbia*
[3]*University of Novi Sad, Faculty of Sport and Physical Education, Novi Sad, Serbia*

Received: 25.03.2021.
Accepted: 17.04.2021.

**Corresponding author:**

**Marko Dimitrijevic**

University of Kragujevac, Faculty of Medical Sciences, Department of Physiology, Kragujevac, Serbia

E-mail: dimitrijevic_marko@yahoo.com

sciendo

UDK: 612.769:796.42.012.1-051
Eabr 2024; 25(2):127-135
DOI: 10.2478/sjecr-2021-0026

## ABSTRACT

*Studies examining correlation of existing anthropometric methods developed for specific and general athlete population and BIA method are much more scarce and often conducted using only one anthropometry method for comparison with BIA method per study. Aim: Examination of the correlation between different anthropometric methods and BIA method in assessing body fat percentage of general male athlete population. The study was conducted using 85 professional athletes from Serbia, average age of 23,7 ± 4,3 years. Correlation between anthropometric methods and BIA method was examined using Spearman rang correlation. Sixteen anthropometric equations using a total of ten skinfolds were selected from eleven anthropometric methods developed for specific or general male athlete population. All sixteen anthropometric equations revealed a strong correlation with BIA method. Faulkner's anthropometric skinfold equation (%BF = 5,783 + (0,153 (triceps + subscapular + supra-iliac + abdominal)) revealed the strongest correlation coefficient ($r_s$ = 0,792) and the shortest bias-corrected and accelerated confidence interval length (BCa CI 95% (0,712 - 0,849)). Even though ten of the sixteen anthropometric equations revealed a very strong correlation, Faulkner's equation showed the largest Spearman's correlation coefficient with BIA method in assessing body fat of professional male athletes. Faulkner's equation may be the best candidate that can be used as replacement of BIA method for general male athlete population. It would be useful and interesting to repeat a similar study with the addition of one of the referent methods from the second level of validity group.*

***Keywords***: *Body fat, anthropometry, skinfolds,anthropometric equation, male athletes,bioelectrical impedance, BIA.*

## INTRODUCTION

Body composition component in form of fat tissue is very important for sports performance (1,2,3,4,5,6,7) It is known that body fat percentage affects the cardiorespiratory ability of male athletes (8), as well that both high and low levels of body fat can put athletes in an unwanted situation (9). Today we are familiar with a large number of methods that can be applied in the analysis of body composition. More precise methods for body composition analysis such as magnetic resonance imaging (MRI), computed tomography (CT), dual-energy X-ray absorptiometry (DXA), plethysmography (ADP) and other second level validity methods are rarely available to us due to financial constraints and the need for trained staff. Because of this, alternative, third level validity methods such as anthropometry and bioelectrical impedance analysis are far more often used on a daily basis for general population, i.e. for non-athletes, people who do recreational sports and athletes. Besides a far more affordable price, the advantages of these alternative methods are also reflected in non-invasiveness, portability and in their simple and fast application in body composition analysis.

On the other hand, one of the biggest disadvantages of these methods is that they are considered less accurate than the aforementioned second level validity methods. In practice we can find numerous anthropometric methods, but the most common ones are those using measured values of skinfolds thickness at defined points of the body and specific mathematical formulas to estimate the body fat percentage. The most common bioelectrical impedances (BIA) are portable models, which today can be seen more and more often in fitness and wellness centers, but also in private homes. Both BIA and anthropometric methods are considered to have a measurement error in estimating body fat of about ± 3.5%, assuming that all preconditions for measurement and analysis are fulfilled (10). However, in situations where athletes have to travel, anthropometric methods still show certain portable advantages. Anthropometric equipment is more practical for transporting compared to BIA analyzers being bigger in size, robust and carry the risk of electronic component damage or failure. Bioelectrical impedance also requires an athlete preparation protocol starting 48 hours prior to measurement which is not practical when going on a trip, while with anthropometry this is not the case. There is also the possibility of temporal disruption of physiological systems caused by air travel or any longer land travel that may lead to somewhat reduced accuracy of BIA, which is not the case with anthropometry where the measurement is performed anatomically. This can influence coaches, sports experts or sports physicians to use anthropometry, especially in situations where athletes often change location and travel to away games, competitions and preparation camps. When it comes to male athletes, Forsythe and Sinning already investigated back in 1973. and pointed out that anthropometric equations developed for the general non-athletic population are not accurate enough in estimating body fat in male athletic population. (11). Throughout decades, numerous anthropometric methods based on sport specificity have been developed through research (12,13,14) and also based on general samples of athletes from different sports, by determining the correlation of these methods with one of the second level validity reference methods (11,15,16,17,18,19) in evaluating body fat of athletes. A smaller number of studies have been conducted in examining the correlation between anthropometric methods and BIA method in general population of male athletes or in sport-specific male population, where second level validity reference method was not included (20,21). However, these studies often examined the correlation of anthropometric methods and BIA method by using only one sports anthropometric method and equation in the study. Determining whether some of the already existing and represented sports anthropometric methods (sports-specific or general sports methods) can replace BIA method in estimating body fat percentage of general male athlete population could be one of the solutions for athletes, coaches and sports experts to avoid confusion and encourage them to use anthropometry in the field of practice, either for traveling needs or using it as personal preference.

In accordance with the previous, the aim of this study is to examine the correlation of different anthropometric methods and BIA methods in estimating body fat percentage of male professional athletes from different sports.

## MATERIALS AND METHODS

### Participants

The study included eighty five professional athletes (N=85), 17 - 33 years of age, recruited from four different sports, wrestling (n=28), football (n=28), boxing (n=15) and basketball (n=14). All recruited athletes were members of FIT IN health-related fitness club in Belgrade, where they performed part of their conditioning procedures. The inclusion criteria included athletes who were competing in sports for more than 3 years and not having any long training breaks or any rest caused by an injury or any other factor within last six months.

### Procedures

Athletes were examined in the laboratory for sports medicine and exercise therapy at the Institute of Physiology "Richard Burian" in Belgrade. Anthropometric measurement procedures was conducted in accordance with the guidelines and recommendations of International Standards for Anthropometric Assessment (ISAK) (22,23). Procedure for BIA analysis was conducted using BIA pre-test guidelines (24). Athletes were not pressured to participate in the study and after being well informed they voluntarily signed the consent form for participating in the study.

**Table 1.** Athlete characteristics

| Sport / Variables | Basketball (n=14) X ± SD range | Football (n=28) X ± SD range | Boxing (n=15) X ± SD range | Wrestling (n=28) X ± SD range | Total (N=85) X ± SD range |
|---|---|---|---|---|---|
| **Age (years)** | 25.4 ± 4.2<br>17.2 - 31 | 23.9 ± 4.2<br>17.5 - 33 | 23.687 ± 4.2<br>17.4 - 32.2 | 21.4 ± 6.4<br>17.5 - 32.9 | 23.7 ± 4.3<br>17.2 - 33 |
| **Height (cm)** | 198.3 ± 10.8<br>171.2 - 211 | 181.9 ± 5.1<br>169.0 - 190.5 | 186.4 ± 7.2<br>175 - 198 | 176.7 ± 7.7<br>155.0 - 191.5 | 183.7 ± 10.4<br>155 - 211 |
| **Weight (kg)** | 96.1 ± 19.2<br>43.7 - 120.6 | 77.2 ± 5.6<br>67.3 - 86.5 | 87.7 ± 17.5<br>59.8 - 123.4 | 80.6 ± 11.7<br>59.5 - 105.2 | 83.3 ± 14.4<br>43.7 - 123.4 |
| **BMI ($kg/m^2$)** | 24.1 ± 3<br>14.9 - 27.3 | 23.3 ± 1.1<br>21.2 - 25.3 | 25.1 ± 3.4<br>19.3 - 32.3 | 25.7 ± 2.5<br>22.4 - 31.2 | 24.6 ± 2.6<br>14.9 - 32.3 |
| **FFMI ($kg/m^2$)** | 21.7 ± 2.5<br>14 - 25.4 | 21.2 ± 0.9<br>19.7 - 22.9 | 21.9 ± 2.2<br>17.6 - 26.4 | 22.4 ± 1.7<br>20.1 - 26.1 | 21.8 ± 1.8<br>14 - 26.4 |
| **BIA-BF (%)** | 10 ± 3.2<br>5.5 - 15.4 | 8.8 ± 2.1<br>169.0 - 190.5 | 12.2 ± 3.6<br>7 - 19.2 | 12.6 ± 2.8<br>7.4 - 18.4 | 10.8 ± 3.3<br>4.9 - 19.2 |

X - mean; SD - standard deviation; n - number of subjects within a group; N - total number of subjects; BMI - body mass index; FFMI - fat-free mass index; BIA-BF - body fat percentage estimated with bioelectrical impedance.

**Equipment**

Skinfolds measurement was performed using Harpenden caliper (model HSB-BI, produced by company HaB Direct, United Kingdom) with measuring range from 0 to 80 mm (caliper needle can go four full circles around a dial scale with gradation from 0 to 20 mm), measuring pressure on a lifted skinfold of 10 gr/mm² and reading accuracy of 0.2 mm. Athletes height was measured with roll-up measuring tape with wall attachment (model SECA 206, produced by SECA, Germany), providing measuring range of 0 - 220 cm with 1 mm gradation. Body weight measurement and estimation of body fat were conducted using hand-to-foot type BIA (model InBody 230, produced by InBody, Republic of Korea). All additional needed equipment was prepared and calibrated before measurement took place.

**Anthropometric and BIA measurement**

Anthropometric measurement of skinfolds was conducted using ISAK guidelines and recommendations (22,23). Bioelectrical impedance analysis was conducted according to the manufacturer's instructions for model InBody 230. Complete testing of every individual athlete was conducted on the same day. Upon testing arrival, athletes performed BIA analysis first, having their body fat percentage assessed and their body weight measured. After BIA analysis was completed anthropometric measurements of body height and skinfolds thickness were conducted. An anthropometrist with a decade of experience in practice was recruited for anthropometric measurement.

**Anthropometric methods**

Eleven anthropometric methods designed for different male athlete populations were selected for the study and then a total of sixteen skinfold equations (formulas) were selected from these methods (Table 2). The inclusion criterion for anthropometric equations was met with equations being developed for a specific sport population or for general male sport population, by using only measurements of skinfolds or measurements of skinfolds combined with some of the basic anthropometric or descriptive characteristics such as body height and weight, body mass index and age. Also, only equations developed through regression analysis with the highest multiple correlation coefficients between a dependent variable and a group of independent variables (R) or that explained the largest variance in dependent variable by using independent variables ($R^2$) (depending on what was reported in an individual study, R or $R^2$), when these anthropometric equations were correlated with referent methods within a study.

**Table 2.** Selected anthropometric methods and equations developed for assessing body fat in different male athlete populations.

| Author(s)/ method | Anthropometric equation |
|---|---|
| Yuhasz (25) | Equation using 6 skinfolds. %BF = 3.64 + (0.097 (Ch + Tr + Sb + Si + Ab + Th)) |
| Faulkner (26) | Equation using 4 skinfolds, today considered a modified Yuhasz method (27). %BF = 5.783 + (0.153 (Tr + Sb + Si + Ab)) |
| Forsyth & Sinning 1 (11) | Equation using 2 skinfolds (equation no. 2a). BD = 1.103 − (0.00168 x Sb) − (0.00127 x Ab) |
| Forsyth & Sinning 2 (11) | Equation using 4 skinfolds (equation no. 2b). BD = 1.10647 − (0.00162 x Sb) − (0.00144 x Ab) − (0.00077 x Tr) + (0.00071 x Ma) |
| Forsyth & Sinning 3 (11) | Equation using 2 skinfolds and height (equation no. 3a). BD = 1.02415 − (0.00169 x Sb) + (0.00444 x Ht) - (0.00130 x Ab) |
| Forsyth & Sinning 4 (11) | Equation using 4 skinfolds and height (equation no. 3b). BD = 1.03316 − (0.00164 x Sb) + (0.00410 x Ht) - (0.00144 x Ab) - (0.00069 x Tr) + (0.00062 x Ma) |
| White et al. (12) | Equation using 2 skinfolds. BD = 1.0958 − (0.00088 x Si) − (0.0006 x Th) |
| Thorland et al. 1 (19) | Equation using 7 skinfolds. BD = 1.1091 − (0.00052 (Tr + Sb + Ma + Si + Ab + Th + Ca)) + (0.00000032 (Tr + Sb + Ma + Si + Ab + Th + Ca)$^2$) |
| Thorland et al. 2 (19) | Equation using 3 skinfolds. BD = 1.1136 − (0.00154 (Tr + Sb + Ma)) + (0.00000516 (Tr + Sb + Ma)$^2$) |
| Withers et al. (28) | Equation using 7 skinfolds, not fully published in the original 1987 paper by Withers et al. (28), but can be found in Reilly et al. study (13) derived from Withers et al. data. BD = 1.0988 − (0.0004 (Tr + Sb + Bc + Sp + Ab + Th + Ca)) |
| Evans et al. 1 (18) | Equation using 7 skinfolds, gender and race. %BF = 10.566 + (0.12077 (Sb + Tr + Ch + Ma + Si + Ab + Th)) - (8.057 x gender) − (2.545 x race) |
| Evans et al. 2 (18) | Equation using 3 skinfolds, gender and race. %BF = 8.997 + (0.24658 (Ab + Th + Tr)) - (6.343 x gender) - (1.998 x race) |
| Oliver et al. (14) | Equation using 7 skinfolds (equation model number 3). %BF = 3.53 + (0.132 (Ch + Tr + Sb + Ma + Si + Ab + Th)) |
| Reilly et al. (13) | Equation using 4 skinfolds. %BF = 5.174 + (0.124 x Th) + (0.147 x Ab) + (0.196 x Tr) + (0.13 x Ca) |
| Civar et al. (16) | Equation using 3 skinfolds and weight. BF% = (0.432 x Tr) + (0.193 x Ab) + (0.364 x Bc) + (0.077 x Wt) - 0.891 |
| Stewart & Hannan (17) | Equation using 2 skinfolds and weight. This equation estimates body fat in grams, which are then converted into body fat percentage for BIA comparison. BFM = (331.5 x Ab) + (356.2 x Th) + (111.9 x Wt) − 9108 |

Ht - height; Wt - weight; BD - body density; BF% - body fat percentage; BFM - body fat mass in grams; Tr - triceps skinfold; Ma - midaxilar skinfold; Sb - subscapular skinfold; Ab - abdominal skinfold; Si - suprailiac skinfold; Sp - supraspinale skinfold; Th - quadriceps skinfold; Ca - calf skinfold (medial calf); Ch - chest skinfold; Bc - biceps skinfold; gender - men = 1; race - African American = 1, Caucasian = 0.

Anthropometric measurement included the following ten skinfolds: subscapular, midaxillar, chest (pectoral), abdominal, biceps, triceps, suprailiac, supraspinale, quadriceps and medial calf. Locating and measuring skinfolds was conducted accordance with ISAK guidelines and recommendations (22). Additionally, Siri equation was applied to convert body density to body fat percentage for anthropometric equations that only estimated only body density (29). Determining the test-retest reliability of anthropometric measurement was performed using the method of technical measurement error (TEM) of a measurer, where a deviation of up to 7.5% for skinfolds and up to 1.5% for other anthropometric measures is considered acceptable. The calculation of the TEM was carried out according to the recommendations by Norton (23).

**Statistical analysis**

Statistical analysis was conducted using SPSS statistical program, package version 25 (30). Linearity for model validity, outliers and data normality distribution were checked using scatter plot graph, Q-Q plot, histogram, skewness and kurtosis and Kolmogorov-Smirnov test. Based on this, examining the correlation of anthropometric methods and BIA method was conducted using Spearman's rang correlation ($r_s$), where values of $r_s$ = 0.0 - 0.09) were considered trivial, $r_s$ = 0.10 - 0,29 small, $r_s$ = 0.30 - 0.49 moderate, $r_s$ = 0.50 - 0.69 large, 0.70 - 0.89 very large, 0.90 - 0.99 almost perfect and $r_s$ = 1 perfect correlation (31). Descriptive data was described through means and standard deviations (mean ± SD). Statistical significance was set at 0,05. Confidence interval was set at 95%.

## RESULTS

Ten anthropometric equations revealed a very large correlation with BIA method (rs = 0.70 – 0.89) while 6 anthropometric equations revealed a large correlation with BIA method (rs = 0.50 – 0.69). All sixteen anthropometric equations showed correlation statistical significance of $p < 0.001$. Out of the ten anthropometric equations with a very large correlation coefficient, six equations slightly isolated and showed a correlation of 0.760 or larger (Yuhasz, rs = 0.769; Faulkner, rs = 0.792; White et al., rs = 0.761; Thorland et al. 1, rs = 0.760; Evans et al. 1, rs = 0.761; Oliver et al., rs = 0.761). Out of these six equations, along with their highest correlation coefficients, the narrowest bias-corrected and accelerated confidence interval was revealed in equations of Yuhasz with interval length of 0.191 (BCa CI 95% (0.649 – 0.840)), Faulkner with interval length of 0.137 (BCa CI 95% (0.712 – 0.849)) and White et al. with interval length of 0,174 (BCa CI 95% (0.665 – 0.837)), isolating these three equations furthermore from the rest.

**Table 3.** Correlation of different anthropometric methods and BIA method in assessing body fat percentage of professional male athletes.

| Method | | N | $r_s$ | BCa CI 95% lower - upper |
|---|---|---|---|---|
| Yuhasz (25) | vs BIA | 85 | 0.769 *** | 0.649 - 0.840 |
| Faulkner (26) | vs BIA | 85 | 0.792*** | 0.712 - 0.849 |
| Forsyth & Sinning 1 (11) | vs BIA | 85 | 0.743 *** | 0.619 - 0.823 |
| Forsyth & Sinning 2 (11) | vs BIA | 85 | 0.738 *** | 0.627 - 0.019 |
| Forsyth & Sinning 3 (11) | vs BIA | 85 | 0.676 *** | 0.536 - 0.775 |
| Forsyth & Sinning 4 (11) | vs BIA | 85 | 0.685 *** | 0.545 - 0.786 |
| White et al. (12) | vs BIA | 85 | 0.761 *** | 0.665 - 0.837 |
| Thorland et al. 1 (19) | vs BIA | 85 | 0.760 *** | 0.650 - 0.848 |
| Thorland et al. 2 (19) | vs BIA | 85 | 0.736 *** | 0.613 - 0.830 |
| Whiters et al. (13) | vs BIA | 85 | 0.674 *** | 0.502 - 0.796 |
| Evans et al. 1 (18) | vs BIA | 85 | 0.761 *** | 0.642 - 0.845 |

| Method | | N | $r_s$ | BCa CI 95% lower - upper |
|---|---|---|---|---|
| Evans et al. 2 (18) | vs BIA | 85 | 0.674 *** | 0.518 - 0.791 |
| Oliver et al. (14) | vs BIA | 85 | 0.761 *** | 0.614 - 0.843 |
| Reilly et al. (13) | vs BIA | 85 | 0.681 *** | 0.535 - 0.793 |
| Civar et al. (16) | vs BIA | 85 | 0.740 *** | 0.625 - 0.819 |
| Stewart & Hannan (17) | vs BIA | 85 | 0.681 *** | 0.543 - 0.787 |

BIA - bioelectrical impedance; $r_s$ -Spearman's correlation coefficient; p - statistical significance;
*** - $p < 0.001$; BCa CI 95% - bias-corrected and accelerated confidence interval, set at 95% confidence.

## DISCUSSION

The aim of this study was to identify if any of the existing anthropometric methods developed for male athlete population (general or specific) are applicable to general male athlete population as replacement for BIA method. A trend can be noticed of publishing studies in journals across the world that are developing and suggesting new population-specific anthropometric methods and equations for determination body fat percentage. It is also noticeable that the most numerous of these population-specific methods are developed for specific or general athlete populations (13,14,16,17,32) and for nation-specific populations (specific to anthropology or characteristics of a certain nation) (32-37). Publishing and suggesting a large number of anthropometric methods and equations for athlete population, which amounts up to tens of equations developed for popular sports, can be confusing and exhausting for coaches and sport experts when they are making a decision in selecting and applying anthropometric method for their athletes. Also, being exposed to numerous anthropometric methods increases the chances for selecting inadequate anthropometric method for their athletes which can lead to significant mismanagement in regulation of body fat percentage. Examples of inadequate selection of anthropometric methods in practice can be noticed when coaches and sport experts apply popular anthropometric methods developed for general or general male non-athlete population such as Jackson and Pollock (38), Durnin & Womersley (39), Sloan (40) or Lohman (41) for their male athlete population.

The specificity of anthropometric methods should cover parameters or factors of gender, race, age, method and protocol used for skinfold measuring, condition level or competition level, nation (anthropology) etc. All these factors should be taken into consideration during the selection of specific or general athlete anthropometric methods and equations. This means that even if coaches or sport experts decide to select an anthropometric method developed on the sample of athletes from the same sport, chances are that even that method won't be precise enough for their athletes unless all aforementioned factors of specificity match with the athletes which comprised the sample in the development of that anthropometric method. Considering everything said, it can be roughly concluded that the only precise anthropometric method for athletes would have to include coaches or sport experts conducting their own anthropometric measurement and applying regression analysis, thereby developing their own anthropometric equations using only their athletes as the sample. These kind of complications and uncertainties can influence coaches and sport experts to avoid using anthropometry and to prefer the use of BIA method for assessing body fat percentage. As aforementioned, anthropometry also has advantages in field practice. For example, anthropometric equipment takes up a lot less space than BIA instruments, it weights less and doesn't possess any electrical components therefore creating almost no risk from damage during transport. These can be significant advantages of anthropometry compared to BIA when athletes are obligated to travel to preparation camps or competitions, especially if we are considering transporting a higher quality and bigger size (therefore more expensive as well) BIA instrument.

Precision of BIA analysis can be affected by physiological oscillations in human body and potential physiological oscillations during airplane travel or longer land travel, and also it requires athletes to deal with a long and unpopular preparation protocol (48 hours) and requires coaches trust that athlete fully complied with the preparation protocol before BIA analysis, while anthropometry is based on anatomical measurements which require a much simpler athlete testing preparation. In conjunction with the previous, authors of this study considered that it would be useful to examine and provide athletes, coaches and other sport experts with an option of applying an existing anthropometric method to general male athlete population that reveals the closest correlation coefficient to BIA method and therefore can be used as BIA replacement in field practice, either by circumstantial need, personal preference, or simply to eliminate uncertainty and potential selection of inadequate anthropometric methods for specific athletes, which are usually lacking specificity factors.

Anthropometric methods and equations today are numbered by the hundreds. For this study, we selected more common and known anthropometric methods developed for athletes that are used in practice up to a few decades back.

Results of all sixteen anthropometric equations revealed a strong correlation with BIA method, which is somewhat interesting considering that some of the included anthropometric methods and equations were developed using samples of athletes coming from different sports, using general samples of athletes, using different reference methods (DXA, MRI, CT, ADP etc.), applying different models for assessing body composition (two-component, three-component, four-component, etc.), probably with large technical error of skinfold measurement caused by different anthropometry measurers (inter-tester TEM) and protocols, and in the time span of more than 40 years (changes in average athletes body composition and constitution over decades), so it would be more logical that some anthropometric methods reveal much more different correlation coefficients than others in comparison with BIA method.

Results of this study showed that six anthropometric equations with Spearman's coefficient of $r_s$ = 0.760 or stronger, somewhat distanced themselves in correlation with BIA method compared to other methods, even though this distance was minimal. Out of these six equations, Yuhasz, Faulkner and White et al. equations separate themselves furthermore at the top with correlation coefficients of $r_s$ = 0,769, $r_s$ = 0.792 i $r_s$ = 0.761, and with bias-corrected and accelerated confidence interval length of 0.191 (BCa CI 95% (0.649 – 0.840)), 0.137 (BCa CI 95% (0.712 – 0.849)) and 0.174 (BCa CI 95% (0.665 – 0.837)). Even though it used to be seen mostly in studies examining statistical difference, lately, a trend of calculating and adding confidence intervals as important correlation indicators can been noticed in correlation studies as well. The reason for this is that correlation coefficients attained in correlation studies refer to our observed sample from a specific population, while for example a confidence interval of 95% tells us that in 95% of cases a true correlation coefficient for our targeted population (in this case professional male athletes) should fall within attained confidence interval range of an individual anthropometric method and BIA method. A shorter length (narrower range) of confidence interval leads to the assumption that the correlation coefficient for our observed sample ($r_s$) must be close to the true correlation coefficient for our specific population, or at least closer than those correlation coefficients with wider confidence interval lengths. Besides revealing the highest correlation coefficients, Yuhasz, Faulkner and White et al. anthropometric equations also revealed the shortest confidence intervals ranges, and alongside Thorland et al. 1 and Civar et al. equations, these three were the only equations revealing confidence intervals shorter than 0.2 and therefore indicated correlation coefficients closer to the true correlation coefficient than other anthropometric methods when correlated with BIA method.

Faulkner's anthropometric method or equation revealed the highest correlation coefficient, reaching almost $r_s$ of 0.80 when compared with BIA method. Faulkner's equation was originally considered a method developed for a population of swimmers (26), however motivated by the lack of evidence of it's development, in 2007 Pires-Neto and Graner managed to reveal and point out that this method is actually a modified Yuhasz method (27). Furthermore, by answering the question proposed by Pires-Neto and Graner in 2006 about this methods origin, Faulkner reveals that this equation was modified by Yuhasz himself by combining data of two anthropometric equations which were previously published in his dissertation in 1962. (42), but he couldn't remember how exactly Yuhasz performed this modification (27). Pires-Neto and Graner then suggested that Faulkner's equation should be addressed as Yuhasz's unpublished equation, because evidence revealed that Faulkner did not develop this equation by using a sample of swimmers. By further analyzing Faulkner's equation and comparing it with other studies, among other finding Pires-Neto and Graner state da Faulkner's equation is applicable to young trained male population (27). This part of Pires-Neto and Graner's conclusion matches the results obtained in this study. A young trained male population can be compared with a sample of relatively young athletes (23.7 ± 4.3 years of age) from this study, while a sample of young athletes from different sports in this study (wrestling, football, boxing, basketball) can be compared with the sample used for Yuhasz's method (university martial arts athletes and swimmers, basketball players selected for Olympics and others), or in other words, can be compared with the sample from Yuhasz's population from which the Faulkner's equation was developed.

One of the main limitations of this study was the lack of reference method of second level of validity for estimating body fat, by which besides determining the correlation with BIA method we could also determine if one of the selected anthropometric methods for athletes in this study correlates more accurately than BIA method, for our professional male athlete population. Without a reference method, results of this study can only showcase if one of the existing anthropometric methods is applicable as a replacement for BIA method on general male athlete population. By adding a second level of validity reference method, we would also be able develop a new anthropometric equation based on the athlete sample like the one in this study.

## CONCLUSION

This study examined weather any of existing and relatively used anthropometric methods reveal sufficiently similar results to BIA method within male population of professional athletes. This can provide coaches and sports experts an easier selection and enable them an option to replace BIA method with one of the already existing sports anthropometric methods, eliminating at the same time the risk of selecting an inadequate method. Faulkner's anthropometric method (unpublished Yuhasz's equation) showed the largest correlation and the narrowest bias-corrected and accelerated confidence interval with BIA method thus suggesting that this correlation coefficient probably deviates least from the professional male athletes population's true correlation coefficient. This further indicates that it would be very useful and interesting to repeat this kind of study or similar one with the addition of one of the second level of validity reference

methods such as magnetic resonance, computed tomography or dual-energy X-ray absorptiometry.

## ACKNOWLEDGEMENTS

None

## CONFLICT OF INTEREST

Authors declare no conflict of interest.

## FUNDING

None.

## REFERENCES

1. Ostojic SM. Changes in body fat content of top-level soccer players. J Sports Sci Med. 2002;1(2):54-5.
2. Reilly T. Science and Soccer. In: Reilly T, editor. London: E. & F.N. Spon; 1996. p. 25-49.
3. Ostojic SM, Zivanic S. Effects of training on anthropometric and physiological characteristics of elite Serbian soccer players. Acta Biol Med Exp. 2001;(27):48.
4. Reilly T, Collins K. Science and the Gaelic sports: Gaelic football and hurling. Eur J Sport Sci. 2008;8(5):231-40.
5. Torres Navarro V, Campos Granell J, Aranda Malavés R. Influencia de la masa grasa para el VO2max y Umbrales Ventilatorios en jóvenes deportistas de especialidades deportivas de resistencia. Sport Sci J Sch Sport Phys Educ Psychomot. 2016;3(1):530.
6. Ramos NJ, Zubeldía GD. Masa Muscular y Masa Grasa, y su relación con la Potencia Aeróbica y Anaeróbica en Futbolistas de 18 a 20 años de Edad (Parte II). PubliCE. 2003;173.
7. Kelly RA, Collins K. The seasonal variations in anthropometric and performance characteristics of elite intercounty gaelic football players. J Strength Cond Res. 2018;32(12):3466-73.
8. Stojanović D, Branković N. Association Between Body Composition and Cardiorespiratory Fitness of Adolescents. Facta Univ Ser Phys Educ Sport. 2018;16(2):297.
9. Mooses M, Hackney AC. Anthropometrics and Body Composition in East African Runners: Potential Impact on Performance. Int J Sports Physiol Perform. 12(4):422-30.
10. Heyward VH, Wagner D. Applied Body Composition Assessment. 2nd ed. Champaign (IL): Human Kinetics; 2004. 280 p.
11. Forsyth HL, Sinning WE. The anthropometric estimation of body density and lean body weight of male athletes. Med Sci Sports. 1973;5(3):174-80.
12. White J, Mayhew JL, Piper FC. Prediction of body composition in college football players. J Sports Med Phys Fitness. 1980;20(3):317-24.
13. Reilly T, George K, Marfell-Jones M, Scott M, Sutton L, Wallace JA. How well do skinfold equations predict percent body fat in elite soccer players? Int J Sports Med. 2009;30(8):607-13.
14. Oliver JM, Lambert BS, Martin SE, Green JS, Crouse SF. Predicting football players' dual-energy x-ray absorptiometry body composition using standard anthropometric measures. J Athl Train. 2012;47(3):257-63.
15. Bell W. Football Players. 1995;29(1):46-51.
16. Civar S, Aktop A, Tercan E, Ozdol Y, Ozer K. Validity of leg-to-leg bioelectrical impedance measurement in highly active women. J Strength Cond Res. 2006; 20(2):359-65.
17. Stewart AD, James Hannan W. Prediction of fat and fat-free mass in male athletes using dual x-ray absorptiometry as the reference method. J Sports Sci. 2000;18(4):263-74.
18. Evans EM, Rowe DA, Misic MM, Prior BM, Arngrímsson SÁ. Skinfold prediction equation for athletes developed using a four-component model. Med Sci Sports Exerc. 2005;37(11):2006-11.
19. Thorland W, Johnson G, Tharp G, Housh T, Cisar C. Estimation of body density in adolescent athletes. Hum Biol. 1984;56:439-45.
20. Ostojic SM. Estimation of body fat in athletes: Skinfolds vs bioelectrical impedance. J Sports Med Phys Fitness. 2006;46(3):442-6.
21. Utter AC, Scott JR, Oppliger RA, Visich PS, Goss FL, Marks BL, et al. A Comparison of Leg-to-Leg Bioelectrical Impedance and Skinfolds in Assessing Body Fat in Collegiate Wrestlers. J Strength Cond Res. 2001;15(2):157-60.
22. Stewart A, Marfell-Jones M, Olds T, de Ridder H. Preliminary considerations. In: Stewart A, Marfell-Jones M, Olds T, de Ridder H, editors. International Standards for Anthropometric Assessment. 3rd ed. Lower Hutt, New Zealand: International Society for the Advancement of Kinanthropometry; 2011. p. 12.
23. Norton K. Standards for anthropometry assessment. In: Norton, K., Eston, R. (Eds.), Kinanthropometry and Exercise Physiology. London: Routledge, Taylor & Francis Group; 2018. 131-2 p.
24. Gibson, Ann L, Wagner, Dale R, Heyward VH. Advanced Fitness Assessment and Exercise Prescription. 8th ed. Champaign, Ilinois: Human Kinetics; 2018. 262 p.
25. Yuhasz MS. Physical Fitness Manual. 1ª. London, Ontario: University of Western Canada; 1974.
26. Faulkner JA. Physiology of swimming and diving. In: Falls H Exercise physiology. Baltimore: Academic Press; 1968. p. 415-46.
27. Pires-Neto SC, Glaner MF. Ponto de vista "Equação de Faulkner" para predizer a gordura corporal: O fim de um mito The "Faulkner equation" for predicting body fat:

The end of a myth. Rev Bras Cineantropometria e Desempenho Hum. 2007;9(1415-8426):207-13.
28. Withers R, Craig N, Bourdon P, Norton K. The relative body fat and anthropometric predicition of body density of male athletes. Eur J Appl Physiol Occup Physiol. 1987;56(2):191-200.
29. Siri WE. Body composition from fluid spaces and density: Analysis of methods. In: Brožek, J.Hanschels A, editor. Techniques for Measuring Body Composition. Washington, D.C.: National Academy of Science; 1961. p. 223.
30. IBM SPSS Statistics for Windows. Armonk, NY: IBM Corp; 2017.
31. Hopkins WG, Marshall SW, Batterham AM, Hanin J. Progressive statistics for studies in sports medicine and exercise science. Med Sci Sports Exerc. 2009; 41(1): 3-13.
32. Riyahi-Alam S, Mansournia MA, Kabirizadeh Y, Mansournia N, Steyerberg E, Kordi R. Development and Validation of a Skinfold Model for Estimation of Body Density for a Safe Weight Reduction in Young Iranian Wrestlers. Sports Health. 2017;9(6):564-9.
33. Eston RG, Fu F, Fung L. Validity of conventional anthropometric techniques for predicting body composition in healthy Chinese adults. Br J Sports Med. 1995;29(1):52-6.
34. Demura S, Yamaji S, Goshi F, Kobayashi H, Sato S, Nagasawa Y. The validity and reliability of relative body fat estimates and the construction of new prediction equations for young Japanese adult males. J Sports Sci. 2002;20(2):153-64.
35. Davidson LE, Wang J, Thornton JC, Kaleem Z, Silva-Palacios F, Pierson RN, et al. Predicting fat percent by skinfolds in racial groups: Durnin and womersley revisited. Med Sci Sports Exerc. 2011;43(3):542-9.
36. Hastuti J, Kagawa M, Byrne NM, Hills AP. Development and validation of anthropometric prediction equations for estimation of body fat in indonesian men. Asia Pac J Clin Nutr. 2013;22(4): 522-9.
37. Liu X, Sun Q, Sun L, Zong G, Lu L, Liu G, et al. The development and validation of new equations for estimating body fat percentage among Chinese men and women. Br J Nutr. 2015;113(9):1365-72.
38. Jackson AS, Pollock ML. Generalized equations for predicting body density of men. 1978;British Jo(40):497-504.
39. Durnin J, Womersley J. Body fat assessed from total body density and its estimation from skinfold thickness: measurements on 481 men and women aged from 16 to 72 years. Br J Nutr. 1974;32(1):77-97.
40. Sloan AW. Estimation of body fat in young men. J Appl Physiol. 1967;23(3):311-5.
41. Lohman TG. Skinfolds and body density and their relation to body fatness: a review. Hum Biol. 1981;53(2):181-225.
42. Yuhasz MS. The effects of sports training on body fat in man with predictions of optimal body weight. [Doctoral Dissertation - Phylosophy in Physical Education in the Graduate College of the University of Illinois]. Urbana (IL): University of Illinois; 1962.

sciendo

# STEROID HORMONES OF FOLLICULAR FLUID AND THE OUTCOME OF IN VITRO FERTILIZATION

Aleksandra Gavrilovic[1,2], Jelena Cekovic[1], Aida Parandilovic[1], Aleksandar Nikolov[1], Predrag Sazdanovic[1,3], Aleksandra Velickovic[4], Marija Andjelkovic[4,5] and Marija Sorak[1,6]

[1]*Clinical Center Kragujevac, Clinic of Obstetrics and Gynecology, Department for Biomedically Assisted Fertilization, Kragujevac, Serbia*
[2]*University of Kragujevac, Faculty of Medical Sciences, PhD student, Kragujevac, Serbia*
[3]*University of Kragujevac, Faculty of Medical Sciences, Department for Anatomy, Kragujevac, Serbia*
[4]*Clinical Center Kragujevac, Department for Laboratory Diagnostics, Kragujevac, Serbia*
[5]*University of Kragujevac, Faculty of Medical Sciences, Department for Biochemistry, Kragujevac, Serbia*
[6]*University of Kragujevac, Faculty of Medical Sciences, Department for Obstetrics and Gynecology, Kragujevac, Serbia*

Received: 20.10.2020.
Accepted: 03.02.2021.

**Corresponding author:**

**Aleksandra Gavrilovic**

Clinical Center Kragujevac, Clinic of Obstetrics and Gynecology, Department for Biomedically Assisted Fertilization, Kragujevac, Serbia

E-mail: alexstojanovic2207@gmail.com

## ABSTRACT

*One of the succes factors of biomedically assisted fertilization is the regular maturation of one or more oocytes. The quality of the oocytes is significantly influenced by the environment in which it is located, the so-called „microenvironment" that includes cumulus cells, follicular fluid in which hormones and growth factors involved in its growth and development are secreted. The main aim was to examine whether the concentration of steroid hormones in the follicular fluid affects the rate of fertilization and the outcome of the in vitro fertilization process itself. The study included 31 patients who were included in vitro fertilization procedure at the Department for Biomedically Assisted Fertilization, Clinic for Gynecology and Obstetrics, Clinical Center Kragujevac. We used follicular fluid as biological material for analysis. Examination of the obtained follicular fluid and collection of oocytes under a stereomicroscope was done in the embryological laboratory at the Department. Biochemical parameters of follicular fluid were analyzed in the Department for Laboratory Diagnostics, Clinical Center Kragujevac. In vitro fertilization (IVF) or intracytoplasmic sperm injection (ICSI) methods were used as the fertilization method. The criteria of the Istanbul Consensus of Clinical Embryologists were used as a reference framework for embryo quality assessment. Pregnancy was confirmed by a positive serum level of the hormone β-hCG 14 days after embryo transfer. A software package SPSS 20 was used for statistical data processing. The results of the analysis of follicular fluid samples show that there was no statistically significant difference in the concentration of estradiol, progesterone and testosterone in follicular fluid in relation to fertilization rate and the outcome of in vitro fertilization. Based on our results, it can be concluded that the concentration of steroid hormones did not affect fertilization rate and the outcome of in vitro fertilization.*

***Keywords***: *Biomedically assisted fertilization, follicular fluid, oocytes, steroid hormones.*

sciendo

UDK: 618.177-089.888.11
615.357:[577.175.6:547.92
Eabr 2024; 25(2):137-143
DOI: 10.2478/sjecr-2021-0018

## INTRODUCTION

One of the most serious problems which couples face in today's world is infertility; our country is not exception to this rule. Infertility affects approximately 10-15% of the world's population and it is constantly growing in the last decade. Globally, one in six/seven couples worldwide has some difficulty conceiving (1). Although the frequency and cause(s) of infertility are not fully characterized, current studies show that approximately 40% of cases can be attributed to the male factor, 40% to the female factor and 20% to combined problems of both sexes (2). Consequnetly, assisted reproductive techniques are developing rapidly and today include many methods for achieving pregnancy (3).

One of the factors for success of biomedically assisted fertilization is proper maturation of one or more oocytes. The main objective of embryologists is to asses the quality of oocyte based on morphology of cumulus-oocyte complex and of the oocyte itself after the removal of the cumulus cells. The oocyte quality is significantly influenced by the environment in which it is located i.e. microenvironment that includes cumulus cells as well as follicular fluid. Hormones are secreted in follicular fluid thus contributing to growth of oocyste and development (4). Therefore, in order to increase the success of biomedically assisted fertilization methods it is necessary to focus on determining critical "microenvironment" parameters that allow us to estimate the quality of oocytes easily and quickly. Any change in follicular fluid composition can affect the oocyte which may potentially affect its development and quality, fertilization and early embryonic development (5-8).

Estradiol, progesterone and testosterone are the main steroid hormones that play an important role during the follicular and luteal phases of the menstrual cycle. Nevertheless, there are still inconsistencies in the literature regarding the concentrations of estradiol and other steroid hormones in follicular fluids (9). Higher estradiol and progesterone levels were found in follicles from which oocyte with higher fertilization rate were obtained. These observations, however, have not been confirmed by other studies, but it has been proven that the quality of the embryo was not related to the levels of follicular estradiol and progesterone. Regarding pregnancy rates, increased estradiol and progesterone levels in follicular fluid were associated with greater success (10). Lower progesterone concentrations and higher testosterone concentrations were measured in follicular fluid containing germinal vesicle oocytes (*germinal vesicle* - GV) compared to follicular fluid containing MII oocytes (11).

## THE AIM

This study focuses on examining the levels of estradiol, progesterone and testosterone in the follicular fluid obtained from stimulated cycles. The main goal is to examine whether the concentration of steroid hormones in follicular fluid affects fertilization rate and the outcome of in vitro fertilization process itself.

## METHODS

### Patients

The study included 31 patients who were included in the in vitro fertilization procedure at the Department for Biomedically Assisted Fertilization, Clinic for Gynecology and Obstetrics, Clinical Center Kragujevac. All participants were informed about the objectives of the research before joining the research and all of them signed the consent for participation in the research.

The including criteria were: spouses, respectively extramarital partners who have exhausted other possibilities of infertility treatment, spouses or extramarital partners who in the existing community have one child obtained in the IVF procedure, preserved ovarian function, normal body mass index of a woman (BMI). Also, patients had to have the results of the following analyzes and diagnostics:

- microbiological tests (bacterial vaginosis, vaginal and cervical swabs for bacteria, fungi and *Chlamydia trachomatis*), virological tests (*Hepatitis B* (HbsAg), *Hepatitis C virus* (HCV), human immunodeficiency virus (HIV)), hormonal status (2-3 days of menstrual cycle - follicle-stimulating hormone (FSH), luteinizing hormone (LH), estradiol, progesterone, testosterone, prolactin, thyroid-stimulating hormone (TSH), triiodothyronine hormone (Triiodothyronine- FT3), thyroxine (Thyroxine- FT4), Anti-Mullerian hormone (AMH), cervical screening (Pap smear, colposcopy), ultrasound examination performed with a vaginal probe, hysterosalpingography (HSG).

All results had to be within the reference values.

Criteria for exclusion from the study were: Couples who have not exhausted other options for treating infertility, women who have not preserved ovarian reserve, women who have BMI >30 kg/m², anomalies and benign tumors of the uterus, fallopian tubes and ovaries that prevent the process of in vitro fertilization, the occurrence and pregnancy development, the presence of malignant or suspected tumors of the uterus, fallopian tubes and ovaries, any diseases (internal medicine, immunology, infectology, neurology, psychiatry) if they are without permission to perform the IVF procedure of the appropriate specialist, diseases in which anesthesia or pregnancy would potentially endanger the patient's life. Those patients who suffer from any other endocrine disease that has been confirmed to affect fertility were excluded from the study.

We used follicular fluid as biological material for analysis. Follicular fluid was obtained by puncturing the follicles from 18 mm to 20 mm after controlled ovarian stimulation in the intervention room at the Department for Biomedically Assisted Fertilization. Examination of the obtained follicular fluid and collection of oocytes under a stereomicroscope was done in the embryological laboratory at the Department for Biomedically Assisted Fertilization. Biochemical parameters

of follicular fluid were analyzed in the Department for Laboratory Diagnostics, Clinical Center Kragujevac.

**Stimulation of ovulation**

Stimulation of ovulation is a procedure to stimulate ovulation and controlled ovarian hyperstimulation using various stimulation protocols and the use of gonadotropin drugs, GnRH antagonists and agonists, as well as drugs that belong to the group of selective estrogen receptor blockers (SBER) (Klomifen and Letrozol).

All patients were determined for basal hormonal status, on the second or the third day of the cycle, before being included in the procedure. Serum levels of estradiol, progesterone, follicle-stimulating hormone and luteinizing hormone were determined.

A short stimulation protocol was used according to a certain scheme, depending on the gynecologist's assessment based on the ultrasound findings and hormonal status.

During the stimulation procedure, drugs belonging to the group of selective estrogen receptor blockers (SBER), injections of human menopausal gonadotropin (HMG) such as Merional or Menopur and drugs from the group of antagonists (Cetrotide) were used to counteract the effects of natural pituitary hormones.

During the stimulation, the growth of follicles and the level of sex hormones in the blood were monitored by ultrasound, with successive ultrasound and laboratory examinations.

Stimulation lasted until the leading follicle reached a diameter of 20 mm or two or more follicles with a diameter of 18 mm.

When the increase in serum estradiol concentration corresponded to the presence of two or more follicles > 18 mm, human chorionic gonadotropin (Pregnyl, Organon, the Netherlands) was administered at a dose of 5000 IU, 34-36 hours before oocyte aspiration.

**Follicular fluid and oocytes**

Oocyte aspiration is a surgical intervention and is performed by ultrasound control while the patient is under general anesthesia. The intervention lasts about 15 to 20 minutes, depending on the number and availability of follicles in the ovaries. After the aspiration of the follicles was completed, the obtained follicular fluid was examined under a microscope in the embryological laboratory and the oocyte number and quality were determined.

Follicular fluids were isolated in which oocytes were found for laboratory analysis. The entire amount of follicular fluid was centrifuged at 3000 rpm for 10 minutes to separate pure follicular fluid, without cellular elements. For the analysis itself, 5 ml of the total amount of follicular fluid was taken.

In vitro fertilization (IVF) or intracytoplasmic sperm injection (ICSI) methods were used as the fertilization method. After incubation, 16-20 hours after fertilization it is checked whether fertilization has occurred or not. Fertilization has occured if two pronuclei and / or two polar bodies are present.

The fertilization rate is calculated according to the following formula:

$$\frac{Number\ of\ fertilized\ oocytes}{Total\ number\ of\ obtained\ oocytes} \times 100$$

The criteria of the Istanbul Consensus of Clinical Embryologists were used as a reference framework for embryo quality assessment (12). Criteria include assessment of the fragmentation degree and symmetry of the blastomeres. Embryos are divided into class A (excellent, without or 1-10% fragmentation, perfect symmetry), class B (medium, 11-25% fragmentation, moderate asymmetry), class C (poor, > 25% fragmentation, expressed asymmetry). An embryo transfer of a maximum of three embryos was performed under the control of transabdominal ultrasound on the third or the fifth day after oocyte aspiration. From the day of oocyte aspiration, the patients received progesterone depot intramuscularly on the second and the fifth day as a support of the luteal phase. Pregnancy was confirmed by a positive serum level of the hormone β-hCG 14 days after embryo transfer, while clinical pregnancies were confirmed by transvaginal ultrasound findings of a gestational sac with a vital embryo at 6 weeks of gestation.

The implantation rate is calculated according to the following formula:

$$\frac{Total\ number\ of\ pregnancies}{Total\ number\ of\ transfered\ embryos} \times 100$$

The variables measured in the study were: the concentration of hormones (estradiol, progesterone and testosterone) in the follicular fluid.

The values of estradiol, progesterone and testosterone in the follicular fluid were analyzed by chemiluminescent immunoassay on the device UniCel 600, Becman Coulter in the Department for Laboratory Diagnostics, Clinical Center Kragujevac. Follicular fluid samples were diluted to determine estradiol (1: 1000) and progesterone (1: 1000) concentrations, while no follicular fluid dilution was required to determine testosterone concentration.

**Statistical data processing**

Regularity of the distribution of obtained values was confirmed by using the Kolmogorov-Smirnov test before statistical data processing. Based on the obtained value of p, the test used for statistical analysis was determined (ANOVA parametric test for $p < 0.05$ - samples having normal

distribution or nonparametric Mann-Whitney, Kruskal-Wallis and Hi square test test if $p > 0.05$ - samples that do not have a normal distribution). The value of the obtained data was considered statistically significant if $p < 0.05$. The software package SPSS 20 was used for statistical data processing. All values are expressed as a mean value and are presented in a table.

## RESULTS

Table 1 presents the relevant results and characteristics of the study group. In total 31 patients were involved, starting from age of 29 till 46. On average 9.1 oocytes were obtained per woman, however, there is a strong deviation between individual participant going from 1 till 20. Only 172 cells were normally fertilized (around 60,5%). It should be pointed out that about 58% of pregnancies were successful. Results show that measured data for estradiol concentration in follicular fluid, progesterone concentration in follicular fluid, and testosterone concentration in the follicular fluid is widely dispersed from the mean.

**Table 1.** Relevant characteristics and results of the study group

| | |
|---|---|
| Number of patients | 31 |
| Years - mean | 36,33 (29-46) |
| Total number of oocytes | 284 |
| Mean value of oocytes per patient | 9,16 (1-20) |
| Number of fertilized oocytes | 172 (1-11) |
| Number of unfertilized oocytes | 112 (0-15) |
| Fertilization rate | 60,5% |
| Achieved pregnancies (β-HCG>5) | 18 |
| Implantation rate | 31% |
| Pregnancy rate | 58% |
| Mean estradiol concentration in follicular fluid (ng/L) | 1974,65 (115,11-4859,85) |
| Mean value of progesterone concentration in follicular fluid (µg/L) | 11,44 (1,72- 20.48) |
| Mean value of testosterone concentration in the follicular fluid (ng/ml) | 5,53 (1,43-13,33) |

High p-values imply that the oocyte fertilization rate is not direclty related to the concentration of estradiol, progesterone and testosterone in the follicular fluid (see, Table 2). Nerevetheless, it should be noted that in case of normally fertilized oocytes in follicular fluid estradiol and progesterone levels were slightly lower, while testosterone levels were slightly higher. In addition, statisitcaly looking the fertilization rate is not related to the outcome of IVF (see, Table 3).

**Table 2.** Relationship between steroid hormone concentration in follicular fluid and fertilization rate

| Steroid hormones of follicular fluid | Hormone concentrations in follicular fluid (Mean 95%) | | |
|---|---|---|---|
| | Normal fertilization (172) | Poor fertilization (112) | p* |
| Estradiol ng/ml | 1821,79 | 1872,07 | 0,639 |
| Progesterone µg/ml | 10,71 | 11,01 | 0,673 |
| Testosterone ng/ml | 5,27 | 5,13 | 0,956 |

p* Statistical significance

**Table 3.** Relationship between fertilization rate and realized pregnancies

| | Positive pregnancy outcome | Negative pregnancy outcome | *p |
|---|---|---|---|
| Fertilization rate (mean value) | 67,34 (±15,15) | 61,31 (±19,22) | 0,379 |

p* Statistical significance

Analysis show that there is no statisticaly significant relation between the achieved pregnancies and applied fertilization method (see, Table 4). The pregnancies via IVF were 49% successful, while via the ICSI method 51%. Further, results indicate that there is no dependency between embryo quality and fertilization methods ($p=0,832$; $p>0,05$). Also, there is no statisitcly significant difference between participant age and realized pregnancies within the study group (see, Table 5).

**Table 4.** Relationship between in vitro fertilization outcomes and oocyte fertilization methods

| IVF outcome | Метода | | p* |
|---|---|---|---|
| | IVF | ICSI | |
| Positive outcome (β-HCG>5) | 9 (49%) | 10 (51%) | 0,121 |
| Negative outcome (β-HCG<5) | 2 (16,71%) | 10 (83,3) | |

p* Statistical significance

**Table 5.** Relationship between mean values of hormone concentrations in follicular fluid and in vitro fertilization outcomes

| Steroid hormones of follicular fluid | Hormone concentrations in follicular fluid (Mean 95%) | | |
|---|---|---|---|
| | Positive outcome (β-HCG<5) | Negative outcome (β-HCG>5) | p* |
| Estradiol ng/L | 1860,27 (115,11-4857,85) | 2133,01 (426,33-4626,82) | 0,540 |
| Progesterone µg/L | 11,28 (1,93-20,48) | 11,67 (1,72-19,56) | 0,859 |
| Testosterone ng/ml | 5,55 (2,51-13,33) | 5,48 (1,43-7,70) | 0,708 |

p* Statistical significance

Results show that there is no statisticly significant deviation between the value of estradiol in follicular fluid of pregnant women and the value of estradiol in the follicular fluid of non-pregnant women (see, Table 5). This also applies to the variation of estradiol values in follicular fluid by age of women (see, Table 6).

The value of progesterone and testosterone in the follicular fluid of pregnant women did not differ statistically from the value of progesterone in the follicular fluid of women who were not pregnant (see, Table 6). Variations in progesterone and testosterone levels in follicular fluid by age of women were also not statistically significant (see, Table 5).

**Table 6.** Relationship between follicular fluid hormone concentration and age, and between in vitro fertilization outcome and age

| Steroid hormones | Mean value of hormone concentration in follicular fluid by age | | | p* |
|---|---|---|---|---|
| | 30-34 | 35-39 | 39-42 | |
| Estradiol (ng/ ml) | 1978,97 (957,96-4626,82) | 1981,28 (426,33-4857,85) | 1959,10 (115,11-2817,11) | 0,859 |
| Progesterone (µg/ml) | 10,83 (5,96-15,62) | 10,99 (1,72-20,48) | 12,98 (7,23-17,98) | 0,626 |
| Testosterone (ng/ml) | 5,77 (2,51-13,33) | 5,01 (1,43-7,82) | 5,86 (3,52-7,70) | 0,598 |
| Positive outcome (β-HCG>5) | 8 | 8 | 2 | 0,051 |
| Negative outcome (β-HCG<5) | 4 | 3 | 6 | |

p* Statistical significance

## DISCUSSION

Approximately 10% of women are unable to naturally become pregnant until the age of 34, and for women between 40 and 45 this is 87%. Although IVF can to a certain extend increase the number of achieved pregnacnies among younger women (i.e. age below 40), these numbers are still relatively low among older women (i.e. age group 40+). All of this is associated with decreased oocyte number and poor oocyte quality with increasing age, along with a higher rate of aneuploidy (13).

It should be pointed out that not all oocytes from all follicles are of the same quality and at the same stage of maturity. Based on the defined monitoring parameters, it is not possible to know in advance which oocyte will be fertilized and provide quality embryos. Embryos of the same patient can be of different quality and still at the end not all embryos will result in pregnancy (10, 14). The various components of the follicular fluid that contains the oocytes can be used as parameters to predict the quality of the oocyte that will be fertilized and give a potentially good embryo resulting in pregnancy. Steroid hormones are important parameters among these components (15).

When comparing the outcome of IVF with the age of women who participated in the study, it can be seen that similar success rates were among women who are in the age group 30–34 and 35–39. On the other hand, the women in the age group 40–42 had the lowest pregnancy success rate. As expected fertility significantly decreases as a woman ages. Results show that steroid hormone concentrations were not in correlation with age of participants.

In this study, a combination of two methods i.e. ICSI and conventional IVF methods were used for fertilization. The results show that the success of achieving pregnancy does not depend on the method of fertilization, and the quality of the embryo does not depend on the method of fertilization. More IVF were successful after the application of the ICSI method for fertilization of oocytes.

Furthermore, no significant correlation was observed between the concentration of steroid hormones and the rate of fertilization, nor in relation to the outcome of IVF. During the study it was noticed that the concentrations of estradiol and progesterone were slightly lower, while testosterone levels were slightly higher in case of the successful IVF. This was not confirmed in an earlier study (10). Carpintero et al. noticed that elevated levels of estradiol and progesterone in the follicular fluid were associated with an increased chance of pregnancy (10). Estradiol concentrations were slightly elevated in age group 35–39. On the other hand, the concentrations of progesterone were slightly elevated, as well as the concentrations of testosterone in age group 40–42.. In-depth analysis didn't show any statistically significant difference in the concentration of estradiol, progesterone and testosterone in follicular fluid between fertilized or unfertilized oocytes. Caprineto et al. pointed out that testosterone concentrations

increased slightly with good fertilization, which was also confirmed in this study. On the other hand, Lamb et al. results show that there was no difference in testosterone concentration in follicular fluid in cases of normal fertilization compared to cases without fertilization (10,16).

Numerous studies have performed 'target analysis' but failed to identify a clinically useful biomarker(s) due to well known limitations within current medical practice. There is a still long way to go to overcome these issues (17-19). One of the major issues is the fact that transfer is done with two embryos. For example, in a situation when only one embryo was successfully implanted, it is difficult to say which embryo was implanted. Furthermore, the process of ovarian stimulation can change the composition of follicular fluid (18). Finnaly, follicular fluid contamination with a follicle flush medium that contains numerous metabolites (e.g. glucose) is possible. Some IVF centers use this method when aspirating follicular fluid. Additionaly, follicular fluid from a previously aspirated follicle can lead to fluid contamination of the next follicle.

Overall, further research is needed to enable more successful in vitro fertilization. A much larger number of follicular fluid samples are needed to more reliably determine which parameters affects the quality of oocytes and to what extent, thus the rate of fertilization i.e. the outcome of IVF.

## CONCLUSION

In today's world infertility must be perceived as a complex issue which is challenging to overcome. Even though there are constant breakthroughs within medicine, it is difficult to discover the real cause of infertility. Extra attention is being paid to the composition of follicular fluid as a possible cause of infertility. From the results, it can be concluded that the concentration of steroid hormones does not affect the fertilization rate and the outcome of in vitro fertilization. Consequnetly, the next step in research would be to further study other sex hormones in addition to steroid hormones among larger number of patients. Punctureing each follicle with multiple stitches using a separate needle for each follicle would be more insightful research, however, this is not feasible in clinical practice at the moment.

## CONCLUSION

The authors declare that there is no conflict of interest. The authors are solely responsible for the content of this article.

## CONFLICTS OF INTEREST

The authors declare no financial or commercial conflicts of interest.

## FUNDING

None.

## REFERENCES

1. Sharma R, Biedenharn KR, Fedor JM, Agarwal A. Lifestyle factors and reproductive health: taking control of your fertility. Reprod Biol Endocrinol. 2013;11:66.
2. Sharlip ID, Jarow JP, Belker AM, Lipshultz LI, Sigman M, Thomas AJ, et al. Best practice policies for male infertility. Fertil Steril. 2002;77(5):873-82.
3. Kamel RM. Assisted reproductive technology after the birth of louise brown. J Reprod Infertil. 2013;14(3):96-109.
4. Nagy B, Poto L, Farkas N, Koppan M, Varnagy A, Kovacs K, et al. Follicular fluid progesterone concentration is associated with fertilization outcome after IVF: a systematic review and meta-analysis. Reprod Biomed Online. 2019;38(6):871-882.
5. Karaer A, Tuncay G, Mumcu A, Dogan B. Metabolomics analysis of follicular fluid in women with ovarian endometriosis undergoing in vitro fertilization. Syst Biol Reprod Med. 2019;65(1):39-47.
6. Walters KA, Eid S, Edwards MC, Thuis-Watson R, Desai R, Bowman M, et al. Steroid profiles by liquid chromatography-mass spectrometry of matched serum and single dominant ovarian follicular fluid from women undergoing IVF. Reprod Biomed Online. 2019;38(1):30-37.
7. Basuino L, Silveira CF Jr. Human follicular fluid and effects on reproduction. JBRA Assist Reprod. 2016;20(1):38-40.
8. Oktem O, Urman B. Understanding follicle growth in vivo. Hum Reprod. 2010;25(12):2944-54.
9. Von Wolff M, Stute P, Eisenhut M, Marti U, Bitterlich N, Bersinger NA. Serum and follicular fluid testosterone concentrations do not correlate, questioning the impact of androgen supplementation on the follicular endocrine milieu. Reprod Biomed Online. 2017;35(5):616-623.
10. Carpintero NL, Suárez OA, Mangas CC, Varea CG, Rioja RG. Follicular steroid hormones as markers of oocyte quality and oocyte development potential. J Hum Reprod Sci. 2014;7(3):187-93.
11. Da Broi MG, Giorgi VSI, Wang F, Keefe DL, Albertini D, Navarro PA. Influence of follicular fluid and cumulus cells on oocyte quality: clinical implications. J Assist Reprod Genet. 2018;35(5):735-751.
12. Alpha Scientists in Reproductive Medicine and ESHRE Special Interest Group of embryology. The Istambul Consensus workshop of embyo assessement: procedings ofan expert meeting. J Hum Reproduction. 2011, 1–14.
13. Kim HO, Sung N, Song IO. Predictors of live birth and pregnancy success after in vitro fertilization in infertile women aged 40 and over. Clin Exp Reprod Med. 2017;44(2):111-117.
14. Kim HO, Sung N, Song IO. Predictors of live birth and pregnancy success after in vitro fertilization in infertile women aged 40 and over. Clin Exp Reprod Med. 2017;44(2):111-117.

15. O'Brien Y, Wingfield M, O'Shea LC. Anti-Müllerian hormone and progesterone levels in human follicular fluid are predictors of embryonic development. Reprod Biol Endocrinol. 2019, 17(1):47.
16. Lamb JD, Zamah AM, Shen S, McCulloch C, Cedars MI, Rosen MP. Follicular fluid steroid hormone levels are associated with fertilization outcome after intracytoplasmic sperm injection. Fertil Steril. 2010;94(3):952-7.
17. Revelli A, Delle Piane L, Casano S, Molinari E, Massobrio M, Rinaudo P. Follicular fluid content and oocyte quality: from single biochemical markers to metabolomics. Reprod Biol Endocrinol. 2009;7:40.
18. De los Santos MJ, García-Láez V, Beltrán-Torregrosa D, Horcajadas JA, Martínez-Conejero JA, Esteban FJ, et al Hormonal and molecular characterization of follicular fluid, cumulus cells and oocytes from pre-ovulatory follicles in stimulated and unstimulated cycles. Hum Reprod. 2012;27(6):1596-605.
19. Costermans NGJ, Soede NM, Blokland M, van Tricht F, Keijer J, Kemp B, et al. Steroid profile of porcine follicular fluid and blood serum: Relation with follicular development. Physiol Rep. 2019;7(24):e14320.

sciendo

# GENDER DIFFERENCES IN THE MORPHOLOGICAL CHARACTERISTICS OF THE NASOPALATINE CANAL AND THE ANTERIOR MAXILLARY BONE - CBCT STUDY

Pavle Milanovic* and Milica Vasiljevic*

*University of Kragujevac, Faculty of Medical Sciences, Department of Dentistry, Serbia*
** Pavle Milanovic and Milica Vasiljevic contributed equally (50% each) to this work, and both should be considered first authors*

Received: 25.03.2021.
Accepted: 25.03.2021.

**Corresponding author:**

**Pavle Milanovic**

University of Kragujevac, Faculty of Medical Sciences, Department of Dentistry, Serbia

E-mail: pavle11@yahoo.com

sciendo

UDK: 611.716.068-055.1/.2
615.33.015.4
Eabr 2024; 25(2):145-155
DOI: 10.2478/sjecr-2021-0029

## ABSTRACT

*The aim of this study was to investigate the gender differences in anatomical and morphometric characteristics of the nasopalatine canal-NPC and horizontal dimensions of the anterior maxilla by CBCT, which could be of interest for clinicians who perform implant surgery in this region. A retrospective quantitative study was conducted using CBCT images from the radiological database of the Department of Dentistry (Kragujevac) on a total of 113 participants (63 male and 50 female). The results of our study confirmed no gender difference in the distribution of NPC type, while the most frequent NPC type confirmed gender variations (cylindrical in females, funnel in males), but the lowest incidence of NPC type in both males and females was banana-type. The NPC length was significantly increased in males with no significant gender impact on medio-lateral (M-L) and antero-posterior (A-P) dimensions of the incisive foramen, as well as the A-P dimension of the nasal foramen. Linear regression analysis revealed the significant correlation between the M-L dimension of incisive foramen and the anterior maxilla diameter at all bone levels for males, and between the NPC length and the anterior maxilla diameter only in females at the level D. Also, both NPC type and gender significantly affected the correlations between the estimated parameters (females showed significant correlation only in funnel NPC type at the level D, while males showed significant correlation in both funnel NPC type at the level A, but also in hourglass-type at the level D). Those results imply significant gender impact in planning of various surgical interventions in the anterior maxilla region.*

***Keywords***: *Nasopalatine canal - NPC, anterior maxilla, cone beam computed tomography - CBCT, morphometric analysis, gender differenc.*

## INTRODUCTION

Surgical procedures in the anterior maxillary region include surgical extraction of impacted teeth, implant placement, endodontic treatment, periodontal surgery, the enucleation of cysts, and orthognathic surgery (1). Clinicians, such as oral, maxillofacial and plastic surgeons, which perform surgical interventions in the mouth and surrounding structures, require more detailed insight into anatomy and variations of the NPC (2). This anatomical structure forms a relationship between the nasal and oral cavity and contains the nasopalatine nerve, the descending branch of the nasopalatine artery, fibrous connective tissue and salivary glands (3).

In order to prevent NPC damage during implant surgery, radiological diagnostic is crucial to assist surgeons in the evaluation of the morphological variations of the NPC (4). The current literature described several NPC shapes. Mardinger and coworkers have classified NPC into four types (banana-, hourglass-, cylindrical- and funnel-shaped) using sagittal cross-section slices at CBCT (5). The same classification was described by Guncu and coworkers (6). However, Liang and collaborators defined the NPC shape as conical and cylindrical (7), while Etoz and colleagues (8) classified six NPC types (tree branch, cylindrical, banana-like, funnel-like, cone-like, and hourglass). Saffi and collaborators (9) proposed the classification of sagittal NPC shape into four groups (cylindrical, funnel, hourglass, and spindle). Beside, the researchers also recommend the evaluation of the NPC location and extension for the planning procedures in implant surgery (10).

In addition to the analysis of the NPC (shape, location and dimensions), the horizontal maxillary bone diameter is the most important factor for successful implant therapy (11). It is not surprising that evaluation of the labiopalatal width of the alveolar ridge is necessary before dental implant placement (12). Accordingly, Al-Amery and coworkers used three different levels for the assessment of the horizontal anterior maxilla dimensions (13). On the other hand, Salemi and collaborators measured buccal bone thickness at four levels anterior to the NPC (14). All of mentioned characteristics of both the NPC and anterior maxilla have been reported to vary depending on gender, age, ethnicity and dental status (6, 15, 16).

The numerous complications during implant surgery in the anterior maxilla were described in a literature. Namely, osseointegration failure and short-term sensory disorder are the two most frequent adverse events that have been associated with the implant placement in this region. Implant contact with the neural tissue had been reported as a prediction factor for osseointegration failure. Furthermore, NPC perforation is often accompanied with the neurovascular bundle injury, bleeding during surgery, and the formation of the NPC cyst (2, 17, 18, 19). There are many radiological modalities available for analysis of the alveolar bone dimensions and surrounding anatomical structures that may be helpful in prevention of these complications (20, 21). However, CBCT with 3D properties provides much more morphometric data for the implant placement planning than the two-dimensional radiographs (22, 23). Also, in recent years, the usage of CBCT had been widely spread for the estimation of anatomical and morphological NPC characteristics for numerous purposes (9, 24, 25).

Hence, the aim of this study was to investigate the gender differences in anatomical and morphometric characteristic of the NPC and horizontal dimensions of the anterior maxilla by CBCT, which could be of interest for clinicians who perform implant surgery in the region of the anterior maxilla.

## MATERIALS AND METHODS

### Patients' selection

A retrospective quantitative study was conducted using CBCT images from the radiological database of the Department of Dentistry, Faculty of Medical Sciences, University of Kragujevac. Radiographic images were obtained during six months (April to October 2020). The study protocol was approved by the Institutional review board of the Faculty of Medical Sciences, Unversity of Kragujevac (approval ID 01-4376).

The inclusion criteria for involvement in this study were: patients over the age of 18, presence of both lateral and central incisors, and formal consent for usage of personal clinical data in scientific purposes. The exclusion criteria were established as: low image quality, patients with systemic diseases (such as hyperparathyroidism, Paget's disease, osteoporosis), maxillary osteonecrosis, as well as the pathological entities in the NPC surrounding region (nasopalatine duct cyst, tumors, impacted teeth, cleft lips, periodontal diseases of central and lateral incisors - radiographic bone level from cementoenamel junction >3 mm). Patients with orthodontic braces, metal restoration, dental implants, bone grafting and spaced dentition were also excluded from this study. Therefore, a total of 113 participants fulfilled the inclusion criteria, 63 male and 50 female (an average age of 45.20 ± 2.14 and 41.06 ± 1.96, respectively).

### Imaging procedures

The CBCT images were obtained using an Orthophos XG 3D device (Sirona Dental Systems GmbH, Bensheim, Germany). Operating parameters were set - 85 kV/6 mA, exposure time - 14.3 s or 85 kV/10 mA, exposure time - 5.0 s, and a voxel size of 160 μm or 100 μm. The field of view was 8×8 cm for all CBCT images, and the Frankfort horizontal plane was perpendicular to the floor. GALAXIS software v1.9.4 (Sirona Dental Systems GmbH, Bensheim, Germany) was used to analyze images. The examiners analyzed the CBCT images using a monitor (23-inch Philips LED) with 1920x1080 screen resolution in a room with dim lightening.

Morphology and dimensions of nasopalatine canal and anterior maxilla

According to previously defined criteria (5), we classified the NPC into four groups (banana-, hourglass-, cylindrical- and funnel-type). The estimation of predefined NPC morphometric parameters was performed at different sections: anteroposterior (A-P) dimension of the nasal foramen, length of the NPC, A-P dimension of the incisive foramen, and mediolateral (M-L) dimension of the incisive foramen. We used sagittal CBCT slice for all morphometric analyzes of the NPC, except for the M-L dimension of incisive foramen, which was evaluated at axial CBCT slice (Figure 1). For the evaluation of the horizontal diameter of the anterior maxilla, we used sagittal CBCT slice, and measurement was obtained at four predefined levels, as shown in Figure 1. The values of all parameters were expressed in mm. All measurements were independently performed by two investigators (blind to the protocol), with high inter-rater reliability (Pearson's r=0.95). The mean value for each parameter was used for further analysis.

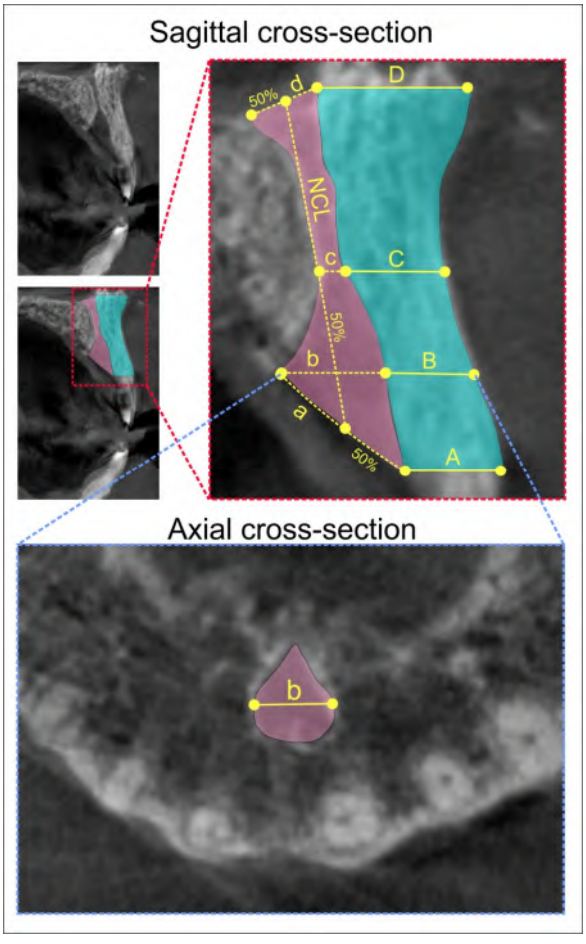


**Figure 1.** CBCT image analysis strategy.

**Sagittal cross-section with the region of interest (top)**; (a) A-P dimension of the incisive foramen, (b) level for the M-L measurement of the incisive foramen, (c) mid-length of the NPC, (d) A-P dimension of the nasal foramen, NCL (NPC length), (A) horizontal diameter of the anterior maxilla from the buccal border of incisive foramen to the facial aspect of buccal bone plate, (B) horizontal diameter of the anterior maxilla from the buccal wall of the NPC to the facial aspect of buccal bone plate using a horizontal line from the palatal border of the incisive foramen, (C) horizontal diameter of the anterior maxilla from the buccal border at the midpoint level of the NCL to the facial aspect of buccal bone plate, (D) horizontal diameter of the anterior maxilla from the buccal border of nasal foramen to the facial aspect of buccal bone plate; **Axial cross-section with the region of interest (bottom)**; (b) M-L diameter of the incisive foramen.

### Statistical analysis

The data presented here was expressed as the means ± SEM. The parameters were initially submitted to Levene's test for homogeneity of variance and to the Shapiro-Wilk test of normality. Comparisons between groups were performed using independent t-test, Pearson's chi-squared test, and/or one-way ANOVA, followed by Scheffe's post hoc test. Pearson's coefficient of correlation was used to analyze relationships between parameters, and simple linear regression analyses were performed. A value of $p<0.05$ was considered to be significant. Statistical analysis was performed with the SPSS version 20.0 statistical package (IBM SPSS Statistics 20).

## RESULTS

Results presented in Figure 2 confirmed no significant difference by means of distribution in the NPC type between male and female subjects (Pearson Chi-Square F=1.742, df=3, p=0.628). However, the distribution of the NPC type for both male and female subjects showed significant differences (Chi-Square F=11.095 and 9.040, p=0.011 and 0.029, respectively). The frequency of banana shape was the lowest for both estimated genders, but the highest incidence in male subjects was observed for funnel-type of the NPC (36.51%) while the most frequent NPC type in females was cylindrical (36%).

As presented in Figure 3, the dimensions at different sections of the nasopalatine canal and the horizontal diameter of the anterior maxilla were not significantly gender-dependent by means of both the mediolateral and anteroposterior dimension of the incisive foramen (Fig. 3A/1 and A/2, respectively). The similar situation was observed for the anteroposterior dimension of the nasal foramen (Fig. 3A/3). In contrast, the nasopalatine canal length (Fig. 3A/4) was significantly higher in male subjects ($p<0.01$). The horizontal diameter of the anterior maxilla was not significantly affected by means of gender difference at the levels of A, B, and C (Fig. 3B/1-3, respectively), but again male subjects showed significant augmentation in diameter of the anterior maxilla at the D level (Fig. 3B/4, $p<0.05$).

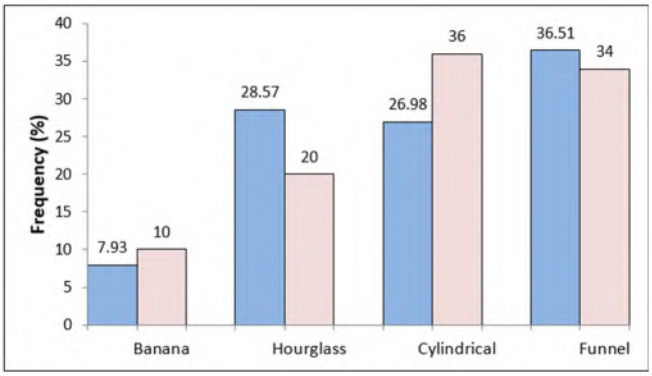


**Figure 2.** The frequency of the NPC type appearance. Blue bars represents male subjects (n=63), pink bars represents female subjects (n=50).

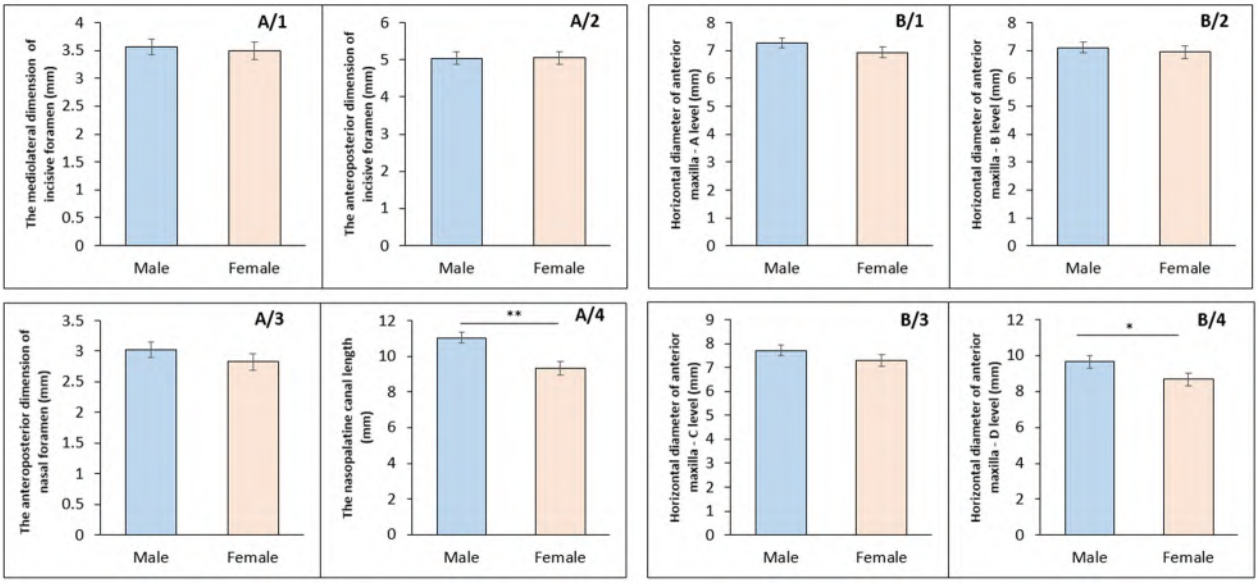


**Figure 3.** The dimensions at different sections of the nasopalatine canal and the horizontal diameter of the anterior maxilla (mm).A - different sections of NPC: A/1 - the mediolateral dimension of incisive foramen, A/2 - the anteroposterior dimension of the incisive foramen, A/3 -the anteroposterior dimension of the nasal foramen, A/4 - the nasopalatine canal length. B - horizontal diameter of anterior maxilla: B/1 - A level, B/2 - B level, B/3 - C level, B/4 - D level. Values are expressed as the mean ± SEM. * Denotes a significant difference, $p<0.05$, ** denotes a significant difference, $p<0.01$.

The results presented in Figure 4 showed that there was no significant difference between the estimated parameters - the mediolateral and anteroposterior dimension of the incisive foramen (Fig. 4A and B, df=7, F=1.818 and 1.660, respectively), as well as the anteroposterior dimension of the nasal foramen (Fig. 4C, F=2.494) and the NPC length (Fig. 4D, F=2.031) depending on NPC type. Also, there was no statistically significant gender difference in any estimated parameter for predefined NPC types.

The estimation of correlation between the dimension at different sections of the NPC and the anterior maxilla diameter at various levels (Table 1) showed that the M-L dimension of the incisive foramen significantly correlated with the anterior maxilla horizontal diameter at all levels for male subjects, but only at level B and C for females, while no significant correlation between the A-P dimension of the incisive foramen and the anterior maxilla horizontal diameter was observed. As shown in Table 1, the A-P dimension of the nasal foramen significantly correlated with the anterior maxilla horizontal diameter at all levels for male subjects, but only at level D for females. In contrary, NPC length analysis showed no significant correlation with the anterior maxilla horizontal diameter in male subjects, while females showed significant correlation at D level.

The horizontal diameter of the anterior maxilla at all estimated levels (A-D, Fig. 5A-D, respectively) was significantly affected neither by the NPC type nor gender.

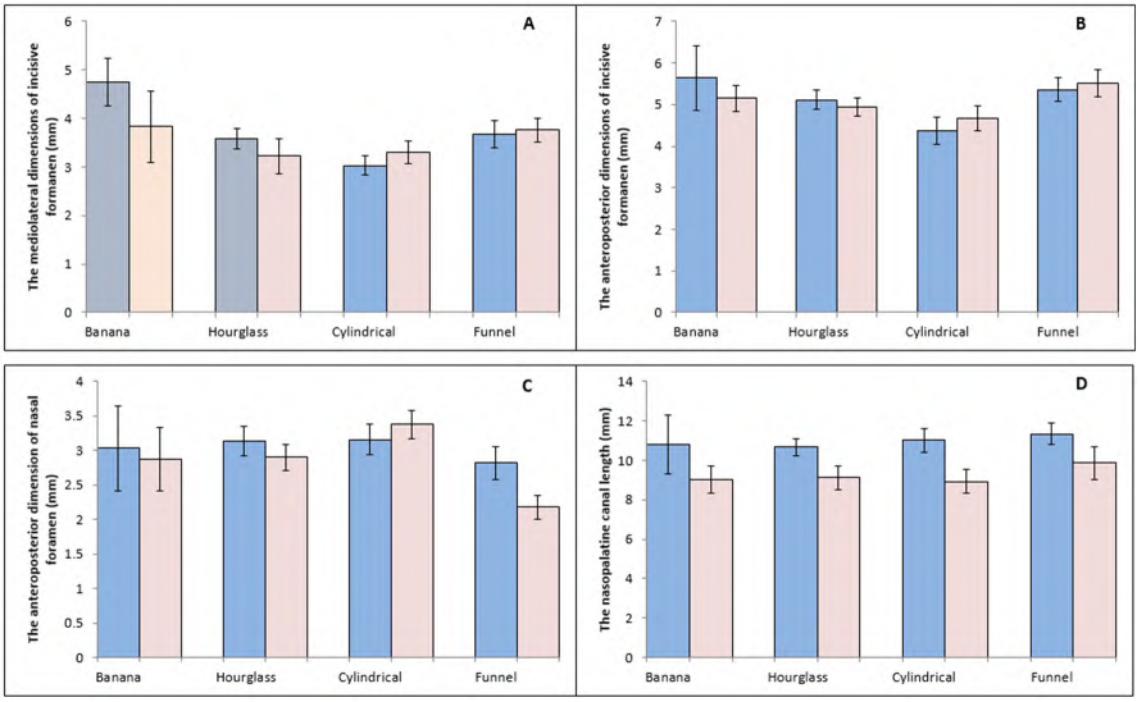


**Figure 4.** The dimensions of the NPC up to the NPC type in sagittal cross-section (in mm). A - M-L dimension of the incisive foramen; B - A-P dimension of the incisive foramen; C - A-P dimension of the nasal foramen; D - NPC length. Values are expressed as the mean ± SEM.

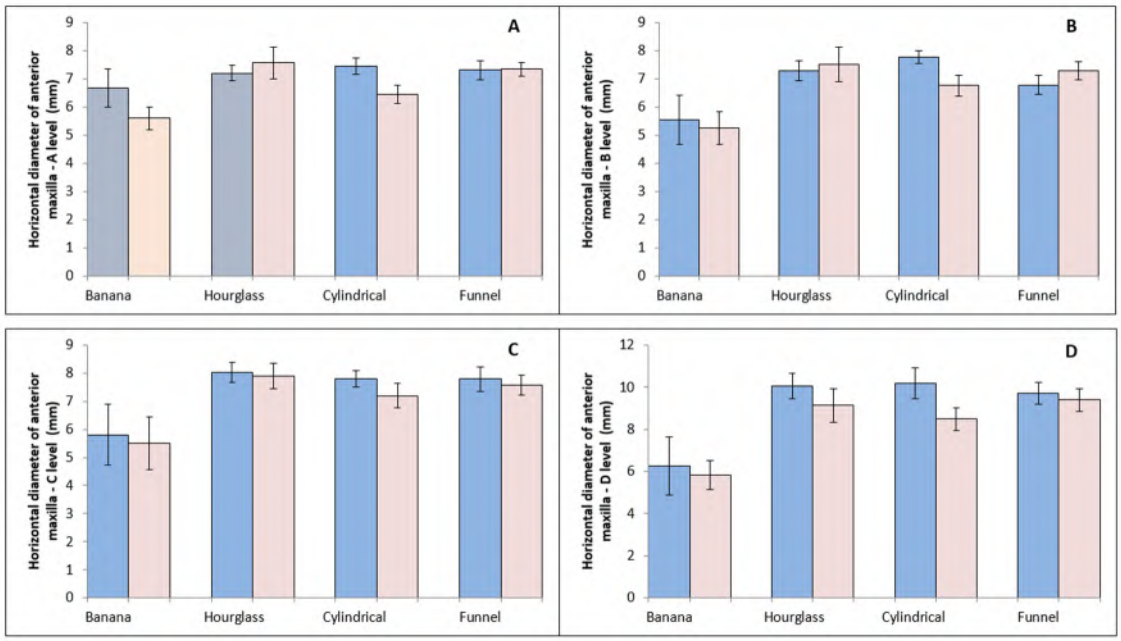


**Figure 5.** The horizontal diameter of the anterior maxilla at different levels according to the NPC type in sagittal cross-section (in mm). A - horizontal diameter of the anterior maxilla - A level; B - horizontal diameter of the anterior maxilla - B level; C - horizontal diameter of the anterior maxilla - C level; D - horizontal diameter of the anterior maxilla - D level. Values are expressed as the mean ± SEM.

As shown in Table 2, the M-L dimension of the incisive foramen at level A and B significantly correlated with the horizontal diameter of the anterior maxilla at level A and B for banana and funnel NPC types in male subjects, while the significant correlation in females was observed only in the hourglass NPC type, with no significant correlation for either gender in the cylindrical NPC type. Again, female subjects showed the significant correlation between the M-L

dimension of incisive foramen and the horizontal diameter of anterior maxilla at level C in the hourglass type. The significant correlation between those parameters in male subjects was observed in the cylindrical NPC type, but both gender statistics confirmed significant correlation at the level C of the anterior maxilla only in funnel NPC type. The analysis performed at level C of the anterior maxilla showed no significant correlation in either gender.

Interestingly, the significant correlation between the A-P dimension of the incisive foramen and the anterior maxilla diameter was observed only in female subjects at the level A and B for the hourglass, and level B for the cylindrical NPC type (Table 3), while males did not show any significant correlation between those parameters at all levels.

As shown in Table 4, A-P dimension of the nasal foramen significantly correlated with the anterior maxilla diameter at levels A, B, and C only for the funnel NPC type in male subjects, whit no significant correlations with the NPC type in females.

On the other hand, female subjects expressed significant correlation between the A-P dimension of the nasal foramen and the anterior maxilla diameter at level C for the hourglass type, and level D for the cylindrical NPC type.

Results presented in Table 5 showed that there was no significant correlation between the NPC length at all estimated levels and the anterior maxilla diameter for banana and cylindrical NPC types in both populations. At the same time, the significant correlation was confirmed between the NPC length and the anterior maxilla diameter at the level D for the hourglass type, and level A for the funnel NPC type in male subjects. Finally, the significant correlation for female participants was confirmed only between the NPC length and the anterior maxilla diameter at the level D for the funnel NPC type.

**Table 1.** The correlation between the dimension at different sections of the NPC and the anterior maxilla diameter at various levels (significant correlations are bolded, blue fields represent significant correlations only for male subjects, pink fields represent significant correlations only for female subjects, gray fields represent significant correlations for both gender).

| The sections of the NPC | Gender | The levels of anterior maxilla horizontal diameter | | | |
|---|---|---|---|---|---|
| | | A level | B level | C level | D level |
| **The M-L dimension of incisive foramen** | Male | $R^2 = 0.2223$ **$p = 9.61x10^{-5}$** | $R^2 = 0.309$ **$p = 2.25x10^{-6}$** | $R^2 = 0.2788$ $p =$ **$8.7x10^{-6}$** | $R^2 = 0.0908$ **$p = 0.016$** |
| | Female | $R^2 = 0.027$ $p = 0.254$ | $R^2 = 0.0903$ **$p = 0.034$** | $R^2 = 0.1872$ $p =$ **$0.002$** | $R^2 = 0.0443$ $p = 0.142$ |
| **The A-P dimension of incisive foramen** | Male | $R^2 = 0.0064$ $p = 0.532$ | $R^2 = 0.0538$ $p = 0.067$ | $R^2 = 0.0036$ $p = 0.641$ | $R^2 = 0.001$ $p = 0.804$ |
| | Female | $R^2 = 0.0015$ $p = 0.791$ | $R^2 = 0.0054$ $p = 0.612$ | $R^2 = 1x10^{-7}$ $p = 0.998$ | $R^2 = 0.0013$ $p = 0.804$ |
| **The A-P dimension of nasal foramen** | Male | $R^2 = 0.0727$ **$p = 0.033$** | $R^2 = 0.1011$ **$p = 0.011$** | $R^2 = 0.2882$ **$p = 5.7x10^{-6}$** | $R^2 = 0.0788$ **$p = 0.026$** |
| | Female | $R^2 = 0.0328$ $p = 0.208$ | $R^2 = 0.0033$ $p = 0.690$ | $R^2 = 0.0336$ $p = 0.203$ | $R^2 = 0.1827$ **$p = 0.002$** |
| **The NPC length** | Male | $R^2 = 0.0048$ $p = 0.590$ | $R^2 = 0.0005$ $p = 0.856$ | $R^2 = 0.0015$ $p = 0.766$ | $R^2 = 0.0036$ $p = 0.462$ |
| | Female | $R^2 = 0.0003$ $p = 0.901$ | $R^2 = 0.002$ $p = 0.760$ | $R^2 = 0.0012$ $p = 0.814$ | $R^2 = 0.100$ **$p = 0.025$** |

**Table 2.** The correlation between the M-L dimension of the incisive foramen and anterior maxilla diameter at various levels depending on the canal type at the sagittal cross-section (significant correlations are bolded, blue fields represent significant correlations only for male subjects, pink fields represent significant correlations only for female subjects, gray fields represent significant correlations for both gender).

| **The correlation between the M-L dimension of incisive foramen and anterior maxilla diameter on different levels** | **Gender** | **The NPC type at the sagittal cross-section** | | | |
|---|---|---|---|---|---|
| | | **Banana** | **Hourglass** | **Cylindrical** | **Funnel** |
| **The M-L dimension of incisive foramen *vs.* A level** | Male | $R^2 = 0.8776$ **p = 0.019** | $R^2 = 0.135$ p = 0.134 | $R^2 = 0.0123$ p = 0.672 | $R^2 = 0.3015$ **p = 0.007** |
| | Female | $R^2 = 0.519883$ p = 0.169 | $R^2 = 0.4546$ **p = 0.032** | $R^2 = 0.0504$ p = 0.672 | $R^2 = 0.0005$ p = 0.935 |
| **The M-L dimension of incisive foramen *vs.* B level** | Male | $R^2 = 0.8946$ **p = 0.015** | $R^2 = 0.0641$ p = 0.311 | $R^2 = 0.0273$ p = 0.526 | $R^2 = 0.4272$ **p = 0.001** |
| | Female | $R^2 = 0.7471$ p = 0.059 | $R^2 = 0.6061$ **p = 0.008** | $R^2 = 0.0944$ p =0.215 | $R^2 = 0.2092$ p =0.065 |
| **The M-L dimension of incisive foramen *vs.* C level** | Male | $R^2 = 0.7564$ p = 0.0553 | $R^2 = 0.2071$ p = 0.058 | $R^2 = 0.2285$ **p = 0.030** | $R^2 = 0.2049$ **p = 0.030** |
| | Female | $R^2 = 0.4326$ p = 0.228 | $R^2 = 0.6925$ **p = 0.003** | $R^2 = 0.0016$ p = 0.874 | $R^2 = 0.4137$ **p = 0.005** |
| **The M-L dimension of incisive foramen *vs.* D level** | Male | $R^2 = 0.0094$ p = 0.876 | $R^2 = 0.1275$ p = 0.146 | $R^2 = 0.1387$ p = 0.141 | $R^2 = 0.0062$ p = 0.722 |
| | Female | $R^2 = 0.0032$ p = 0.928 | $R^2 = 0.0362$ p = 0.598 | $R^2 = 0.1404$ p = 0.125 | $R^2 = 0.0324$ p =0.489 |

**Table 3.** The correlation between the A-P dimension of the incisive foramen and the anterior maxilla diameter at various levels depending on the canal type at the sagittal cross-section (significant correlations are bolded, blue fields represent significant correlations only for male subjects, pink fields represent significant correlations only for female subjects, gray fields represent significant correlations for both gender).

| **The correlation between the A-P dimension of nasal foramen and anterior maxilla diameter on different levels** | **Gender** | **The NPC type at the sagittal cross-section** | | | |
|---|---|---|---|---|---|
| | | **Banana** | **Hourglass** | **Cylindrical** | **Funnel** |
| **The A-P dimension of nasal foramen *vs.* A level** | Male | $R^2 = 0.5001$ p = 0.182 | $R^2 = 0.0042$ p = 0.855 | $R^2 = 0.0094$ p = 0.711 | $R^2 = 0.2443$ **p = 0.016** |
| | Female | $R^2 = 0.4523$ p = 0.214 | $R^2 = 0.0602$ p = 0.494 | $R^2 = 0.0116$ p = 0.670 | $R^2 = 6x10^{-5}$ p = 0.075 |
| **The A-P dimension of nasal foramen *vs.*** | Male | $R^2 = 0.6757$ p = 0.088 | $R^2 = 0.0324$ p = 0.475 | $R^2 = 0.0528$ p = 0.359 | $R^2 = 0.2772$ **p = 0.009** |

| The correlation between the A-P dimension of nasal foramen and anterior maxilla diameter on different levels | Gender | The NPC type at the sagittal cross-section | | | |
|---|---|---|---|---|---|
| | | **Banana** | **Hourglass** | **Cylindrical** | **Funnel** |
| **B level** | Female | $R^2 = 0.1552$<br>$p = 0.518$ | $R^2 = 0.1011$<br>$p = 0.370$ | $R^2 = 0.0004$<br>$p = 0.937$ | $R^2 = 0.009$<br>$p = 0.717$ |
| **The A-P dimension of nasal foramen** ***vs.*** **C level** | Male | $R^2 = 0.7152$<br>$p = 0.071$ | $R^2 = 0.2715$<br>**$p = 0.027$** | $R^2 = 0.2028$<br>$p = 0.069$ | $R^2 = 0.3381$<br>**$p = 0.004$** |
| | Female | $R^2 = 0.3094$<br>$p = 0.330$ | $R^2 = 0.1200$<br>$p = 0.327$ | $R^2 = 0.0052$<br>$p = 0.775$ | $R^2 = 0.0883$<br>$p = 0.247$ |
| **The A-P dimension of nasal foramen** ***vs.*** **D level** | Male | $R^2 = 0.0074$<br>$p = 0.890$ | $R^2 = 0.0575$<br>$p = 0.338$ | $R^2 = 0.1558$<br>$p = 0.117$ | $R^2 = 0.1492$<br>$p = 0.069$ |
| | Female | $R^2 = 0.0782$<br>$p = 0.649$ | $R^2 = 0.3954$<br>$p = 0.051$ | $R^2 = 0.3125$<br>**$p = 0.016$** | $R^2 = 0.0799$<br>$p = 0.272$ |

**Table 4.** The correlation between the A-P dimension of the nasal foramen and the anterior maxilla diameters at various levels depending on the canal type at the sagittal cross-section (significant correlations are bolded, blue fields represent significant correlations only for male subjects, pink fields represent significant correlations only for female subjects, gray fields represent significant correlations for both gender).

| The correlation between the A-P dimension of nasal foramen and anterior maxilla diameter on different levels | Gender | The NPC type at the sagittal cross-section | | | |
|---|---|---|---|---|---|
| | | **Banana** | **Hourglass** | **Cylindrical** | **Funnel** |
| **The A-P dimension of nasal foramen** ***vs.*** **A level** | Male | $R^2 = 0.5001$<br>$p = 0.182$ | $R^2 = 0.0042$<br>$p = 0.855$ | $R^2 = 0.0094$<br>$p = 0.711$ | $R^2 = 0.2443$<br>**$p = 0.016$** |
| | Female | $R^2 = 0.4523$<br>$p = 0.214$ | $R^2 = 0.0602$<br>$p = 0.494$ | $R^2 = 0.0116$<br>$p = 0.670$ | $R^2 = 6x10^{-5}$<br>$p = 0.075$ |
| **The A-P dimension of nasal foramen** ***vs.*** **B level** | Male | $R^2 = 0.6757$<br>$p = 0.088$ | $R^2 = 0.0324$<br>$p = 0.475$ | $R^2 = 0.0528$<br>$p = 0.359$ | $R^2 = 0.2772$<br>**$p = 0.009$** |
| | Female | $R^2 = 0.1552$<br>$p = 0.518$ | $R^2 = 0.1011$<br>$p = 0.370$ | $R^2 = 0.0004$<br>$p = 0.937$ | $R^2 = 0.009$<br>$p = 0.717$ |
| **The A-P dimension of nasal foramen** ***vs.*** **C level** | Male | $R^2 = 0.7152$<br>$p = 0.071$ | $R^2 = 0.2715$<br>**$p = 0.027$** | $R^2 = 0.2028$<br>$p = 0.069$ | $R^2 = 0.3381$<br>**$p = 0.004$** |
| | Female | $R^2 = 0.3094$<br>$p = 0.330$ | $R^2 = 0.1200$<br>$p = 0.327$ | $R^2 = 0.0052$<br>$p = 0.775$ | $R^2 = 0.0883$<br>$p = 0.247$ |
| **The A-P dimension of nasal foramen** ***vs.*** **D level** | Male | $R^2 = 0.0074$<br>$p = 0.890$ | $R^2 = 0.0575$<br>$p = 0.338$ | $R^2 = 0.1558$<br>$p = 0.117$ | $R^2 = 0.1492$<br>$p = 0.069$ |
| | Female | $R^2 = 0.0782$<br>$p = 0.649$ | $R^2 = 0.3954$<br>$p = 0.051$ | $R^2 = 0.3125$<br>**$p = 0.016$** | $R^2 = 0.0799$<br>$p = 0.272$ |

**Table 5.** The correlation between the nasopalatine canal length and anterior maxilla diameters at various levels depending on the canal type at the sagittal cross-section (significant correlations are bolded, blue fields represent significant correlations only for male subjects, pink fields represent significant correlations only for female subjects, gray fields represent significant correlations for both gender).

| The correlation between NPC length and anterior maxilla diameter on different levels | Gender | The NPC type at the sagittal cross-section | | | |
|---|---|---|---|---|---|
| | | **Banana** | **Hourglass** | **Cylindrical** | **Funnel** |
| **NPC length *vs.* A level** | Male | $R^2 = 0.5000$ p = 0.182 | $R^2 = 0.0657$ p = 0.651 | $R^2 = 0.0022$ p = 0.858 | $R^2 = 0.2551$ **p = 0.014** |
| | Female | $R^2 = 0.4606$ p = 0.208 | $R^2 = 0.0268$ p = 0.651 | $R^2 = 0.0292$ p = 0.498 | $R^2 = 0.0077$ p = 0.738 |
| **NPC length *vs.* B level** | Male | $R^2 = 0.6587$ p = 0.095 | $R^2 = 0.0569$ p = 0.340 | $R^2 = 0.0078$ p = 0.736 | $R^2 = 0.1649$ p = 0.054 |
| | Female | $R^2 = 0.2089$ p = 0.439 | $R^2 = 0.0001$ p = 0.993 | $R^2 = 0.0130$ p = 0.652 | $R^2 = 0.0042$ p = 0.806 |
| **NPC length *vs.* C level** | Male | $R^2 = 0.3954$ p = 0.256 | $R^2 = 0.0778$ p = 0.262 | $R^2 = 0.0001$ p = 0.979 | $R^2 = 0.1580$ p = 0.060 |
| | Female | $R^2 = 0.533$ p = 0.161 | $R^2 = 0.0121$ p = 0.762 | $R^2 = 0.0110$ p = 0.678 | $R^2 = 0.0083$ p = 0.728 |
| **NPC length *vs.* D level** | Male | $R^2 = 0.1125$ p = 0.581 | $R^2 = 0.3829$ **p = 0.006** | $R^2 = 0.0083$ p = 0.727 | $R^2 = 0.0052$ p = 0.743 |
| | Female | $R^2 = 0.6497$ p = 0.099 | $R^2 = 0.2256$ p = 0.165 | $R^2 = 0.0413$ p = 0.419 | $R^2 = 0.428$ **p = 0.004** |

## DISCUSSION

A growing interest for a variety of surgical protocols in dentistry implies the necessity for upgraded planning of such interventions. One of the most complex issues that employs regions in oral and maxillofacial surgery is focused on the anterior maxilla. Therefore, the development of methodology for better knowledge of morphometric properties of the NPC and faster acquisition may be substantially important. In order to establish the methodology that could be helpful by means of duration in surgical interventions planning, we performed the estimation of the morphometric analysis of the NPC and the anterior maxilla, based on the NPC type classification, according to gender.

The results of our study confirmed no gender difference in the distribution of the NPC type. Our results are in line with studies by Guncu (6) and Thakur and coworkers (20). However, as shown in Figure 2, the frequency of appearance for different NPC types did not follow equal distribution for both male and female subjects. Interestingly, the most frequent NPC type confirmed gender variations (cylindrical in females, funnel in males), but the lowest incidence of the NPC type in both male and female participants was the banana-type of the NPC. This is also in accordance with Guncu and collaborators (6).

The analysis of the dimensions at different sections of the NPC showed no significant gender impact on M-L and A-P dimensions of the incisive foramen, as well as the A-P dimension of the nasal foramen. In contrast,the NPC length was significantly increased in male participants. The results for the NPC length and the A-P dimension of the nasal foramen are in accordance with previous reporst of Kajan and collaborators (26), but they found statistical difference in the A-P dimension of incisive foramen between male and female. However, the study of Soumya and coworkers showed that gender did not have an impact on any of the estimated dimensions of the NPC sections (16). The observed differences could be attributed to different methodologies applied. Furthermore, analysis of the horizontal diameter of the anterior maxilla at different levels also showed the gender impact

manifested as significant augmentation of distance between the nasal foramen and cortical layer of the anterior maxilla in male subjects, with no significant difference at the lower parts of the anterior maxilla. Our results are in line with research groups of Salemi (14) and Gonul (27). However, our findings are not in accordance with the results presented by Lopez (1) and Hakbilen and colleagues (28). A potential explanation could be found in obvious differences in population characteristics, age of participants, total number of subjects, and/or predefined inclusion/exclusion criteria. Also, there was a substantial variability in methodology (number and definition of NPC sections, as well as the classification of NPC types).

According to the results obtained in this study none of the parameters (the dimensions of NPC up to NPC type in sagittal cross-section) was significantly different according to gender (Fig. 4). However, we are not able to compare the results obtained in this study with other published material due to lack of literature data.

Linear regression analysis (Table 1) revealed the significant correlation between the M-L dimension of the incisive foramen and the anterior maxilla diameter at all bone levels for male subjects, while this relation in female participants was present only in the mid part of the anterior maxilla (level B and C). A similar finding was observed for the A-P dimension of the nasal foramen, where again significant correlation was confirmed in male subjects, but the A-P dimension of the nasal foramen correlated significantly with the anterior maxilla diameter only at the highest evaluated level (level D) in females. The opposite finding was achieved concerning the relationship between the NPC length and alveolar bone thickness. Namely, the significant correlation between the NPC length and the anterior maxilla diameter was observed only in female participants at the level D. Furthermore, the horizontal diameter of the anterior maxilla at different levels according the NPC type in sagittal cross-section showed no significant difference according to gender (Fig. 5).

The correlation between the M-L dimension of the incisive foramen and the anterior maxilla diameter at various levels depending on the canal type at the sagittal cross-section was variously affected by gender (Table 2). In male subjects, significant correlation between the M-L dimension of the incisive foramen and lower parts of the alveolar ridge (level A and B) was observed in the banana- and funnel-type of NPC, while with the higher regions of the anterior maxilla (level C) significant correlation was present in the cylindrical- and funnel-type of NPC. In contrast, females expressed significant correlation between the M-L dimension of the incisive foramen and the anterior maxilla thickness only in the hourglass-type of NPC at the levels A, B, and C, as well as the funnel NPC type at the level C.

The linear regression analysis revealed significant correlation between the A-P dimension of the incisive foramen and the anterior maxilla diameter only for females with the hourglass-type at levels A and B, and for the cylindrical-type of NPC at level B, with no significant correlations for male participants.

Furthermore, the estimation of interconnection between the A-P dimension of the nasal foramen and anterior maxilla diameters at different levels depending on the canal type at the sagittal cross-section confirmed that no significant correlation for either gender in the banana NPC type. At the same time, male subjects showed significant correlation between the A-P dimension of the nasal foramen and buccal bone in the funnel NPC type at all levels except the highest (D level), and the hourglass-type at the level C. Unlike for males, female participants confirmed significant correlation between the A-P dimension of nasal foramen and anterior maxilla thickness in the cylindrical-type of NPC at the highest level (level D).

Finally, the linear regression analysis for the relationship between the NPC length and the anterior maxilla diameters at various levels depending on the canal type revealed that in female subjects significant correlation was present only in the funnel NPC type at the level D. In contrast, male participants showed significant correlation in both the funnel NPC type at level A, but also in the hourglass-type at the level D.

Unfortunately, we are not able to compare the mathematical analysis that gives an insight into the relationship between the anterior maxilla dimensions and morphometric characteristics of the NPC according to the NPC type, since to our knowledge this interconnection was not yet evaluated. Thus, it is even more not possible to estimate the gender impact on those relationships. However, our principle intention was to allow the more accurate data for morphometric quantification in order to achieve advanced planning of various surgical interventions in the anterior maxilla region. Future investigations on this topic, accompanied with the standardized methodology for evaluation, will allow more reliable information for clinical practice.

## ACKNOWLEDGEMENT

None

## CONFLICT OF INTEREST

The authors declare no financial or commercial conflict of interest.

## REFERENCES

1. López JP, Boix P, Sanchez PA, Boracchia A. Morphological Characterization of the Anterior Palatine Region Using Cone Beam Computed Tomography. Clin Implant Dent Relat Res. 2015; e459-64.
2. Bahşi I, Orhan M, Kervancıoğlu P, Yalçın ED, Aktan AM. Anatomical evaluation of nasopalatine canal on cone beam computed tomography images. Folia Morphol (Warsz). 2019; 78(1): 153-162.
3. Peñarrocha M, Carrillo C, Uribe R, García B. The nasopalatinecanal as an anatomic buttress for implant

placement in theseverely atrophic maxilla: a pilot study. Int J Oral MaxillofacImplants. 2009; 24(5): 936-942.
4. Costa EDD, Nejaim Y, Martins LAC, Peyneau PD, Ambrosano GMB, Oliveira ML. Morphological Evaluation of the Nasopalatine Canal in Patients With Different Facial Profiles and Ages. J Oral Maxillofac Surg. 2019; (4): 721-729.
5. Mardinger O, Namani SN, Chaushu G, Schwartz AD. Morphologic Changes of the Nasopalatine Canal Related to Dental Implantation: A Radiologic Study in Different Degrees of Absorbed Maxillae. J Periodontol. 2008; 79 (9): 1659-1662.
6. Güncü GN, Yıldırım YD, Yılmaz HG, Galindo-Moreno P, Velasco-Torres M, Al-Hezaimi, K, Al-Shawaf R, Karabulut E, Wang, H.L, Tözüm TF. Is there a gender difference in anatomic features of incisive canal and maxillary environmental bone? Clin Oral Implants Res. 2013; 24 (9): 1023-1026.
7. Liang X, Jacobs R., Martens W, Hu Y, Adriaensens P, Quirynen M, Lambrichts I. Macro- and micro-anatomical, histological and computed tomography scan characterization of the nasopalatine canal. J Clin Periodontol. 2009; 36 (7): 598-603.
8. Etoz M, Sisman Y. Evaluation of the nasopalatine canal and variations with cone-beam computed tomography. Surg Radiol Anat. 2014; 36 (8): 805-812.
9. Safi Y, Moshfeghi M, Rahimian S, Kheirkhahi M, Manouchehri, ME. Assessment of Nasopalatine Canal Anatomic Variations Using Cone Beam Computed Tomography in a Group of Iranian Population. Iran J Radiol. 2017; 14(1): e13480.
10. Buser D, Chappuis V, Belser UC, Chen S. Implant placement post extraction in esthetic single tooth sites: When immediate, when early, when late? Periodontology 2000. 2016; 73(1): 84-102.
11. Mounir M, Beheiri G, El-Beialy W. Assessment of marginal bone loss using full thickness versus partial thickness flaps for alveolar ridge splitting and immediate implant placement in the anterior maxilla. Int J Oral Maxillofac Surg. 2014; 43(11): 1373-1380.
12. Kan JYK, Rungcharassaeng K, Deflorian M, Weinstein T, Wang HL, Testori T. Immediate implant placement and provisionalization of maxillary anterior single implants. Periodontology 2000. 2018; 77(1): 197-212.
13. Al-Amery SM, Nambiar P, Jamaludin M, John J, Ngeow WC. Cone beam computed tomography assessment of the maxillary incisive canal and foramen: considerations of anatomical variations when placing immediate implants. PLoS One. 2015; 10(2): e0117251.
14. Salemi F. Moghadam FA, Shakibai, Z, Farhadian M. Three-dimensional Assessment of the Nasopalatine Canal and the Surrounding Bone Using Cone-beam Computed Tomography. J. Periodontol. Implant Dent. 2016; 8(1): 1-7.
15. Panda M, Shankar T, Raut A, Dev S, Kar AK, Hota S. Cone beam computerized tomography evaluation of incisive canal and anterior maxillary bone thickness for placement of immediate implants. J Indian Prosthodont Soc. 2018; 18(4): 356-363.
16. Soumya P, Koppolu P, Pathakota, KR, Chappidi V. Maxillary Incisive Canal Characteristics: A Radiographic Study Using Cone Beam Computerized Tomography. Radiol Res Pract. 2019; 2019: 6151253.
17. Peñarrocha D, Candel E, Guirado JLC, Canullo L, Peñarrocha M. Implants Placed in the Nasopalatine Canal to Rehabilitate Severely Atrophic Maxillae: A Retrospective Study with Long Follow-up. J Oral Implantol. 2014; 40(6): 699-706.
18. McCrea SJJ. Aberrations Causing Neurovascular Damage in the Anterior Maxilla during Dental Implant Placement. Case Rep Dent. 2017; 2017: 5969643.
19. Mraiwa N, Jacobs R, Van CJ, et al. The nasopalatine canal revisited using 2D and 3D CT imaging. Dentomaxillofac Radiol. 2004; 33(6): 396-402.
20. Canto G. Comparative analysis of imaging techniques for diagnostic accuracy of peri-implant bone defects: a meta-analysis. Oral Surg Oral Med Oral Pathol Oral Radiol. 2017; 124(4): 432-440.e5.
21. Wanner L, Ludwig U, Hövener JB, Nelson K, Flügge T. Magnetic resonance imaging-a diagnostic tool for postoperative evaluation of dental implants: a case report. Oral Surg Oral Med Oral Pathol Oral Radiol. 2018; 125(4): e103-e107.
22. Sahota J, Bhatia A, Gupta M, Singh V, Soni J, Soni R. Reliability of Orthopantomography and Cone-beam Computed Tomography in Presurgical Implant Planning: A Clinical Study. J Contemp Dent Pract. 2017; 18(8): 665-669.
23. Jacobs R, Salmon B, Codari M, Hassan B, Bornstein MM. Cone beam computed tomography in implant dentistry: recommendations for clinical use. BMC Oral Health. 2018; 18(1): 88.
24. Alkanderi A, Al Sakka Y, Koticha T, Li J, Masood F, Suárez-López Del Amo F. Incidence of nasopalatine canal perforation in relation to virtual implant placement: A cone beam computed tomography study. Clin Implant Dent Relat Res. 2020; 22(1): 77-83.
25. Thakur AR, Burde K, Guttal K, Naikmasur VG. Anatomy and morphology of the nasopalatine canal using cone-beam computed tomography. Imaging Sci Dent. 2013; 43(4): 273-281.
26. Kajan ZD, Kia J, Motevasseli S, Rezaian SR. Evaluation of the nasopalatine canal with cone-beam computed tomography in an Iranian population. Dent Res J (Isfahan). 2015; 12(1): 14-19.
27. Gönül Y, Bucak A, Atalay Y, Beker-Acay M, Çalişkan A, Sakarya G, Soysal N, Cimbar M, Özbek M. MDCT evaluation of nasopalatine canal morphometry and variations: An analysis of 100 patients. Diagn Interv Imaging. 2016; 97(11): 1165-1172.
28. Hakbilen S, Magat G. Evaluation of anatomical and morphological characteristics of the nasopalatine canal in a Turkish population by cone beam computed tomography. Folia Morphol (Warsz). 2018; 77(3): 527-535.

sciendo

# ASSESSMENT OF INDIVIDUAL CARDIOVASCULAR RISK AMONG POPULATION IN PUBLIC PHARMACIES USING THE HEART-SCORE QUESTIONNAIRE

Vesna Maksimovic and Biljana Jakovljevic

*Academy of Vocational Studies Belgrade, Department of Health School, Serbia*

Received: 16.12.2020.
Accepted: 09.01.2021.

**Corresponding author:**

**Biljana Jakovljevic**

Academy of Vocational Studies Belgrade, Department of Health School, Serbia

E-mail: jakovljevic.biljana@yahoo.com

## ABSTRACT

*The SCORE model was calibrated according to mortality statistics for each European country. If it is used for the population aged 40-65, it will predict the possibility of fatal cardiovascular consequences that will appear after 10 years. The aim of this study was to investigate individual risk factors for cardiovascular complications in the adult population in the city of Belgrade. The study was designed as a cross-sectional study. Using Heart Score tool for determining of the total risk of CVD, could be projected to the age of 60, which may be of particular importance for guiding young adults, aged 20 to 30, with low absolute risk but already with an unhealthy risk profile, which will lead to a much higher risk as they age. In our study, predominately were present female participants without hypertension, then male and were dominate frequent non-smokers compared with smokers in male and female. Furthermore, in study population were more present smokers with longer duration of smoking (>10 years). After calculated Heart Score, we can see that 25.6% of respondents have a high risk of cardiovascular event, of which 19.6% high risk, 4.4% very high risk, and 1.6% extremely high risk of developing some an adverse fatal cardiovascular event. The present risk factors and high mortality and morbidity from cardiovascular disease indicate the need for taking preventive measures already in children, with the parallel implementation of population strategies and high risk.*

***Keywords***: *Heart Score, cardiovascular risk, public pharmacies.*

sciendo

UDK: 616.1-02(497.11)
Eabr 2024; 25(2):157-164
DOI: 10.2478/sjecr-2021-0017

## INTRODUCTION

Cardiovascular disease are the leading cause of mortality in all region of world, except in Sub - Saharan Africa. It accounts for about 49% of all deaths and 30% lost years of life in Europe. They are a significant cause of disability, large health care costs and premature mortality. WHO estimates say that in 2020, 70% of all causes of death will be related to lifestyle, where the most important risk factors are:Unbalanced and improper diet (overweight, obesity), Physical inactivity, Smoking and Alcohol consumption (1-5)

Risk factors for cardiovascular disease are numerous and have cumulatively effect. Most of the risk factors that are associated with the behavior, such as diet and lifestyle, sedentary life at an early age and have a persistent character (6-8). The most significant risk factors that can be prevented are: high blood pressure, smoking, high cholesterol, diabetes mellitus, obesity, inadequate nutrition, and physical inactivity. In stopping the unfavorable trend in CVD, the greatest importance that there should be primary prevention. Patients who have already had a cardiovascular event should be subjected to secondary prevention measures (9-11).

In stopping the unfavorable trend of CVD, primary prevention should be of the greatest importance (12). Patients who have already had an ischemic event should undergo secondary prevention measures, especially in view of advances in the interventional, medical and surgical approaches (13-16). Cardiovascular diseases are the most significant cause of death in men and women, and they can be prevented. CVD prevention lasts a lifetime, and the best time to start is before birth, by educating young, future parents, and then should continue in preschool (kindergarten), as well as through failure in the school system. During this phase, the emphasis should be on enjoying a healthy diet and joy and a sense of well-being related to physical activity, instead of focusing on disease prevention. Starting from the 6th grade of primary school (11-12 years, or even earlier, depending on the social environment), a smoke-free lifestyle should be encouraged (17-20).

Secondary prevention is a set of therapeutic measures that reduce the occurrence of recurrent, recurrent cardiovascular events in patients with confirmed atherosclerosis, including coronary heart disease, patients with cerebrovascular disease, peripheral artery and carotid artery disease, and atherosclerotic aortic atherosclerotic disease (21). Equivalents in terms of risk level are people with diabetes, as well as people with chronic kidney disease, and people with asymptomatic atherosclerosis can also be classified in some way (22).

The recommended model for total risk assessment is based on the SCORE (Systematic Coronary Risk Evaluation) system. The SCORE risk assessment is based on a large number of data from prospective European studies and predicts fatal atherosclerotic cardiovascular diseases over a period of 10 years (23, 27). This risk assessment is based on the following risk factors: gender, age, smoking, systolic blood pressure, and total cholesterol (24, 25). The SCORE model was calibrated according to mortality statistics for each European country. If it is used for the population aged 40-65, it will predict the possibility of fatal cardiovascular consequences that will appear after 10 years (26, 29).

The aim of this study was to investigate individual risk factors for cardiovascular complications in the adult population in the city of Belgrade.

## PATIENTS AND METHODS

### Ethical Concerns

This study was performed in accordance with Declaration of Helsinski (1964) and with all relevant ethical guidelines.

### Design of study

The study was designed as a cross-sectional study, with using of a survey or specially designed questionnaire as an instrument. All subjects were adults or more then 18 years old. A questionnaire was created for the needs of the research. The questionnaire consisted of 17 questions, both closed and open. The research was conducted in privately owned pharmacies in the municipalities of New Belgrade, Vracar and Zemun, during January and February 2016. Subjects were selected by random sampling. The survey was anonymous and respondents signed an informed consent form by completing the questionnaire. To determine the sample size, it was estimated that 138 subjects were needed (test power 80%, error level 0.05).

As a research instrument, a specially designed questionnaire was used, which consists of 3 parts: the first part presents sociodemographic data on respondents, the second part records of present, already diagnosed diseases in respondents, and the third behavior of respondents, ie detection of personal risk factors for cardiovascular diseases. These three sections applied to all respondents.

### Heart Score Tool

Using Heart Score tool for determining of the total risk of CVD, could be projected to the age of 60, which may be of particular importance for guiding young adults, aged 20 to 30, with low absolute risk but already with an unhealthy risk profile, which will lead to a much higher risk as they age (29).

The 2003 guidelines used the SCORE assessment for risk assessment, based on data from 12 European cohort studies; it included 205,178 subjects, surveyed between 1970 and 1988 with 2.7 million years of follow-up and 7,934 cardiovascular deaths. In this way the SCORE risk function was confirmed (23, 29).

Risk tables, such as SCORE, aim to facilitate risk assessment in seemingly healthy individuals. Patients who have had a clinical event such as acute coronary syndrome (ACS)

or stroke automatically qualify for intensive care and risk factor management. SCORE differs from previous risk assessment systems in several important ways, and has been modified to some extent for current guidelines. The SCORE system assesses the risk of 10 years to the first fatal atherosclerotic case, whether a heart attack, stroke, aortic aneurysm, or some other (29).

### Statistical analysis

The collected data were then coded and entered into Microsoft Excel 2016. The statistical program Excel 2016 was used for descriptive data analysis. PASW v18 was used for regression analysis.

## RESULTS

Demographic characteristic of study population

In Table 1 are shown basic data about study population.

We observed distribution of location of public pharmacies, age, gender, marital status and education level of participants.

**Table 1.** Distribution of basic demographic characteristic in study population

| | | Frequency | Percent (%) | Valid Percent (%) | Cumulative Percent (%) |
|---|---|---|---|---|---|
| City | Zemun | 79 | 31,6 | 31,6 | 31,6 |
| | Novi Beograd | 89 | 35,6 | 35,6 | 67,2 |
| | Vracar | 60 | 24,0 | 24,0 | 91,2 |
| | Other | 22 | 8,8 | 8,8 | 100,0 |
| Age (years) | | Frequency | Percent (%) | Valid Percent (%) | Cumulative Percent (%) |
| | <30 | 83 | 33,2 | 33,2 | 33,2 |
| | 31-50 | 51 | 20,4 | 20,4 | 53,6 |
| | 51-65 | 30 | 12,0 | 12,0 | 65,6 |
| | >65 | 86 | 34,4 | 34,4 | 100,0 |
| Gender (m/f) | | Frequency | Percent (%) | Valid Percent (%) | Cumulative Percent (%) |
| | Male | 93 | 37,2 | 37,2 | 37,2 |
| | Female | 157 | 62,8 | 62,8 | 100,0 |
| Merital status | | Frequency | Percent (%) | Valid Percent (%) | Cumulative Percent (%) |
| | Not Merried | 94 | 37,6 | 37,6 | 37,6 |
| | Merried | 108 | 43,2 | 43,2 | 80,8 |
| | Divorced | 15 | 6,0 | 6,0 | 86,8 |
| | Widover | 33 | 13,2 | 13,2 | 100,0 |

| | | Frequency | Percent (%) | Valid Percent (%) | Cumulative Percent (%) |
|---|---|---|---|---|---|
| Education | Primary school | 7 | 2,8 | 2,8 | 2,8 |
| | High school | 130 | 52,0 | 52,0 | 54,8 |
| | Faculty | 113 | 45,2 | 45,2 | 100,0 |

**Hypertension as a cardiovascular risk factor in study population**

In our study, predominately were present female participants without hypertension, then male. Similar, were frequently male and female participants with hypertension (Figure 1). Also, in the same group, we observed the most frequent self-measuring of blood pressure compared with other groups (Figure 2).

**Figure 1.** HTA distribution in study population

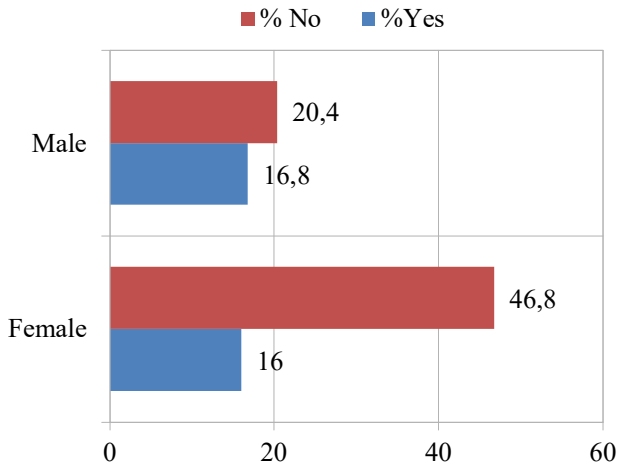


**Figure 2** Self-measuring of BP distribution in study population

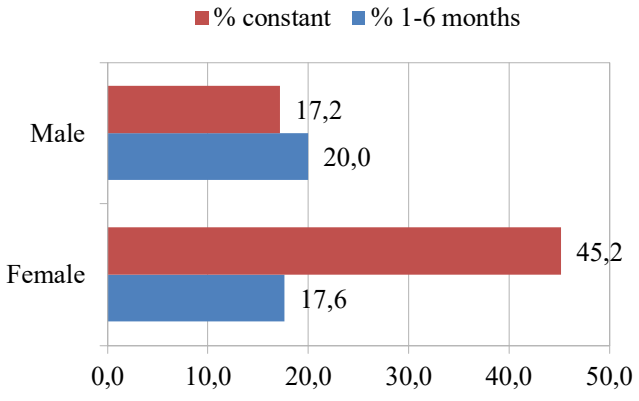


**Smoking as a cardiovascular risk factor in study population**

As we can see on Figure 3, in our study were dominate frequent non-smokers compared with smokers in male and female (Figure 3). Furthermore, in study population were more present smokers with longer duration of smoking (>10 years) (Figure 4). Also, in smokers group there were higher percent of participants who smoked more than 20 cigarets per day (Figure 5)

**Figure 3.** Smokers and non-smokers distribution in study population

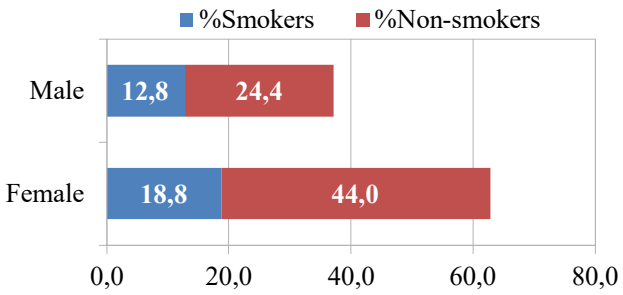


**Figure 4.** Duration of smoking in participants

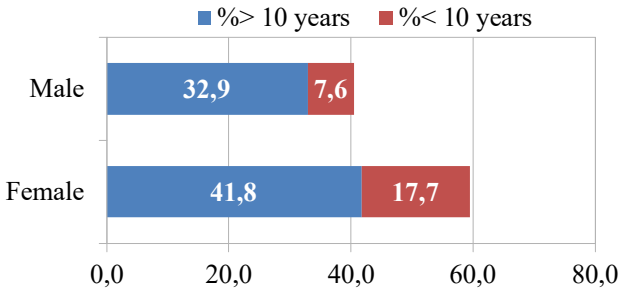


**Figure 5.** Intensity of smoking in male and female

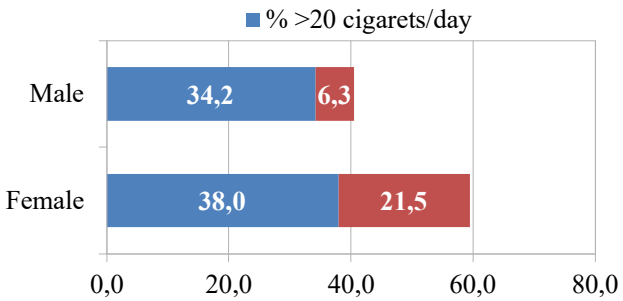

Body weight as a cardiovascular risk factor in study population

Regarding the body weight, we measured waist size and body mass index of each participant. The most frequent were female participant without CVD risk, and the most unfrequent were male participant without risk (Figure 6). Also, BMI below 30 was significantly present in our study population (Figure 7).

**Figure 6.** Waist size in study population

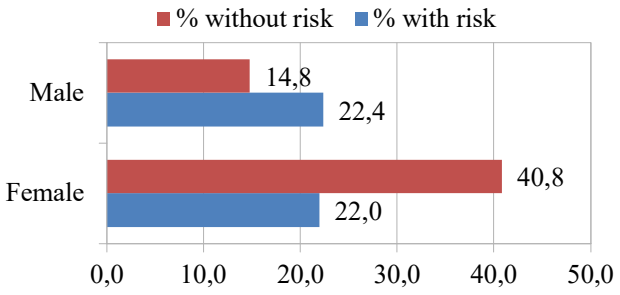


**Figure** 7. BMI in study population

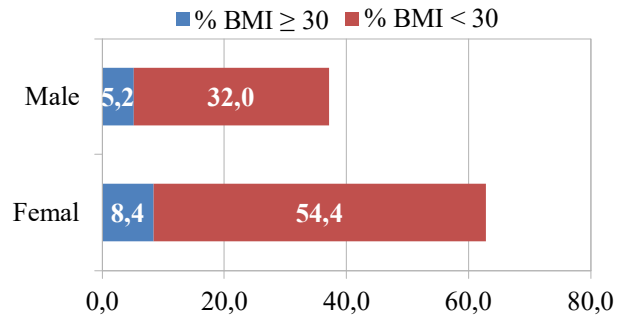


**Heart Score in study population**

We categorized participant into two categories: participants with HS higher than 5 and lower than 5. In our study, in 19,6% were present male with HS higher than 5 and in 6% were female with higher HS than 5 (Fig. 8). Also, after calculated Heart Score, we can see that 25.6% of respondents have a high risk of cardiovascular event, of which 19.6% high risk, 4.4% very high risk, and 1.6% extremely high risk of developing some an adverse fatal cardiovascular event. The workload in relation to gender is 52.7% of all men included in the sample have a high or very high and extreme risk compared to only 6% of all surveyed women. Using regression analysis, it was found that the factors that have statistical significance for the assessment of Heart Score are as follows: age of subjects (F = 12,023; p <0,001), sex of subjects (F = 20,685; p <0,001), smoking (F = 6,249; p = 0.003) and systolic pressure (F = 10.553; p <0.001). Other variables had no effect on the Heart Score value.

Regarding the variables, the age of the subjects and the value of systolic pressure, with increasing values, the risk measured by Heart Score also increased, which was to be expected. Men also had a higher risk of an unwanted CV event than women. An interesting result was obtained for the variable smoking in the sense that the respondents who smoked had the highest risk, but on the other hand a higher estimated risk was recorded in respondents who did not smoke than in respondents who recently quit smoking.

**Figure** 8. Heart Scores in study population

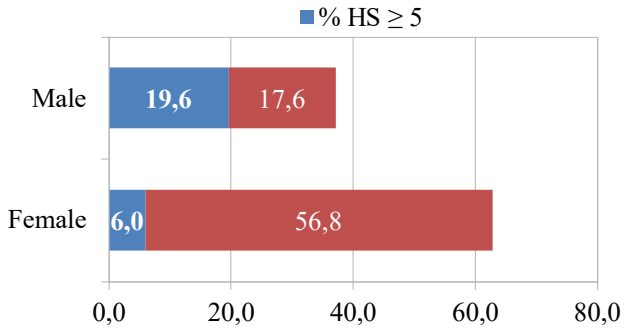


## DISCUSSION

According to the results of the research, more than 1⁄4 of the examined population of adult inhabitants of the city of Belgrade has a high Heart Score (value higher than 5) (29). Risk factors that affected the value of the Heart Score were: age of the subjects, sex of the subjects, smoking and the value of systolic pressure. Other variables had no effect on the Heart Score value, which can be explained by the relatively small sample examined (14-23).

Cardiovascular diseases are still leading in the number of patients - both in the world and in our country. About 17.3 million people die each year, most often from heart attacks and strokes. These are conditions that can be treated, and it is possible to prevent them. It is best if we deal with our own cardiovascular risk on time. This mostly applies to men over 40 and women over 45 (11, 30).

According to WHO experts, the number of people suffering from CVD will continue to grow from year to year until 2020 (15, 29). These diseases are increasingly affecting the working age population, and their immediate cause is stress, low standard, daily struggle for survival, low level of general awareness and education about the importance of adequate prevention, which, in addition to proper nutrition, physical activity, includes regular visits to check-ups and taking prescribed therapy (31-33).

Mortality, incidence and fatal outcomes of CVD are declining in most countries of northern, southern and western Europe, but either not declining or even rising in Central and Eastern Europe. Although CVD mortality rates are declining in the EU, the number of men and women living with these diseases is growing (34). This paradox is related to increased longevity and improved survival of patients with CVD. The burden of these diseases is unevenly distributed in the world, with higher mortality of people who are in a worse socio-

economic position. In Serbia, every hour, from various manifestations of CVD, 6 people die, of which every eighth is in the most productive years of life (from 25 to 64 years). Compared to all other causes of death during 2013, 24,505 men (45.9% of all causes of death) and 28,862 women (54.1%) died of heart and blood vessel diseases in Serbia. Compared to 2012, when the mortality rate from CVD was 763.6 per 100,000 inhabitants, in 2013 the mortality rate dropped to 744.9 per 100,000 inhabitants (32-36).

From 2001 to 2010, the CVD mortality rate in Serbia fell by 14% for women and by 16% for men, but despite the registered decline in the mortality rate, Serbia is in the group of countries with a higher-than-average risk for the countries of the European region (29, 36). The lack of CVD prevention is evident in the Republic of Serbia. According to a study of the workload of the KVB society (37), Serbia spent much more money on the treatment of cardiovascular diseases and its complications than on prevention; more than 60% of direct health care costs can be attributed to hospitalizations, surgical and diagnostic procedures. An additional problem in the Republic of Serbia is incomplete or missing data regarding funds invested in prevention activities, such as smoking cessation campaigns.

Alarming trends for chronic diseases, such as obesity, cardiovascular diseases and diabetes mellitus, affect people at the earliest age, which indicates a significant need not only for primary and secondary prevention, but also for primordial prevention. Primordial prevention is defined as preventing the development of risk factors, such as smoking, being overweight or consuming alcohol. Smoking significantly reduces the chances of survival in middle age. Three times the percentage of heavy smokers (≥ 20 cigarettes per day) dies from cardiovascular disease compared to people who have never smoked. The beneficial effect of smoking cessation is more pronounced in earlier years, but it is also present in people who quit smoking in their 50s or 60s (38). It has been documented that prevention strategies are not only cost-effective, but also strategies that bring certain savings to the health system. The company's programs aimed at increasing physical activity, improving nutrition, and preventing smoking provide a return on investment in the sense that for every dollar spent, the company returns $ 5.6 within 5 years. Smoke-free enclosed regulations are also estimated to bring the United States savings in the health care system of $ 10 billion a year (31, 34).

Being overweight has also been shown to be an independent risk factor for CVD. In Serbia, prevention programs are experiencing a low level of implementation. Even more worrying is the fact that only half of the population has received counseling from health professionals to change life risk factors, but only one third of those have actually changed some of their risk factors. Less than 1% of smokers used the smoking cessation counseling service (29-34).

However, these diseases can be largely prevented. The WHO estimates that a simultaneous reduction in blood pressure, obesity, cholesterol and tobacco use in the majority of the population would more than double the incidence of CVD (39). The presented risk factors and high mortality and morbidity from cardiovascular diseases indicate the need to take preventive measures as early as possible, with the parallel implementation of population strategy and high-risk strategy. The possibility of risk assessment is a step forward in the prevention of CVD.

## CONCLUSION

The present risk factors and high mortality and morbidity from cardiovascular disease indicate the need for taking preventive measures already in children, with the parallel implementation of population strategies and high risk.

## CONFLICTS OF INTEREST

The authors declare no financial or commercial conflicts of interest.

## FUNDING

None.

## REFERENCES

1. Mirzaei M, Truswell AS, Taylor R, Leeder SR. Coronary heart disease epidemics: not all the same. Heart 2009;95:740-746.
2. WHO. MONICA monograph and multimedia sourcebook. World s largest study of heart disease, stroke, risk factors and population trends 1979-2002. Tunstall-Pedoe H. ed, 2003.
3. Nacionalni vodič za lekare u primarnoj zdravstvenoj zaštiti, Prevencija kardiovaskularnih bolesti, Republička stručna komisija za izradu i implementaciju vodiča u klinikoj praksi, Ministarstvo zdravlja Republike Srbije 2004.
4. National Institute for Health and Clinical Excellence. Prevention of Cardiovascular Disease: Costing Report. 2010. Nice Public Health Guidance 25.
5. Clark AM, Hartling L, Vandermeer B, McAlister FA. Meta-analysis: secondary prevention programs for patients with coronary artery disease. Ann Intern Med. 2005;143:659-672.
6. Doll R, Peto R, Wheatley K, Gray R, Sutherland I. Mortality in relation to smoking: 40 years' observations on male British doctors. BMJ. 1994;309: 901-911.
7. Huisman M, Kunst AE, Mackenbach JP. Inequalities in the prevalence of smoking in the European Union: comparing education and income. Prev Med 2005;40: 756-764. BMJ 2004;328:217-219. 215.
8. Prescott E, Hippe M, Schnohr P, Hein HO, Vestbo J. Smoking and risk of myocardial infarction in women and men: longitudinal population study. BMJ 1998; 316:1043-1047.
9. World Health Organization. Global Health Observatory Data Repository.

10. O'Leary DH, Polak JF, Kronmal RA, Manolio TA, Burke GL, Wolfson SK Jr. Carotid- artery intima and media thickness as a risk factor for myocardial infarction and stroke in older adults. Cardiovascular Health Study Collaborative Research Group. N Engl J Med. 1999;340:14-22.
11. Chambless LE, Heiss G, Folsom AR, Rosamond W, Szklo M, Sharrett AR, et al. Association of coronary heart disease incidence with carotid arterial wall thickness and major risk factors: the Atherosclerosis Risk in Communities (ARIC) Study, 1987 - 1993. Am J Epidemiol. 1997;146:483- 494.
12. US Department of Health and Human Services.2008 Physical Activity Guidelines for Americans. 2008
13. Williams PT. Physical fitness and activity as separate heart disease risk factors: a meta- analysis. Med Sci Sports Exerc. 2001;33:754-761.
14. American College of Sports Medicine.ACSM's Guidelines for Exercise Testing and Prescription. 8th ed. Baltimore, MD: Lippincott, Williams and Wilkins; 2009.
15. World Health Organization. Obesity: Preventing and Managing the Global Epidemic. Report of a WHO Consultation. World Health Organization Technical Report Series, Report No. 894. 1998.
16. Fry J, Finley W. The prevalence and costs of obesity in the EU. Proc Nutr Soc. 2005;64:359-362.
17. Romero-Corral A, Montori VM, Somers VK, Korinek J, Thomas RJ, Allison TG, Mookadam F, Lopez-Jimenez F. Association of bodyweight with total mortality and with cardiovascular events in coronary artery disease: a systematic review of cohort studies. Lancet. 2006;368:666-678.
18. Poirier P, Giles TD, Bray GA, Hong Y, Stern JS, Pi-Sunyer FX, et al. Obesity, cardiovascular disease: pathophysiology, evaluation, effect of weight loss: an update of the 1997 American Heart Association Scientific Statement on Obesity and Heart Disease from the Obesity Committee of the Council on Nutrition, Physical Activity, and Metabolism. Circulation. 2006;113:898-918.
19. Freiberg MS, Pencina MJ, D'Agostino RB, Lanier K, Wilson PW, Vasan RS. BMI vs. waist circumference for identifying vascular risk. Obesity (Silver Spring) 2008;16: 463- 469.
20. Pischon T, Boeing H, Hoffmann K, Bergmann M, Schulze MB, Overvad K, et al. General and abdominal adiposity and risk of death in Europe. N Engl J Med. 2008;359:2105-2120.
21. Lewington S, Clarke R, Qizilbash N, Peto R, Collins R. Age-specific relevance of usual blood pressure to vascular mortality: a meta-analysis of individual data for one million adults in 61 prospective studies. Lancet 2002;360:1903-1913.
22. Franklin SS, Larson MG, Khan SA, Wong ND, Leip EP, Kannel WB, et al. Does the relation of blood pressure to coronary heart disease risk change with aging? The Framingham Heart Study. Circulation. 2001;103:1245-1249.
23. Mancia G, Laurent S, Agabiti-Rosei E, Ambrosioni E, Burnier M, Caulfield MJ, et al. Reappraisal of European guidelines on hypertension management: a European Society of Hypertension Task Force document. J Hypertens. 2009;27:2121 -2158.
24. O'Brien E, Asmar R, Beilin L, Imai Y, Mallion JM, Mancia G, et al. European Society of Hypertension recommendations for conventional, ambulatory and home blood pressure measurement. J Hypertens. 2003;21: 821-848.
25. Verberk W, Kroon AA, de Leeuw PW. Masked hypertension and white-coat hypertension prognosis. J Am Coll Cardiol. 2006;47:2127; author reply 2127-2128.
26. Ministarstvo zdravlja Srbije. Istraživanje zdravlja stanovnika republike Srbije. 2013.Izveštaj.
27. Cooney MT, Dudina A, De Bacquer D, Fitzgerald A, Conroy R, Sans S, et al. How much does HDL cholesterol add to risk estimation? A report from the SCORE Investigators. Eur J Cardiovasc Prev Rehabil. 2009;16:304-314.
28. Cooney MT, Dudina A, De Bacquer D, Wilhelmsen L, Sans S, Menotti A, et al. HDL cholesterol protects against cardiovascular disease in both genders, at all ages and at all levels of risk. Atherosclerosis. 2009;206:611-616.
29. https://www.heartscore.org last visit 27/07/2020.
30. UK Prospective Diabetes Study Group. Effect of intensive blood-glucose control with metformin on complications in overweight patients with type 2 diabetes (UKPDS 34). Lancet. 1998;352:854-865.
31. Albus C, Jordan J, Herrmann-Lingen C. Screening for psychosocial risk factors in patients with coronary heart disease—recommendations for clinical practice. Eur J Cardiovasc Prev Rehabil. 2004;11:75 -79.
32. Rozanski A, Blumenthal JA, Davidson KW, Saab PG, Kubzansky L. The epidemiology, pathophysiology, and management of psychosocial risk factors in cardiac practice: the emerging field of behavioral cardiology. J Am Coll Cardiol. 2005;45:637-651.
33. Kotseva K, Wood D, De Backer G, De Bacquer D, Pyorala K, Keil U. Cardiovascular prevention guidelines in daily practice: a comparison of EUROASPIRE I, II, and III surveys in eight European countries. Lancet. 2009;373:929 -940.
34. Rayner M, Allender S, Scarborough P. Cardiovascular disease in Europe. Eur J Cardiovasc Prev Rehabil. 2009;16(Suppl 2):S43-S47.
35. Cuende JI, Cuende N, Calaveras-Lagartos J. How to calculate vascular age with the SCORE project scales: a new method of cardiovascular risk evaluation. Eur Heart J 2010;31:2351-2358.
36. Conroy RM, Pyorala K, Fitzgerald AP, Sans S, Menotti A, De Backer G, et al. Estimation of ten-year risk of fatal cardiovascular disease in Europe: the SCORE project. Eur Heart J. 2003;24:987-1003.
37. Sofi F, Abbate R, Gensini GF, Casini A. Accruing evidence on benefits of adherence to the Mediterranean diet on health: an updated systematic review and meta-analysis. Am J Clin Nutr. 2010;92:1189-1196.

38. Conroy RM, Pyörälä K, Fitzgerald AP, Sans S, Menotti A, De Backer G, et al. Estimation of ten-year risk of fatal cardiovascular disease in Europe: the SCORE project. Eur Heart J. 2003;24(11):987-1003.
39. Lakic D, Tasic Lj, Kos M. Economic burden of cardiovascular disease in Serbia. Vojnosanit Pregled. 2014;71(2):137-147.

# IMMUNOHISTOCHEMICAL ANALYSIS OF THE EXPRESSION OF THE GLYCODELIN CYTOKINE IN ENDOMETRIAL TISSUE AND THE ENDOMETRIAL POLYP, BEFORE AND AFTER HYSTEROSCOPY, IN INFERTILE FEMALE PATIENTS

Aleksandar Devic[1], Ana Devic[1], Marija Sorak[2], Goran Zajic[3] and Slobodanka Mitrovic[4]

[1] *Clinical Hospital Center Zemun, Hospital for Gynecology and Obstetrics, Serbia*
[2] *University of Kragujevac, Faculty of Medical Sciences, Department of Gynecology, Kragujevac, Serbia*
[3] *Academy of Technical and Art Applied Studies Belgrade- ICT College of Applied Studies, Belgrade, Serbia*
[4] *University of Kragujevac, Faculty of Medical Sciences, Department of Pathology, Kragujevac, Serbia*

Received: 20.02.2021.
Accepted: 07.04.2021.

**Corresponding author:**

**Ana Devic**

Clinical Hospital Center Zemun, Hospital for Gynecology and Obstetrics, Serbia

Phone: +381 63 8138333

E-mail: anavjestica74@gmail.com

## ABSTRACT

*An endometrial polyp is most commonly a benign, localized proliferation of the glands and the endometrial stroma, covered with epithelium and protruding above the level of the mucosa. These polyps are most often diagnosed during investigation into the causes of irregular menstrual bleeding or infertility. It is produced in the highest concentration during the secretory phase of the endometrial cycle. The level of glycodelin reaches its peak 12 days after ovulation. The aim of this paper was to determine the changes in the immunohistochemical expression of glycodelin at the level of the endometrium and in the tissue of the polyp, before and after hysteroscopic polypectomy, in infertile female patients with an endometrial polyp, and in the endometrial tissue of female patients without an endometrial polyp. The study included 82 infertile female patients. The infertile patients were divided into two groups. The first was the experimental group which included 56 infertile female patients who had an endometrial polyp. The second group was the control group, composed of 26 infertile female patients who did not have an endometrial polyp. The results obtained primarily indicate the existence of changes in the immunohistochemical expression of the cytokine glycodelin in the female patients from both the experimental and the control group, not only prior to but also after hysteroscopy. A larger number of patients who have an endometrial polyp show a lack of glycodelin expression, more pronouncedly so in the bioptate of the endometrium than in the endometrial polyp.*

***Keywords***: *Glycodelin, polyp, endometrium, infertility.*

sciendo

UDK: 618.177-076
618.14-006
Eabr 2024; 25(2):165-170 DOI:
10.2478/sjecr-2021-0027

## INTRODUCTION

According to the World Health Organization (WHO), infertility is a disease of the reproductive system defined by the failure to achieve a clinical pregnancy after a year or more of regular unprotected sexual intercourse (1). In the world, around 10% of couples are infertile, and in Serbia the percentage of infertile couples is 15% (1). Endometrial polyps are thickenings of the uterine mucosa consisting of endometrial glands, stroma and blood vessels (2). A polyp is formed as a focal proliferation of the endometrial basal layer, while thickened blood vessels can be found in the base of the polyp (3, 4). The rate of recurrence of endometrial polyps in the overall population is around 24%. Pathological uterine bleeding is the most common clinical symptom of an endometrial polyp. In infertile women, the diagnosis of an endometrial polyp is usually a coincidental finding (4).

The diagnosis of endometrial polyp is established on the basis of histopathology and sonographic findings. Hysteroscopy is the golden standard in the diagnosis and therapy of endometrial polyps (5, 6, 7). Cytokines are polypeptides and glycopeptides with a molecular mass of 6 - 10 kDa. Cytokines demonstrate their effects through specific receptors within the cell or in the cell membrane (8). With the activation of specific receptors, certain genes are activated, and as a result of this activation, phenotypic and functional changes occur in the target cell. Cytokines may be positive or negative regulators of immune response. The basic function of cytokines is in intercellular communication (9). The activity of cytokines depends on their concentration. Depending on the influence that they have on the inflammatory reaction, cytokines are divided into proinflammatory and anti-inflammatory cytokines (10). Glycodelin, placental protein-14 or osteopontin (8) is a glycoprotein deposited in the glandular and epithelial cells of the endometrium (11, 12). It affects the endometrium through different cells (13).

In the human endometrium, during ovulation, the level of glycodelin is low 6 days before and 5 days after ovulation (14, 15). This can facilitate or allow fertilization to occur (16). During implantation the level of glycodelin significantly increases, prevents the action of NK cells, prepares the endometrium for implantation, and, to a certain extent, protects the embryo from the harmful effect of NK cell activity (17).

## MATERIALS AND METHODS

The research was conducted in the form of a randomized cross-sectional study on a sample of 82 infertile female patients, in the generative period. The first, experimental group comprised 56 infertile female patients with a diagnosis of endometrial polyp. The second, control group, consisted of 26 infertile patients who did not have an endometrial polyp. The study was carried out at the Obstetrics and Gynecology Clinic Narodni Front in Belgrade and at the Center for Molecular Medicine and Stem Cell Research of the Faculty of Medical Sciences, University of Kragujevac. The criteria for inclusion in the study were: infertility lasting at least one year, age between 20 and 42 years, regular menstrual cycle, no use of any type of hormonal contraceptives or other hormone products in the six months prior to the study, the finding of an endometrial polyp confirmed by transvaginal 2D ultrasound examination or by SIS (for the experimental group, only), no other endometrial pathology confirmed by transvaginal ultrasound examination (4). The criteria for exclusion from the study, for both groups of patients, were: the presence of submucosal myoma, endometriosis, endometrial carcinoma, uterine anomalies, patients who had undergone surgery of the uterus and fallopian tubes, patients with previous unsuccessful ovulation stimulation, and patients aged over 42 years. The study was approved by the Ethics Committee of the Obstetrics and Gynecology Clinic Narodni Front, No. 04-24 / 3-1i and by the Ethics Committee of the Faculty of Medical Sciences, University of Kragujevac, No: 01-3593 (4). Surgical procedures were performed on infertile patients in the first phase of the menstrual cycle, when the endometrial mucosa is the thinnest and when there is the least probability of interfering with early undiagnosed pregnancy (4, 7).

### Research Methodology

For the purpose of immunohistochemical analysis, the tissue of the endometrium and the polyp were fixed for 24 hours in 4% neutral buffered formalin, at room temperature. Then, the tissue sections were dehydrated, cleared in xylol and infiltrated with paraffin in the apparatus for automatic tissue sample fixation – the Leica TP1020 Tissue Processor and were then embedded into paraffin blocks. Paraffin molds obtained in this way were sectioned in the automatic Leica RM2155 Rotary Microtome into 4μm sections; they were then immersed in water at 56 °C and were finally placed on Superfrost glass microscope slides (18).

### Hematoxylin and Eosin Staining (HE)

The staining of paraffin tissue sections was performed by the application of Heidenhain's hematoxylin-eosin method and in keeping with Gurr's recommendations (19, 20). Slides with tissue sections obtained in this way were buffered in formaldehyde buffer for 10 seconds, rinsed with running water and finally immersed for two minutes in Mayer's hematoxylin (Merck). The tissue sections were then rinsed for one minute in running water and stained with alcoholic eosin (Merck) for one minute. After dehydration, tissue sections were dipped in a series of increasing ethanol concentrations, after which the clearing procedure was carried out, when the sections were immersed for 50 seconds in a mixture of xylol and ethanol (ratio 1:1), and then twice in pure xylol, 50 seconds each time. A drop of Canada balsam (Centrohem, Serbia) was placed on the tissue sections. The tissue sections were covered with cover slips. After drying for 24 hours, the preparations were analyzed under a light microscope (21, 22).

Tissue sections were heated at 56 ºC for a period of 60 minutes and were mounted onto adherent SuperFrost® slides. The slides with tissue sections were immersed in xylol, and then in a series of decreasing concentrations of ethanol. For the purpose of antigen unmasking, tissue sections were heated in a microwave oven in citrate buffer (pH = 6.0) for a period of 21 minutes. After cooling down, the preparations were rinsed in distilled water and were then incubated three times, 10 minutes each time, in phosphate buffered saline (PBS). For the purpose of fixation and permeabilization of the tissue sections, the slides with tissue sections were immersed in icy cold acetone, at 4 ºC, for 10 minutes. They were then rinsed in PBS. For the purpose of blocking the activity of endogenous peroxidase, several drops of Hydrogen Peroxide Blocking Reagent were applied on them. After ten minutes of incubation, the preparations were rinsed twice with PBS and then several drops of Protein Block were applied on them. After a ten-minute incubation period, the Protein Block was rinsed out, once, in PBS.

### Immunohistochemical staining

Tissue sections were incubated overnight with primary antibodies in a humidity chamber at 4 ºC. The appropriate mouse monoclonal antibodies (Ab17247, monoclonal 001-13, provided by Abcam) were used in the appropriate attenuation (1:200) dissolved in PBS (22). Tissue sections were rinsed in PBS, and appropriate commercial detection kits were used for antigen visualization (4, 23, 24).The reparations were covered with glycerol and a cover slip. Immunohistochemical staining was performed, with control for quality and specificity of staining, in keeping with the UK NEQAS (UK National External Quality Assessment Scheme for Immunocytochemistry) standards, and with the use of positive and negative controls (20). Different expression of epithelial endometrial cells was obtained with staining, in proportion to the binding of the dye to the cells (21).

### Statistical data processing

Sample size was determined on the basis of the formula for calculating large samples, implemented in the PASS 11.0 software. All the data obtained were processed using descriptive statistics methods (25). All results were processed with the aid of the SPSS 22.0 software package (26). The results obtained were compared to those of other authors available in literature (27). Conclusions were made on the basis of the results obtained (4, 22). For values that had a normal distribution, we used the Student's t test and Student's paired t test, and for other distributions nonparametric Mann-Whitney and Wilcoxon test is used. All statistical analyzes were performed with a 95% confidence interval. If the probability level of the null hypothesis is <5%, and if the significance of the test is $p < 0.05$ the results of the statistical analysis were accepted as statistically significant.

## RESULTS

This segment presents the analysis of the expression of the cytokine glycodelin obtained through the application of the immunohistochemistry method.

### Immunohistochemical expression of glycodelin

Table 1 and Graph 1 show the immunohistochemical (IHC) expression of the cytokine glycodelin in the polyp and the endometrium of the patients belonging to the experimental group and the endometrium of the patients from the control group.

**Table 1.** Immunohistochemical expression of glycodelin, in polyp tissue, endometrial biopsy of patients with polyp and without polyp

| **Experimental group** | N | % |
|---|---|---|
| Polyp | 9 | 18 |
| Bioptate of the endometrium | 1 | 2 |
| **Control group** | | |
| Bioptate of the endometrium | 1 | 3.8 |

N – number of patients
% – number of patients in percentages

**Graph 1.** Immunohistochemical expression of glycodelin, in polyp tissue, endometrial biopsy of patients with polyp and without polyp

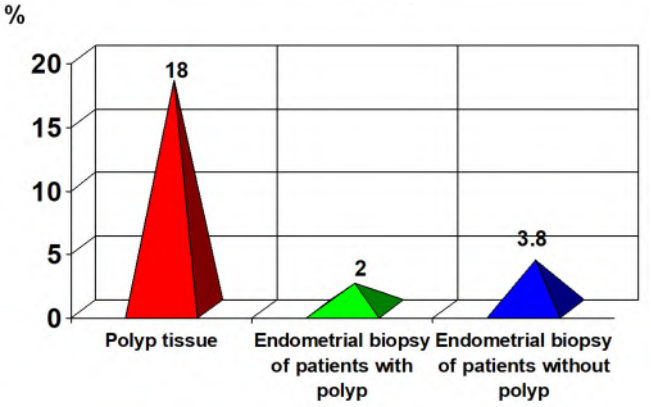


Statistical processing of the data shown in Table 1 and Graph 1 found that a very highly statistically significantly greater number of patients from the experimental group did not have IHC expression of glycodelin in the polyp ($\chi 2 = 20.480$; $p<0.001$), as compared to the patients within the group who did have IHC expression of glycodelin in the polyp. In the endometrial bioptate of the same patient group a very highly statistically significantly greater number of patients did not demonstrate IHC expression of glycodelin ($\chi 2 = 46.080$; $p<0.001$) as compared to those within this group who did demonstrate IHC expression in the endometrial bioptate. In the control group of infertile female patients there was also a very highly statistically significantly larger

number of patients who did not demonstrate IHC expression of glycodelin in the endometrial bioptate as compared to the number of patients in whom IHC expression of glycodelin was found in the endometrial bioptate ($\chi 2$ = 22.154; $p<0.001$).

When IHC glycodelin expression was compared between the polyp and the endometrial bioptate of the experimental group of patients, a statistically significant difference in IHC glycodelin expression was found (Z = -2.530; $p<0.05$).

**Signal intensity of immunohistochemical glycodelin expression**

Table 2 and Graph 2 show the signal intensity of glycodelin immunohistochemical expression in the polyp and the endometrium of the patients from the experimental group and the endometrium of the patients from the control group.

As shown in Table 2 and Graph 2, in most subjects, an IHC signal of glycodelin expression was registered neither in the polyp or the endometrial bioptate of the experimental patient group, nor in the endometrial bioptate of the control group of patients. In the polyp of the experimental group, in patients who demonstrated glycodelin expression, a low-intensity signal was registered in 5 (10%) of patients, a medium-intensity signal was registered in three (6%) patients, and a high-intensity signal was registered in one (2%) patient. In the endometrial bioptate of the experimental group, a low-intensity signal of ICH glycodelin expression was registered in only one (2%) patient, which was also the case in the control group of patients – a low-intensity signal was registered in one (3,8%) patient.

**Table 2.** Signal intensity of IHC glycodelin expression, in polyp tissue, endometrial biopsy of patients with polyp and without polyp

| **Experimental group** | Low-intensity signal (%) | Medium-intensity signal (%) | High-intensity signal (%) |
|---|---|---|---|
| Polyp | 10 | 6 | 2 |
| Bioptate of the endometrium | 2 | 0 | 0 |
| **Control group** | | | |
| Bioptate of the endometrium | 3.8 | 0 | 0 |

Signal intensity: low-intensity signal, medium-intensity signal, high-intensity signal

**Graph 2.** Signal intensity of IHC glycodelin expression, in polyp tissue, endometrial biopsy of patients with polyp and without polyp

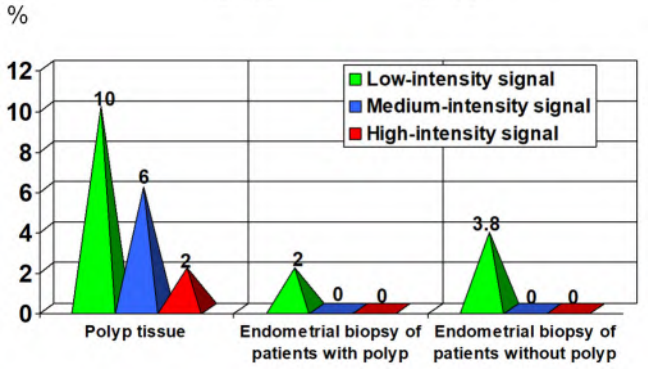


Statistical processing of the data shown in Table 2 and Graph 2 found a very highly statistically significant difference in the signal intensity of IHC glycodelin expression, both in the polyp ($\chi 2$ = 87.280; $p<0.001$) and in the endometrial bioptate ($\chi 2$ = 46.080; $p<0.001$) of the experimental group of patients. The same was true for the control group. The frequency of no signal registered was very highly statistically significantly greater than the registering of a low-intensity signal ($\chi 2$ = 22.154; $p<0.001$). In the experimental group of patients, the distribution of IHC glycodelin expression signal intensity was statistically significantly different between the endometrial bioptate and the polyp (Z = -2.511; $p<0.05$). The signal intensity of IHC glycodelin expression in the polyp of the experimental group of patients and the endometrial bioptate of the control group of patients did not show a statistically significant difference (Z = -1.753; $p>0.05$), as was the case within the control group of patients among the endometrial bioptate specimens. (Z = 0.474; $p>0.05$).

**Microscopic view of immunohistochemical glycodelin expression**

Image 1 shows the microscopic view of the signal intensity of IHC glycodelin expression in the endometrial bioptate of the patients from the control group, at x10 magnification. Images 2 and 3 represent microscopic views of the signal intensity of IHC glycodelin expression in the endometrial polyp of the experimental patient group, at x10 and x20 magnification, respectively. Image 4 shows a microscopic view of the signal intensity of IHC glycodelin expression in the endometrial bioptate of patients from the control group, at x10 magnification. Image 5 shows a microscopic view of IHC glycodelin expression in the tissue of the placenta and the epithelium of the chorionic villi, at x20 magnification (external positive control of immunohistochemical staining).

**Image 1.** Microscopic view of IHC glycodelin expression in the endometrial bioptate of the infertile patients without a verified endometrial polyp ( x10 magnification)

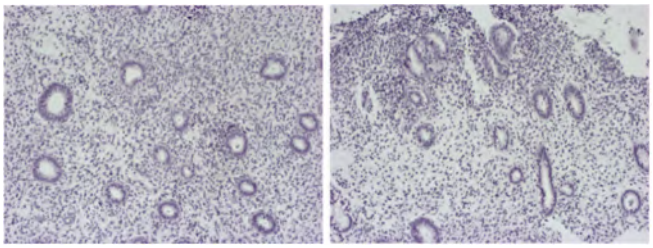

**Image 2.** Microscopic view of IHC glycodelin expression in the tissue of the endometrial polyp of infertile patients without a verified endometrial polyp ( x10 magnification)

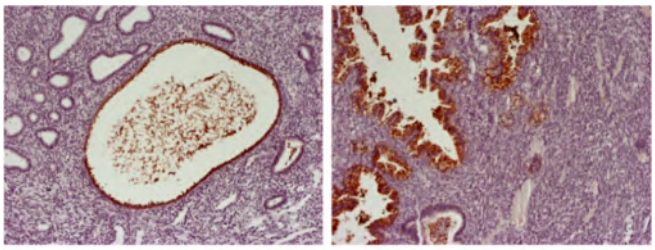

**Image 3.** Microscopic view of IHC glycodelin expression in the tissue of the endometrial polyp of infertile patients with a verified endometrial polyp ( x20 magnification)

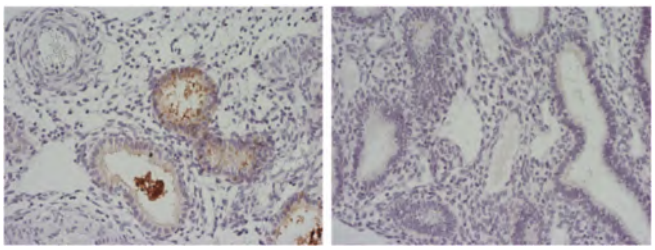

**Image 4.** Microscopic view of IHC glycodelin expression in the endometrial bioptate of infertile patients without a verified endometrial polyp( x10 magnification)

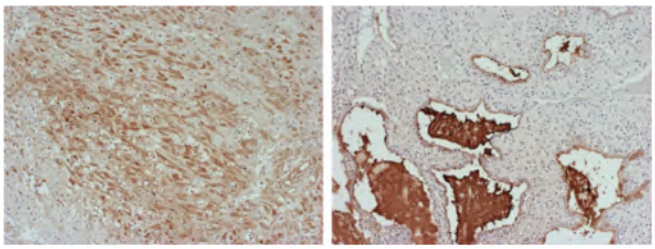

**Image 5.** Microscopic view of IHC glycodelin expression in the tissue of the placenta and the epithelium of the chorionic villi (external positive control of immunohistochemical staining, x20 magnification)

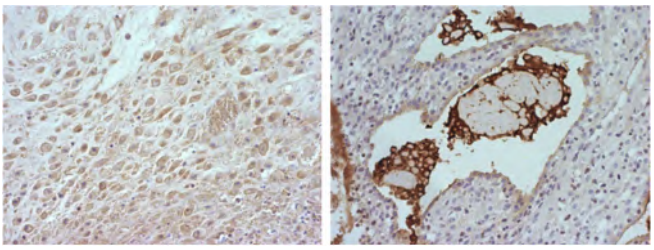

## LITERATURE


1. Zegers-Hochschild F, Adamson GD, de Mouzon J, Ishihara O, Mansour R, Nygren K, Sullivan E, Van der Poel S. The international committee for monitoring assisted reproductive technology (ICMART) and the world health organization (WHO) revised glossary on ART terminology. Hum Reprod. 2009 Oct 4;24(11):2683-7.
2. Bassil S. Changes in endometrial thickness, width, length and pattern in predicting pregnancy outcome during ovarian stimulation in in vitro fertilization. Ultrasound Obstet Gynecol. 2001 Sep;18:258-63.
3. Mahajan N, Kaur S, Alonso MR. Window of implantation is significantly displaced in patients with adenomyosis with previous implantation failure as determined by endometrial receptivity assay. J Hum Reprod Sci. 2018 Oct;11(4):353.
4. Sorak M, Devic A. Analysis of Glycodelin Levels Before and After Hysteroscopic Polypectomy in Infertile Patients. Serbian Journal of Experimental and Clinical Research. 2018 Oct 29; 19(3): 247-253.
5. Nijkang NP, Anderson L, Markham R, Manconi F. Endometrial polyps: Pathogenesis, sequelae and treatment. SAGE open medicine. 2019 Apr;7:2050 312119848247.
6. Banas T, Pitynski K, Mikos M, et al. Endometrial polyps and benign endometrial hyperplasia have increased prevalence of DNA fragmentation factors 40 and 45 (DFF40 and DFF45) together with the antiapoptotic B-cell lymphoma (Bcl-2) protein compared with normal human endometria. Int J Gynecol Pathol 2018; 37(5): 431–440.
7. Munro MG. Practical aspects of the two FIGO systems for management of abnormal uterine bleeding in the reproductive years. Best Pract Res Clin Obstet Gynaecol 2017; 40: 3–22.
8. Ferreira VL, Borba HHL, Bonetti AF, Leonart LP, Pontarolo R. Cytokines and interferons: types and functions. In: Ali Khan W, editor. *Autoantibodies and Cytokines*. IntechOpen (2018).

9. Kopitar Jerala N. The Role of Interferons in Inflammation and Inflammasome Activation. Frontiers in Immunology. 2017; 8:873
10. Pattelongi I, Massi MN, Idris I, Bukhari A, Wahyu Widodo AD, Achmad H. Research Reviews on Effect of Exercise on DAMP's, HMGB1, Proinflammatory Cytokines and Leukocytes. Systematic Reviews in Pharmacy. 2020 Apr 1;11(4):306-312.
11. Koistinen H, Pasanen A, Hautala L. [abstract]. In: Proceedings of the 107th Annual Meeting of the American Association for Cancer Research; 2016 Apr 16-20; New Orleans, LA. Philadelphia (PA): AACR; Cancer Res 2016;76(14 Suppl):Abstract nr 436.
12. Dantzer R. Expression and action of cytokines in the brain: mechanisms and pathophysiological Implications. In: Ader R editor. Psychoneuroimmunology (4th edition), Vol I:271-80. Amsterdam: Elsevier Inc.;2007 Dec 1.
13. Mylonas I, Speer R, Makovitzky J, Richter DU, Briese V, Jeschke U, Friese K. Immunohistochemical analysis of steroid receptors and glycodelin A (PP14) in isolated glandular epithelial cells of normal human endometrium. Histochem Cell Biol. 2000 Nov 1;114(5):405-411.
14. Ben-Nagi J, Miell J, Yazbek J, Holland T, Jurkovic D. The effect of hysteroscopic polypectomy on the concentrations of endometrial implantation factors in uterine flushings. Reprod Biomed Online. 2009 Nov; 19(5): 737-44.
15. Ben-Nagi J, Miell J, Mavrelos D, Naftalin J, Lee C, Jurkovic D. Endometrial implantation factors in women with submucous uterine fibroids. Reprod Biomed Online. 2010 Nov; 21(5):610– 5.
16. Cui J, Liu Y, Wang X. The roles of glycodelin in cancer development and progression. Front Immunol. 2017 Nov 29;8:1685.
17. Weber R, Meister M, Muley T, Thomas M, Sültmann H, Warth A, Winter H, Herth FJ, Schneider MA. Pathways regulating the expression of the immunomodulatory protein glycodelin in non-small cell lung cancer. Int J Oncol. 2019 Feb 1;54(2):515-26.
18. Kim SW, Roh J, Park CS. Immunohistochemistry for pathologists: protocols, pitfalls, and tips. J Pathol Transl Med. 2016 Nov;50(6):411.
19. Gurr GT. Biological staining methods. Biological Staining Methods. Chadwell Heath: Hopkin and Williams; 1979 (9th Edition).
20. Heidenhain M. Noch einmal uber die darstellung der centralkorper durch eisnhamatoxylin nebst einigen allgemeinen bemerkungen uber die hamatoxylinfarben. Z Wiss Mikrosk. 1896;13:186.
21. Renshaw S, editor. Immunohistochemistry and immunocytochemistry: Essential methods. John Wiley & Sons; 2017 Feb 6.
22. Dević A, Vasiljević M, Šorak M, Dević A, Rudić-Biljić-Erski I, Zajić G. The effect of hysteroscopic polypectomy on the concentrations of tumour necrosis factor-α (TNF-α) in uterine flushings and serum in infertile women. Srpski arhiv za celokupno lekarstvo. 2020(00):120-120.
23. Seshi R. Sompuram, Kodela Vani, Anika K. Schaedle, Anuradha Balasubramanian, Steven A. Bogen, Selecting an Optimal Positive IHC Control for Verifying Antigen Retrieval, J Histochem Cytochem. 2019 Apr; 67(4): 275–289.
24. Seshi R. Sompuram, Kodela Vani, Brian Tracey, Debra A. Kamstock, Steven A. Bogen, Standardizing Immunohistochemistry: A New Reference Control for Detecting Staining Problems, J Histochem Cytochem. 2015 Sep; 63(9): 681–690.
25. Barton B, Peat J. Medical statistics: A guide to SPSS, data analysis and critical appraisal. John Wiley & Sons; 2014 Aug 6.
26. Belinda Barton, Jennifer Peat, Medical Statistics: A Guide to SPSS, Data Analysis and Critical Appraisal 2nd Edition, Wiley, dec 2017, ISBN-13: 978-1118589939
27. Katabi N, Xu B, Jungbluth AA, et al. PLAG1 immunohistochemistry is a sensitive marker for pleomorphic adenoma: a comparative study with PLAG1 genetic abnormalities. Histopathology. 2018;72(2):285-293.
28. Ferenczy A, Giudice LC. The Endometrial Cycle: Morphologic and Biochemical Events. In: Adashi EY, Rock JA and Rosenwaks Z, editors. Reproductive Endocrinology, Surgery, and Technology. New York: Raven Press; 1995; 1:171-94.
29. Lee C-L, Vijayan M, Wang X, Lam KKW, Koistinen H, Seppälä M et al. Glycodelin-A stimulates the conversion of human peripheral blood CD16(-)CD56(bright) NK cell to a decidual NK cell-like phenotype. Hum Reprod. 2019 Apr;34(4):689-701.

# MICROINFLAMMATION IN PATIENTS ON HEMODIALYSIS: A PRACTICAL APPROACH

Marko Nenadovic[1], Aleksandra Nikolic[2], Marijana Stanojevic Pirkovic[3], Tomislav Nikolic[1,4], Dejan Petrovic[1,4] and Jasna Trbojevic-Stankovic[5,6]

[1]*Faculty of Medical Sciences, University of Kragujevac, Kragujevac, Serbia*
[2]*Clinic of Internal Medicine, Clinical Center Kragujevac, Kragujevac, Serbia*
[3]*Department of Biochemistry, Faculty of Medical Sciences, University of Kragujevac, Kragujevac, Serbia*
[4]*Clinic of Urology, Nephrology and Dialysis, University Clinical Center Kragujevac, Kragujevac, Serbia*
[5]*Faculty of Medicine, University of Belgrade, Belgrade, Serbia*
[6]*University Hospital Center "Dr Dragisa Misovic - Dedinje", Belgrade, Serbia*

Received: 01.10.2021
Accepted: 15.10.2021.

**Corresponding author:**

**Prof. dr Dejan Petrovic**

Faculty of Medical Sciences, University of Kragujevac, Clinic of Urology, Nephrology and Dialysis, University Clinical Center Kragujevac, Kragujevac, Serbia

E-mail: dejan.petrovic@fmn.kg.ac.rs

## ABSTRACT

*Microinflammation is a non-traditional risk factor for the development of cardiovascular diseases in patients on hemodialysis. It occurs in 30-50% of these patients, and its main causes are: uremic toxins, oxidative stress, metabolic acidosis, vitamin D deficiency, overhydration, altered intestinal microbiome, impaired intestinal epithelial barrier integrity, increased translocation of endotoxin from the intestinal lumen into the systemic circulation, occult infection of the vascular approach for hemodialysis, periodontal disease, bioincompatibility of the hemodialysis membrane and the presence of endotoxin in the hemodialysis solution. The main clinical consequences of microinflammation are: accelerated atherosclerosis, malnutrition, anemia, resistance to the action of erythropoietin, hemoglobin variability and dialysis-related amyloidosis. Postdilution online hemodiafiltration, extended and adsorptive hemodialysis prevent the development of microinflammation. Optimal control of microinflammation prevents the development of cardiovascular diseases, improves the quality of life and the outcome of patients who are treated with regular hemodialysis.*

***Keywords***: *Microinflammation, postdilution online hemodiafiltration, extended hemodialysis, adsorptive hemodialysis.*

sciendo

UDK: 616.12:616.61-78-056.24
Eabr 2024; 25(2):171-179
DOI: 10.2478/sjecr-2021-0047

## INTRODUCTION

Cardiovascular diseases are the leading cause of death in patients treated with regular hemodialysis (1-4). Uremic toxins, microinflammation, malnutrition, oxidative stress, endothelial dysfunction, erythropoietin resistance and anemia are significant non-traditional risk factors for the development of cardiovascular disease. Microinflammation occurs in 30-50% of patients on hemodialysis, and its main clinical consequences are: accelerated atherosclerosis, malnutrition and resistance to the action of erythropoietin. Microinflammation plays a key role in the process of atherosclerosis, development and rupture of atherosclerotic plaque, and its early detection and timely application of appropriate treatment significantly reduce the development of cardiovascular morbidity and mortality in patients treated with hemodialysis (5). Early detection and optimal control of nontraditional risk factors play a key role in preventing the development of cardiovascular disease in this patient population (4-6).

### Definition and etiopathogenesis of microinflammation

Microinflammation is defined as a pathological condition, which is characterized by constant low-grade inflammation followed by an increase in the concentration of pro-inflammatory mediators in the serum (concentration of C-reactive protein - CRP ≥ 10 mg/L, IL-6 concentration ≥ 7 pg/mL) (7). The etiopathogenesis of microinflammation is complex and includes multiple factors: uremic toxins, immune system dysfunction in chronic kidney disease, intestinal microbiome dysfunction, dialysis membrane biocompatibility, conventional dialysis solution, presence of endotoxin in dialysis solution, reversible ultrasound hemodialysis, gingival infection (periodontitis), increased extracellular fluid volume (overhydration), metabolic acidosis, vitamin D deficiency (7, 8).

Uremic toxins play a significant role in the development of microinflammation, oxidative stress, accelerated atherosclerosis, and cardiovascular disease in this patient population (8-10). According to the recommendations of the EUTox (European Union Toxin Working Group), uremic toxins are divided into three groups. The first group consists of uremic toxins of low molecular weight (MW < 500 Da). These toxins are soluble in water and are effectively removed by standard high-flux hemodialysis. The second group consists of uremic toxins that bind in a high percentage to plasma proteins (degree of binding to plasma proteins > 90%). They are mainly low molecular weight (MW < 500 Da) and are efficiently removed by hemodialysis with membranes that have the ability to adsorb. Middle molecular weight uremic toxins (MW = 0.5-60 kDa) belong to the third group of uremic toxins. These uremic toxins are effectively removed by postdilution online hemodiafiltration and extended hemodialysis - ED (Expanded Dialysis). Middle molecular weight uremic toxins include proinflammatory cytokines (interleukin-1β, interleukin-6, interleukin-18, tumor necrosis factor alpha - TNFα), proinflammatory proteins (pentraxin-3, YKL-40) and adipokines (adiponectin, visfatin, leptin). Proinflammatory cytokines, proteins and adipokines play a significant role in the development of microinflammation and malnutrition in patients treated with regular hemodialysis. Microinflammation, malnutrition and oxidative stress are significant non-traditional risk factors, which result in the development of accelerated atherosclerosis (atherosclerotic cardiovascular disease), amyloidosis associated with hemodialysis, erythropoietin resistance, and anemia (8-10).

In the end-stage of chronic kidney disease, due to the accumulation of uremic toxins, the function of the immune system is disturbed. We distinguish between disorders of the innate and acquired immune system. Disorders of the innate immune system in patients on hemodialysis include: constant activation of neutrophils and low-grade peripheral blood monocytes, which results in an increased risk of developing microinflammation and atherosclerotic cardiovascular diseases. Due to the reduced function of phagocytosis of neutrophils and monocytes, as well as the reduced function of NK cells, the risk of bacterial infections is increased. Disorder of the acquired immune system is characterized by a decrease in the number and function of B and T lymphocytes, which results in an increased risk of viral infections and malignant diseases (11). The two most significant uremic toxins that alter the function of the immune system in this patient population are indoxyl sulfate and p-cresyl sulfate. Indoxyl sulfate stimulates monocytes to enhance the production and release of proinflammatory cytokines, while p-cresyl sulfate reduces phagocytosis function and NADPH oxidase activity in neutrophils, as well as antigen presentation by dendritic cells (11).

Hemodialysis membranes play a key role in the process of hemodialysis and hemodiafiltration. They can be natural or artificial (synthetic). Natural membranes are derivatives of cellulose (cuprophan), they are "low-flux", they are less biocompatible compared to synthetic membranes and they have a small clearance of uremic toxins of middle molecular weight. Synthetic membranes (polysulfone, polyethersulfone, polyarylethersulfone, ethylene vinyl alcohol, polyamide, polyacrylnitrile, polymethylacrylate, helixone) are highly biocompatible “high-flux” membranes, which have a good clearance of middle molecular weight uremic toxins (12-14). The composition of the dialysis membrane (cellulose membrane), the sterilization method (ethylene oxide) and bisphenol A can be triggers of bioincompatibility reactions. During hemodialysis, the blood comes into direct contact with the synthetic material of the dialysis membrane and extracorporeal circulation, and as a consequence various reactions can occur: activation of neutrophils and peripheral blood monocytes, activation of the complement system, activation of coagulation and platelet systems, hypersensitivity reactions (allergic reactions). Activated neutrophils increase the production and release of proteinases (elestase, myeloperoxidase), lactoferrin, cathepsin, chemokines (IL-8, CCL2, CCL3) and cytokines (IL-1, IL-6, TNFα, TGFβ). Released mediators intensify microinflammation. In clinical practice, the concentration of neutrophilic elastase and myeloperoxidase (released from granules due to neutrophil activation) in serum is measured to assess the biocompatibility of the

dialysis membrane, while the concentration of platelet factor 4 and β-thromboglobulin is measured to assess platelet activation. All of these serum parameters are measured at the start of the dialysis session, after 15 minutes, 60 minutes, and at the end of the dialysis session (12-14). Due to the activation of neutrophils and peripheral blood monocytes, there is an increased production of oxygen free radicals, and due to increased loss of trace elements and water-soluble antioxidants during the hemodialysis session, the activity of antioxidant enzymes decreases (increased oxidative stress) (12-14).

Allergic reactions associated with hemodialysis are classified as type A and type B reactions. Type A reactions occur 5-30 minutes after the start of dialysis, are mediated by IgE class antibodies (anaphylactic reactions), releasing histamine, leukotrienes, prostaglandins and cytokines from mast cells and basophils, resulting in itching, runny nose, abdominal cramps, tingling in the vascular approach to hemodialysis, urticaria, bronchospasm, angioedema, and anaphylactic shock (15, 16). Type A reactions are repeated when the same type of dialyzer is used. Type B reactions occur later (> 30 minutes from the start of the hemodialysis session), are not mediated by IgE class antibodies (anaphylactoid reactions), are triggered by activation of the complement system, clinical symptoms are less pronounced: headache, nausea, vomiting, back and/or chest pain, hypotension (15, 16).

The microbiological quality of the hemodialysis solution is a risk factor for the development of microinflammation and accelerated atherosclerosis. During the hemodialysis session, bacterial products (endotoxins) through the processes of backdiffusion and back ultrafiltration (backdiffusion/backfiltration) from the dialysis solution, through the dialysis membrane, reach the patient's blood and activate monocytes. Activated monocytes intensively produce and release pro-inflammatory cytokines (IL-1, IL-6, TNFα), which results in the development of persistent low-grade microinflammation and the development of accelerated atherosclerosis. High-flux hemodialysis, postdilution online hemodiafiltration, and extended hemodialysis require an ultrapure dialysis solution. It is defined as a solution in which the bacterial concentration is < 0.1 CFU/mL and the endotoxin concentration is less than 0.03 EU/mL. In postdilution online hemodiafiltration, a sterile substitution solution is used, and it is defined as a solution in which the bacterial concentration is < 10-6 CFU/ml and the endotoxin concentration is less than 0.03 EU/mL (17).

Metabolic acidosis occurs in 15-20% of patients with chronic kidney disease. It is defined as a serum bicarbonate concentration of less than 22 mmol/L. The main clinical consequences of metabolic acidosis are: microinflammation, increased protein catabolism (decrease in muscle mass), progression of chronic kidney disease, development of osteoporosis, insulin resistance, decreased albumin synthesis in the liver (hypoalbuminemia), increased risk of adverse outcome in these patients. The target serum bicarbonate concentration in patients with chronic kidney disease should be - $HCO3^- \geq$ 22 mmol/L (optimal $HCO3^-$ concentration should be: 22-26 mmol/L) (21, 22). For the treatment of metabolic acidosis, sodium bicarbonate (650 mg tablets) is used twice a day until the target serum bicarbonate concentration is reached (18, 19).

Oxidative stress is a non-traditional risk factor for the development of cardiovascular diseases in the population of patients treated with regular hemodialysis. Hemodialysis is itself a trigger for increased oxygen free radical formation. The two main pathophysiological mechanisms of enhanced oxygen free radical formation during a hemodialysis session are: bioincompatibility of the dialysis membrane and the presence of endotoxin in the dialysis solution. In contact with the blood and the dialysis membrane, NADPH neutrophil oxidase is activated, oxygen free radicals are formed, and myeloproxidase - MPO (Myeloperoxidase) is released from the neutrophil granules. Measurement of serum myeloperoxidase concentration during a hemodialysis session is an indicator of the severity of oxidative stress induced by a bioincompatible dialysis membrane. Endotoxin and other bacterial products, through backdiffusion/backfiltration processes, pass from the dialysis solution through the dialysis membrane into the patient's circulation and activate neutrophils and monocytes to increase the production and release of oxygen free radicals and proinflammatory cytokines. This results in the development of oxidative stress, microinflammation and accelerated atherosclerosis. In patients treated with regular hemodialysis, the activity of enzymatic and non-enzymatic antioxidant systems is reduced. During the hemodialysis session, trace elements (zinc, selenium, copper) are lost, and this results in reduced activity of antioxidant enzymes, such as superoxide dismutase and glutathione peroxidase. Vitamin E-coated dialysis membrane reduces the concentration of lipid peroxidation parameters in the serum of patients treated with high-flux hemodialysis and postdilution online hemodiafiltration (20, 21).

Intestinal microbiome disorder (intestinal dysbiosis) is defined as a change in the composition and function of intestinal microorganisms. Studies show that intestinal microbiome disorder is a non-traditional risk factor for the development of cardiovascular disease in patients treated with regular hemodialysis. As a consequence of intestinal microbiome disorders, indoxyl sulfate and p-cresyl sulfate are increasingly formed. These uremic toxins bind in a high percentage to plasma proteins, are poorly removed by high-flux hemodialysis, extended hemodialysis, and postdilution online hemodiafiltration. They stimulate the activation and adhesion of leukocytes to endothelial cells, increase and release inflammatory mediators, stimulate oxidative stress and the formation of foam cells, cause endothelial dysfunction and reduced production of nitric oxide, which begins the process of atherosclerosis (atherosclerotic plaque). High-flux hemodialysis with adsorptive membranes and the oral adsorbent AST-120 play a significant role in reducing the concentration of indoxyl sulfate and preventing the development of atherosclerotic cardiovascular diseases in patients treated with regular hemodialysis (22). Intestinal microbiome disorders and intestinal epithelial barrier integrity disorders play a significant role in the development of microinflammation in

patients treated with regular hemodialysis. Due to the disturbed epithelial barrier of the intestine, bacteria and endotoxins are translocated from the intestinal lumen into the systemic circulation, which activate the innate immune system. Through so many receptors, neutrophils and peripheral blood monocytes are activated, they increase the production and release of proinflammatory mediators (cytokines), resulting in systemic microinflammation (22).

High-flux hemodialysis with adsorptive membranes and the oral adsorbent AST-120 play a significant role in reducing the concentration of indoxyl sulfate and preventing the development of atherosclerotic cardiovascular diseases in patients treated with regular hemodialysis (22). Intestinal microbiome disorders and intestinal epithelial barrier integrity disorders play a significant role in the development of microinflammation in patients treated with regular hemodialysis. Due to the disturbed epithelial barrier of the intestine, bacteria and endotoxins are translocated from the intestinal lumen into the systemic circulation, which activate the innate immune system. Through so many receptors, neutrophils and peripheral blood monocytes are activated, they increase the production and release of proinflammatory mediators (cytokines), resulting in systemic microinflammation (22).

Overhydration is defined as an increase in the volume of extracellular fluid in patients treated with regular hemodialysis. It is a risk factor for the development of microinflammation, malnutrition and cardiovascular diseases. Overhydration causes edema of the intestinal wall and increased translocation of bacteria and endotoxins from the intestinal lumen into the systemic circulation. As a consequence of the activation of the cells of the innate immune system, there is an increased production and secretion of proinflammatory cytokines and the development of microinflammation. The following parameters are used to assess the state of hydration: overhydration (OH) and the ratio of overhydration to extracellular fluid volume (OH/ECW). Normal hydration in hemodialysis patients is present if the OH is in the range of -1.1 to +1.1 liters. Mild hyperhydration exists if OH = 1.1-2.5 liters, and severe excess fluid is defined as OH > 2.5 liters. The OH/ECW ratio > 15% in men and > 13% in women indicates overhydration. Patients treated with hemodialysis in whom OH > 2.5 liters and OH/ECW ratio > 15% have a statistically significantly higher mortality rate compared to patients with normal hydration (23-26).

Vitamin D [25 (OH) D] reduces microinflammation, resistance to the action of erythropoietin, has a protective effect on the cardiovascular and immune system of patients treated with regular hemodialysis. In patients treated with regular hemodialysis, the normal concentration of vitamin D [25 (OH) D] is 30-80 ng/mL, and vitamin D deficiency is defined as a vitamin D concentration of less than 30 ng/mL. Patients with a serum vitamin D concentration of 20-30 ng/mL have a mild deficiency, and a serum vitamin D concentration of 10-20 ng/mL indicates a moderate deficiency. Severe vitamin D deficiency is defined as a vitamin D concentration of less than 10 ng/mL. Vitamin D substitution involves the administration of ergocalciferol or cholecalciferol at a dose of 25,000 IU/week for 3-6 months. In case of severe vitamin D deficiency (< 10 ng/mL), ergolaciferol or cholecalciferol should be administered at a dose of 50,000 IU/week for three to six weeks, until the target serum vitamin D concentration ≥ 30 ng/mL (27).

## Clinical consequences of microinflammation

### *Atherosclerosis and atherosclerotic cardiovascular disease*

Microinflammation, oxidative stress, and hyperhomocysteinemia are significant risk factors for the development of accelerated atherosclerosis in patients undergoing regular hemodialysis. These risk factors block the activity of the enzymes dimethyl-diamino-hydrolase - DDHA (Dimethyl-Diamino-Hydrolase) in the endothelial cells of arterial blood vessels, which breaks down asymmetric dimethylarginine - ADMA (Asymmetric Dimethylarginine) to L-citrulline and methionine. Asymmetric dimethylarginine is the most important endogenous blocker of nitric oxide synthase - NO (Nitrogen Oxide), and reduced production of nitric oxide in endothelial cells plays a key role in initiating the process of atherosclerosis (28). The process of atherosclerosis goes through several stages: increased endothelial permeability, expression of adhesion molecules on the surface of endothelial cells, adhesion and migration of leukocytes and monocytes, formation of foam cells, plaque rupture and thrombus formation. Microinflammation leads to the accumulation of neutrophils and monocytes in atherosclerotic plaque, and the release of cytokines and metalloproteinases causes rupture of the atherosclerotic plaque cap and the development of an acute coronary event (29, 30).

### *Anemia, erythropoietin resistance and hemoglobin variability*

Microinflammation is a risk factor for the development of anemia, resistance to the action of erythropoietin, as well as for the variability of hemoglobin in patients on hemodialysis. The pathophysiological mechanisms of the development of anemia due to microinflammation can be divided into two groups: hepcidin-dependent mechanisms and hepcidin-independent mechanisms. Microinflammation (interleukin-6) stimulates the synthesis of hepcides in liver cells. Hepcidin prevents the release of iron from the cells of the reticulonedothelial system in the liver and spleen and causes a functional lack of iron (reduced amount of iron available for erythrocytopoiesis in the bone marrow). Mechanisms independent of hepcidin include: decreased production of endogenous erythropoietin (IL-1β, TNFα), blocking the proliferation and differentiation of erythrocyte lineage precursor cells in the bone marrow (TNFα, INFγ) and shortened erythrocyte lifespan (neutrophil elestasis) (31 ). Erythropoietin Resistance Index (ERI) is defined as the ratio of the weekly dose of erythropoietin depending on body weight and hemoglobin concentration in the blood. Resistance to the action of short-

acting erythropoietins exists if the resistance index - ERI ≥ 1.0 IU/kg/week/gHb. Resistance index - ERI ≥ 0.005 μg/kg/week/gHb indicates resistance to the action of long-acting erythropoietins. The main risk factors for the development of erythropoietin resistance include: uremic toxins, microinflammation, oxidative stress, iron deficiency, vitamin D deficiency, uncontrolled secondary hyperparathyroidism, excessive hydration, vitamin B12 and folic acid deficiency. The results of clinical trials show that the concentration of CRP in serum ≥ 20 mg/L, tumor necrosis factor - TNFα ≥ 2 ng/mL and interleukin 6 - IL-6 ≥ 40 ng/mL indicates the existence of resistance to the action of erythropoietin in patients who are treated with regular hemodialysis (31).

Hemoglobin variability is a risk factor for adverse outcomes in patients treated with regular hemodialysis. It is defined as an oscillation of the hemoglobin concentration in the blood over a period of 8 weeks, with an amplitude greater than 15 g/L from the set target hemoglobin values (hemoglobin oscillation greater than 15 g/L from the equilibrium point with a return back to the same point during the period of at least 8 weeks). Factors that cause hemoglobin variability can be divided into three groups. The first group consists of drug-related factors (drugs), which include: pharmacokinetic characteristics of erythropoietin, bioavailability and route of administration of erythropoietin (s.c. or i.v.). Factors related to the patient include acute and chronic comorbidities: microinflammation, malnutrition, vitamin D deficiency, secondary hyperparathyroidism. The third group consists of factors related to treatment protocols and costs (refund policy) (32). The strategy to prevent the development of variability includes: more frequent monitoring of hemoglobin concentration in the blood (weekly or biweekly), gradual change of erythropoietin dose (± 25% of the initial dose), preventive increase of erythropoietin dose (inflammatory conditions), optimal microinflammation control, fast and effective treatment of infection , rapid and effective treatment of gastrointestinal bleeding, optimal control of secondary hyperparathyroidism, erythropoietin and iron dosage compliance, erythropoietin change, and individualization of anemia treatment (32).

***Malnutrition: loss of energy due to lack of protein***

Malnutrition is a risk factor for an unfavorable outcome in patients treated with regular hemodialysis. The two main pathophysiological mechanisms of malnutrition due to protein deficiency are: reduced dietary protein intake and increased catabolism of deposited proteins. Reduced dietary protein intake is a consequence of loss of appetite and reduced absorption of nutrients from the gastrointestinal tract. Increased protein catabolism in hemodialysis patients occurs due to microinflammation, oxidative stress, metabolic acidosis, insulin resistance, and testosterone deficiency (33, 34). In hemodialysis patients, dietary protein intake should be ≥ 1.2 g/kg/day and energy intake 35 kcal/kg/day. Oral Nutrition Supplementation (OSN) provides additional protein intake of 0.3-0.4 g/kg/ day and energy of 10 kcal/kg/day. In patients on hemodialysis with proven malnutrition, in whom the spontaneous intake of protein is less than 0.8 g/kg/day and energy is less than 20 kcal/kg/day, intradialysis parenteral nutrition - IDPN (Intradialytic Parenteral Nutrition) is indicated. The commercial bag contains a mixture of amino acids, glucose and lipid emulsions (1 kcal/mL, amino acids 40-60 g/L), administered in the form of IV infusion through the venous line of extracorporeal circulation, 15 minutes after the start of the dialysis session, at a maximum rate of 250 mL/h. It can provide 1000 kcal and 50 g of amino acids during a single hemodialysis session (33, 34).

Diagnosis of PEW includes four categories of clinical criteria: biochemical criteria, body mass, muscle mass, and protein and energy intake. Biochemical criteria include: serum albumin concentration less than 38 g/L, prealbumin concentration less than 0.30 g/L, serum cholesterol concentration less than 2.6 mmol/L (< 100 mg/dL). The body weight category includes the following clinical criteria: body mass index - BMI less than 23 kg/m2, unintentional weight loss ≥ 5% over three months or ≥ 10% over 6 months, total body fat percentage less than 10%. Clinical criteria for assessing muscle mass include: unintentional decrease in muscle mass ≥ 5% over 3 months or ≥ 10% over six months, decreased upper arm muscle volume - MAMC by 10% compared to reference values (Mid-Arm Muscle Circumference) and the kinetics/creatinine index - SCI (Simplified Creatinine Index). The category of dietary intake include: unintentionally low protein intake less than 0.8 g/kg/day for at least two months for patients undergoing hemodialysis and less than 0.6 g/kg/day for patients suffering from chronic kidney disease stage CKD 3b-5, as well as unduly low energy intake, less than 25 kcal/kg/day for at least two months. For the diagnosis of protein deficiency malnutrition (PEW), at least three categories and at least one test result in each of the selected categories must be positive. For the diagnosis of protein deficiency malnutrition (PEW), at least three categories and at least one test result in each of the selected categories must be positive. Each criterion should be documented three times, preferably 2-4 weeks apart (33, 34).

***Amyloidosis associated with dialysis***

Hemodialysis-related amyloidosis occurs as a consequence of $\beta_2$-microglobulin accumulation. In hemodialysis patients, microinflammation and metabolic acidosis promote increased $\beta_2$-microglobulin production. In contact with other biological molecules (glycosaminoglycans, proteoglycans) conformational changes of $\beta_2$-microglobulin occur, amyloid fibers are formed, and their deposition leads to bone and joint disorders, carpal tunnel syndrome (compression of the median tunnel) and carpal tunnel. formation of cystic formations in the bones. In patients with carpal tunnel syndrome, as a consequence of shortening of the flexor tendons of the fingers, a characteristic "guitar sign" appears. Post-dilution online hemodiafiltration and extended hemodialysis, which enable the efficient removal of $\beta_2$-microglobulin from the patient's serum, play a key role in preventing the development and progression of hemodialysis-related amyloidosis. According to the recommendations of the JSN (Japanese Society of Nephrology), the target predialysis concentration of $\beta_2$-

microglobulin in the serum should be less than 30 mg/L (ideally less than 25 mg/L) (35).

**Prevention and treatment of microinflammation**

*Postdilution online hemodiafiltration - OL-HDF*

Postdilution online hemodiafiltration is a method to replace kidney function that effectively removes uremic toxins of middle molecular weight in the range of 0.5-60 kDa. Studies show that it reduces microinflammation, oxidative stress, malnutrition due to protein deficiency, resistance to the action of erythropoietin and the development of accelerated atherosclerosis (36-41). High-volume postdilution online hemodiafiltration (Vconv = 22-30 liters per session) prevents the development of atherosclerotic cardiovascular diseases, reduces the risk of cardiovascular mortality and improves the quality of life of patients with end-stage chronic kidney disease (42-47). For optimal control of oxidative stress and microinflammation, high-flux hemodialysis and postdilution online hemodiafiltration with dialysis membranes coated with vitamin E are used (48-50).

The efficiency of postdilution online hemodiafiltration depends on the total convective volume - Vconv. The target total convective volume should be - Vconv = 22-30 liters per session. It depends on the rate of blood flow through the arteriovenous fistula (Qavf ≥ 600 mL/min), the rate of blood flow (Qb ≥ 350 mL/min) and the characteristics of the dialyzer. The main characteristics of dialyzers used for postdilution online hemodiafiltration are: high ultrafiltration coefficient (Kuf > 40 mL/h x mmHg), sieving coefficient for $\beta_2$-microglobulin greater than 0.60, sieving coefficient for albumin less than 0.01 (albumin loss per session less than 4.0 g), capillary density greater than 11,000 per cross-sectional area of the dialyzer allows the flow of dialysis solution - Qd = 500 mL/min, the inner diameter of the dialyzer capillaries greater than 200 μm. Dialyzers with dialysis membranes with an area of ≥ 2.0 $m^2$ should be used to optimize the filtration fraction in postdilution online hemodiafiltration (51, 52). For postdilution online hemodiafiltration, the maximum conductivity of water from the reverse osmosis system should be up to 5 μS/cm. Ultrapure dialysis solution (bacterial concentration < 0.1 CFU/mL, endotoxin concentration < 0.03 EU/mL) and sterile substitution solution (bacterial concentration < 10-6 CFU/mL, endotoxin concentration < 0.03 EU/mL (51, 52).

***Extended hemodialysis - MCO hemodialysis***

Extended hemodialysis is a method to replace kidney function that effectively removes uremic toxins of medium molecular weight, including proinflammatory cytokines, by a diffusion process and an internal filtration process. With an MCO membrane of 2.0 $m^2$, the internal filtration is high and amounts to 30-50 mL/min. Less than 4.0 g/4h is lost during a single session of extended MCO hemodialysis, which is of great importance in order to prevent malnutrition due to protein loss. It reduces microinflammation, oxidative stress, malnutrition due to protein deficiency, resistance to the action of erythropoietin and prevents the development of accelerated atherosclerosis (53-57).

Optimization of diffusion and convective transport capacity in MCO dialysis membrane depends on blood flow rate (Qb ≥ 300 mL/min), net ultrafiltration flow rate (Qnuf), internal filtration flow rate, single session duration and dialyzer characteristics. Internal filtration depends on the membrane ultrafiltration coefficient, the internal diameter of capillary fibers (< 200 μm), the net ultrafiltration flow rate and the sieving coefficient for individual uremic toxins. It increases in proportion to the strength of blood flow and the area of the MCO membrane. High internal filtration and increased MCO membrane sieving capacity enable high clearance of middle molecular weight uremic toxins. The target spKt/V index for a single session of extended MCO hemodialysis should be ≥ 1.20 (53-57).

***Adsorptive hemodialysis - PMMA hemodialysis***

Adsorptive hemodialysis is a method for replacing kidney function that effectively removes uremic toxins of medium and large molecular weight, as well as uremic toxins that bind in a high percentage to plasma proteins - PBUT (Protein-Bound Uremic Toxins). It combines diffusion, convection and adsorption. PMMA (Polymethyl Methacrylate) dialysis membranes have a high adsorption capacity of $\beta_2$-microglobulin, proinflammatory cytokines (IL-6, IL-8, TNFα, HMGB-1), free light chains of monoclonal immunoglobulins and uremic toxins that in high percentage bind to plasma proteins (indoxyl sulfate, p-cresyl sulfate). Clinical studies show that adsorptive hemodialysis reduces microinflammation (removes proinflammatory cytokines), prevents malnutrition and muscle loss, significantly reduces uremic itching and the development of atherosclerotic cardiovascular diseases in the population of patients treated with regular hemodialysis (58-60). Optimization of diffusion capacity, convective transport and adsorption capacity of PMMA dialysis membrane depends on blood flow rate (Qb ≥ 300 mL/min), dialysate flow rate (Qd ≥ 500 mL/min), net ultrafiltration flow rate (Qnuf), duration of individual sessions and characteristics of the dialyzer: inner diameter of capillary fibers of 200 μm, membrane wall thickness of 30 μm. The target spKt/V index for a single session of adsorptive PMMA hemodialysis should be ≥ 1.20 (58-60).

**CONCLUSION**

Microinflammation is a risk factor for an unfavorable outcome in patients treated with regular hemodialysis. Its prevalence in the final stage of chronic kidney disease is 30-50%. Postdilution *online* hemodiafiltration, extended and adsorptive hemodialysis prevent the development of microinflammation. Optimal control of microinflammation reduces the risk of accelerated atherosclerosis, malnutrition, resistance to the action of erythropoietin, improves the quality of life and reduces the rate of cardiovascular morbidity and mortality in patients treated with regular hemodialysis.

## ACKNOWLEDGEMENTS

The authors would like to express their deepest gratitude to the Ministry of Education, Science and Technological Development of the Republic of Serbia for Grant N0175014 and also to the Faculty of Medical Sciences University of Kragujevac for their Junior Project grants N002/19 and N022/20 from which the funds were used as one of the sources to financially support this paper.

## CONFLICT OF INTEREST

The authors declare no financial or commercial conflict of interest.

## REFERENCES

1. Cozzolino M, Mangano M, Stucchi A, Ciceri P, Conte F, Galassi A. Cardiovascular disease in dialysis patients. Nephrol Dial Transplant 2018; 33(1):28-34. Doi: 10.1093/ndt/gfy174.
2. Escoli R, Carvalho MJ, Cabrita A, Rodrigues A. Diastolic Dysfunction, an Understimated New Challenge in Dialysis. Ther Apher Dial 2019; 23(2): 108-17. Doi: 10.1111/1744-9987.12756.
3. Ahmadmehrabi S, Tang WHW. Hemodialysis-induced Cardiovascular Disease. Semin Dial 2018; 31(3): 258-67. Doi: 10.1111/sdi.12694.
4. Genovesi S, Boriani G, Covic A, Vernooij RWM, Combe C, Burlacu A, et al. Sudden cardiac death in dialysis patients: different causes and management strategies. Nephrol Dial Transplant 2021; 36(3): 396-405. Doi: 10.1093/ndt/gfz182.
5. Levi A, Simard T, Glover C. Coronary Artery Disease in Patients with End-Stage Kidney Disease; Current perspective and gaps of knowledge. Semin Dial 2020; 33(3): 187-97. Doi: 10.1111/sdi.12886.
6. Roehm B, Gulati G, Weiner DE. Heart failure management in dialysis patients: Many treatment options with no clear evidence. Semin Dial 2020; 33(3): 198-208. Doi: 10.1111/sdi.12878.
7. Akchurin OM, Kaskel F. Update on Inflammation in Chronic Kidney Disease. Blood Purif 2015; 39(1-3): 84-92. Doi: 10.1159/000368940.
8. Wolley MJ, Hutchison CA. Large uremic toxins: an unsolved problem in end-stage kidney disease. Nephrol Dial Transplant 2018; 33(Suppl 3): 6-11. Doi: 10.1093/ndt/gfy179.
9. Kaesler N, Babler A, Floege J, Kramann R. Cardiac Remodeling in Chronic Kidney Disease. Toxins 2020; 12(3): 161. Doi: 10.3390/toxins12030161.
10. Velasquez MT, Centron P, Barrows I, Dwivedi R, Raj DS. Gut Microbiota and Cardiovascular Uremic Toxicities. Toxins 2018; 10(7): 287. Doi: 10.3390/toxins10070287.
11. Espi M, Koppe L, Fouque D, Thaunat O. Chronic Kidney Disease-Associated Immune Dysfunctions: Impact of Protein-Bound Uremic Retention Solutes on Immune Cells. Toxins 2020; 12: 300. Doi: 10.3390/toxins12050300.
12. Ronco C, Clark WR. Haemodialysis membranes. Nat Rev Nephrol 2018; 14(6): 394-410. Doi: 10.1038/s41581-018-0002-x.
13. Haroon S, Davenport A. Choosing a dialyzer: What clinicians need to know. Hemodialysis Int 2018; 22(Suppl 2): 65-74. Doi: 10.1111/hdi.12702.
14. Kohlova M, Amorim CG, Araujo A, Santos-Silva A, Solich P, Montenegro MCBS. The biocompatibility and bioactivity of hemodialysis membranes: their impact in end-stage renal disease. Int J Artif Organs 2019; 22(1); 14-28. Doi: 10.1007/s10047-018-1059-9.
15. Chen DP, Flythe JE. Dialysis-associated allergic reactions during continuous renal replacement therapy and hemodialysis: A case report. Hemodialysis Int 2020; 24(1): 5-9. Doi: 10.1111/hdi.12801.
16. Martin-Navarro J, Esteras R, Castillo E, Carriazo S, Fernandez-Prado R, Gracia-Iguacel C, et al. Reactions to Synthetic Membranes Dialyzers: Is there an Increase in Incidence? Kidney Blood Press Res 2019; 44(5): 907-14. Doi: 10.1159/000501035.
17. Glorieux G, Neirynck N, Veys N, Vanholder R. Dialysis water and fluid purity: more than endotoxin. Nephrol Dial Transplant 2012; 27(11): 4010-21. Doi: 10.1093/ndt/gfs306.
18. Kraut JA, Madias NE. Metabolic Acidosis of CKD: An Update. Am J Kidney Dis 2016; 67(2): 307-17. Doi: 10.1053/j.ajkd.2015.08.028.
19. Raphael KL. Metabolic Acidosis in CKD: Core Curriculum 2019. Am J Kidney Dis 2019; 74(2): 263-75. Doi: 10.1053/j.ajkd.2019.01.036.
20. Liakopoulos V, Roumeliotis S, Zarogiannis S, Eleftheriadis T, Mertens PR. Oxidative stress in hemodialysis: Causative mechanisms, clinical implications, and possible therapeutic interventions. Semin Dial 2019; 32(1): 58-71. Doi: 10.1111/sdi.12745.
21. Yang SK, Xiao L, Xu B, Xu XX, You F, Liu FY, Sun L. Effects of vitamin E-coated dialyzer on oxidative stress and inflammation status in hemodialysis patients: a systematic review and meta-analysis. Ren Fail 2014; 36(5): 722-31. Doi: 10.3109/0886022X.2014.890858.
22. Jovanovich A, Isakova T, Stubbs J. Microbiome and Cardiovascular Disease in CKD. Clin J Am Soc Nephrol 2018; 13(10): 1598-604. Doi: 10.2215/CJN.12691117.
23. Van der Sande FM, Van de Wal-Visscher ER, Suard S, Moissi U, Kooman JP. Using Bioimpedance Spectroscopy to Assess Volume Status in Dialysis Patients. Blood Purif 2020; 49(1-2): 178-84. Doi: 10.1159/000504079.
24. Dekker MJE, Van der Sande FM, Van den Berghe F, Leunissen KML, Kooman JP. Fluid Overload and Inflammation Axis. Blood Purif 2018; 45(1-3): 159-65. Doi: 10.1159/000485153.
25. Dekker MJE, Konings C, Canaud B, Usvyat L, Kotanko P, Kooman JP. Interactions Between Malnutrition, Inflammation, and Fluid Overload and Their Associations With Survival in Prevalent Hemodialysis

Patients. J Ren Nutrition 2018; 28(6): 435-44. Doi: 10.1053/j.jrn.2018.06.005.
26. Dekker MJE, Marcelli D, Canaud BJ, Carioni P, Wang Y, Grassmann A, et al. Impact of fluid status and inflammation and their interaction on survival: a study in an international hemodialysis patient cohort. Kidney Int 2017; 91(5): 1214-23. Doi: 10.1016/j.kint.2016.12.008.
27. Icardi A, Paoletti E, De Nicola L, Mazzaferro S, Russo R, Cozzolino M. Renal anemia and EPO hyporesponsiveness associated with vitamin D deficiency: the potential role of inflammation. Nephrol Dial Transplant 2013; 28(7): 1672-9. Doi: 10.1093/ndt/gft021.
28. Tain YL, Hsu CN. Toxic Dimethylarginines: Asymetric Dimethylarginine (ADMA) and Symmetric Dimethylarginine (SDMA). Toxins 2017; 9(3): 92. Doi: 10.3390/toxins9030092.
29. Weiss G, Ganz T, Goodnough LT. Anemia of inflammation. Blood 2019; 133(1): 40-50. Doi: 10.1182/blood-2018-06-856500.
30. Szeto CC, McIntyre CW, Li PKT. Circulating Bacterial Fragments as Cardiovascular Risk Factors in CKD. J Am Soc Nephrol 2018; 29(6): 1601-8. Doi: 10.1681/ASN.2018010068.
31. Gluba-Brzozka A, Franczyk B, Olszewski R, Rysz J. The Influence of Inflammation on Anemia in CKD Patients Int J Mol Sci 2020; 21(3): 725. Doi: 10.3390/ijms21030725.
32. Kalantar-Zadeh K, Aronoff GR. Hemoglobin Variability in Anemia of Chronic Kidney Disease. J. Am Soc Nephrol 2009; 20(3): 479-87. Doi: 10.1681/ASN.2007070728.
33. Ikizler TA, Burrowes JD, Byham-Gray LD, Campbell KL, Carrero JJ, Chan W, et al. KDOQI clinical practice guidelines for nutrition in CKD: 2020 Update. Am J Kidney Dis 2020; 76(3 Suppl 1): 1-107. Doi: 10.1053/j.ajkd.2020.05.006.
34. Sabatino A, Piotti G, Cosola C, Gandolfini I, Kooman JP, Ficcadori E. Dietary protein and nutritional supplements in conventional hemodialysis. Semin Dial 2018; 31(6): 583-91. Doi: 10.1111/sdi.12730.
35. Kaneko S, Yamagata K. Hemodialyis-related amyloidosis: Is it still relevant? Semin Dial 2018; 31(6): 612-8. Doi:10.1111/sdi.12720.
36. Wolley M, Jardine M, Hutchison CA. Exploring the Clinical Relevance of Providing Increased Removal of Large Middle Molecules. Clin J Am Soc Nephrol 2018; 13(5): 805-14. Doi:10.2215/CJN.12631117.
37. Canaud B, Vienken J, Ash S, Ward R. Hemodiafiltration to Addres Unmet Medical Needs ESKD Patients. Clin J Am Soc Nephrol 2018; 13(9):1435-43.
38. Nenadovic M, Jacovic S, Nikolic A, Kostovic M, Draskovic B, Jovanovic M, Nikolic T, Petrovic D. Postdilution online hemodiafiltration: basic principles and clinical significance. Ser J Exp Clin Res 2020; Doi: 10.2478/sjecr-2020-0055.
39. Nenadovic M, Jacovic S, Nikolic A, Kostovic M, Draskovic B, Jovanovic M, Nikolic T, Petrovic D. Assessment of the influence of postdilution online hemodiafiltration on the rate of removal of middle molecular weight uremic toxins. Ser J Exp Clin Res 2021; Doi: 10.2478/sjecr-2021-0005.
40. Nenadovic M, Nikolic A, Kostovic M, Draskovic B, Jovanovic M, Nikolic T, Petrovic D. Poredjenje efikasnosti uklanjanja uremijskih toksina srednje molekulske mase izmedju visokopropusne hemodijalize i postdilucione online hemodijafiltracije. Med Cas 2021; 55(1): 7-17. Doi: 10.5937/mckg55-31062.
41. Nenadovic M, Petrovic D, Trbojevic-Stankovic J. Beta-2-microglobulin removal with postdilution online hemodiafiltration - comparison of three different dialysis membranes. Srp Arh Celok Lek 2021; 149(7-8): 422-7. Doi: 10.2298/SARH210329048N.
42. Marcelli D, Scholz C, Ponce P, Sousa T, Kopperschmidt P, Grassmann A, et al. High-Volume Postdilution Hemodiafiltration Is a Feasible Option in Routine Clinical Practice. Artif Organs 2015; 39(2): 142-9. Doi: 10.1111/aor.12345.
43. Marcelli D, Kopperschmidt P, Bayh I, Jirka T, Merello JI, Ponce P, et al. Modifiable factors associated with achievement of high-volume post-dilution hemodiafiltration: results from an international study. Int J Artif Organs 2015; 38(5): 244-50. Doi: 10.5301/ijao.5000414.
44. De Roij van Zuijdewijn CLM, Chapdelaine I, Nube MJ, Blankestijn PJ, Bots ML, Konings CJAM, Hovinga TKK, et al. Achieving high convection volumes in postdilution online hemodiafiltration: a prospective multicenter study. Clin Kidney J 2017; 10(6): 804-12. Doi: 10.1093/ckj/sfw140.
45. Chapdelaine I, De Roij van Zuijdewijn CLM, Mostovaya IM, Levesque R, Davenport A, Blankestijn PJ, et al. Optimization of the convection volume in online postdilution haemodiafiltration: practical and technical issues. Clin Kidney J 2015; 8(2): 191-8. Doi: 10.1093/ckj/sfv003.
46. Panichi V, Scatena A, Rosati A, Giusti R, Ferro G, Malagnino E, et al. High-volume online haemodiafiltration improves erythropoiesis-stimulating agent (ESA) resistance in comparison with low-flux bicarbonate dialysis: results of the REDERT study. Nephrol Dial Transplant 2015; 30(4): 682-9. Doi: 10.1093/ndt/gfu345.
47. Rosati A, Ravaglia F, Panichi V. Improving Erythropoiesis Stimulating Agent Hyporesponsiveness in Hemodialysis Patients: The Role of Hepcidin and Hemodiafiltration Online. Blood Purif 2018; 45(1-3): 139-46. Doi: 10.1159/000485314.
48. Locatelli F, Andrulli S, Vigano SM, Concetti M, Urbini S, Giacchino F, et al. Evaluation of the Impact of a New Synthetic Vitamin E-Bonded Membrane on the Hypo-Responsiveness to the Erythropoietin Therapy in Hemodialysis Patients: A Multicenter Study. Blood Purif 2017; 43(4): 338-45. Doi: 10.1159/000453442.
49. Antic S, Draginic N, Pilcevic D, Zivkovic V, Srejovic I, Jeremic N, Petrovic D, Jakovljevic V. The influence of vitamin E coated dialysis membrane on oxidative stress

during the single session of online hemodiafiltration. Vojnosanit Pregl 2021, 78(5): 511-8. Doi: 10.2298/VSP190730097A.
50. Kiaii M, Aritomi M, Nagase M, Farah M, Jung B. Clinical evaluation of performance, biocompatibility, and safety of vitamin E-bonded polysulfone membrane hemodialyzer compared to non-vitamin E-bonded hemodialyzer. J Artif Org 2019; 22: 307-15. Doi: 10.1007/s10047-019-01110-w.
51. Maduell F. Hemodiafiltration versus conventional hemodialysis: Should "convencional" be redefined? Semin Dial 2018; 31(6): 625-32. Doi: 10.1111/sdi.12715.
52. Guedes M, Dambiski AC, Canhada S, Barra ABL, Poli-De-Figueiredo CE, Cuvello Neto AL, et al. Achieving high convective volume in hemodiafiltration: Lessons learned after successful implementation in the HDFit trial. Hemodialysis Int 2021; 25(1): 50-9. Doi: 10.1111/hdi.12891.
53. Florens N, Juillard L. Expanded haemodialysis: news from the field. Nephrol Dial Transplant 2018; 33(Suppl 3): 48-52. Doi: 10.1093/ndt/gfy203.
54. Ronco C, Marchionna N, Brendolan A, Neri M, Lorenzin A, Rueda AJM. Expanded haemodialysis: from operational mechanism to clinical results. Nephrol Dial Transplant 2018; 33(Suppl 3): 41-7. Doi: 10.1159/000489993.
55. Lorenzin A, Neri M, Lupi A, Todesco M, Santimaria M, Alghisi A, et al. Quantification of Internal Filtration in Hollow Fiber Hemodialyzers with Medium Cut-Off Membrane. Blood Purif 2018; 46(3): 196-204. Doi: 10.1159/000489993.
56. Nenadovic M, Nikolic A, Kostovic M, Draskovic B, Jovanovic M, Nikolic T, Petrovic D. Assessment of the influence of expanded hemodialysis on the rate of removal of middle molecular weight uremic toxins. Med Cas 2020; 54(3): 96-104. Doi: 10.5937/mckg54-30496.
57. Lim JH, Jeon Y, Yook JM, Choi SY, Jung HY, Choi JY, et al. Medium cut-off dialyzer improves erythropoiesis stimulating agent resistance in a hepcidin-independent manner in maintenance hemodialysis patients: results from a randomized controlled trial. Rep Sci 2020; 10(1): 16062. Doi: 10.1038/s41598-020-73124-x.
58. Masakane I, Esashi S, Yoshida A, Chida T, Fujieda H, Ueno Y, et al. A new polymethylmethacrylate membrane improves the membrane adhesion of blood components and clinical Efficacy. Ren Repl Ther 2017; 3: 32. Doi: 10.1186/s41100-017-0112-0.
59. Van Gelder MK, Middel IR, Vernooij RWM, Bots ML, Verhaar MC, Masereeuw R, et al. Protein-Bound Uremic Toxins in Hemodialysis Patients Relate to Residual Kidney Function, Are Not Influenced by Convective Transport, and Do Not Relate to Outcome. Toxins 2020; 12(4): 234. Doi: 10.3390/toxins12040234.
60. Maduell F, Broseta JJ, Rodriguez-Espinosa D, Hermida-Lama E, Rodas LM, Gomez M, et al. Evaluation and comparison of polysulfone TS-UL and PMMA NF-U dialyzers versus expanded hemodialysis and postdilution hemodiafiltration. Artif Organs 2021; Doi: 10.111/aor.13968.

# EVALUATION OF NASAL DECONGESTANTS BY LITERATURE REVIEW

Stasa Petkovic[1], Ivana Maletic[2], Sonja Djuric[3], Ninoslava Dragutinovic[4] and Olivera Milovanovic[5]

[1]*Health Institution - Pharmacy Benu, Belgrade, Serbia*
[2]*KBC Zemun, Clinic of ENT, Belgrade, Serbia*
[3]*Gentext Research Group, University of Valencia, Spain*
[4]*Health system Medi Group, Department of ENT, Belgrade, Serbia*
[5]*University of Kragujevac, Serbia, Faculty of Medical Sciences, Department of Pharmacy*

Received: 16.12.2018.
Accepted: 17.01.2019.

**Corresponding author:**

**Stasa Petkovic**

Health Institution - Pharmacy Benu, Belgrade, Serbia

E-mail: stasa.petkovic@yahoo.com

## ABSTRACT

*Over-the-counter drugs are medicines that are available to consumers without a prescription. The most common over - the-counter preparations in self - medication are nasal decongestants that can be used systemically or locally in the form of drops or nasal sprays. The most common indications for nasal decongestants are viral infections and allergic conditions in order to alleviate the symptoms so it is necessary to inform the users about the type of drug, the active substance it contains and the correct dosage regimen. Given their availability and the prevailing safety precaution, these preparations can lead to numerous prolonged conditions and complications. The mechanism of action of nasal decongestants is based on the reduction of blood vessels' swelling in the nose, which helps the opening of the airway. As a result, most nasal decongestants cause vasoconstriction (narrowing of blood vessels). There are nasal decongestants that block histamine and have a good effect on people who suffer from seasonal allergies. Availability (free sale) and prolonged use of the decongestant lead to a decrease in the sensitivity of the alpha receptor, which leads to the need to increase the dose at shorter time intervals to achieve the same effect. As a consequence, patients use excessive, uncontrolled doses of nasal decongestants, which is a public problem and warns of the necessity of identification and the taking of measures to prevent their uncontrolled procurement and use.*

***Keywords***: *Nasal decongestants, ephedrine, pseudoephedrine, oxymetazoline, intranasal corticosteroids.*

sciendo

UDK: 615.451.3
Eabr 2024; 25(2):181-187
DOI: 10.2478/sjecr-2019-0002

## INTRODUCTION

Drugs without prescription available to consumers - OTC drugs play a key role in the health care system and modern pharmaceutical practices. Currently, there are over 300.000 different OTC drugs available in the United States (1).

The US Food and Drug Administration (FDA) determines whether OTC drugs are safe and effective for use, and decides on the safety of drug sales directly, without a prescription. This regulatory process allows American population to take an active role in their health care, which requires the maturity of population that is able to make right decisions in the process of self-medication (2). Self-medication is a process that requires a high level of awareness, knowledge and general education of people, as well as satisfactory socio-economic status. Access to information, the quality of information, and the skills in interpreting and applying information to OTC drugs are important to support the process of self-medication (3). In order to safely and efficiently use an OTC drug, the consumer must accurately identify the symptoms, set the therapeutic goal, choose the product to use, determine the appropriate dose and method of dosing, taking into account contraindications, associated illnesses and medications that are taken regularly because of chronic problems, as well as tracking response to treatment with the identification of possible adverse effects (4).

The general rule for OTC drugs is to be used primarily for the treatment of conditions that do not require direct medical attention with the recognition and proper interpretation of the symptoms and the accompanying instructions on the medicine.

Research suggests that self-medication improves health care and reduces the economic costs of the health care system (5). Although there is an opinion that OTC drugs are safe and effective, it must be emphasized that they are not completely harmless. Acting on symptoms, they often mask the underlying disease and can cause unwanted side effects (6). Self-medication carries a serious risk of drug interactions, polypharmacy, wrong diagnosis, overuse of drug dosing, prolonged drug use, inappropriate drug selection, rare but serious adverse events, addiction, abuse and increased antimicrobial resistance (7). Doctors and pharmacists play a very important role in creating awareness about self-medication in patient education (8). When making a decision to purchase as well as when purchasing OTC drugs, patients are directly referred to pharmacists. Therefore, before proposing any OTC drugs, a pharmacist should thoroughly assess the nature and degree of patient's condition and recommend them to seek professional care when necessary.

Motivating factors for self-medication could be: easy availability of many drugs, lack of strict control over medical advertising, low medical literacy of the population, prices of medical examinations, long wait in public health institutions, etc.

Therefore, very important step for this type of medication is the public education of the population about recognition of the symptoms of illness in the process of self-medication, as well as education on the use of OTC drugs and precautionary measures and information about the possible consequences and possibilities of their abuse (9).

The most commonly used OTC drugs are nasal decongestants that are used systemically or locally in the form of drops or nasal sprays. These preparations are most commonly used in viral infections to alleviate the symptoms (nasal obstruction, vomiting, increased nasal secretion, difficulty breathing, etc.), but it is necessary to inform the users about the type of preparation, the active substance it contains and the correct dosage regimen. Given their availability and the prevalence of safety precautions, these preparations can lead to numerous prolonged conditions and complications (medicaments rhinitis). Also, an increasing number of allergens, in many parts of the world, and climate change, cause allergic manifestations, so the users decide on the solubility and purchase of drops or sprays without consultation with a physician or pharmacist. Due to the long-lasting symptoms with short periods of improvement, nasal drops/nasal sprays are increasing used for months, even for years. However, it is necessary to inform that many products have restrictions in use, which depend on age, and some are contraindicated in children younger than two years of age, pregnant women, persons with thyroid gland diseases, cardiovascular diseases, prostate problems.

Decongestants are a group of drugs that can provide short-term relief of nasal congestion.

The mechanism of action is based on the reduction of blood vessels' swelling in the nose, which helps in the opening of the airway. Decongestants are used to reduce nasal obstruction and relieve pain in common colds, flu, sinusitis, acute or chronic rhinitis, upper respiratory tract allergy, pollen cough, septum deviation, nasal mucosa hypotrophy, nasal polyps, etc (10).

Allergic rhinitis is one of the clinical conditions when nasal decongestants are most commonly used. This condition is present in about 10% to 20% of the world population and in 15% to 25% of children and adolescents (11). Among sympathomimetic vasoconstrictors for topical use in the nose, imidazole (naphazoline, oxymetazoline and xylomethazoline) and catecholamine derivatives (epinephrine, ephedrine and phenylephrine) produce vasoconstriction of the nasal blood vessels by stimulation through the endogenous release of noradrenaline, which acts on alpha receptors (12, 13).

However, prolonged use of nasal decongestants leads to side effects, e.g. medicamentous rhinitis. Because of this, local application of vasoconstrictor can be carried out only for a short period of time and for no longer than four or five days, due to the risk of damage to the mucociliary epithelium and

reverse vasodilatation. Prolonged use of a decongestant leads to a decrease in the sensitivity of the alpha receptor, which leads to the need to increase the dose at shorter intervals to achieve the same effect. As a consequence, patients use excessive, uncontrolled doses of nasal decongestants (14), which are a public problem and warn of the necessity of identification and the taking of measures to prevent uncontrolled procurement and the use of nasal decongestants (15, 16).

Decongestants may comprise pseudoephedrine, phenylephrine, oxymetazolin or ksilometosolin. Nasal decongestants are available in the form of tablets, drops or nasal sprays. They are generally available as OTC drugs, and are often used without restriction, for a long period of time (17). It is recommended that they should not be given to children under the age of six (18) due to the risk of increased mucous membrane edema after cessation of decongestant use. It is advised that the use of a decongestant should not be longer than five days. Nasal decongestants generally act locally, but may have systemic effects, such as hypertension, headache, nausea, insomnia and dizziness (19). Using decongestant, individuals may develop tachyflilax (a rapid reduction in drug response after repeated doses over a short period of time). Therefore, long-term use of decongestants is not recommended because they lose their effectiveness after a few days.

**Efedrine and pseudoefedrine**

Ephedrine and pseudoephedrine are the earliest molecules known in the treatment of nasal congestion. Their vasoconstrictive actions on the nasal mucosa make them highly effective amines in the treatment of nasal congestion. However, over the past few years, the French National Drugs Safety Agency (NSA), in its action plan of July 2013 (20), has reported against their use in rhinology, saying that vasoconstrictors "include the risk of stroke and severe neurological effects" and that they are "often too risky to use in a simple cold″ (21).

Thanking to their molecular structure, these two sympathomimetic amines (ephedrine and pseudoephedrine) stimulate the adrenergic receptor system at the interface between the sympathetic nerve and the smooth muscles of the blood vessels, thus simulating the vasoconstrictive effect of norepinephrine, which is physiologically produced by the sympathetic nerve fiber. In the nose, the regulation of the vascular network of mucous membranes and, in particular, the filling and discharge of cavernous venous plexus, is essential for regulation of airflow, and hence for the feeling of obstruction (22). Venous plexus, as well as arterioles that accompany them, are surrounded by adrenergic nerve fibers that are associated with α and β adrenergic receptors: β receptors are vasodilators, and α receptors are vasoconstrictor and prevail. Efedrine and pseudoephedrine, therefore, perform a vasoconstriction effect on the blood vessels, which is the basis of the mechanism for reducing obstruction of the nose.

Studies have shown that repeated stimulation of α-2 receptors induces intense vasoconstriction with mucosal ischemia and interstitial edema, while in long-term use, the effect of regulating α-2 receptors is the opposite, i.e. there is a relative dilatation and a tachyphilactic effect leading to an increased need for decongestant (23).

Efedrine applied to the nasal mucosa reduces nasal resistance faster and stronger than oral pseudoephedrine over a short time interval (24).

However, at the end of therapy, a rebound effect may occur with increased nasal resistance and repeated obstruction of the nose. Several research studies have shown the efficacy of oral pseudoephedrine against nasal obstruction during an ordinary cold (25, 26).

Eccles et al., in a prospective randomized double blind study compared to placebo, which included 238 patients with a common cold, reported anti-obstruction without side effects: a dose of 60 mg of oral pseudoephedrine for 3 days (27).

Ephedrine and pseudoephedrine belong to the amphetamine family. In France, in 2008 and again in 2012, the National Pharmacovigilance Commission (28) emphasized their psychotropic effect and cardiovascular side effects. The vasoconstriction effect in oral use or directly by application to the nasal mucosa significantly increases blood pressure and leads to vasospasm (29). This effect, which lasts 5 to 6 times longer than adrenaline, can cause episodes of hypertension, myocardial infarction, stroke and various neurological symptoms (30, 31). Different cardiovascular adverse effects may occur after individual or long-term therapy (for more than 5 days) regardless of vascular status and age (31). The same dangers led to the fact that the French National Agency for the Protection of Health (Agence nationale de sécurité du médicament) in 2013 reassigned preparations containing only pseudoephedrine as medicinal products which are issued on a medical prescription (20, 32). The current literature review shows that their vasoconstrictive effects on the nasal mucosa make ephedrine and pseudoephedrine highly effective against nasal congestion. Given the serious, harmful cardiovascular and neurological effects that can occur even at low doses, it is necessary for doctors to conduct a rigorous assessment of the benefits in prescribing these drugs in allergic rhinitis (33).

Oral phenylephrine is generally used to alleviate symptoms associated with colds and flu, and no change in blood pressure is observed in the short duration of the use of phenylephrine. Several studies on the oral examination of phenylephrine in the recommended dosage of 10 mg have shown that phenylephrine was well tolerated in patients with obstruction of the nose. However, these studies focused on phenylephrine as a single agent, not in combination with paracetamol where its bioavailability is increased, while maximum plasma concentrations are two to four times higher (34).

Given these risks, it is recommended that distribution should be regulated by translating these products from the list of OTC drugs to the list of medicines that are issued on a prescription.

**Oxymetazoline**

Oxymetazoline is a sympathomimetic amine that has vasoconstrictor effects and reduces the mucous membrane.

After application in the nose, the inflamed nasal mucous membrane is reduced, eliminating increased secretion and allowing breathing through the nose. Oxymetazoline is characterized by the dominant α -2 adrenergic activity. Its effect occurs within a few minutes of application and lasts for an average of 6 to 8 hours. Studies with oxymetazoline, a marked isotope, have shown that intranasally administered oxymetazoline had no systemic effect. In double blind studies in healthy volunteers, a dose of 1.8 mg of oxymetazoline (3.6 ml of 0.05% solution) was followed by non-specific ECG (electrocardiography) changes, but without a change in blood pressure or heart rate frequency.

Oxymetazoline, an imidazoline derivative, causes a reduced blood flow to the nose. Vaidyanathan with the coauthors conducted the research which aim was to evaluate the duration of action of oxymetazoline on nasal respiratory resistance and blood flow of nasal mucosa. During eight hours of measurement, blood flow was reduced by 30-40% over a period of six hours. A similar decongestant effect of about 30% was observed in the following period. The pharmacological profile of oxymetazoline is controversial, since the reduced blood flow to the nose may not be significant in the treatment of upper respiratory tract infections. Oxymetazoline-induced tachyphylaxis is contrary to the intranasal fluticasone effect. Further studies require an assessment of the combination of decongestant nasal sprays and corticosteroids in an effective strategy for the elimination of tachyphylaxis and the treatment of rhinitis (35).

After intranasal administration of multiple doses of the recommended amount, the absorbed amount cannot result in systemic cardiovascular effects. There are no data on the distribution of oxymetazoline in the human body. However, the following instruction indicates the precautionary measure: ″The combination of two decongestants is contraindicated, regardless of the mode of administration (oral and/or nasal): such an application is useless and dangerous and corresponds to abuse“ (36) Also, the drug is not recommended for use, due to the risk of vasoconstriction and/or hypertensive crises associated with its sympathomimetic alpha activity, with the following drugs: non-selective MAO inhibitors - monoamine oxidase inhibitors (iproniazid), vasoconstrictors (dihydroergotamine, ergotamine, methylergometrine) and drugs that reduce the epileptogenic threshold (37). However, in the literature, undesirable effects of oxymetazoline have been observed: increased nasal secretion, blurred vision, rapid, irregular heartbeats, headache, dizziness, drowsiness, appetite increased, high blood pressure, syncope, nervousness, trembling, sleep problems and weakness (38).

**Intranasal corticosteroids**

Intranasal corticosteroids are recommended as first-line therapy for patients with moderate to severe allergic rhinitis, especially when nasal congestion is the main symptom (39). Intranasal corticosteroids perform their antiinflammatory effect by inhibiting the production of many different cytokines, chemokines, enzymes and cell adhesion molecules, after their interactions with intracellular glucocorticoid receptors. The main advantage of intranasal corticosteroids is that high drug concentrations, with rapid onset of action, can be delivered directly to the target organ, so that systemic effects are minimal if they occur.

Fluticasone furoate is a topical corticosteroid with a high local potential and low potential for systemic effects, and is a good choice for the treatment of rhinitis (40). After intranasal application of one or more doses, the plasma fluticasone furoate concentration is below the lower limit of quantification for most (41). One study reported that only 2% of patients receiving 110 μg of fluticasone furoate had plasma quantitative concentrations (42).

It is known that many patients use intranasal corticosteroids independently, based on subjective symptoms, and stop using them when the symptoms are significantly reduced. In support of this approach, studies have shown that intermittent use of intranasal corticosteroids is moderately effective in many patients (43).

Also, additives and preservatives included in intranasal corticosteroids to prevent bacterial growth, add flavor and aroma, absorb additional water and maintain adequate levels of moisture, can irritate or dehydrate the nasal tissue and lead to hypersensitivity. Benzalkonium chloride, polysorbate, and carboxymethylcellulose are present in the fluticasone furoate formulation.

Benzalkonium chloride is a cationic surfactant used as a preservative in nasal solutions. Studies have shown that it can cause nasal mucous dysfunction, nasal irritation and hyper secretion, degenerative changes in stimulating and olfactory cells, and squamous cell metaplasia (44). However, clinical trials' results of these effects on the nasal mucosa are often different (45, 46).

A parallel, randomized, double-blind study was performed in 30 healthy subjects to investigate the effects on the nasal mucosa of a one-month treatment with nasal sprays. Ten subjects received oxymetazoline nasal spray; 10 subjects used a nasal spray containing the preservative benzalkonium chloride, and the rest were treated with a placebo nasal spray. The three variables that were studied - nasal mucosal swelling, symptom scores, and nasal reactivity - were estimated by histamine challenge before and after 28 days of treatment.

Rhinostereometry was used to measure nasal mucosal swelling and nasal reactivity. After 28 days of use, benzalkonium chloride spray alone induced an increase in nasal mucosal swelling, which explains why the presence of this preservative in a decongestant spray aggravates rhinitis medicamentosa (47).

Polysorbates are non-ionic surfactants and emulsifiers used as additives in drugs, shampoos and lotions. Polysorbate 80, depending on the concentration, reversibly inhibits the frequency of the ciliary epithelium in cultured human epithelial cells in the nose and is associated with allergy or sensitivity (48).

Carboxymethylcellulose is a thixotropic agent that increases the concentration of nasal drugs, but it also provides viscosity to the solution of intranasal corticosteroids, which is one of the reasons why the suspension must be shaken prior to use (49). It has been observed that it leads to drying of the nasal mucosa, which can contribute to the incidence of epistaxis, and in rare cases, to allergic anaphylactic reactions (50).

Oral antihistamines are often used concomitantly with intranasal corticosteroids in clinical practice, but serious adverse effects of chronic therapy with systemic corticosteroids have been demonstrated in many studies (51, 52). A literature review of the negative effects of local nasal steroids is confusing, but it is indisputable that each of these drugs causes unwanted events. The clinically significant fact is the suppression of the hypothalamic pituitary-adrenal axis and, most importantly, that these drugs have a negative effect on growth in children and osteoporosis in postmenopausal women (53).

## CONCLUSION

Nasal decongestants, as OTC drugs, are available to a large number of users in the process of self-medication. Due to altered climate change, the occurrence of a large number of allergens, their use is increased, as well as uncontrolled. Opinion on their safety suggests users to take them for an extended period of time, which leads to the absence of the expected effect and damage to the function of the mucociliary epithelium (atrophic rhinitis and anosmia).

Decongestants can be absorbed from the nose and give systemic effects, mainly stimulation of the central nervous system and the increase in the blood pressure, so that the ignorance about contraindications of their use can lead to deterioration of the general health condition.

Medical and pharmaceutical practices have a new task, involving primarily user education and monitoring the issuance of nasal decongestants.

## ACKNOWLEDGEMENT

None

## CONFLICT OF INTEREST

Authors declare no conflict of interest.

## REFERENCES

1. U.S. Food and Drug Administration. (2012). Drug applications for over-the-counter (OTC) drugs. Retrieved February 20, 2013, from http://www.fda.gov/drugs/developmentapprovalprocess/howdrugsaredevelopedandapproved/approvalapplications/over-the-counterdrugs/default.htm
2. U.S. Food and Drug Administration (FDA). (2013). Over-the-Counter Medicines: What's Right for You? Retrieved February 20, 2013, from March 09, 2013, from
3. https://www.fda.gov/drugs/resourcesforyou/consumers/buyingusingmedicinesafely/understandingover-the-countermedicines/choosingtherightover-the-counter-medicineotcs/ucm150299.htm
4. Bond, C., Blenkinsopp, A. & Raynor, D. K. (2012). Prescribing and partnership with patients. British journal of clinical pharmacology. 74(4): 581-588. DOI: 10.1111/j.1365-2125.2012.04330.x.
5. Westerlund, T., Barzi, S. & Bernsten, C. (2017). Consumer views on safety of over-the-counter drugs, preferred retailers and information sources in Sweden: after re-regulation of the pharmacy market. Pharmacy practice. 15(1): 894. DOI: 10.1007/s11096-012-9724-1.
6. Shankar, P. R., Partha, P. & Shenoy, N. (2002). Self-medication and non-doctor prescription practices in Pokhara valley, Western Nepal: a questionnaire-based study. BMC family practice, 3, 17. DOI:10.1186/1471-2296-3-17.
7. Sleath, B., Rubin, R. H., Campbell, W., Gwyther, L. & Clark. T.(2001). Physician-patient communication about over-the-counter medications. Soc Sci Med. 53(3); 357-369. PMID: 11439819
8. Sansgiry, S. S., Bhansali, A. H., Bapat, S. S. & Xu, Q. (2016). Abuse of over-the-counter medicines: a pharmacist's perspective. Integrated pharmacy research & practice. 6: 1-6. DOI:10.2147/IPRP.S103494.
9. Homedes, N. & Vgailde, A. (2001). Improving Use of Pharmaceuticals Through Patient and Community Level Intervention. Soc Sci Med. 52 (1): 99-134. PMID:11144920
10. Parikh, D., Sattigeri, BM., Kumar, A. & Brahmbhatt, S. (2013). A survey study on use of over the counter (OTC) drugs among medical students, nursing and clerical staff of a tertiary care teaching rural hospital. Int J Res Med Sci. 1(2): 83-86. DOI: 10.5455/2320-6012.
11. Zaffani, E. R., Kamimura, GF., Maniglia, AJV. & Fernades , AM. (2007) Perfil epidemiológico dos pacientes usuários de descongestionantes nasais tópicos do ambulatório de otorrinolaringologia de um hospital universitário. Arq. Ciênc. Saúde. 14(2); 95-98.
12. Baumann, LM., Romero, KM., Robison, CL., Hansel, NN., Gilman, RH., Hamilton, RG., Lima, JJ., Wise, RA. & Checkley, W.(2015). Prevalence and risk factors for allergic rhinitis in two resource-limited settings

in Peru with disparate degrees of urbanization. Clinical and experimental allergy: journal of the British Society for Allergy and Clinical Immunology. 45(1): 192-9. DOI: 10.1111/cea.12379.

13. Bernstein, DI., Schwartz, G. & Bernstein, JA. (2012). Allergic Rhinitis: Mechanisms and Treatment. Immunol Allergy Clin North Am. 36(2): 261-78. DOI: 10.1016/j.iac.2015.12.004.
14. Corboz, M.R., Rivelli, M.A., Mingo, G.G., Mcleod , R.L., Varty, L. & Jia Y.A. (2008). Mechanism of decongestant activity of alpha 2-adrenoceptor agonists. Pul. Pharmacol. 21(3): 449-454. DOI: 10.1016/j.pupt. 2007.06.007.
15. Doshi, J. (2009). Rhinitis medicamentosa: what an otolaryngologist needs to know. Eur. Arch. Otorhinolaryngol. 266(5): 623-625. DOI:10.1007/s00405-008-0896-1.
16. Servidoni, AB., Coelho, L., Navarro, ML., Ávila, FG. & Mezzalira R. (2006). Perfil da automedicação nos pacientes otorrinolaringológicos. Rev. Bras. Otorrinolaringol. 72(1): 83-88. DOI: org/10.1590/S0034-72992006000100013.
17. Lenz, D., Cardoso, KS., Bitti, AC. & Andrade, TU. (2011). Evaluation of the use of topic nasal decongestants in university students from health sciences courses. Brazilian Journal of Pharmaceutical Sciences. 47(4): 761-767. DOI: org/10.1590/S1984-82502011000400 013.
18. Eccles, R., Eriksson, M., Garreffa, S. & Chen. SC. (2008). The nasal decongestant effect of xylometazoline in the common cold. American Journal of Rhinology. 22(5): 491-496. DOI: 10.2500/ajr.2008.22.3202.
19. Lui, CT. (2017). Prescription practice of antihistamines for acute upper respiratory tract infections in pediatric patients in a local emergency department in Hong Kong. World J Emerg Med. 8(1): 47-54. DOI: 10.5847/wjem. j.1920-8642.
20. Zeynettin, K. & Abdullah, T., (2013). Adverse Cardiac Effects of Decongestant Agents. Eur J Gen Med. 10(1): 32-35. DOI: https://doi.org/10.29333/ejgm/82301
21. ANSM - Juillet 2013. Plan d'action sur les médicaments contenant des vasoconstricteurs à visée décongestionnante. Retrieved ANSM - Juillet 2013, from https://ansm.sante.fr/var/ansm_site/storage/original/application/c6285e0a4e1f950eaa262d4d788f134c.pdf
22. Hallas, J., Bjerrum, L. Stovring, H. & Andersen, M. (2008). Use of a prescribed ephedrine/caffeine combination and the risk of serious cardiovascular events: a registry-based case-crossover study. Am J Epidemiol. 168(8): 966-73. DOI: 10.1093/aje/kwn191.
23. Stewart, M., Ferguson, B. & Fromer, L. (2010). Epidemiology and burden of nasal congestion. International journal of general medicine. 3: 37-45. Published 2010 Apr 8.
24. Mortuaire,G., de Gabory L., François, M., Massé, G., Bloch, F., Brion, N., Jankowski R. & Serrano, E. (2013). Rebound congestion and rhinitis medicamentosa: nasal decongestants in clinical practice. Critical review of the literature by a medical panel. Eur Ann Otorhinolaryngol Head Neck Dis. 130(3): 137-144. doi: 10.1016/ j.anorl.2012.09.005.
25. Eccles R. (2006). Substitution of phenylephrine for pseudoephedrine as a nasal decongestant. An illogical way to control methamphetamine abuse. British journal of clinical pharmacology. 63(1): 10-4. DOI: 10.1111/j.1365-2125.2006.02833.x
26. Eccles, R., Martensson, K. & Chen, SC. (2010). Effects of intranasal xylometazoline, alone or in combination with ipratropium, in patients with common cold. Curr Med Res Opin. 26(4): 889-99. DOI: 10.1185/03007991003648015.
27. Mortuaire, G., de Gabory, L., François, M., Massé, G., Bloch, F., Brion, N., Jankowski, R.& Serrano.E. (2013). Effet rebond et rhinite aux vasoconstricteurs nasaux en pratique clinique. Revue critique de la littérature par un groupe d'experts. Annales Françaises d'Oto-Rhino-Laryngologie et de pathologie cervico-faciale. 130 (3): 140-148. Doi : 10.1016/j.aforl.2012.11.007.
28. Eccles, R., Jawad, MS., Jawad, SS., Angello, JT. & Druce, HM. (2005). Efficacy and safety of single and multiple doses of pseudoephedrine in the treatment of nasal congestion associated with common cold. Am J Rhinol. 19(1): 25-31. DOI:10.1177/1945892405019001 05.
29. ANSM. Commission Nationale de Pharmacovigilance du 20 novembre 2012. http://www.ansm.sante.fr/var/ansm_site/storage/original/application/c9e15dee904acc 094f9b909eea1634a2.pdf
30. Nathan, R.A., Finn AF Jr., La Force, C., Ratner, P., Chapman, D., de Guia, EC., Hewlett, D. & Kramer, B. (2006). Comparison of cetirizine-pseudoephedrine and placebo in patients with seasonal allergic rhinitis and concomitant mild-to-moderate asthma: randomized, double-blind study. Ann Allergy Asthma Immunol. 97(3): 389-396. DOI:10.1016/S1081-1206(10)60806-X.
31. Browning, MG., Seddon, JO., Yung, LT. & Gough, G. (2011). An unusual case of systemic cardiovascular side effects from the application of over-the-counter nasal decongestion drops. BMJ Case Rep. 2011; 2011:bcr0620103078. Published 2011 Mar 24. DOI: 10.1136/bcr.06.2010.3078.
32. Rimsza, M.E. & Newberry, S. (2008). Unexpected infant deaths associated with use of cough and cold medications. Pediatrics. 122(2): 318-322. DOI: 10.1542/peds. 2007-3813.
33. Abood, E. A., Scott, J., & Wazaify, M. (2018). User Experiences of Prescription and Over-The-Counter Drug Abuse in Aden City, Yemen. Pharmacy (Basel, Switzerland), 6(3): 99. DOI:10.3390/pharmacy6030099.
34. Laccourreye, O., Werner, A., Giroud, J.P., Couloigner, V., Bonfils, P. & Emmanuelle Bondon-Guitton. (2015). Apport, dangers et limites de l'éphédrine et de la pseudoéphédrine en tant que décongestionnant nasal. Annales françaises d'Oto-rhino-laryngologie et de Pathologie Cervico-faciale. 132(1): 28-31. DOI: 10.1016/j. aforl.2014.11.007.
35. Atkinson , HC., Stanescu, I. & Anderson, BJ.(2014). Increased phenylephrine plasma levels with administration

of acetaminophen. N Eng J Med. 370(12): 1171-1172. doi: 10.1056/NEJMc1313942.
36. Vaidyanathan , S., Williamson, P., Clearie, K., Khan , F. & Lipworth, B.(2010). Fluticasone Reverses Oxymetazoline-induced Tachyphylaxis of Response and Rebound Congestion. 182 (1); 19-24. DOI: 10.1164/rccm.200911-1701OC.
37. Pray SW, Pray JJ. Safe Use of Nasal Decongestants. US Pharmacist. 2004;29(7).
38. Fabi, M., Formigari, R. & Picchio FM. (2009). Are nasal decongestants safer than rhinitis? A case of oxymetazoline-induced syncope. Cardiol Young. 19: 633-634. DOI: 10.1017/S1047951109990722.
39. Dokuyucu, R., Gokce, H., Sahan, M., Sefil, F., Tas, ZA., Tutuk, O., Ozturk. A., Tumer, C. & Cevik, C. (2015). Systemic side effects of locally used oxymetazoline. Int J Clin Exp Med. 8 (2): 2674-2678. Published online 2015 Feb 15.
40. Antonicelli, L., Micucci, C., Voltolini, S., Senna, GE., Di Blasi, P., Visonà, G., De Marco, R. & Bonifazi F. (2007). Relationship between ARIA classification and drug treatment in allergic rhinitis and asthma. Clin Exp Allergy. 62(9): 1064-1070. DOI: 10.1111/j.1398-9995.2007.01470.x
41. Giavina-Bianchi, P., Agondi, R., Stelmach, R., Cukier, A. & J.Kalil. (2008). Fluticasone furoate nasal spray in the treatment of allergic rhinitis. Ther Clin Risk Manag. 4(2): 465-472.
42. Martin, BG., Ratner, PH., Hampel, FC., Andrews, CP., Toler, T., Wu, W., Faris, MA. & Philpot, EE. (2007). Optimal dose selection of fluticasone furoate nasal spray for the treatment of seasonal allergic rhinitis in adults and adolescents. Allergy Asthma Proc. 28 (2): 216-225. DOI: https://doi.org/10.2500/aap.2007.28.2983
43. Hampel, FC. Jr, Jacobs, R., Martin, B., Toler, T., Ellsworth, A. & Philpot, E. (2007). Once-daily fluticasone furoate nasal spray (FF) provides 24-hour symptom relief in subjects with seasonal allergic rhinitis (SAR) caused by mountain cedar pollen . J Allergy Clin Immunol. 119(1): 304-5. DOI:https://doi.org/10.1016/j.jaci.2006.12.563
44. Juel-Berg, N., Darling, P., Bolvig, J.,Foss-Skiftesvik, MH., Halken, S. &Winther, L.(2017). Intranasal corticosteroids compared with oral antihistamines in allergic rhinitis: A systematic review and meta-analysis. Am J Rhinol Allergy. 31(1): 19-28. DOI: 10.2500/ajra.2016.30.4397.
45. Meltzer, EO. (2007). Formulation considerations of intranasal corticosteroids for the treatment of allergic rhinitis. Ann Allergy Asthma Immunol. 98(1); 12-21. DOI: 10.1016/S1081-1206(10)60854-X.
46. Verret, DJ. & Marple, BF.(2005). Effect of topical nasal steroid sprays on nasal mucosa and ciliary function. Curr Opin Otolaryngol Head Neck Surg. 13(1): 14-18.
47. Riechelmann, H., Deutschle, T., Stuhlmiller ,A., Gronau, S. & Bürner, H. (2004). Nasal toxicity of benzalkonium chloride. Am J Rhinol. 18(5): 291-299. https://doi.org/10.1177/194589240401800506
48. Peter, Graf. & Hans, Hallén. (1996). Effect on the Nasal Mucosa of Long Term Treatment With Oxymetazoline, Benzalkonium Chloride, and Placebo Nasal Sprays. The Laryngoscope. 106 (5 Pt 1), 605-609. DOI:10.1097/00005537-199605000-00016.
49. Dimova, S., Mugabowindekwe, R., Willems, T. Brewster, ME., Noppe, M., Ludwig, A., Jorissen, M., Augustijns, P. (2003). Safety-assessment of 3-methoxyquercetin as an anthirhinoviral compund for nasal application: effect on ciliary beat frequency. Int J Pharm. 263(1): 95-103.
50. Meltzer, EO. (2007). Formulation considerations of intranasal corticosteroids for the treatment of allergic rhinitis. Ann Allergy Asthma Immunol. 98(1): 12-21. DOI: 10.1016/S1081-1206(10)60854-X.
51. Oppliger, R. & Hauser, C. (2004). Anaphylaxis after injection of corticosteroid preparations-carboxymethylcellulose as a hidden allergen [in German]. J Dtsch Dermatol Ges. 2(11): 928-930.
52. Kirtsreesakul, V., Wongsritrang, K. & Ruttanaphol, S. (2011). Clinical efficacy of a short course of systemic steroids in nasal polyposis. Rhinology. 49(5): 525-532.
53. DOI: 10.4193/Rhino11.140.
54. Vaidyanathan, S., Barnes, M., Williamson, P., Hopkinson, P., Donnan, P.T. & Lipworth, B. (2011). Treatment of chronic rhinosinusitis with nasal polyposis with oral steroids followed by topical steroids: A randomized trial. Ann Intern Med. 154 (5): 293-302. DOI: 10.7326/0003-4819-154-5-201103010-00003.
55. Sastre, J. & Mosges, R. (2012). Local and systemic safety of intranasal corticosteroids. J Investig Allergol Clin Immunol. 22(1): 1-12.

# LYMPHOEPITHELIAL CARCINOMA OF THE PALATINE TONSIL

Milica Jevtić[1,2], Dejan Milić[2], Marina Jovanović[1,2], Nenad Relić[1,2], Andra Jevtović[1,2] and Natalija Božović[1,2]

[1] *University of Kragujevac, Faculty of Medical Sciences, Department of Otorhinolaryngology, Kragujevac, Serbia*
[2] *Clinical Centre Kragujevac, Clinic of Otorhinolaryngology, Kragujevac, Serbia*

Received: 01.02.2021.
Accepted: 23.02.2021.

**Corresponding author:**

**Milica Jevtic, MD**

University of Kragujevac, Faculty of Medical Sciences, Department of Otorhinolaryngology, Kragujevac,Clinical Centre Kragujevac, Clinic of Otorhinolaryngology, Kragujevac, Serbia

E-mail: milicazjevtic@gmail.com

## ABSTRACT

*Lymphoepithelial carcinoma is an undifferentiated carcinoma with nonneoplastic lymphoplasmacytic infiltrate, mostly located in the nasopharynx, while it is extremely rare in the oropharynx. We present a rare case of lymphoepithelial carcinoma arising from palatine tonsil. A 81-year old male patient complained of dysphagia, hypersalivation and bloody sputum. Clinical examination revealed hypertrophy of the right palatine tonsil and ipsilateral cervical lymphadenopathy. Biopsy and histopathological analysis confirmed the diagnosis of lymphoepithelial carcinoma. Multi-slice computed tomography showed a 33x31x38 mm heterodense mass in the region of the right palatine tonsil, and 37x30 mm and 21x20 mm lymph nodes on the right side of the neck. The patient was reffered to an oncology council, which suggested radiotherapy and concurrent chemotherapy. Although rare in clinical practice, lymphoepithelial carcinoma should be considered in cases of tonsil cancer.*

***Keywords***: *Oropharyngeal cancer, palatine tonsil, lymphoepithelial, squamous cell, undifferentiated.*

sciendo

UDK: 616.322-006-07
Eabr 2024; 25(2):189-192
DOI: 10.2478/sjecr-2021-0039

## INTRODUCTION

Head and neck cancers are the 6th most common malignancy worldwide.(1) Squamous cell carcinoma (SCC) represents 90% of head and neck cancers, predominantly affecting mucosal lining of oral cavity, oropharynx and larynx.(2) Between 70% and 80% of oropharyngeal SCC are located in the palatine tonsil.(3) Lymphoepithelial carcinoma (LEC) is a particular histological type, defined as an undifferentiated carcinoma, accompanied by reactive lymphoplasmacytic infiltrate. It is mostly located in the nasopharynx, where it is called undifferentiated carcinoma of nasopharyngeal type (UCNT).(4) We present a rare case of LEC of the palatine tonsil in 81-year old male patient.

## CASE REPORT

A 81-year old male patient was admitted to our clinic due to dysphagia, hypersalivation and bloody sputum. Dysphagia was present for 2 months prior to hospitalization, which had been gradually worsening, while hypersalivation was present for 8 months. Bloody sputum appeared 3 days before hospitalization. The patient is a nonsmoker and does not drink. Oropharyngoscopy revealed significant hypertrophy of the right palatine tonsil, partly covered with white deposits and pushing the uvula towards the opposite side (Figure 1). Neck examination showed a firm non-tender mass in region II of the right side of the neck (Figure 2).

We performed incisional biopsy of the right tonsil. Histopathology analysis revealed tissue sample with preserved covering epithelium, with sheets and islands of polymorphic and polygonal cells, vesicular nuclei, dispersed chromatin, noticeable pathological mitosis and areas of geographic necrosis. Immunohistochemistry analysis showed an expression of p63 and Epstein-Barr virus (EBV. Histopathology and immunohistochemistry reports confirmed the diagnosis of undifferentiated carcinoma of nasopharyngeal type (UCNT), or in other words LEC.

**Figure 1.** Oropharyngoscopy showing significant hypertrophy of the right palatine tonsil.

**Figure 2.** Neck examination showing regional cervical lymph node metastases in the region II of the neck.

**Figure 3.** Multi-slice computed tomography showing a heterodense mass in the right palatine tonsil, extending toward the lingual side of the epiglottis (arrows showing the tumor).

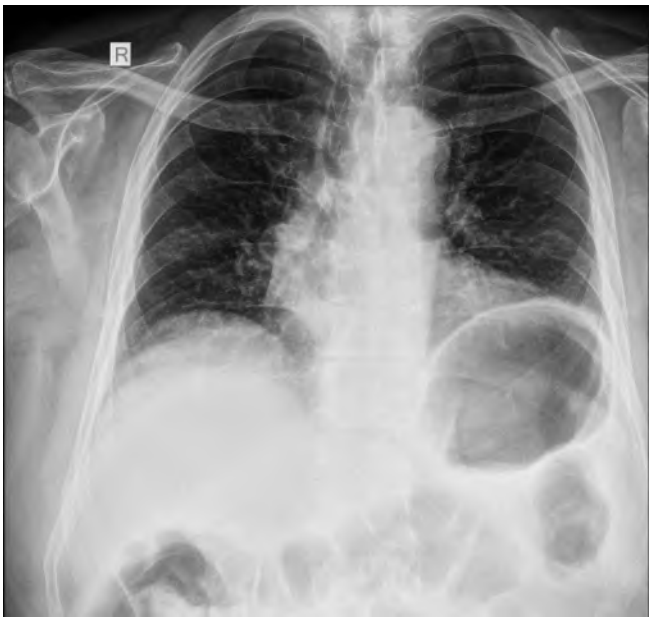


**Figure 4.** Chest X-ray showing no abnormalities.

Multi-slice computed tomography detected a 33x31x38 mm heterodense mass of the right tonsil, extending toward the lingual side of the epiglottis, as well as 37x30 mm and 21x20 mm lymph nodes on the right side of the neck (Figure 3). Chest X-ray showed no abnormalities (Figure 4). Considering the histological type and local and regional spread of the tumor, the patient was referred to an oncology council, which decided upon radical radiotherapy and chemotherapy potentiation once a week during radiotherapy. The patient was advised to come in for a follow-up 1 month after the oncology treatment.

## DISCUSSION

SCC accounts for more than 95% of oropharyngeal cancers.(5) Among these, a particular histological type is LEC, morphologically identical to undifferentiated nonkeratinizing nasopharyngeal cancer (UCNT, earlier known as WHO type 3).(3,6) LEC is very rare in the oropharynx and oral cavity, where it represents only 0,8-2% of all cancers. In more than 90% of cases, LEC is located in the palatine tonsil or the base of the tongue,(7) as in our case. 75% of LEC arise from the nasopharynx, where it represents 40% of all tumors and is almost exclusively related to EBV, which was immunohistochemically proved in our case. Outside of the nasopharynx, LEC is considerably more rare, usually occuring in young males and in more advanced stage compared to nasopharyngeal LEC.(8)

Known risk factors for tonsil cancer are tobacco smoking and alcohol consumption, acting individually and synergistically.(9) However, our patient was a nonsmoker and a nondrinker. Even though tobacco and alcohol use have significantly decreased in the past 50 years, incidence rates for oropharyngeal cancers have increased. Possible explanation is human papillomavirus infection, which is present in up to 47% of oropharyngeal cancers.(10)

Clinical manifestations of tonsil cancer include sore throat, globus sensation, ipsilateral ear pain, dysphagia, odynophagia and trismus as a sign of local invasion.(11,12) Up to 60% of cases present with regional lymph node metastases upon first examination.(5) Our patient complained of dysphagia, hypersalivation and bloody sputum. Hypersalivation was secondary to dysphagia and accumulation of saliva in the mouth, while blood in the sputum was a result of tumor haemorrhage.

Diagnosis of tonsil cancer is based on anamnesis, clinical ENT examination, radiology imaging methods and histopathology analysis.(11) Clinical examination revealed notable enlargement of the right palatine tonsil, partially covered with white deposits, pushing the uvula toward the left side and cervical lymphadenopathy on the side of the enlarged tonsil. Tonsil asymmetry, id est unilateral tonsil hypertrophy, can be the only sign of disease in otherwise asymptomatic patients and the reason for an ENT referral.(12) Among imaging methods, computed tomography is the method of choice, used for estimating the tumor size and its regional and distant spread.(11,12) Histopathology analysis is necessary for definitive diagnosis. Histological characteristics of LEC include the presence of lobules, sheets or islands of polygonal or spindle-shaped tumor cells, round or oval, vesicular nuclei with moderate to marked nuclear pleomorphism, as well as nonneoplastic lymphoplasmacytic cell infiltrate between tumor cells. Increased mitotic activity and necrosis are also frequently found. Immunohistochemistry analysis shows reactivity for cytokeratins and epithelial membrane antigen, focal or diffuse reactivity for p63, while in situ hybridization shows presence of EBV.(4) These characteristics were present in our case.

Treatment for tonsil cancer includes surgery, radiotherapy and chemotherapy. The choice of therapeutic modality depends on TNM staging.(13) The course of action for early cases of the disease is monomodality, either surgery or radiotherapy.(9) Unfortunately, only 1/3 of cases are diagnosed in the early phase.(14) Due to cancer radiosensitivity, radiotherapy combined with concurrent chemotherapy or with surgery for residual disease are applied in advanced cases,(13) as were in our case.

## CONCLUSION

Lymphoepithelial carcinoma is a rare histological entity and is typically found in the nasopharynx, very rarely in the oropharynx and tonsils. Risk factors for this cancer include tobacco and alcohol use, Epstein-Barr virus infection mostly in the endemic regions and human papillomavirus infection. Although a rare histological type, lymphoepithelial carcinoma should always be considered in cases of tonsil cancer in clinical practice.

## ACKNOWLEDGEMENT

None

## CONFLICT OF INTEREST

The authors declare no financial or commercial conflict of interest.

## REFERENCES

1. Solomon B, Young RJ, Rischin D. Head and neck squamous cell carcinoma: Genomics and emerging biomarkers for immunomodulatory cancer treatments. Semin Cancer Biol. 2018;52:228-40.
2. Winquist E, Agbassi C, Meyers BM, Yoo J, Chan KKW. Systemic therapy in the curative treatment of head and neck squamous cell cancer: a systematic review. J Otolaryngol - Head Neck Surg. 2017;46(1):1-11.
3. Ahmadi N, Chan M, Ruth Y, Sritharan N, Chin RY. Survival outcome of tonsillar squamous cell carcinoma (TSCC) in the context of human papillomavirus (HPV): A systematic review and meta-analysis. Surg. 2019; 17 (1):6-14.
4. Wenig BM. Lymphoepithelial-like carcinomas of the head and neck. Semin Diagn Pathol. 2015;32(1):74-86.
5. Fossum CC, Chintakuntlawar A V, Price L, Garcia JJ. Characterization of the Oropharynx: Anatomy, Histology, Immunology, Squamous Cell Carcinoma & Surgical Resection. Histopathology. 2017;70(7):1021-9.
6. Rytkönen AE, Hirvikoski PP, Salo TA. Lymphoepithelial Carcinoma: Two Case Reports and a Systematic Review of Oral and Sinonasal Cases. Head Neck Pathol. 2011;5(4):327-34.
7. Barnes L, Eveson JW, Reichart P, Sidransky D. World Health Organization Classification of Tumours Pathology & Genetics Head and Neck Tumours IARC WHO Classification Head and Neck Tumours. 2005.
8. Bai J, Zhao F, Pan S. Clinicopathological characteristics and survival of lymphoepithelial carcinoma of the oral cavity and pharynx: a population-based study. BioRxiv. 2019;669671.
9. Laccourreye O, Rubin F, Badoual C, Halimi P, Giraud P. The keys to conservative treatment of early-stage squamous cell carcinoma of the tonsillar region. Eur Ann Otorhinolaryngol Head Neck Dis [Internet]. 2017;3-8. Available from: http://dx.doi.org/10.1016/j.anorl.2017.03.007
10. De Santis S, Spinosi MC, Cambi J, Bengala C, Boccuzzi S. Oropharyngeal squamous cell carcinoma and HPV. Systematic review on overall management. J Stomatol Oral Maxillofac Surg. 2017;118(2):103-8.
11. Jamal Z, Anjum F. Oropharyngeal Squamous Cell Carcinoma Histopathology. StatPearls Publ. 2020.
12. Williamson AJ, Mullangi S, Gajra A. Tonsil Cancer. StatPearls Publ. 2020.
13. Marur S, Forastiere AA. Head and Neck Squamous Cell Carcinoma: Update on Epidemiology, Diagnosis, and Treatment. Mayo Clin Proc. 2016;91(3):386-96.
14. Economopoulou P, de Bree R, Kotsantis I, Psyrri A. Diagnostic tumor markers in head and neck squamous cell carcinoma (HNSCC) in the clinical setting. Front Oncol. 2019;9:827.

# SYNCHRONOUS NECK MELANOMA AND PAPILLARY THYROID CANCER: A CASE REPORT

Vladimir Pantelic[1], Sasa Zunjic[1], Dusan Ruzicic[1], Ivan Radosaljevic[2], Ivan Paunovic[3] and Vladan Zivaljevic[3]

[1]*Department of Surgery, General Hospital Valjevo, Serbia*
[2]*University of Kragujevac, Faculty of Medical Sciences, Department of Surgery, Serbia*
[3]*Center for Endocrine Surgery, Institute of Endocrinology, Diabetes and Diseases of Metabolism, Clinical Center of Serbia, Belgrade, Serbia*

Received: 05.01.2021.
Accepted: 02.03.2021.

**Corresponding author:**

**Vladimir Pantelic, MD**

Department of Surgery, General Hospital Valjevo, Serbia Obrena Nikolica 5, 14000 Valjevo

E-mail: vladimir.pantelic2610@gmail.com

## ABSTRACT

*The synchronous malignant melanoma of the neck and papillary thyroid cancer is rare but severe condition. Here, we describe the case of a patient with papillary thyroid cancer and melanoma invasivum cutis. A 49-year-old man had a change on the neck at the last 3-4 months that he accidentally noticed. He had hoarse voice, was afebrile, did not sweat more than usual and feel exhausted, without rash or itching. MR examination of the neck and upper mediastinum before the surgery indicated a hyperintense focal change in the left thyroid gland which dimensions was 19·15mm and several hyperintense inhomogeneous lymph glands of the jugular chain, on the both sides, with different sizes. On the basis of the conducted analyzes, in addition to total thyroidectomy, two-sided functional dissection of the lymph nodes of the neck was performed. The pathohistological diagnosis of the left lobus was: Carcinoma papillary glandulae thyreoideae invasivum (G-I, nG-I, pT2, Lx, Vo). CT of head, neck and thorax were made, where it was noticed that the CT of the head and lungs were normal. PET/CT findings indicated that there was no rest or recurrence of the tumor. The message from this case report is that when diagnosing and treating thyroid cancer, the observed changes in the neck lymph nodes also indicate cancers of non-thyroid pathology such as malignant melanoma.*

***Keywords***: *Papillary thyroid cancer, malignant melanoma, lymph nodes.*

sciendo

UDK: 616.441-006.6
Eabr 2024; 25(2):193-197
DOI: 10.2478/sjecr-2021-0012

## INTRODUCTION

Worldwide malignant melanoma is the commonest tumor of the skin, though it occurs in many other organs. Malignant melanoma is a skin cancer that is caused by the malignant transformation of melanocytes. Melanocytes are neural crest-derived cells that migrate to the skin, mucous membranes and several other sites. The incidence of melanoma has been steadily increasing in the past several decades with an annual increase of 3-8% worldwide (1). Most common form of melanoma are the cutaneous and the ocular form. It occurs slightly more often in males 2.8:1 male to female ratio and the age range is from. 20-83 years worth an average age of 56 years (2). Malignant melanoma can be successfully treated if it is detected in the early stages of development. Surgery is the standard treatment for early stage melanoma. However, the prognosis associated with advanced-stage malignant melanoma is poor; the disease accounts for ~4% of all skin cancers, but results in 80% of skin cancer-associated mortality (3, 4).

The clinical presentation of this condition may vary widely which is divided into following five types: Pigmented nodular type, pigmented macular type, pigmented mixed type, non-pigmented nodular type and non-pigmented mixed type (5-7).

On the other hand, cancers of a thyroid gland are the most frequent endocrine cancers, and this is known over a decades (8). Unlike other forms of thyroid cancers (medullary, follicular and anaplastic), whose occurrence remained almost the same over time, the incidence of papillary thyroid cancer strongly increased (9). Indeed, the vast majority of thyroid malignant tumors belong to papillary cancers (around 90%) (10). To date, several factors have been identified to potentiate the occurrence papillary thyroid cancer such as Hashimoto thyroiditis, other thyroid diseases, and early exposure to ionizing radiation (11, 12). Moreover, some evidence indicate that thyroid malignancy can be found more often after other primary cancers, as consequence of radiation therapy or even without it (13, 14). Therefore, much attention has been paid to the assessment of the risk for developmental of thyroid cancers on the field of existence of non-thyroid malignancies. Nevertheless, there are almost no literature data describing synchronous thyroid cancer and additional malignancy.

Here, we describe the case of a patient with synchronous neck melanoma and papillary thyroid cancer.

## CASE REPORT

A 49-year-old man had a change on the neck at the last 3-4 months that he accidentally noticed. He had hoarse voice, was afebrile, did not sweat more than usual and feel exhausted, without rash or itching. At physical examination following was observed: on the neck - right angularly palpable one lymphatic gland (size 1,2 cm, hard painless, weakly movable), left submental palpable one deep and more tiny single painless lymphatic gland. Supraclaviculary and axillary without significant lymphatic glands, spleen palpable to 1 cm, without lymphatic glands in inguinal region, liver not enlarged, airway noise intensified in the lungs.

MR examination of the neck and upper mediastinum before the surgery indicated a hyperintense focal change in the left thyroid gland which dimensions was 19 x 15mm (AP-LL) (Figure 1A) and several hyperintense inhomogeneous lymph glands of the jugular chain, on the both sides, with different sizes (Figure 1B).

**Figure 1.** MR examination of the neck soft tissues. The examination was performed in the axial section and T2W FS sequences.

A) In the left lobe of the thyroid gland there is a clearly separated hyperintense focal change in size 19 x 15 mm (AP-LL). It does not penetrate the thyroid capsule.

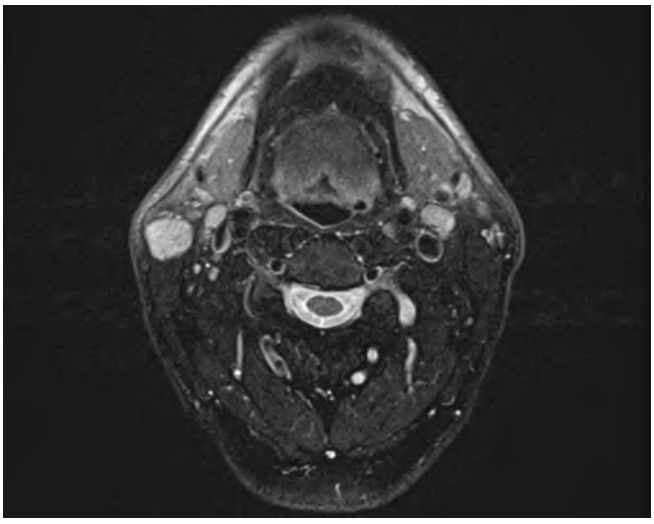

B) In level A and 5A there are several hyperintense inhomogeneous lymph glands on both sides, with different sizes - show pathological signal intensity.

*Ex tempore* analysis indicated that the right lobus was benign, the left lobe was malignant, and the nodus of the right jugular chain was malignant. The pathology report showed that the nodus was most likely malignantly altered due to melanoma and advised to examine the skin of the head and neck intraoperatively. On that occasion pigmented nevus of right tragus was discovered, removed by excision, and confirmed to be malignant. On the basis of the above findings, in addition to total thyroidectomy, two-sided functional dissection of the lymph nodes of the neck was performed. After the operation, Letrox tablets was prescribed a 100 mg 1·1.

The pathohistological diagnosis of the skin with a tumor on a baseline of 15·13·12 mm, light brown color, uneven pigmentation was as follows: Melanoma nodular cutis invasivum (G-II, pT4bN1 (1 + / 4In), Breslow-3, Clark-III, L+, Vx, Ro. Ulceration of surface tumor was present, with peritumoral lymphocytic infiltration. Mitotic index was 4/10HPF, pigment production was minimal with dominant vertical growth phase. The pathohistological diagnosis of the left lobus was: Carcinoma papillary glandulae thyreoideae invasivum (G-I, nG-I, pT2, Lx, Vo). The pathohistological diagnosis of the right lobus was: Struma colloides cystica diffusa glandulae thyreoideae.

During the first CT of head, neck and thorax it was noticed that head and lungs imaging were normal. In the neck region at the height of the oropharynx, alongside the marginal blood vessels, there was one lymph node of 7 mm in size on both sides. Thyroid scintigraphy had shown that there was no accumulation of radioactive iodine and above the thorax finding was neat. A year later, PET/CT of the whole body was made (from the base of the skull to the proximal parts of the femur). Scanning of the entire body was done 60 minutes after i.v. injection of 9 mCi fluordeoxyglucose with fluorine-18 ($^{18}$FDG). PET/CT findings indicated that there was no rest or recurrence of the tumor.

Ultrasound of the neck was done a year after the PET/CT scan. Right in the region of the lower half of the parotid and lateral half of the submandibular gland, three changes were noticed. The largest lymph gland of clear contours was hypoehnogenic structure, diameter 26·9 mm with a clear separation of the cortical layer of the thin and slightly echogenic central matrix. Another lymph gland was with oval structure and diameter of 9·5 mm, and the third was in the parotid parenchyma with diameter of 12·4 mm. In the left region of the lateral half of the submandibular gland was the lymph gland of diameter 15·4mm. There were no signs of recurrence in the thyroid box region. Supraclavicular and the lateral neck chains did not had signed lymph nodes. Taking into account that right submandibular lymph nodes were 26 mm of diameter, and MR inspection was scheduled. The results of thyroid hormones and antibodies were following: PTH intact-55,4 pg/ml (15-65 pg/ml); TSH-78,629 uIU/ml (0,27-4,20 uIU/ml); TT4-0,53 nmol/l (66,0-181,0 nmol/l); TT3-0,45nmol/l (2,7-3,87 nmol/l); Anti Tg-12,5 IU/ml (< 115 IU/ml); TG-0,538 ng/ml (1.4-78 ng/ml). TSH was elevated while TT4, TT3 and TG were lower than reference values. The dose of Letrox was increased to 150 mg daily.

MR imaging after total thyroidectomy and malignant melanoma surgery did not showed detectable recurrence of the tumor.

## DISCUSSION

This case illustrates the presentation, diagnosis, and treatment of a patient with synchronous neck melanoma and papillary thyroid cancer. Literature data have shown that multiple cancers of head and neck are not infrequent malignancies and their incidence is raising (15, 16). Incidence for development of another primary cancer after discovering of the first malignancy, for synchronous cancers is 15 % (17). A careful and systematic triage is thus of the great interest for these patient. Some studies pointed out that synchronous cancers can be detected in 9-14% of patients during routine screening (17).

Malignant melanoma is an aggressive cutaneous melanocytic neoplasia. Although melanoma most commonly metastasizes to regional lymph nodes, mortality from melanoma is due primarily to distant spread to visceral organs, commonly the lungs, liver, and brain (18-20). Considering that metastasis to the thyroid gland is a very rare, after pathohistological analysis of thyroid malignanant tissue diagnosis of synchronous cancers can be confirmed, as seen it this case report.

According to their primary site, melanomas are grouped as cutaneous, ocular, mucosal, and of unknown origin; of all, mucosal melanomas are the least frequent ones (21). Head and neck mucosal melanomas (HNMMs) comprise 0.7% to 0.8% of all melanomas and less than 10% of all head and neck melanomas (22). Malignant melanoma is an aggressive cutaneous melanocytic neoplasm which often metastasizes to regional lymph nodes but whose mortality is mainly determined by tumor dissemination to visceral organs such as the lungs, liver, and brain. Although rare, HNMMs are very aggressive malignant tumors, and their prognosis is worse than that for cutaneous and ocular melanomas (23). However, the occurrence of another primary tumor such as papillary thyroid cancer complicates the diagnostic and therapeutic approach, while the clinical signs may be asymptomatic (24). The prevalence of synchronous non-thyroidal cancers in patients on surgical therapy of papillary thyroid cancer is approximately 14 % (25). The third most frequently associated synchronous non-thyroidal cancers is melanoma (26). When comparing with patients without another malignancy, those with an non-thyroidal cancers were elderly (56.4 ± 15.5 years) and had been exposed to radiation (27). Studies have shown that pathohistological features of papillary thyroid cancers are similar in patients with non-thyroidal cancer compared with ones in patients without additional malignancy (26, 27). Despite the fact that patients with an non-thyroidal cancers were detected at a more severe level of disease than those without, additional estimation of each TNM category have shown absence of statistical distinction in the

primary tumor size, or the rate of nodal or distant metastases. (27).

Having in mind that clinical signs of patients with papillary thyroid cancer are similar to those without accessorial non-thyroidal cancers, they thus must be managed equivalently. Furthermore, surgeons should rise attention of the incidence of synchronous papillary thyroid cancer with these types of cancers and take into account assessment of the neck during thyroidal cancer diagnosis.

Treatment of thyroid malignancies is primarily surgical, but the decision to operate on the patients will depend on their clinical condition, the primary site of the original tumor, presence of other metastases, the degree of dissemination, and symptoms caused by the thyroid mass (25, 26). Surgery may also be important as a palliative treatment to relieve symptoms, particularly those associated with airway compression. No consensus exists on the extent of the surgery, and most authors recommend that isthmectomy and lobectomy be performed in cases with isolated nodules, whereas total or near-total thyroidectomy should be performed in cases with multifocal disease (28).

## CONCLUSION

The message from this case report is that when diagnosing and treating thyroid cancer, the observed changes in the neck lymph nodes also indicate cancers of non-thyroid pathology such as malignant melanoma.

Surgeons should rise attention of the incidence of synchronous papillary thyroid cancer with neck melanoma and take into account assessment of the neck during thyroidal cancer diagnosis. This approach will therefore strongly contribute to the prolonged survival in these patients and prevention of rapid onset of life-threatening complications.

## CONFLICTS OF INTEREST

The authors declare no financial or commercial conflicts of interest.

## FUNDING

None.

## LITERATURE

1. Atkinson V. Recent advances in malignant melanoma. Intern Med J. 2017;47(10):1114-21.
2. Longvert C, Saiag P. Melanoma update. Rev Med Interne. 2019;40(3):178-83.
3. Cabrera R, Recule F. Unusual clinical presentations of malignant melanoma: a review of clinical and histologic features with special emphasis on dermatoscopic findings. Am J Clin Dermatol. 2018;1:15-23.
4. Pavri SN, Clune J, Ariyan S, Narayan D. Malignant melanoma: beyond the basics. Plast Reconstr Surg. 2016;138(2):330e-340e.
5. Leonardi GC, Falzone L, Salemi R, Zanghì A, Spandidos DA, Mccubrey JA, et al. Cutaneous melanoma: from pathogenesis to therapy. Int J Oncol. 2018;52:1071-80.
6. Hartman RI, Lin JY. Cutaneous melanoma-a review in detection, staging, and management. Hematol Oncol Clin North Am. 2019;33(1):25-38.
7. Iglesias-Pena N, Paradela S, Tejera-Vaquerizo A, Boada A, Fonseca E. Cutaneous melanoma in the elderly: review of a growing problem. Actas Dermosifiliogr. 2019;110:434-47.
8. Takano T. Natural history of thyroid cancer. Endocr J. 2017;64:237-44.
9. Luzón-Toro B, Fernández RM, Villalba-Benito L, Torroglosa A, Antiñolo G, Borrego S. Influencers on thyroid cancer onset: molecular genetic basis. Genes (Basel). 2019;10:913.
10. Albi E, Cataldi S, Lazzarini A, Codini M, Beccari T, Ambesi-Impiombato FS, et al. Radiation and Thyroid Cancer. Int J Mol Sci. 2017;18:911.
11. Wang TS, Sosa JA. Thyroid surgery for differentiated thyroid cancer - recent advances and future directions. Nat Rev Endocrinol. 2018;14:670-83.
12. Ferrari SM, Fallahi P, Elia G, Ragusa F, Ruffilli I, Paparo SR, et al. Thyroid autoimmune disorders and cancer. Semin Cancer Biol. 2020;64:135-46.
13. Bhatti P, Veiga LH, Ronckers CM, Sigurdson AJ, Stovall M, Smith SA, et al. Risk of second primary thyroid cancer after radiotherapy for a childhood cancer in a large cohort study: an update from the childhood cancer survivor study. Radiat Res. 2010;174:741-52.
14. Lal G, Groff M, Howe JR, Weigel RJ, Sugg SL, Lynch CF. Risk of subsequent primary thyroid cancer after another malignancy: latency trends in a population-based study. Ann Surg Oncol. 2012;19:1887-96.
15. Leemans CR, Snijders PJF, Brakenhoff RH. The molecular landscape of head and neck cancer. Nat Rev Cancer. 2018;18:269-82.
16. Hahn LD, Kunder CA, Chen MM, Orloff LA, Desser TS. Indolent thyroid cancer: knowns and unknowns. Cancers Head Neck. 2017;2:1.
17. Serafini MS, Lopez-Perez L, Fico G, Licitra L, De Cecco L, Resteghini C. Transcriptomics and Epigenomics in head and neck cancer: available repositories and molecular signatures. Cancers Head Neck. 2020;5:2.
18. Ascierto PA, Accorona R, Botti G, Farina D, Fossati P, Gatta G, et al. Mucosal melanoma of the head and neck. Crit Rev Oncol Hematol. 2017;112:136-52.
19. Nenclares P, Ap Dafydd D, Bagwan I, Begg D, Kerawala C, King E, et al. Head and neck mucosal melanoma: The United Kingdom national guidelines. Eur J Cancer. 2020;138:11-18.
20. Green B, Elhamshary A, Gomez R, Rahimi S, Brennan PA. An update on the current management of head and neck mucosal melanoma. J Oral Pathol Med. 2017; 46:475-79.

21. Jaballah Vinckenbosch P, Litzistorf Y, Gaide O, Özdemir BC, Michielin O, Reinhard A. ENT management of head and neck cutaneous melanoma. Rev Med Suisse. 2020;16:1853-59.
22. Lerner BA, Stewart LA, Horowitz DP, Carvajal RD. Mucosal melanoma: new insights and therapeutic options for a unique and aggressive disease. Oncology. 2017;31:e23-e32.
23. Mihajlovic M, Vlajkovic S, Jovanovic P, Stefanovic V. Primary mucosal melanomas: a comprehensive review. Int J Clin Exp Pathol. 2012;5:739-53.
24. Coca-Pelaz A, Shah JP, Hernandez-Prera JC, Ghossein RA, Rodrigo JP, Hartl DM, et al. Papillary thyroid cancer-aggressive variants and impact on management: a narrative review. Adv Ther. 2020;37:3112-28.
25. Haroon Al Rasheed MR, Xu B. Molecular alterations in thyroid carcinoma. Surg Pathol Clin. 2019;12:921-30.
26. Costa MM, Belo S, Capela-Costa J, Costa J, Carvalho D. Malignant melanoma with synchronous thyroid metastases: case report and literature review. Arch Endocrinol Metab. 2017;61:193-97.
27. Heroiu Cataloiu AD, Danciu CE, Popescu CR. Multiple cancers of the head and neck. Maedica (Bucur). 2013;8:80-85.
28. Miccoli P, Bakkar S. Surgical management of papillary thyroid carcinoma: an overview. Updates Surg. 2017;69:145-50.

# INFORMATION FOR AUTHORS

## AIMS AND SCOPE

*Experimental and Applied Biomedical Research* (*EABR)* former *Serbian Journal of Experimental and Clinical Research* is a peer-reviewed, open access journal which publishes original research articles, reviews, case reports and letters to the editor in all areas of the biomedical sciences that have not been published previously. The journal comprises both basic and clinical research in the field of biomedicine. Current acceptance rate is 60%. *EABR* was founded in 2000 under the name *Medicus* and over more than two decades has grown into one of the leading national journals in the field of biomedical sciences. *Experimental and Applied Biomedical Research* is owned and published by Faculty of Medical Sciences University of Kragujevac. The journal adheres to the policies of the International Committee of Medical Journal Editors (ICMJE) and publishing ethics guidelines provided by the Committee on Publication Ethics (COPE).

## TYPES OF MANUSCRIPTS

- *Original research articles*: *EABR* considers all original research manuscripts which present the results of an original research study (experimental or clinical). These manuscripts must contain sufficient information on all relevant research methods, as well as a detailed analysis of the results obtained.

- *Reviews*: *EABR* considers literature reviews, systematic reviews and meta analyses addressed to a particular subject area, with special reference to new knowledge and facts. Manuscripts in this category must not be shorter than 6000 words, the text must cite more than 70 references of which 50% have been published in the previous 5 years. Systematic reviews should follow the PRISMA guidelines.

- *Case reports*: *EABR* considers case reports presenting detailed information on the symptoms, signs, diagnosis, treatment (including all types of interventions), and outcomes of an individual patient. Case reports should usually describe new or uncommon conditions that serve to enhance medical care or highlight diagnostic approaches. Case reports should follow the CARE guidelines.

- *Letters to the editor: EABR* considers letters to the editor related to different clinico-laboratory observations. They should be titled, not exceed 500 words, and have a maximum of 5 references. Up to 1 table or figure may be submitted, but will be published at the discretion of the Editor. No more than 3 authors should appear.

## MANUSCRIPT SUBMISSION

Manuscripts submitted to *Experimental and Applied Biomedical Research* must neither be published previously nor be under consideration for publication in another journal. Manuscripts are acompanied with a suitable *cover letter* stating that: the manuscript is not

submitted for publication elsewhere; all authors have agreed to submission; the study is carried out in accordance with relevant ethical international guidelines.

*EABR* considers only manuscripts written in English using *Microsoft Office Word* format and uploaded online at https://www.editorialmanager.com/sjecr/.

Plagiarism, data fabrication and image manipulation are not tolerated. Plagiarism includes copying text, ideas, images, or data from another source, even from authors own publications, without providing any reference to the original source. If a study's design or the manuscript's structure or language has been inspired by previous works, these papers must be explicitly cited. All manuscripts submitted to *Experimental and Applied Biomedical Research* are checked for plagiarism using the academic standard software prior to the first step of the editorial process.

## MANUSCRIPT PREPARATION AND ORGANISATION

### *Title Page*

The Title Page should contain the following informations:

- Manuscript title
- Full author(s) names
- The affiliation(s) of the author(s)
- A clear indication and an active e-mail address of the corresponding author

Manuscript title should be concise and informative.

It is necessary to state the full names and surnames (middle letter or name is optional) of all authors and the exact affiliations of all authors - institution, (department), city, (state), country. *Experimental and Applied Biomedical Research* remains neutral with regard to jurisdictional claims in institutional affiliations. Responsibility for affiliations ultimately rests with the author.

### *Abstract*

Provide an abstract of 150 to 250 words. Abstract should be structured (Background, Methods, Results, Conclusion), citation-free, without abbreviations if possible.

### *Keywords*

Three to five relevant keywords need to be added after the abstract. Keywords should be specific to the manuscript, yet reasonably common within the subject discipline.

### *Text Formatting*

Manuscripts should be submitted in *Microsoft Office Word*. The authors should use normal, plain *Times New Roman* font (12pt) for text. Pages should be numbered automatically. Italics may be used for emphasis. Abbreviations should be defined at the first mentioning in the text and used consistently thereafter (do not use a separate subtitle for abbreviations only). Please use no more than three levels of displayed headings. International System (SI) of Units should be used (imperial, US customary and other units should be converted to SI units).

*Original research articles* should contain following sections: Introduction, Materials and Methods, Results, Discussion, Conclusions, Acknowledgments, Conflict of Interest, and References. *Reviews* may require different formats, while *Case reports* manuscripts should follow the CARE guidelines.

*Introduction.* This section should contain context or background for the study, rationale, clear aim of research or tested hypothesis.

*Materials and Methods*. This section should provide sufficient detail for replication of the study. If more than one method is used in the research, use subsections with appropriate subheadings. The *Materials and Methods* section should also contain following statements:

a) Informed Consent Statement. In cases where the identification of personal information is necessary for scientific reasons, authors should obtain informed consent from all individuals included in the study
b) Human Right Statement. Manuscripts containing information related to human should clearly state that the research has complied with all relevant international and national regulations and institutional policies and has been approved by the authors' institutional Ethics committee.
c) Animal Right Statement. Manuscripts containing information related to animals should clearly state that the research has complied with all relevant international and national regulations and institutional policies and has been approved by the authors' institutional Ethics committee.

For details and examples of statements please see part ‘Research and publication ethics’.

*Results.* The results should be presented in logical sequence in the manuscript. Do not repeat all the data in the tables or figures in the text.

*Conclusions*. Within the *Conclusions* section the authors should clearly explain the main conclusions of the article, highlighting its importance and relevance.

*Acknowledgments*. Acknowledgments of people, grants, funds, etc. should be placed in a separate section after the Conclusions section. The names of funding organizations should be written in full. This may include administrative and technical support, or donations in kind (e.g., materials used for experiments).

*Conflict of Interest.* Authors must declare all relevant interests that could be perceived as conflicting. If there is no conflicts exist, the authors should state this. Submitting authors are responsible for coauthors declaring their interests.

*References*. *References* must be numbered in order of appearance in the text (including table captions and figure legends) and listed individually at the end of the manuscript. In the text, reference numbers should be placed in round brackets ( ), and placed before the punctuation – e.g. (1), (1–3) or (1, 3). The list of references should only include works that are cited in the text and that have been published or accepted for publication. Personal communications and unpublished works should only be mentioned in the text.

The reference list should include contain surnames and the first letter of the author's name, full title, abbreviated title of the journal, year of publication, volume, number and pagination (Vancouver style guide). In case where the list of authors are more than six, please use et al. after the sixth author.

The examples of correct referencing:

*For journal papers:*
Shoji F, Haro A, Yoshida T, Ito K, Morodomi Y, Yano T, et al. Prognostic significance of intratumoral blood vessel in- vasion in pathologic stage IA non-small cell lung cancer. Ann Thorac Surg. 2010;89(3):864-9.

*For journal papers by DOI*:
Ewy MW, Patel A, Abdelmagid MG, Mohamed Elfadil O, Bonnes SL, Salonen BR, et al. Plant-Based Diet: Is It as Good as an Animal-Based Diet When It Comes to Protein? Curr Nutr Rep. 2022. doi: 10.1007/s13668-022-00401-8.

*For books:*
Kleiner FS, Mamiya CJ, Tansey RG. 2001. Gardner's art through the ages (11th ed.). Fort Worth, USA: Harcourt College Publishers.

*For chapter in an edited book:*
Mettam GR, Adams LB. How to prepare an electronic version of your article. In: Jones BS, Smith RZ, editors. Introduction to the electronic age, New York: E-Publishing Inc; 2009, p. 281–304.

**Tables, figures and images**

*Tables*

Tables should always be cited in text in consecutive numerical order. For each table, please supply a table caption (title) explaining the components of the table. Identify any previously published material by giving the original source in the form of a reference at the end of the table caption. Footnotes to tables should be indicated by superscript lower-case letters (or asterisks for significance values and other statistical data) and included beneath the table body.

*Figures*

Please submit each figure as an individual file separate from the manuscript text. All figures are to be numbered using Arabic numerals. Figures should always be cited in text in consecutive numerical order. Each figure should have a concise caption describing accurately what the figure depicts. Include the captions in the text file of the manuscript, not in the figure file.

For vector graphics, the preferred format is EPS, for halftones, please use TIFF format. *Microsoft Office* files are also acceptable. Vector graphics containing fonts must have the fonts embedded in the files.

*Line art*:

- Definition: Black and white graphic with no shading.
- Do not use faint lines and/or lettering and check that all lines and lettering within the figures are legible at final size.
- All lines should be at least 0.1 mm (0.3 pt) wide.
- Scanned line drawings and line drawings in bitmap format should have a minimum resolution of 1200 dpi.
- Vector graphics containing fonts must have the fonts embedded in the files.

*Halftone art*:

- Definition: Photographs, drawings, or paintings with fine shading, etc.
- If any magnification is used in the photographs, indicate this by using scale bars within the figures themselves.
- Halftones should have a minimum resolution of 300 dpi.

*Images*

Supply vector-based files such as those produced by *CorelDraw*, *Adobe Illustrator* or similar software. Vector files give us maximum flexibility for sizing your figures properly. Do not rasterize line art or text. Photographic images should have a minimum resolution of 300 dpi at final print size. Embedded images within a vector file should also have a minimum resolution of 300 dpi. Up sampling artwork (artificially increasing file size or resolution) will not improve quality and causes production problems. At final print size, line weights can be no thinner than 0.28 pt.

**PEER REVIEW PROCESS**

All submitted manuscripts received by the Editorial Office will be evaluated by a professional *Editorial board* to determine whether they posses sufficient quality, are they properly prepared and follow the ethical policies of *Experimental and Applied Biomedical Research*. Manuscripts that do not fit with the quality and ethical standards of *EABR* will be rejected before peer-review. Manuscripts that are not properly prepared according to the Instruction for authors will be returned to the authors for revision and resubmission.

Once a manuscript passes the initial evaluation, it will be assigned to at least two independent experts for single-blind peer-review process. If the outcomes of the performed reviews are opposite, the third review is required. The peer-review outcomes are one of following:

- *Accept (without any changes)* - the journal will publish the paper in its original form. This type of decision outcome is rare.
- *Minor revision* - the manuscript have high chance to be accepted after fulfillment of minor corrections. Authors will be asked to resubmit the revised manuscript within a suitable time frame, and the revised version will be returned to the reviewer for further comments.
- *Reconsider after Major Revision* - the acceptance of the manuscript would depend on the revisions. The authors are required to perform extensive and significant

improvements in their manuscript. Authors will be asked to resubmit the revised manuscript within a suitable time frame, and the revised version will be returned to the reviewer for further comments.

- *Reject* - the manuscript is rejected for two reasons: 1. it has serious flaws, and/or makes no original significant contribution; 2. corrections and improvements during the (major) revision were not sufficient and satisfactory. No offer of resubmission to the journal is provided.

All reviewer comments should be responded point-by-point in a separate document entitled 'Answers to reviewers comments'. Corrections should be marked within the text in a red colour or as a track changes. During the submission process, author should suggest two potential reviewers with the appropriate expertise to review the manuscript. Proposed reviewers should be from different institutions than the authors.

Upon editor's approval, after received positive manuscript reviews, the manuscript is accepted in the system, and the corresponding author receives information about the manuscript accepted for publication to the email address. Once accepted, the manuscript will undergo professional copy-editing, English editing, proofreading by the authors, pagination and publication. The Editorial board reserves the right to correct the English language after proofreading by the authors.

DOI number is assigned to the paper and, after proofreading and text break according to the Journal instructions, the paper is published as *Ahead of Print* first on *Sciendo* platform (https://sciendo.com/journal/sjecr) and then in one of the next issues of the Journal.

## RESEARCH AND PUBLICATION ETHICS

### Research Involving Human Subjects

When reporting on research that involves human subjects, human material, human tissues, or human data, authors must declare that the investigation was carried out following the rules of the Declaration of Helsinki of 1975 (https://www.wma.net/what-we-do/medical-ethics/declaration-of-helsinki/), revised in 2013. As a minimum, a statement including number of approval and name of the ethics committee must be stated in Section 'Statement of Human Rights' of the article. In addition, the protection of privacy is a legal right that must not be breached without individual informed consent. In cases where the identification of personal information is necessary for scientific reasons, authors should obtain full documentation of informed consent, including written permission from the patient prior to inclusion in the study.

*Example of Statement of Human Rights*: "The study was conducted in accordance with the Declaration of Helsinki, and the protocol was approved by the Ethics Committee of *Name of the Institution* (No. *number of approval*)."

*Example of Statement of Informed Consent*: "All subjects gave their informed consent for inclusion before they participated in the study".

For non-interventional studies (e.g. surveys, questionnaires, social media research), all participants must be fully informed if the anonymity is assured, why the research is being conducted, how their data will be used and if there are any risks associated. As with all

research involving humans, ethical approval from an appropriate ethics committee must be obtained prior to conducting the study.

**Research involving Animals**

When reporting on research that involves animal subjects, animal material or animal tissues, authors must declare that the investigation was carried out following the rules of the European Directive for the welfare of laboratory animals (No. 2010/63/EU) and national and institutional regulations. As a minimum, a statement including number of approval and name of the ethics committee must be stated in Section 'Statement of Animal Rights' of the article. Statements on animal welfare should confirm that the study complied with all relevant legislation. Also, authors must include details on housing, husbandry and pain management in their manuscript (section Materials and methods).

*Example of Statement of Animal Rights*: "All research procedures were carried out in strict accordance with the European Union Directive for the welfare of laboratory animals (No. 2010/63/EU) and approved by the Ethics Committee of *Name of the Institution* (No. *number of approval*)."


sciendo